

# Final Report

## Updating the Hydrogeologic Framework for the Northern Portion of the Gulf Coast Aquifer

*Prepared by*

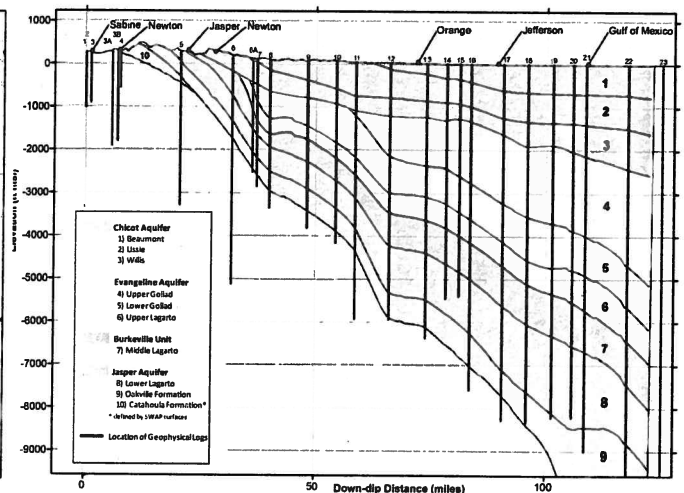
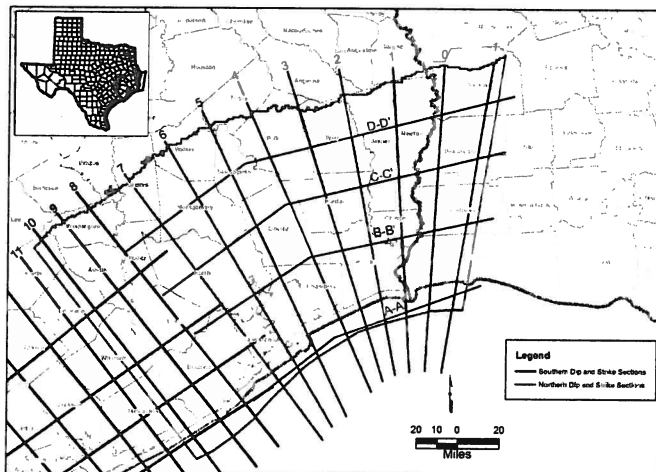
**Steven C. Young, Ph.D., P.E., P.G.**

**Tom Ewing, Ph.D., P.G.**

**Scott Hamlin, Ph.D., P.G.**

**Ernie Baker, P.G.**

**Daniel Lupton**



*Prepared for:*

**Texas Water Development Board**

**P.O. Box 13231, Capitol Station**

**Austin, Texas 78711-3231**



**June 2012**

2012 JUN 29 AM 10:18

CONTACT ADMINISTRATION

**1004831113\_Final Report**

# Final Report

## Updating the Hydrogeologic Framework for the Northern Portion of the Gulf Coast Aquifer

*Prepared by*

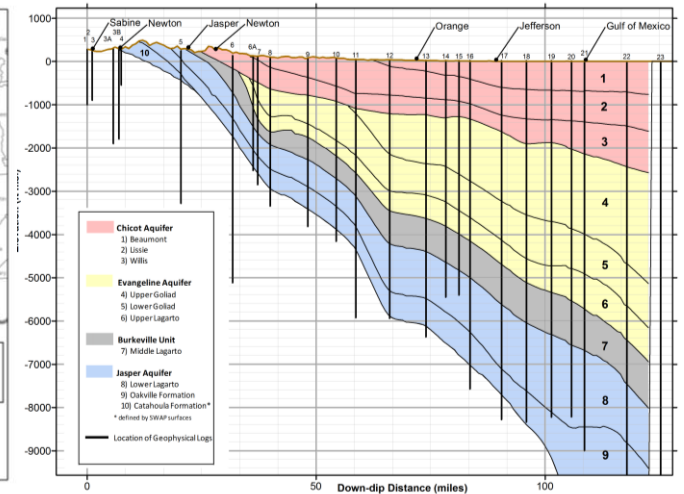
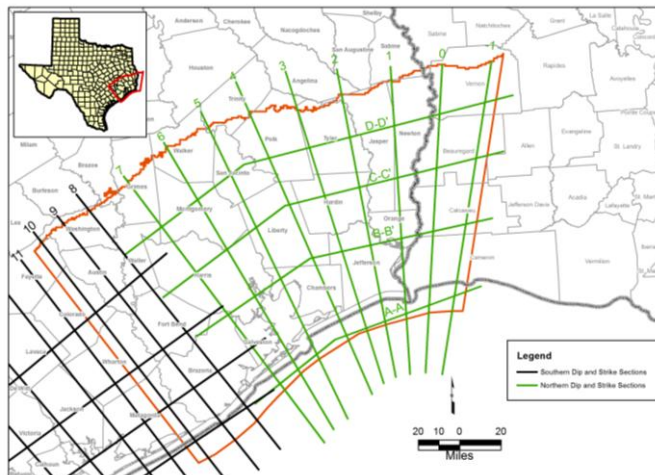
**Steven C. Young, Ph.D., P.E., P.G.**

**Tom Ewing, Ph.D., P.G.**

**Scott Hamlin, Ph.D., P.G.**

**Ernie Baker, P.G.**

**Daniel Lupton**



*Prepared for:*

**Texas Water Development Board**

**P.O. Box 13231, Capitol Station**

**Austin, Texas 78711-3231**



**June 2012**





**Texas Water Development Board**

**Final Report  
Updating the Hydrogeologic Framework for  
the Northern Portion of the Gulf Coast Aquifer**

**Steven C. Young, Ph.D., P.E., P.G.  
Daniel Lupton  
INTERA Incorporated**

**Tom Ewing, Ph.D., P.G.  
Frontera Exploration Consultants**

**Scot Hamlin, Ph.D., P.G.**

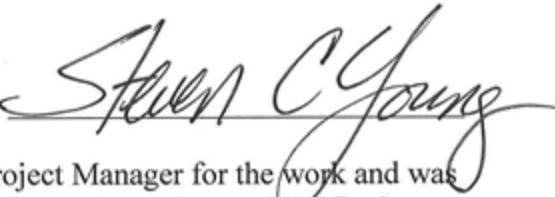
**Ernie Baker, P.G.**

**June 2012**

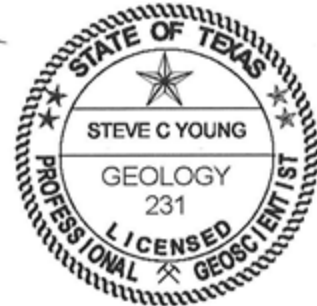
## Geoscientist seal

This report documents the work of the following Licensed Geoscientists:

Steve C. Young, P.G.



Dr. Young was the Project Manager for the work and was responsible for oversight on the project and the final interpretation of the lithologic and water quality analysis of the geophysical logs.



Thomas E Ewing, P.G. #1320



Dr. Ewing was primarily responsible for developing the chronostratigraphy of the Gulf Coast Aquifer.

*This page is intentionally blank.*

## Table of Contents

Executive Summary .....	xiii
1.0 Introduction .....	1-1
1.1 Approach for Defining Stratigraphy .....	1-2
1.2 Approach for Defining Lithology and Generating Sand Maps .....	1-3
2.0 Gulf Coast Aquifer Geologic Setting .....	2-1
2.1 Overview.....	2-1
2.2 Structural Features .....	2-4
2.2.1 Faulting and Subsidence.....	2-4
2.2.2 Salt Domes in Southeast Texas and Southwest Louisiana .....	2-7
2.2.2.1 Salt Dome Geology.....	2-8
2.2.2.2 Natural Resources .....	2-12
2.2.2.3 Groundwater Chemistry.....	2-16
2.3 Depositional Systems.....	2-17
2.4 Depositional History .....	2-18
3.0 Stratigraphic and Hydrogeologic Framework .....	3-1
3.1 Previous Studies.....	3-1
3.2 Fleming Group: Oakville and Lagarto Formations .....	3-4
3.3 Goliad Formation.....	3-8
3.4 Willis Formation.....	3-12
3.5 Lissie Formation .....	3-13
3.6 Beaumont Formation .....	3-13
3.7 Holocene Deposits .....	3-14
4.0 Information sources.....	4-1
4.1 Geophysical Logs .....	4-1
4.1.1 Resistivity Logs.....	4-2
4.1.2 Spontaneous Potential Logs .....	4-3
4.1.3 American Petroleum Institute Format .....	4-4
4.2 Approach for Obtaining Geophysical Logs.....	4-5
4.2.1 Geophysical logs' Sources .....	4-6
4.2.2 Geophysical Logs Selected for the Study.....	4-6
4.3 Literature Review .....	4-7
4.4 Paleontology Data.....	4-8
5.0 Approach for Stratigraphic Interpretation .....	5-1
5.1 Chronostratigraphic Conceptual Framework.....	5-1
5.2 Methodology.....	5-4
6.0 Gulf Coast Aquifer Stratigraphy .....	6-1
6.1 Chronostratigraphic Surfaces and Aquifer Boundaries .....	6-1
6.2 Structural Configuration of Surfaces .....	6-2

7.0	Approach for Lithologic Interpretation .....	7-1
7.1	Lithology Classification.....	7-1
7.2	Depositional Facies Classification.....	7-2
8.0	Gulf Coast Aquifer Lithology .....	8-1
8.1	Sand Thickness and Percent .....	8-1
8.1.1	Chicot Aquifer .....	8-3
8.1.2	Evangeline Aquifer.....	8-3
8.1.3	Middle Lagarto (Burkeville confining unit).....	8-3
8.1.4	Jasper Aquifer.....	8-4
8.2	Depositional Facies .....	8-4
8.2.1	Chicot Aquifer .....	8-5
8.2.2	Evangeline Aquifer.....	8-5
8.2.3	Middle Lagarto Unit (Burkeville confining unit).....	8-6
8.2.4	Jasper Aquifer.....	8-6
9.0	Gulf Coast Water Quality.....	9-1
9.1	Terminology .....	9-1
9.1.1	Fresh and Brackish Groundwater .....	9-1
9.1.2	Total Dissolved Solids and Specific Conductivity.....	9-1
9.2	Analysis of Geophysical Logs .....	9-3
9.2.1	Approach .....	9-3
9.2.2	Results .....	9-4
9.3	Analysis of Water Well Measurements .....	9-7
9.3.1	Approach .....	9-7
9.3.2	Results .....	9-7
10.0	References .....	10-1
Appendix A	Geophysical Logs Listing, including Location and Use	
Appendix B	Listing of Geophysical Logs Stratigraphic Contacts	
Appendix C	Estimated Total Sand Thickness at Each Geophysical Log Location	
Appendix D	Response TWDB Comments on Draft Report and Responses to Comments	

## List of Figures

Figure 1-1	Map of the study area showing the locations of the dip-oriented and strike-oriented cross-sections used to develop the stratigraphic surfaces. ....	1-5
Figure 2-1	Map of the Gulf of Mexico basin showing major structural elements and stratigraphic provinces. Modified from Ewing (1991). ....	2-21
Figure 2-2	Regional dip-oriented cross section of Cenozoic strata on the northwestern margin of the Gulf of Mexico basin. Modified from Galloway and others (1991) and Sharp and others (1991). ....	2-21
Figure 2-3	Map showing major growth fault zones and shallow salt domes in the onshore part of the Texas coastal zone. Modified from Ewing (1990) and Hamlin (2006). ....	2-22
Figure 2-4	Schematic cross section showing active surface fault. The fault zone is composed of deformed sediment having high vertical hydraulic conductivity locally. Aquifer sands are offset across the fault and commonly are thicker on the downthrown side owing to greater subsidence and sedimentation there. Modified from Verbeek and Clanton (1979). ....	2-22
Figure 2-5	Cross section showing typical surface expression of an active fault. The fault scarp is generally modified by erosion into a subtle topographic step. Vegetation changes near the fault line mark the boundary between dryland on the upthrown block and wetland on the downthrown block. Modified from Verbeek and Clanton (1979). ....	2-23
Figure 2-6	Lineation map of the Texas coastal zone in the Houston Embayment area. Lineations are the surface expressions of faults or fractures (Kreitler, 1976). The entire Texas coastal plain is covered by lineations, although only the more coastward lineations are mapped here. Modified from Fisher and others (1972, 1973) and McGowen and others (1976). ....	2-23
Figure 2-7	Map of subsidence and active surface faults in the Houston metropolitan area. Modified from Holzer (1984) and Shah and Lanning-Rush (2005). ....	2-24
Figure 2-8	Map showing locations of salt domes in southeast Texas and southwest Louisiana. Approximate dome sizes, shapes, and depths are shown. Individual salt domes identified by number (Table 1). ....	2-25
Figure 2-9	Cross section of Barbers Hill salt dome in Chambers County showing the salt stock, cap rock mineralogical zones, and enclosing hydrostratigraphic intervals (modified from Hamlin and others, 1988). This cross section has no vertical exaggeration (vertical and horizontal scales are equal). Cap-rock layering is generally more complicated than shown here and varies widely among domes. ....	2-26
Figure 2-10	Regional dip-oriented cross section of the upper Texas Gulf Coast showing salt domes and enclosing strata (modified from Hamlin, 1986). Line of section located in Figure 2-8. ....	2-26
Figure 2-11	Cross section of Boling salt dome in Wharton County showing salt stock, cap rock, and surrounding sediments (modified from Seni and others, 1985). Freshwater sands surround the dome, but muds and thin saline-	



	water sands overlie the dome. Groundwater salinities are interpreted from resistivity logs (freshwater sands have >20 ohm-m resistivity). ....	2-27
Figure 2-12	Map of lower Chicot sand thickness around Barbers Hill salt dome (modified from Hamlin and others, 1988). The lower Chicot sand is widespread in the Houston area (Wesselman, 1971, 1972; Baker, 1979). ....	2-27
Figure 2-13	Map of surficial sediments and depositional facies around Barbers Hill salt dome (from Fisher and others, 1972). Pleistocene channel sand follows peripheral low area east of the dome, whereas fine-grained interchannel facies cover the dome crest. ....	2-28
Figure 2-14	Photograph showing catastrophic collapse and sinkhole that formed over Hull salt dome in 2008 in the town of Daisetta, Liberty County, Texas (from Horswell, 2009). ....	2-29
Figure 2-15	Map of Barbers Hill salt dome showing locations of storage caverns in the salt stock and brine disposal wells in the cap rock as they existed in 1984 (modified from Seni and others, 1984c). ....	2-30
Figure 2-16	Cross section showing storage caverns and brine disposal wells at Barbers Hill salt dome (modified from Seni and others, 1984c). Line of section located in Figure 8. Storage cavern locations, depths, and dimensions are accurate, but geometric details are generalized. Storage cavern geometries are commonly delineated using sonar, and a sonar survey was available for one cavern on this section (third cavern from the right). ....	2-31
Figure 2-17	Cross section of Barbers Hill salt dome showing salt stock, cap rock, and surrounding sediments (modified from Hamlin and others, 1988). Groundwater salinities are interpreted from resistivity logs. Sands become thinner and more saline with proximity to the dome. Sand thickness of the lower Chicot sand is shown in Figure 2-12. ....	2-31
Figure 2-18	Hydrograph of a long-term cap rock injection test at Barbers Hill salt dome showing brine-level changes in a cap rock observation well during controlled brine disposal in two other cap rock wells (from Hamlin and others, 1988). Water levels in nearby Chicot aquifer and Evangeline aquifer water wells are around 100 feet below sea level or similar to cap rock brine levels when no disposal is occurring. However, water levels in nearby water wells were not monitored during the injection test. ....	2-32
Figure 2-19	Resistivity map of the lower Chicot aquifer at Barbers Hill salt dome (modified from Hamlin and others, 1988). Water wells completed in this lower Chicot sand are also shown along with total dissolved solids measurements. Low resistivities around the southern and southwestern dome flanks delineate a high-salinity plume extending away from the salt dome in the down-flow direction. ....	2-32
Figure 2-20	Schematic diagram showing a fluvial depositional system with its component depositional environments and resulting genetic facies. Modified from Galloway and others (1979). ....	2-33
Figure 2-21	Schematic drawing of Quaternary depositional systems of the Texas Coastal Plain. Modified from Winker (1979) and Galloway and others (1986). ....	2-33

Figure 2-22	Positions of principal fluvial-deltaic depocenters and interdeltic shorelines for selected depositional episodes, northwest GOM. Modified from Galloway (1989b) and Galloway and others (2000). .....	2-34
Figure 2-23	Chronostratigraphic chart of Miocene to Holocene depositional episodes, northwest GOM. ....	2-35
Figure 3-1	Geologic map of the Texas Coastal Plain. Source: Barnes (1992). ....	3-16
Figure 3-2	Schematic dip cross section showing relationships between outcropping formations and subsurface stratigraphy, central coastal plain, Texas. Modified from Doering (1956). ....	3-17
Figure 3-3	Schematic cross section of lower Miocene stratigraphy showing depositional sequences and lithostratigraphic and biostratigraphic boundaries. Source: Galloway and others. (1986). ....	3-17
Figure 3-4	Net-sandstone isopach map of the Oakville Formation also showing depositional systems. Red dotted line separates updip fluvial systems from downdip delta and shore-zone systems. Modified from Galloway and others. (1986). ....	3-18
Figure 3-5	Net-sandstone isopach map of the Lagarto Formation also showing depositional systems. Red dotted line separates updip fluvial systems from downdip delta and shore-zone systems. Modified from Galloway and others. (1986). ....	3-18
Figure 3-6	Schematic cross section of middle-upper Miocene stratigraphy showing depositional sequences and lithostratigraphic and biostratigraphic boundaries. From Morton and others. (1988). ....	3-19
Figure 3-7	Percent sandstone maps of Goliad and equivalent middle-upper Miocene sequences. From Hoel (1982) and Morton and others, (1988). ....	3-20
Figure 3-8	Sand percent map of the Willis Formation, southeast Texas and south Louisiana. Modified from Weiss (1992). ....	3-21
Figure 3-9	Sand percent map of the Lissie Formation, southeast Texas and south Louisiana. Modified from Weiss (1992). ....	3-21
Figure 3-10	Simplified map of surface sediment types covering Matagorda County to the Louisiana border showing Pleistocene (Beaumont Formation) and Holocene deposits. Modified from Fisher and others (1972, 1973) and McGowen and others (1976a,b). ....	3-22
Figure 4-1	Idealized SP and resistivity curve showing the responses corresponding to alternating sand and clay strata that are saturated with groundwater that has significant increases in total dissolved concentrations with depth. Modified from Driscoll (1986). ....	4-9
Figure 4-2	Schematic showing the location of the Kelly Bushing relative to the ground level and the oil rig. ....	4-10
Figure 4-3	Example of a geophysical well log that uses the American Petroleum Institute format. ....	4-10
Figure 4-4	Location of the approximately 800 logs used to characterize the stratigraphy and lithology of the northern portion of the Gulf Coast Aquifer System. ....	4-11

Figure 5-1	Schematic cross section showing small-scale depositional cycles (parasequences) and larger-scale sequence bounded by maximum flooding surfaces. ....	5-8
Figure 5-2	Schematic cross section showing correlation strategies. ....	5-8
Figure 5-3	Schematic cross section comparing (a) chronostratigraphic correlation to (b) lithostratigraphic correlation. ....	5-9
Figure 6-1	Stratigraphic column showing correlations among age, geologic formations, hydrogeologic units, paleomarkers, and relative change of coastal onlap.....	6-9
Figure 6-2	Contours for the Oakville geologic unit showing: (a) base elevation and (b) thickness. ....	6-10
Figure 6-3	Vertical cross-section of the geological units near dip section 9 in Figure 1-1. ....	6-11
Figure 6-4	Vertical cross-section of the geological units near dip section 7 in Figure 1-1. ....	6-12
Figure 6-5	Vertical cross-section of the geological units near dip section 5 in Figure 1-1. ....	6-13
Figure 6-6	Vertical cross-section of the geological units near dip section 3 in Figure 1-1. ....	6-14
Figure 6-7	Vertical cross-section of the geological units near dip section 1 in Figure 1-1. ....	6-15
Figure 6-8	Vertical cross-section of the geological units near dip section -1 in Figure 1-1. ....	6-16
Figure 6-9	Vertical cross-section of the geological units near strike section B-B'. ....	6-17
Figure 6-10	Contours for the lower Lagarto geologic unit showing: (a) base elevation and (b) thickness. ....	6-18
Figure 6-11	Contours for the Jasper Aquifer showing: (a) base elevation and (b) thickness.....	6-19
Figure 6-12	Contours for the middle Lagarto Formation, which is associated with the Burkeville Unit, showing: (a) base elevation and (b) thickness. ....	6-20
Figure 6-13	Contours for the upper Lagarto geologic unit showing: (a) base elevation and (b) thickness. ....	6-21
Figure 6-14	Contours for the lower Goliad geologic unit showing: (a) base elevation and (b) thickness. ....	6-22
Figure 6-15	Contours for the upper Goliad geologic unit showing: (a) base elevation and (b) thickness. ....	6-23
Figure 6-16	Contours for the Evangeline Aquifer showing: (a) base elevation and (b) thickness.....	6-24
Figure 6-17	Contours for the Willis geologic unit showing: (a) base elevation and (b) thickness.....	6-25
Figure 6-18	Contours for the Lissie geologic unit showing: (a) base elevation and (b) thickness.....	6-26
Figure 6-19	Contours for the Beaumont geologic unit showing: (a) base elevation and (b) thickness.....	6-27
Figure 6-20	Contours for the Chicot Aquifer showing: (a) base elevation and (b) thickness.....	6-28

Figure 6-21	Schematic showing outcrop and subcrop locations of geologic units in a three-dimensional block (a) and in a map view (b). .....	6-29
Figure 6-22	Surface geology map from Barnes (1992) showing the estimated locations of the subcrop of selected geologic units. ....	6-30
Figure 7-1	Example calculation of net and percent sand from a spontaneous potential (SP) log curve. ....	7-6
Figure 7-2	Example analysis of a geophysical log showing a binary and four-phase classification of lithology (taken from Young and Kelley, 2006). ....	7-7
Figure 7-3	Example analysis of a geophysical log showing a binary and four-phase classification of lithology (taken from Young and Kelley, 2006). ....	7-8
Figure 7-4	Example analysis of a geophysical log showing a binary and four-phase classification of lithology (taken from Young and Kelley, 2006). ....	7-9
Figure 8-1	Map of the Chicot Aquifer showing total sand thickness. ....	8-7
Figure 8-2	Map of the Beaumont geologic unit showing: (a) percentage sand coverage and (b) depositional facies. ....	8-8
Figure 8-3	Map of the Beaumont geologic unit showing total sand thickness. ....	8-9
Figure 8-4	Map of the Lissie geologic unit showing: (a) percentage sand coverage and (b) depositional facies. ....	8-10
Figure 8-5	Map of the Lissie geologic unit showing total sand thickness. ....	8-11
Figure 8-6	Map of the Willis geologic unit showing: (a) percentage sand coverage and (b) depositional facies. ....	8-12
Figure 8-7	Map of the Willis geologic unit showing total sand thickness. ....	8-13
Figure 8-8	Map of the Evangeline Aquifer showing total sand thickness. ....	8-14
Figure 8-9	Map of the upper Goliad geologic unit showing: (a) percentage sand coverage and (b) depositional facies. ....	8-15
Figure 8-10	Map of the upper Goliad geologic unit showing total sand thickness. ....	8-16
Figure 8-11	Map of the lower Goliad geologic unit showing: (a) percentage sand coverage and (b) depositional facies. ....	8-17
Figure 8-12	Map of the lower Goliad geologic unit showing total sand thickness. ....	8-18
Figure 8-13	Map of the upper Lagarto geologic unit showing: (a) percentage sand coverage and (b) depositional facies. ....	8-19
Figure 8-14	Map of the upper Lagarto geologic unit showing total sand thickness. ....	8-20
Figure 8-15	Map of the Burkeville confining unit (middle Lagarto geologic unit) showing: (a) percentage sand coverage and (b) depositional facies. ....	8-21
Figure 8-16	Map of the Burkeville confining unit (middle Lagarto geologic unit) showing total sand thickness. ....	8-22
Figure 8-17	Map of the Jasper Aquifer showing total sand thickness. ....	8-23
Figure 8-18	Map of the lower Lagarto geologic unit showing: (a) percentage sand coverage and (b) depositional facies. ....	8-24
Figure 8-19	Map of the lower Lagarto showing total sand thickness. ....	8-25
Figure 8-20	Map of the Oakville geologic unit showing: (a) percentage sand coverage and (b) depositional facies. ....	8-26
Figure 8-21	Map of the Oakville geologic unit showing total sand thickness. ....	8-27
Figure 9-1	Specific conductivity of salt solutions (modified from Moore, 1966). ....	9-9

Figure 9-2	Percentage of the Chicot Aquifer estimated to be fresh water with a TDS concentration less than 1,000 ppm, as determined by the analysis of geophysical logs.....	9-10
Figure 9-3	Percentage of the Chicot Aquifer estimated to be slightly saline water with a TDS concentration between 1,000 ppm and 3,000 ppm, as determined by the analysis of geophysical logs.....	9-11
Figure 9-4	Percentage of the Chicot Aquifer estimated to be moderately saline water with a TDS concentration more than 3,000 ppm, as determined by the analysis of geophysical logs.....	9-12
Figure 9-5	Percentage of the Evangeline Aquifer estimated to be fresh water with a TDS concentration less than 1,000 ppm, as determined by the analysis of geophysical logs.....	9-13
Figure 9-6	Percentage of the Evangeline Aquifer estimated to be slightly saline water with a TDS concentration between 1,000 ppm and 3,000 ppm, as determined by the analysis of geophysical logs.....	9-14
Figure 9-7	Percentage of the Evangeline Aquifer estimated to be moderately saline water with a TDS concentration more than 3,000 ppm, as determined by the analysis of geophysical logs.....	9-15
Figure 9-8	Percentage of the Burkeville confining unit (middle Lagarto Formation) estimated to be fresh water with a TDS concentration less than 1,000 ppm, as determined by the analysis of geophysical logs. ....	9-16
Figure 9-9	Percentage of the Burkeville confining unit (middle Lagarto Formation) estimated to be slightly saline water with a TDS concentration between 1,000 ppm and 3,000 ppm, as determined by the analysis of geophysical logs.....	9-17
Figure 9-10	Percentage of the Burkeville confining unit (middle Lagarto Formation) estimated to be moderately saline water with a TDS concentration more than 3,000 ppm, as determined by the analysis of geophysical logs. ....	9-18
Figure 9-11	Percentage of the Jasper Aquifer estimated to be fresh water with a TDS concentration less than 1,000 ppm, as determined by the analysis of geophysical logs.....	9-19
Figure 9-12	Percentage of the Jasper Aquifer estimated to be slightly saline water with a TDS concentration between 1,000 ppm and 3,000 ppm, as determined by the analysis of geophysical logs.....	9-20
Figure 9-13	Percentage of the Jasper Aquifer estimated to be moderately saline water with a TDS concentration more than 3,000 ppm, as determined by the analysis of geophysical logs.....	9-21
Figure 9-14	Map of water well locations in the Chicot Aquifer with at least one measurement of TDS concentrations. ....	9-22
Figure 9-15	Map of water well locations in the Evangeline Aquifer with at least one measurement of TDS concentrations. ....	9-23
Figure 9-16	Map of water well locations in the Burkeville confining unit with at least one measurement of TDS concentrations. ....	9-24
Figure 9-17	Map of water well locations in the Jasper Aquifer with at least one measurement of TDS concentrations. ....	9-25

**List of Tables**

Table 2-1 Simplified stratigraphic and hydrogeologic chart of the northwestern Gulf of Mexico basin, Texas coastal zone (Galloway and others, 1991; Sharp and others, 1991)..... 2-3

Table 2-2 Simplified stratigraphic and hydrogeologic chart of the northwestern Gulf of Mexico basin, Texas coastal zone (Galloway and others, 1991; Sharp and others, 1991)..... 2-10

Table 3-1 Fleming Group depositional facies (Galloway and others, 1982, 1986). ..... 3-5

Table 3-2 Fleming Group depositional systems (Spradlin, 1980; Galloway, and others, 1982, 1986). ..... 3-6

Table 3-3 Goliad Formation depositional facies (Hoel, 1982)..... 3-9

Table 3-4 The Goliad Formation fluvial depositional systems (Hoel, 1982; Morton and others, 1988)..... 3-11

Table 4-1 Types of log header data. .... 4-4

Table 4-2 Selected tables and fields from the Microsoft Access database used to manage information on the 666 well logs analyzed for the study. .... 4-7

Table 7-1 Description of the four textural classes used to characterize the lithology of the LCRA-SAWS Water Project (LSWP) wells. .... 7-2

Table 7-2 Depositional Facies Definition and Predicted Flow Characteristics [modified from Table 3.1.3 in Young and Kelley (2006)]. ..... 7-4

Table 9-1 Groundwater classifications based on TDS (from Collier, 1993)..... 9-1

Table 9-2 Relationship among TDS, specific conductivity, and resistivity (from Collier, 1993)..... 9-3

Table 9-3 General criteria used by Mr. Baker to estimate the TDS from the geophysical logs..... 9-4

Table 9-4 Aquifer codes used in Gulf Coast query ..... 9-7

*This page intentionally left blank.*

## **Executive Summary**

This report documents the development of the structure, lithology, and depositional framework for the Gulf Coast Aquifer system from the Brazos River north to the Sabine River and into Louisiana. The project is part of a long-term plan to update the Groundwater Availability Models (GAMs) for the Gulf Coast Aquifer.

The structure of the Gulf Coast Aquifer system is comprised of, from shallowest to deepest, the Chicot Aquifer, the Evangeline Aquifer, the Burkeville confining unit, and the Jasper Aquifer, with parts of the Catahoula Formation acting as the Catahoula Confining System. In this study, aquifer units have been subdivided on the basis of chronostratigraphic correlation to yield subaquifer layers. The boundaries for the geologic units were traced from outcrop formation boundaries to identifiable flooding surfaces in the deeper subsurface, where paleontological control constrained geologic ages of surfaces at nearshore and offshore geophysical log locations.

The Chicot Aquifer subaquifer layers include, from the shallowest to deepest, the Beaumont and Lissie Formations of Pleistocene age and the Pliocene-age Willis Formation. The Evangeline Aquifer subaquifer layers include the upper Goliad Formation of earliest Pliocene and late Miocene age, the lower Goliad Formation of middle Miocene age, and the upper unit of the Lagarto Formation (a member of the Fleming Group) of middle Miocene age. The Burkeville confining unit is defined as the middle unit of the Lagarto Formation of middle and early Miocene age, which is the chronostratigraphic layer with the most widespread clayey interval between the Evangeline and Jasper Aquifers. For this study, the Jasper Aquifer includes the lower Lagarto unit of early Miocene age, the early Miocene Oakville sandstone member of the Fleming Group, and the sandy intervals of the Oligocene-age Catahoula Formation. Elevations from the established base Jasper surface in the Source Water Assessment Program dataset were used close to the outcrop and were merged with the chronostratigraphic base of the Oakville Sandstone defined in this study.

As part of this project, approximately 800 geophysical logs were used to map stratigraphy, lithologic profiles, and estimates of water quality in the northern Gulf Coast Aquifer system. The 800 geophysical logs include 666 wells that were analyzed as part of this study and



approximately 125 logs that were analyzed as part of a similar TWDB study of the southern portion of the Gulf Coast Aquifer (Young and others, 2010).

The method used to develop geologic surfaces focuses on identifying clay-dominated flooding surfaces of the same age that form the boundaries of episodes that deposit the coarse sediment of an aquifer. Depositional facies modeling, including an analysis of depositional cyclicity, was used to better construct a regional framework for the flooding surfaces and the spatial variation of the aquifer-matrix properties. In the northern Gulf Coast region, the existing data from Young and others (2010) was augmented to generate surfaces for nine geologic units along 12 dip sections. In addition, the data from Young and others (2010) was augmented with lithologic picks to develop maps of sand percentages and total sand thickness maps for the Chicot, Evangeline, and Jasper Aquifers and their respective geologic formations. Like the study of Young and others, (2010), lithologic picks are based on a four-class system consisting of: 1) sand; 2) clay; 3) sand-with-clay; and 4) clay-with-sand. Using the lithologic information, geologic layers were developed.

To assist in the development of hydraulic conductivity distributions for each geologic unit, depositional facies maps were developed. The deposition facies provide information on factors that affect groundwater flow such as the sorting, arrangement, and sizes of the particles in a deposit and how the deposit is or is not interconnected to similar and different deposits.

For each of the geophysical logs used for the lithologic interpretation, an estimate of the water quality was made for each interval assigned a lithology classification. For each of these intervals, the water quality was classified as fresh, slightly saline, or moderately saline. These classifications are based on the concentration of Total Dissolved Solids (TDS). Fresh water is defined as having a TDS concentration less than 1,000 ppm. Slightly saline water has a TDS between 1,000 and 3,000 ppm, and moderately saline water has a TDS between 3,000 and 10,000 ppm. Using these results, maps of percent fresh water were generated for the Chicot, Evangeline, and Jasper Aquifer

## **1.0 Introduction**

The current groundwater availability models (GAMs) for the northern region (Kasmarek and Robinson, 2004), the central region (Chowdhury and others, 2004), and the southern region (Chowdhury and Mace, 2007) of the Gulf Coast Aquifer are based on stratigraphy developed from the Source Water Assessment and Protection (SWAP) Program. For these GAMs, the Gulf Coast Aquifer includes the Chicot Aquifer, the Evangeline Aquifer, the Burkeville Confining System, and the Jasper Aquifer. One of the obstacles to improving the GAMs predictive accuracy is that the SWAP database contains limited stratigraphic and lithologic information at the scale of the geologic formations that comprise the aquifers. In a continual effort to improve the GAMs, the Texas Water Development Board (TWDB) has determined that additional stratigraphic and lithologic information beyond what is available from the SWAP data would be beneficial for improving the predictive accuracy of future GAMs.

The primary objective of this study is to provide the stratigraphic surfaces and sand thickness maps of the geological formations that compose the Gulf Coast Aquifer system from the Brazos River north to the Sabine River and the Texas State line and into Louisiana using an approach consistent with the approach used by Young and others (2010). Young and others (2010) used sequence stratigraphy for defining geological units that comprise the Gulf Coast Aquifer System from the Brazos River south to the Rio Grande. For this study, the Chicot Aquifer includes, from the shallowest to deepest, the Beaumont and Lissie Formations of Pleistocene age and the Pliocene-age Willis Formation. The Evangeline Aquifer includes the upper Goliad Formation of earliest Pliocene and late Miocene age, the lower Goliad Formation of middle Miocene age, and the upper unit of the Lagarto Formation (a member of the Fleming Group) of middle Miocene age. The Burkeville confining unit is associated with the middle unit of the Lagarto Formation of middle and early Miocene age. As noted by Baker (1979) the Burkeville is not restricted to a single geological unit and represents the low permeability deposits that contribute to the hydraulically isolating the Jasper and the Evangeline Aquifers. The Jasper Aquifer includes the lower Lagarto unit of early Miocene age, the early Miocene Oakville sandstone member of the Fleming Group, and the sandy intervals of the Oligocene-age Catahoula Formation.

## **1.1 Approach for Defining Stratigraphy**

Investigations of the Gulf Coast Aquifer began in the late 1880's. Since that time, numerous studies have contributed toward our understanding of the formations in that aquifer. Central to our approach are the selected studies that provide an overarching stratigraphic framework.

With regard to naming conventions, we rely on the founding work of Doering (1935), who was perhaps the first to use the nomenclature most commonly used today (from the surface downward), the Beaumont, Lissie, Willis, Goliad, Lagarto, and Oakville. With regard to nomenclature, we also reference Baker (1979). He was among the first to establish an accurate stratigraphic framework using a lithostratigraphic correlation of the Gulf Coast Aquifer that relied on good understanding of geologic processes.

With regard to defining the stratigraphy surfaces, our analysis is based on chronostratigraphic rather than lithostratigraphic correlation techniques. Lithostratigraphic correlations rely on the interpretation from well logs of formation lithologies and boundaries between different lithologies (e.g., mud on sand) and then correlating those boundaries between wells. Prior to the 1980s, lithofacies correlations were the most common technique to define stratigraphy. Since the 1980's, an improved understanding of depositional processes has shown that lithostratigraphic correlations are more suspect for mischaracterizing the continuity and size of a formation than are chronostratigraphic correlations. Chronostratigraphic correlations focus on identifying clay-dominated flooding surfaces of the same age that form the boundaries of episodes that deposit the coarse sediment of an aquifer. As part of our approach, we used depositional facies modeling, including an analysis of depositional cyclicity, to better construct a regional framework for the flooding surfaces and the spatial variation of the aquifer-matrix properties.

Where appropriate, our sequence stratigraphy and chronostratigraphic correlations are based on the concepts and methods used by the Gulf Basin Depositional Synthesis Project (GBDS), the LCRA-SAWS Water Project (LSWP), and the TWDB study for the southern portion of the Gulf Coast Aquifer. The GBDS project conducted by the Texas Bureau of Economic Geology and funded by a consortium of petroleum companies to characterize the Cenozoic depositional history of the Gulf of Mexico Basin. Among the key papers that explains some of these concepts

and methods are Galloway (1989b), Galloway and others (2000), and Galloway (2005). The LSWP project included a chronostratigraphic analysis of the Chicot and Evangeline Aquifers across a 10-county region intersected by the Colorado River. Among the papers that describe the LSWP study are Knox and others (2006), Young and Kelley (2006), and Young and others (2009). The TWDB study is described by Young and others (2010).

Dr. Thomas Ewing is the geologist primarily responsible for making the stratigraphic picks on 350 geophysical logs. Dr. Ewing analyzed logs along twelve dip-oriented cross-sections. These dip sections included three dip sections 10, 9, and 8 presented in Young and others (2010) and eight new dip sections, which are numbered from 7 to -1. Figure 1-1 shows the location of the twelve dip sections. For dip sections 10, 9, and 8 Dr. Ewing picks made his stratigraphic picks on the same geophysical logs used by Mr. Paul Knox (Young and others, 2010).

Within the area of overlapping picks on dip sections 10, 9, and 8, there are locations where Dr. Ewing and Mr. Knox made different picks for the same geologic unit. One of the reasons for these differences is that the two geologist worked toward the dip sections from different directions. Mr. Knox worked northward from the San Marco Arch and Dr. Ewing worked southward from the Houston Embayment. Because of these differences, difference preferences were assigned to each geologist picks based on the log location.

In developing the stratigraphic surfaces, all of the picks associated with dip section 10 are those made by Mr. Knox. For dip section 9, Mr. Knox's picks were given preference over Dr. Ewing's picks. For dip section 8, Mr. Ewing's picks were given preference over Mr. Knox's picks. These preferences were given so that stratigraphic surfaces generated from this project would be consistent and match with the stratigraphic surfaces provided by Young and others (2010) at dip section 10.

## **1.2 Approach for Defining Lithology and Generating Sand Maps**

Lithologic analyses were performed independently of the stratigraphic correlations. As a result, there are logs that have stratigraphic picks but not lithologic picks and vice versa. The lithology picks are based on using four textural classes instead of the traditional "binary" system of classifying lithology from geophysical logs. The "binary" system classifies lithology into either sand beds or clays beds based on the "kicks" provided by the spontaneous potential log or the

resistivity log. The four textural classes used are (1) sand, basically; (2) clay, basically; (3) sand and clay but basically sand; and, (4) clay and sand but basically clay. This classification scheme is used to provide a more accurate representation of the lithology for vertical intervals where sands and clays are alternating and have individual bed thicknesses of less than 20 feet.

The boundaries between the four textural classes are based on the "kicks" in the resistivity logs and are supplemented by "kicks" in the spontaneous potential logs. Resistivity logs record an apparent electrical resistance in and within the vicinity of the borehole at different depths. Spontaneous potential (SP) logs record naturally occurring electrical potentials (voltages) that occur in the borehole at different depths.

Our textural classes are the same as those used by Young and others (2010) to characterize the southern portion of the Gulf Coast Aquifer. To ensure consistency among all of the lithologic analyses, Mr. Ernie Baker performed all of lithologic analyses for this study. Also, Mr. Baker is the geologist who made all of the lithologic picks used by Young and others (2010).

The sand maps produced for the study area are based on Mr. Baker's lithologic profiles for approximately 590 logs. These maps were generated for selected lithostratigraphic units based on interpolation of the total sand thickness generated at each geophysical log. Interpolation of the sand thickness values was performed using ordinary kriging. Where appropriate, the generated contours were adjusted based on our interpretation of the depositional history and environments responsible for the sand distributions.

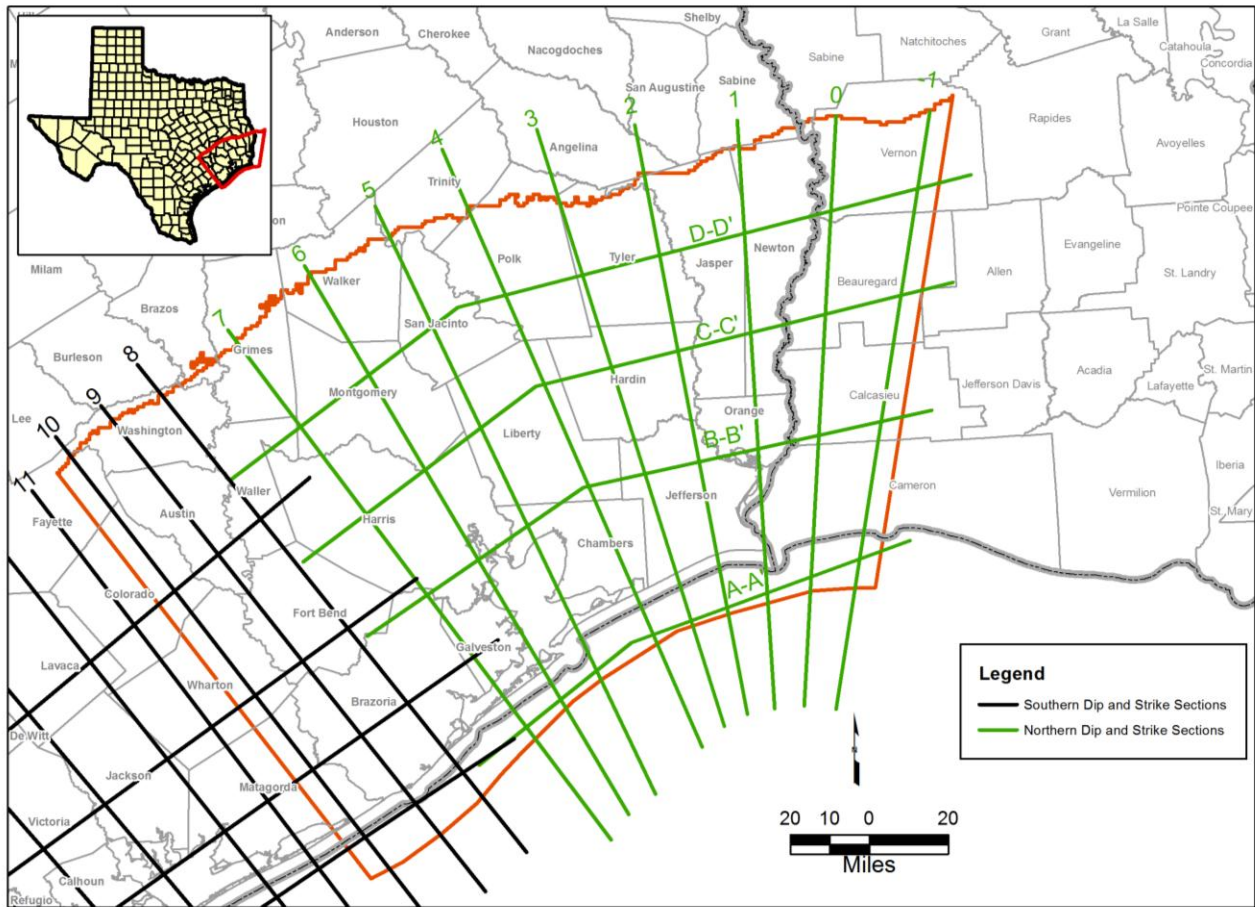


**Figure 1-1** Map of the study area showing the locations of the dip-oriented and strike-oriented cross-sections used to develop the stratigraphic surfaces.

*This page intentionally left blank.*

## **2.0 Gulf Coast Aquifer Geologic Setting**

### **2.1 Overview**

The Gulf of Mexico (GOM) is a small semi-enclosed ocean basin surrounded by continental shelves and coastal plains (Bryant and others, 1991). The GOM is a circular structural basin, 940 miles in diameter, and filled with 0 to 9.4 miles of sediments ranging from Triassic to Holocene in age (Salvador, 1991) (Figure 2-1). The GOM basin probably originated in the Triassic time from rifting within the North American plate as it was drifting away from the African and South American plates (Salvador, 1991). Intermittent marine flooding of the proto-GOM rift valley formed extensive evaporite deposits (mainly salt) during the Jurassic period. Early Cretaceous carbonate platforms and shelf margins rimmed the GOM and provided a foundation for subsequent terrigenous clastic sedimentation during the Cenozoic period (Winker and Buffler, 1988). In the north and west parts of the GOM, Cenozoic sediments form thick sequences of sandstones and mudstones that overlie Cretaceous carbonates and extend basinward to the base of the modern continental slope (Figure 2-2). GOM stratigraphy is generalized in Table 2-1.

Three major stratigraphic-structural margins surround the deep ocean basin that forms the center of the GOM: 1) northern and northwestern margin of terrigenous clastic sedimentation; 2) western and southwestern structurally modified margin; and 3) eastern and southeastern carbonate-evaporite margin (Ewing, 1991; Galloway et al., 1991) (Figure 2-1). The eastern carbonate margin includes the Florida and Yucatan platforms and is characterized by low subsidence and limited clastic sediment input. The Floridian carbonate aquifer system is the main groundwater resource in the U.S. part of the eastern carbonate province (Miller, 1986). The western structurally modified margin of the Gulf Coast in Mexico includes a relatively narrow clastic coastal plain and continental shelf that have been affected by Laramide (early Cenozoic) compressional deformation. Sandy coastal aquifer systems similar to those in Texas are not well developed in Mexico (Sharp and others, 1991). The northern and northwestern clastic margin (northwest GOM) spans coastal Texas, coastal Louisiana, and adjacent offshore areas (Figure 2-1). The northwest GOM includes the major sand and sandstone aquifer systems



of the Gulf Coast (Weiss, 1992; Chowdhury and Turco, 2006) of which one, the Gulf Coast Aquifer, is the focus of this report.

The northwest GOM includes two broad zones that parallel the basin margins: the interior zone and the coastal zone (Ewing, 1991). The interior zone defines the updip margin of the basin and extends downdip to the relict Early Cretaceous shelf margin (Figure 2-1). The interior zone is dominated by Cretaceous carbonates and Paleogene terrigenous clastics (Figure 2-2). The Edwards (Balcones Fault Zone), Carrizo-Wilcox, Queen City-Sparta, and Yegua-Jackson Aquifers occur in the northwest GOM interior zone (Table 2-1). The coastal zone extends from the Early Cretaceous shelf margin to the base of the modern continental slope (Figure 2-1). Basinward of the stable Cretaceous carbonate platform, subsidence increases greatly, and Cenozoic clastic sequences become much thicker. In the onshore part of the coastal zone, Paleogene sediments are dominated by deltaic, shore-zone, and marine depositional systems below the base of fresh water. Overlying Neogene sediments are dominantly nonmarine depositional systems. The Gulf Coast Aquifer of Texas is located within these onshore Neogene sediments (Table 2-1, Figure 2-2).

The northwest GOM encompasses several second-order structural elements inherited from the early formation of the basin. The Rio Grande embayment is an area of enhanced subsidence and greater sediment thickness centered on the modern Rio Grande river in South Texas and northeastern Mexico. The Burgos Basin in northeastern Mexico forms the south part of the Rio Grande embayment (Ewing, 1991; Hernandez-Mendoza and others, 2008). The Houston embayment is a similar subsidence trough centered in southeast Texas (Figure 2-1). The Mississippi embayment is a larger synclinal feature coinciding with the modern lower Mississippi River valley and delta. Although these embayments began in the Mesozoic as active tectonic structures, they became passive loading-induced depocenters during the Cenozoic (Ewing, 1991). In the coastal zone of the northwest GOM, these embayments are distinguished by enhanced subsidence and greater cumulative sediment thickness. The San Marcos arch separates the Rio Grande and Houston embayments in coastal Texas, forming a broad area of relatively lower subsidence and thinner cumulative sediment thickness (Figure 2-1).

**Table 2-1 Simplified stratigraphic and hydrogeologic chart of the northwestern Gulf of Mexico basin, Texas coastal zone (Galloway and others, 1991; Sharp and others, 1991).**

ERA	Period		Epoch	Age (M.Y.)	Stratigraphic Unit	Dominant Lithology	Hydrogeologic Unit			
Cenozoic	Quaternary		Holocene	0.02	Alluvium	sand	Alluvium/Beaumont Aquifer	Gulf Coast Aquifer		
			Pleistocene		Beaumont	sand				
	Tertiary	Neogene	Pliocene		1.8 5.3	Lissie/Alta Loma	sand		Chicot Aquifer	
				Miocene			Goliad		sand	Evangeline Aquifer
							Fleming/Lagarto		mud	Burkeville Aquitard
			Paleogene	Oligocene		23.9	Fleming/Oakville		sand	Jasper Aquifer
							Catahoula/Frio/Anahuac		sand and mud	aquitard
				Eocene		33.9	Vicksburg		mud	aquitard
					Jackson		sand and mud		Yegua-Jackson Aquifer	
					Yegua		sand and mud			
					Sparta		sand		Queen City-Sparta Aquifer	
					Queen City		sand and mud			
		Paleocene		55.8	Upper Wilcox/Carrizo	sand	Carrizo-Wilcox Aquifer			
					Middle Wilcox	mud				
					Lower Wilcox/Simsboro	sand and mud				
			65.5	Midway	mud	aquitard				
Mesozoic	Cretaceous	Upper		145.5		carbonate				
		Lower			Edwards	carbonate	Edwards (BFZ) Aquifer			
	Jurassic	Upper				carbonate				
		Middle		201.6	Louann salt	evaporite	salt domes			
	Triassic									

The northwest GOM coastal zone is composed of terrigenous clastic sediments and sedimentary rocks that dip gently and thicken toward the center of the GOM. Older sediments are more indurated and dip more steeply than younger sediments (Figure 2-2). These stratigraphic patterns reflect increasing subsidence toward the central GOM and progradational deposition (infilling incrementally from the margin). Paleo-shoreline positions typically oscillated broadly in response to relative sea-level fluctuations, but continental margin outbuilding was progressive so that each successive major stratigraphic interval (e.g., Carrizo-Wilcox) extends basinward of the underlying interval. Minor stratigraphic intervals (e.g., Queen City-Sparta) typically do not extend basinward but instead stack vertically (aggradational deposition) upon underlying intervals (Figure 2-2).

## **2.2 Structural Features**

Geologic structures related mainly to sediment loading and gravity tectonics disrupt and deform Cenozoic sediments in the northwest GOM. Growth faults are syndepositional normal faults that form mainly by gravitational failure during rapid sediment loading along an unstable shelf margin and upper slope (Winker and Edwards, 1983). Coast-parallel growth fault zones mark shelf-margin positions of major Cenozoic depositional episodes, which get younger basinward (Figure 2-3). Sediments deposited during active growth faulting typically thicken on the downthrown sides of the faults because downward and basinward displacement creates local subsidence troughs and increased accommodation space. Greatest displacement and sediment thickening occur in shelf margin and upper-slope depositional settings.

### ***2.2.1 Faulting and Subsidence***

Faulting and subsidence not only affect aquifer properties and groundwater availability in the Gulf Coast Aquifer but also cause land loss and property damage. In the Houston Embayment, active surface faults are commonly upward extensions of deep-seated growth faults. Surface faults also occur around salt domes, but dome-related faults are shorter (<3 miles) and more localized than are growth faults (>6 miles) (Veerbeek, 1979). Gulf Coast growth faults form by differential sediment loading and gravity slumping near the shelf margin. The seaward side of a growth fault is typically displaced downward relative to the landward side (Figure 2-4). Because the downthrown fault block is topographically lower than the upthrown block, greater

thicknesses of sediment are deposited on the downthrown block (Figure 2-4). Antithetic faults, having opposing sense of movement (downward displacement on the landward side) locally accompany down-to-the-coast growth faults, forming complete fault-bounded blocks that are downthrown on all sides. Maximum displacement (several thousand feet) on growth faults occurs in deep formations, such as the Wilcox and Frio, and decreases upward. In the Gulf Coast aquifer, maximum fault displacements are a few hundred feet, and surface expressions of active faults are generally only a few feet (Verbeek, 1979) (Figure 2-5).

Growth faults are not isolated surfaces but instead form zones of sediment deformation that commonly impede horizontal groundwater flow and enhance vertical flow. Displacement (offset) of sand bodies across fault zones reduces horizontal transmissivity (Kreitler and others, 1977) (Figure 2-4). Fluid-pressure buildup at depth results in upward flow of water, gas, and oil through vertical permeability pathways within fault zones. Linear distributions of saline-water plumes in shallow aquifer sands are associated with active faults in Louisiana (Kuecher and others, 2001). Faults compartmentalize groundwater flow. Pumpage within a fault block can result in water-level declines that are restricted to that block, while water levels in surrounding blocks are less affected (Kreitler, 1977). Decreased fluid pressures in semi-isolated fault blocks may result in increased sediment compaction leading to surface subsidence over the downthrown block. In the natural system through geologic time, sedimentation tends to infill topographically downthrown blocks, accentuating loading and reactivating fault movement. On the modern coastal plain, however, sedimentation may be restricted by dams and channel diversions, and downthrown fault blocks tend to become wetlands or submerged areas (Gagliano, 1999, 2005) (Figure 2-5).

Active faults in the Gulf Coast Aquifer typically display mappable surface expressions. Lineations are straight, lengthy surface features that, in part, represent the surface traces of faults and locally coincide with boundaries between zones of differential subsidence (Kreitler, 1976). Over 7,000 miles of lineations have been mapped on the Texas Coastal Plain (Fisher and others, 1972, 1973; McGowen and others, 1976a,b) (Figure 2-6). Lineations are identified by color variations on aerial photographs and are coincident with geomorphic features, such as rectilinear drainage patterns and vegetation changes (Kreitler, 1976). Not all lineations are active surface faults. The following criteria are used to identify surface faults: (1) breaks in man-made

structures caused by displacement of the land surface, (2) presence of topographic scarps, (3) recognition of faults in the shallow subsurface using electric log correlations, coring, or trenching, and (4) lineations observed on aerial photographs (Kreitler, 1976). Active surface faults commonly display surficial displacement and subtle scarps (Figures 2-4 and 2-5). Recently, Lidar (an acronym for light detection and ranging, analogous to radar but with laser light as a source) has been used to map fault-related scarps having only a few feet of relief (Shah and Lanning-Rush, 2005; Saribudak and Nieuwenhuise, 2006; Engelkemeir and Khan, 2007, 2008). Some active surface faults do not form discrete scarps but instead form zones of deformed ground tens to hundreds of feet wide. Lineation mapping is the best tool for identifying deformed zones in undeveloped areas, but in urban areas, surface deformation is made obvious by cracked foundations, buckled roads, and damaged buildings (Verbeek, 1979).

On the Texas Coastal Plain, the most detailed investigations of shallow faulting have been conducted in the Houston area (Harris County). More than 300 active surface faults with a total length exceeding 300 miles have been mapped in the Houston metropolitan area (Holzer, 1984; Shah and Lanning-Rush, 2005) (Figure 2-6). Houston area active faults typically have 1.0- to 1.5-foot-high scarps and displacement rates of about 1 inch/year (Holzer and Gabrysch, 1987). Some data suggest that fault movement is related to groundwater fluid pressure. Modern displacement rates are greater than estimated prehistoric rates (Holzer and Gabrysch, 1987), and declining pressures in the Gulf Coast Aquifer have accelerated movement on some surface faults (Kreitler, 1976). Geophysical surveys suggest dewatering and compaction on the downthrown sides of active faults (Saribudak and Nieuwenhuise, 2006). Fault displacement rates have decreased in some areas, for example southeast Houston, where groundwater pumpage was reduced and water levels were allowed to recover (Kreitler, 1977; Holzer and Gabrysch, 1987).

Land-surface subsidence has been a particular problem in the Houston area for decades (Coplin and Galloway, 1999) but also occurs widely throughout the Texas and Louisiana coastal zones. In low-lying coastal areas, subsidence is 100 times greater than global sea-level rise and is the main cause of flooding and wetlands loss (Anderson and Milliken, 2005). Subsidence is a natural process resulting from compaction of sediments during burial, but groundwater withdrawal increases compaction within the Gulf Coast Aquifer (Kasmarek and others, 2009). The weight of subsurface material (aquifer matrix plus stored groundwater) is supported by both

fluid pressure and grain-to-grain contacts in the matrix. Lowering fluid pressures puts more of the overburden weight on the sedimentary matrix, causing compaction (rearrangement of clay particles to decrease total aquifer volume). Compaction-related reduction of aquifer volume causes the land surface to subside. A well-defined subsidence bowl is centered on southeast Houston, where land-surface elevations have decreased as much as 10 feet (Figure 2-7).

Subsidence in Houston is closely related to groundwater withdrawal, but the influence of faulting is less well understood (Engelkemeir and Khan, 2007). Clearly, subsidence and faulting have both natural and anthropogenic causes. Regional, long-term subsidence of the Gulf of Mexico basin, sediment loading and compaction around the basin margins, salt movement, and gravity slumping are all natural processes that result in subsidence and faulting (Kuecher and others, 2001). Subsurface fluid withdrawal (groundwater and petroleum) contributes to both regional and local subsidence (Paine, 1993; Sharp and Hill, 1995) and probably also to increased displacement on shallow faults (Kreitler, 1977; Holzer and Gabrysch, 1987).

Groundwater availability and quality in the Gulf Coast Aquifer are affected by faulting and land-surface subsidence. Because compaction is largely irreversible, subsidence results in permanent reduction of aquifer volume and groundwater storage. Groundwater availability may also be limited in a practical way owing to the negative impacts of subsidence. In order to mitigate subsidence in the Houston-Galveston area, for example, a planned transition from groundwater to surface water as the primary source of water supply has been in progress since the 1970s.

Along with salt domes, faults are the primary conduits for vertical groundwater flow and saltwater intrusion in the Gulf Coast Aquifer. Whereas the effects of salt domes are relatively local, growth faults form regional vertical permeability conduits and horizontal transmissivity barriers that are perpendicular to the dominant groundwater flow direction (southeast).

Abundant growth faults at depth and lineations on the land surface suggest that most if not all of the sand bodies in the Gulf Coast Aquifer are intersected by faults.

### ***2.2.2 Salt Domes in Southeast Texas and Southwest Louisiana***

Salt domes are common geologic features along the upper Texas Coast and in southwest Louisiana. In the Texas part of the northern Gulf Coast Aquifer, there are 50 salt domes that are less than 15,000 feet deep (Figure 2-8). An additional 17 salt domes at similar depths are located in southwest Louisiana within 60 miles of the Texas border (Figure 2-8). Many more deep salt

structures exist below 15,000 feet but are not covered in this report. Shallow salt domes have the greatest potential to affect groundwater quality. There are 35 shallow salt domes in the northern Gulf Coast Aquifer in Texas that range in depth from 0 (land surface) to 1,500 feet (Figure 2-8, Table 2-2). The average depth of these shallow Texas domes is 565 feet.

Salt domes typically include three elements: salt stock, cap rock, and surrounding uplifted sediments. The core of a salt dome forms a vertically elongate, cylindrical stock, consisting of 90 to 99 percent crystalline rock salt (halite). Cap rock composed of sulfate and carbonate minerals commonly overlies the crest of the salt stock and drapes down the uppermost flanks (Figure 2-9). Salt stock and cap rock are enclosed in sediments and sedimentary rocks of the Gulf Coast Aquifer and deeper intervals. Salt-dome crests are generally one to three miles in diameter. Gulf Coast salt domes extend downward many 1,000s of feet, but their true shapes at depth are largely unknown.

Shallow salt domes have the potential to increase groundwater salinities in the Gulf Coast Aquifer in two ways: first by direct dissolution and transport of soluble dome minerals and second by providing pathways for groundwater mixing between shallow freshwater and deep saline-water aquifers. The salt domes of the Texas Gulf Coast have been thoroughly explored in the search for oil and gas, but the effects of shallow salt domes on groundwater quality have been less well studied. The purpose of this chapter is to review the available literature on the salt domes of the upper Texas Gulf Coast and summarize our current understanding of salt dome hydrogeology.

#### **2.2.2.1 Salt Dome Geology**

Salt domes are geologic structures that grow and develop as sediments are being deposited around them (Seni and Jackson, 1984; Halbouty, 1979). The salt originally formed bedded evaporite deposits in the ancestral Gulf of Mexico during the Jurassic period. A thick (greater than 20,000 feet) sequence of sedimentary rocks now overlies the salt source layer (Figure 2-10). Salt, which is a low-density, ductile mineral, is gravitationally mobilized by sediment loading, forming a variety of upwelling structures, one of which is the cylindrical salt dome. The growth of salt structures, in turn, influences the structure and stratigraphy of surrounding sediments and sedimentary rocks. Uplift and upward drag occur against the salt stock and over its crest. Steeply dipping strata terminate against the salt stock, and shallower layers arch over the dome

crest (Figure 2-10). The zone of uplift near the dome is surrounded by areas of subsidence and downwarping caused by salt withdrawal at depth (Figure 2-10). Faults and fractures are also common features of salt dome growth.

Salt dome growth also influences the topography of the overlying land surface. Positive topographic relief is linked to dome growth and uplift, whereas subsidence of the topographic surface is linked to dissolution of the dome crest (Seni and Mullican, 1986; Mullican, 1988). Of the shallow domes along the upper Texas Gulf Coast, sixty-three percent have positive topographic relief over their crests (Seni and others, 1984d; Beckman and Williamson, 1990) (Table 2-2). Warping of the depositional surface, either on the coastal plain or in the shallow marine environment, influences sedimentation patterns. On the coastal plain, muddy sediments tend to be deposited over dome crests, and sandy sediments tend to be deposited in surrounding low-lying areas (Figures 2-11, 2-12, 2-13). Elevation of the sea floor over dome crests can decrease water depths sufficiently to allow reefs to grow (Rezak, 1984). The Oligocene *Heterostegina* Limestone, which is composed of carbonate reef facies, occurs within the Anahuac Formation marine shale around Barbers Hill, Boling, Nash, Stratton Ridge, and West Columbia salt domes and is exposed in a quarry at the crest of Damon Mound salt dome (Collins, 1986).

Salt dome cap rock is composed mainly of anhydrite, gypsum, and calcite arranged in heterogeneous layers (Figure 2-9). Cap rock formation results from salt dissolution. Anhydrite (calcium sulfate), the main impurity in the salt stock, forms a residual accumulation at the dome crest. Commonly, a thin layer of loose, sand-size anhydrite crystals directly overlies top of salt. As salt continues to dissolve and more anhydrite accumulates, it compacts and recrystallizes, forming the lower part of the cap rock (Figure 2-9). Circulating groundwater converts anhydrite into gypsum (hydrous calcium sulfate), and sulfate-reducing bacteria convert anhydrite into calcite (calcium carbonate), and to a lesser extent, native sulfur and metallic sulfides (Bodenlos, 1970; Kyle and Price, 1986). Thus, the upper part of the cap rock is typically composed of gypsum and calcite (Figure 2-9). Cap rock layering, however, is irregular and varies greatly from dome to dome. Structural deformation and fracturing are common, as are cavernous voids. Gulf Coast cap rocks range in thickness from 0 to 2,000 feet (Table 2-2). Cap rocks are direct evidence for dissolution of salt by groundwater.



**Table 2-2 Simplified stratigraphic and hydrogeologic chart of the northwestern Gulf of Mexico basin, Texas coastal zone (Galloway and others, 1991; Sharp and others, 1991).**

Map Number (See Figure 2-8)	Salt Dome Name	County or Parish	Depth (ft) to Cap Rock	Depth(ft) to Salt	Land Surface Elevation (ft msl)	Cap-Rock Thickness (ft)	Aquifer at Dome Top	Production		Storage Caverns	Cap-Rock Brine Disposal	Topographic Relief (ft)
								Sulfur	Salt or Brine			
1	ALLEN	BRAZORIA	760	1,380	5	620	Chicot	No	No	No	No	0
2	ARRIOLA	HARDIN	3,930	3,930	40	0	Deep	No	No	No	No	5
3	BARBERS HILL	CHAMBERS	350	1,000	75	650	Chicot	No	Yes	Yes	Yes	55
4	BATSON	HARDIN	1,080	1,400	80	320	Evangeline	No	No	No	No	-4
5	BIG CREEK	FORT BEND	450	600	80	150	Chicot	Yes	No	No	No	5
6	BIG HILL	JEFFERSON	200	1,300	30	1100	Chicot	No	No	Yes	Yes	30
7	BLUE RIDGE	FORT BEND	143	230	85	87	Chicot	No	Yes	Yes	Yes	20
8	BOLING	WHARTON	380	975	75	595	Chicot	Yes	No	Yes	Yes	-44
9	BRENHAM	AUSTIN	700	1,834	300	1134	Jasper	No	No	Yes	No	-30
10	BRYAN MOUND	BRAZORIA	680	1,067	10	387	Chicot	Yes	Yes	Yes	No	12
11	CEDAR POINT	CHAMBERS	10,300	10300	0	0	Deep	No	No	No	No	0
12	CLAM LAKE	JEFFERSON	8,200	8,200	0	0	Deep	No	No	No	No	0
13	CLEMENS	BRAZORIA	600	1,400	13	800	Chicot	Yes	No	Yes	No	-4
14	DAMON MOUND	BRAZORIA	0	530	110	530	Chicot	Yes	No	No	No	86
15	DANBURY	BRAZORIA	5,000	5,000	20	0	Jasper	No	No	No	No	0
16	DAVIS HILL	LIBERTY	800	1,200	100	400	Evangeline	No	No	No	No	165
17	ESPERSON	LIBERTY	6,000	6,000	55	0	Deep	No	No	No	No	0
18	FANNETT	JEFFERSON	740	2,000	15	1260	Chicot	Yes	No	Yes	Yes	5
19	GULF	MATAGORDA	825	1,100	20	275	Chicot	Yes	No	No	No	20
20	HANKAMER	LIBERTY	7,535	7,580	35	45	Deep	No	No	No	No	0
21	HAWKINSVILLE	MATAGORDA	95	600	10	505	Chicot	No	No	No	No	0
22	HIGH ISLAND	GALVESTON	150	1,100	20	950	Chicot	Yes	No	No	No	20
23	HOCKLEY	HARRIS	76	1,000	170	924	Chicot	No	Yes	No	No	-20
24	HOSKINS MOUND	BRAZORIA	574	1,070	20	496	Chicot	Yes	No	No	No	25
25	HULL	LIBERTY	260	600	75	340	Chicot	No	No	Yes	Yes	14
26	HUMBLE	HARRIS	700	1,200	75	500	Chicot	No	No	No	No	-9
27	LONG POINT	FORT BEND	550	930	75	380	Chicot	Yes	No	No	No	8
28	LOST LAKE	CHAMBERS	3,275	5,430	5	2155	Evangeline	No	No	No	No	0
29	MANVEL	BRAZORIA	11,400	11,400	55	0	Deep	No	No	No	No	0
30	MARKHAM	MATAGORDA	1,350	1,420	55	70	Chicot	No	Yes	Yes	Yes	0
31	MOSS BLUFF	LIBERTY	625	1,100	35	475	Chicot	Yes	No	Yes	Yes	22
32	MYKAWA	HARRIS	7,100	7,100	50	0	Deep	No	No	No	No	0
33	NASH	FORT BEND	620	950	55	330	Chicot	Yes	No	No	Yes	5
34	NORTH DAYTON	LIBERTY	580	800	85	220	Chicot	No	No	Yes	Yes	-2
35	ORANGE	ORANGE	7,120	7,120	10	0	Deep	No	No	No	No	0
36	ORCHARD	FORT BEND	285	369	110	84	Chicot	Yes	No	No	Yes	-5

Table 2-2, continued

Map Number (See Figure 2-8)	Salt Dome Name	County or Parish	Depth (ft) to Cap Rock	Depth(ft) to Salt	Land Surface Elevation (ft msl)	Cap-Rock Thickness (ft)	Aquifer at Dome Top	Production		Storage Caverns	Cap-Rock Brine Disposal	Topographic Relief (ft)
								Sulfur	Salt or Brine			
37	PIERCE JUNCTION	HARRIS	730	950	60	220	Chicot	No	Yes	Yes	Yes	8
38	PORT NECHES	ORANGE	6,950	6,950	5	0	Deep	No	No	No	No	0
39	RACCOON BEND	AUSTIN	11,000	11,000	150	0	Deep	No	No	No	No	0
40	SAN FELIPE	WALLER	3,160	4,200	120	1040	Deep	No	No	No	No	0
41	SARATOGA	HARDIN	1,500	1,900	90	400	Evangeline	No	No	No	No	8
42	SOUR LAKE	HARDIN	500	720	50	220	Chicot	No	No	Yes	No	10
43	SOUTH HOUSTON	HARRIS	4,406	4,406	35	0	Jasper	No	No	No	No	0
44	SOUTH LIBERTY	LIBERTY	320	480	20	160	Chicot	No	No	No	No	-16
45	SPINDLETOP	JEFFERSON	700	1,200	20	500	Chicot	Yes	Yes	No	No	12
46	STRATTON RIDGE	BRAZORIA	850	1,308	10	458	Chicot	No	Yes	Yes	No	13
47	SUGARLAND	FORT BEND	3,450	4280	65	830	Jasper	No	No	No	No	-10
48	THOMPSON	FORT BEND	9,315	9,315	55	0	Deep	No	No	No	No	0
49	WEBSTER	HARRIS	10,500	10,500	30	0	Deep	No	No	No	No	0
50	WEST COLUMBIA	BRAZORIA	740	790	30	50	Chicot	No	No	No	No	-15
51	BIG LAKE	CAMERON	12,910	12,910	3	0	Deep	No	No	No	?	?
52	BLACK BAYOU	CAMERON	881	1,035	3	154	Chicot	No	No	Yes	?	?
53	CALCASIEU LAKE	CAMERON	1,490	2,369	3	879	Chicot	No	No	No	?	?
54	CAMERON MEADOWS	CAMERON	4,770	4,770	3	0	Evangeline	No	No	No	?	?
55	EAST HACKBERRY	CAMERON	3,000	3,330	3	330	Evangeline	No	No	Yes	?	?
56	EDGERLY	CALCASIEU	3,800	3,898	10	98	Jasper	No	No	No	?	?
57	IOWA	CALCASIEU	7,902	7,902	20	0	Deep	No	No	No	?	?
58	LOCKPORT	CALCASIEU	8,160	8,160	3	0	Deep	No	No	No	?	?
59	NORTH STARKS	CALCASIEU	9,031	9,031	40	0	Deep	No	No	No	?	?
60	ROANOKE	JEFFERSON DAVIS	11,585	11,585	25	0	Deep	No	No	No	?	?
61	STARKS	CALCASIEU	1,157	1,538	30	381	Chicot	Yes	Yes	No	?	?
62	SULPHUR MINES	CALCASIEU	390	1,460	5	1070	Chicot	Yes	Yes	Yes	?	?
63	SWEET LAKE	CAMERON	8,560	8,560	3	0	Deep	No	No	No	?	?
64	VINTON	CALCASIEU	384	700	3	316	Chicot	No	No	No	?	?
65	WELSH	JEFFERSON DAVIS	6,315	6,315	20	0	Deep	No	No	No	?	?
66	WEST HACKBERRY	CAMERON	1,200	1,790	3	590	Chicot	No	Yes	Yes	?	?
67	WOODLAWN	JEFFERSON DAVIS	10,726	10,726	30	0	Deep	No	No	No	?	?

### 2.2.2.2 Natural Resources

Salt domes provide a variety of natural resources. Structural deformation and cap rock formation have created prolific petroleum reservoirs. Oil and gas are trapped in uplifted strata surrounding or overlying salt domes and in the cap rock itself. In addition to petroleum, salt from the salt stock and sulfur from the cap rock are the main commodities derived from Gulf Coast salt domes in Texas (Table 2-2). Salt is recovered from domes by room and pillar mining and also by dissolution and production through brine wells. Sulfur is also produced through wells. The cap rock is injected with hot water to melt the sulfur, which has a low melting point (245°F), and then molten sulfur and water are produced to the surface.

Salt domes also provide space for storage and disposal (Seni and others, 1985). Solution-mined caverns in the salt stock have been created both for brine production and for storage of various petroleum products, most commonly liquefied petroleum gas (LPG). The volume of some storage caverns exceeds ten million barrels. Storage cavern use has expanded greatly since the 1960's. Crude oil for the U.S. Strategic Petroleum Reserve is stored in caverns at Bryan Mound and Big Hill salt domes. Cavern construction creates large volumes of concentrated brine, and permeable zones in cap rocks are commonly used for brine disposal (Seni and others, 1984c). The potential for disposal and isolation of chemical and radioactive wastes in salt dome caverns in Texas has been evaluated but not put into practice (Seni and others, 1984a).

Resource development and production can create geologic and hydrologic instabilities around salt domes (Seni and others, 1985). Land-surface subsidence, sometimes involving catastrophic collapse and sinkhole formation, is common where large amounts of sulfur, salt, and/or petroleum have been extracted from the salt dome (Mullican, 1988) (Table 2-2). Spectacular examples of surficial collapse and sinkhole formation related to sulfur production have occurred at Boling and Orchard salt domes (Mullican, 1988). More recently (2008), a large sinkhole abruptly formed over Hull salt dome in the town of Daisetta in Liberty County (Figure 2-14). Although sulfur has not been extracted there, Hull salt dome has a long-term history of drilling for oil and gas. The exact cause of the Daisetta sinkhole, however, has not yet been determined (Horswell, 2009).

Anthropogenic sources of aquifer contamination at salt domes include cap-rock brine disposal and storage facility failure. High-volume brine disposal elevates cap rock fluid pressures in shallow intervals laterally adjacent to freshwater sands, reversing pre-development hydraulic gradients and creating the potential for aquifer contamination (Hamlin and others, 1988). Petroleum storage cavern facilities have failed and leaked product into surrounding freshwater sands (Seni and others, 1984b, 1985). Barbers Hill salt dome has the greatest concentration of underground storage caverns in the world and historically has been the site of high-volume cap-rock brine disposal (Figures 2-15, 2-16). Gas storage and transportation facilities are concentrated at Barbers Hill, which is located 20 miles east of Houston, and numerous accidents have occurred, the most recent being in early 2011 (Fowler, 2011). Accidents at salt dome cavern storage operations usually involve failures of well casing strings or surface facilities; the caverns themselves have been remarkably stable (Miyazaki, 2009). The hydrogeology of Barbers Hill salt dome is described in more detail in subsequent sections of this chapter.

### **Hydrogeologic Units**

A salt dome in the Gulf Coast Aquifer forms a complex system of hydrogeologic units. The salt stock is a cylindrical vertical aquiclude. The cap rock rests on the salt stock like an inverted cup. Cap rocks are essentially karstic aquifers whose hydrodynamic properties are controlled by fracturing and dissolution. Irregularly distributed networks of vuggy to cavernous porosity are common in cap rock. Drillers call these networks “lost-circulation zones” because of the difficulty of establishing drilling-fluid circulation in wells penetrating cavernous intervals. These are also the intervals favored for brine disposal because they readily accept high injection rates. However, cap rock also includes areas composed of dense calcite and anhydrite, which have low hydraulic conductivity.

The salt stock and cap rock are encased in interbedded sandy aquifers and muddy aquitards. Even though fine-grained, muddy layers become more abundant with proximity to a salt dome, owing to topographic effects previously discussed, sandy layers commonly overlie domes and locally contact the cap rock surface (Figures 2-11, 2-17). In these interbedded sand and mud layers, hydraulic conductivity in the horizontal direction is typically many times greater than it is in the vertical direction. However, the potential for high vertical hydraulic conductivity exists within the zone of structural deformation around the salt dome. Gulf Coast salt domes contact

freshwater sands in the Chicot, Evangeline, and Jasper aquifers, as well as saline-water sands in more deeply buried intervals (Figures 2-11, 2-17, Table 2-2).

### **Groundwater Flow**

In the salt-dome environment, groundwater flow is driven not only by hydraulic-head gradients but also by density gradients. The density gradients arise from the high thermal conductivity of salt and from groundwater salinity variations due to dissolution of the salt itself (Evans and others, 1991). Few studies have reported head and density distributions in the vicinity of Texas coastal salt domes. Work done in East Texas, where salt domes penetrate the Carrizo-Wilcox aquifer, suggests that dome-related uplift creates local recharge areas over some salt-dome crests, but in general regional flow patterns are not affected by the presence of salt domes (Fogg and others, 1983). Studies in Louisiana, where salt domes penetrate the Gulf Coast Aquifer, document upward groundwater flow around deeper dome flanks but downward flow at shallower levels (Evans and others, 1991), although the focus of the Louisiana studies was the interval below the base of freshwater.

At Barbers Hill salt dome, which penetrates Evangeline and Chicot freshwater sands in Chambers County, head measurements and pumping tests were conducted in the cap rock aquifer, which is saturated with dense brine (Hamlin and others, 1988). Barbers Hill salt dome has a history of intense development, including oil production, salt-cavern storage, and cap rock brine disposal. Water-level data are available from cap rock disposal wells. When the effects of density variations were normalized, a hydraulic gradient directed radially outward and upward from the cap rock was revealed. The present magnitude and direction of this hydraulic gradient is attributable both to lowering of fluid pressures in the Chicot and the Evangeline aquifers by long-term pumping in the Houston area and to elevation of fluid pressures in the cap rock by high-volume brine disposal.

Controlled brine injection tests at Barbers Hill salt dome indicated that the cap rock is a single integrated aquifer with leaky vertical and lateral boundaries. Because of the arched shape of the cap rock, the vertical boundary corresponds to vertical and lateral contacts with freshwater sands, and the lateral boundary is the lower edge down the dome flanks that is in contact with deeper saline-water sands (Figures 2-9, 2-17). Within the cap rock, water levels stabilized in

observation wells during a long-term brine injection test, showing that groundwater must be exiting the cap rock (Figure 2-18). During the brine injection test, however, water levels were not monitored in nearby Chicot and Evangeline water wells, so the exact destination of leaking cap rock brines was not documented.

Development of both fresh groundwater and salt-dome resources has increased the potential for contamination of shallow aquifers. In pre-development steady-state groundwater flow systems, salt-dome related contamination remained localized by high freshwater heads in surrounding sands and the tendency for high-density brines to flow downward. The combination of lowered heads in the Gulf Coast Aquifer and increased heads in cap rocks has created hydraulic gradients directed outward from the salt dome toward adjacent freshwater sands. Resource extraction and leakage of stored petroleum product have further perturbed the natural system. Most of the available evidence for salt-dome-related contamination of the Gulf Coast Aquifer is at least 20 years old. More recent hydraulic and hydrochemical data, including data collected periodically through time, are needed for proper risk analysis and for a more comprehensive understanding of shallow groundwater flow near salt domes.

Numerical modeling of groundwater flow systems around salt domes has proved challenging owing to the complications of extreme salinity and density variations and complex boundary conditions (Konikow and others, 1997). Fogg and others (1983) modeled groundwater flow in the Carrizo-Wilcox aquifer around a salt dome but without explicitly including the dome itself or salinity variations. Their model helped identify recharge and discharge areas and flow paths in freshwater aquifer sands relative to the position of the salt dome, so that the movement of potential dome-related contaminants might be predicted. Their model also showed the importance of sand-body distribution and interconnection as controls on flow near salt domes. Hamlin and others (1988) modeled the cap rock aquifer at Barbers Hill salt dome, using the results of controlled brine injections tests, but did not include the surrounding Chicot and Evangeline sands or salinity/density variations. Nevertheless, their model accurately reproduced water-level measurements and demonstrated that the cap rock boundaries are leaking. Models of groundwater flow around Gulf Coast salt domes in Louisiana, which explicitly include both the salt dome and salinity/density variations, emphasize the importance of density-driven flow

(Evans and others, 1991). The Louisiana models show that salt dissolved at the dome crest is carried down the dome flanks below the zone of freshwater.

### **2.2.2.3 Groundwater Chemistry**

Hydrochemical patterns in groundwater near salt domes provide information about flow of dome-related fluids into surrounding freshwater aquifers. The most commonly available data for measuring groundwater salinities in the near-dome environment are geophysical logs from oil and gas wells, because an empirical relationship can be established between groundwater salinity and electrical conductivity (Jones and Buford, 1951) and because most salt domes have been densely drilled in the quest for petroleum. Using geophysical logs, anomalously high salinities in shallow sands were documented near salt domes in Chambers, Fort Bend, and Jefferson counties (Wesselman, 1971, 1972).

At Barbers Hill salt dome, Hamlin and others (1988) used closely spaced well logs to map individual sand bodies and groundwater salinities near the dome, revealing a complicated pattern of vertical and lateral salinity variation (Figure 2-17). In one lower Chicot aquifer sand, a plume of high-salinity groundwater extends away from the salt dome in the direction of regional groundwater flow (Figure 2-19). Similar saline plumes extending away from salt domes in the direction of groundwater flow have been documented in the Carrizo-Wilcox aquifer in East Texas (Fogg and others, 1983) and in Germany (Klinge and others, 2002).

Chemical and isotopic analyses of groundwater are less abundantly available than are geophysical logs but can be used to reveal both fluid sources and flow patterns. Banga and others (2002) used multi-element chemistry and isotopic tracers to document vertical flow patterns in deep sandstones (below freshwater) around South Liberty salt dome in Liberty County, showing that oil field brines near the salt dome are a mixture of shallow meteoric waters and deep formation waters. The presence of a meteoric component in deep brines indicates downward flow along the flanks of the salt dome. The implication of the South Liberty salt dome study is that shallow fresh groundwater flows across the top of the salt dome, dissolves salt, becomes increasingly dense, and then flows downward along the dome flanks driven by a density gradient.

The evidence for dissolution of salt dome minerals in shallow groundwater is conclusive. Shallow salt domes extend well into the zone of freshwater and are surrounded laterally and vertically by Gulf Coast Aquifer sands. As salt dissolves at the dome crest, an insoluble residue accumulates, forming the cap rock. Within the cap rock itself, chemical reactions occur that require the presence of low-temperature, low-salinity groundwaters (Kyle and Price, 1986). Geophysical logs have been used to identify high-salinity plumes within otherwise freshwater sands near several Gulf Coast salt domes and to map actual sand/dome contacts (Wesselman 1971, 1972; Hamlin and others, 1988). Indeed, dissolution of salt domes by groundwater has been documented, and the amount of salt removed has been quantified (Seni and Jackson, 1984; Bruno and Hanor, 2003).

Although salt actively goes into solution at the crests of shallow salt domes, most of the high-salinity groundwater thus formed flows downward driven by density gradients. Recent studies document downward flow along salt-dome flanks and the control of faults and sand distribution on flow paths (Banga and others, 2002; Bruno and Hanor, 2003). Although upward flow occurs in deep zones below the base of freshwater (Evans and others, 1991), upward movement and mixing of dense saline groundwater from deep zones into the low-density freshwater zones appear unlikely.

### **2.3 Depositional Systems**

A depositional system is a three-dimensional body of sediment deposited in a contiguous suite of process-related sedimentary environments (Fisher and McGowen, 1967). Each sedimentary environment produces specific genetic facies (Figure 2- 20). Neogene Formations of the onshore northwest GOM coastal zone, which includes the Gulf Coast Aquifer, are mainly composed of nonmarine alluvial (fluvial) depositional systems. Because Miocene through Quaternary coastal plains had similar shoreline trends, climate gradients, physiography, and sediment source areas, Quaternary depositional systems that are exposed at the surface provide a good analog for underlying Neogene coastal plain depositional systems (Galloway, 1981).

The Quaternary coastal plain of Texas encompasses a mosaic of fluvial systems of various types, sizes, and sediment composition (Morton and McGowen, 1980; Galloway, 1981; Blum and Price, 1998; Anderson and Fillon, 2004) (Figure 2-21). Extrabasinal rivers have large drainage



basins that extend well beyond the coastal plain, whereas basin-fringe and intrabasinal rivers have drainage basins marginal to and within the coastal plain. Extrabasinal rivers have persistently occupied the major embayments and still do so today; the Rio Grande, Houston, and Mississippi embayments are occupied by the Rio Grande, Colorado/Brazos, and Mississippi rivers, respectively. The point of entry of an extrabasinal river onto the coastal plain is stable owing to valley entrenchment across the slightly uplifted margin of the coastal zone (Winker, 1979). Basinward from the entry point, fluvial systems are free to migrate laterally, constructing alluvial aprons composed of sand-rich channel-fill facies and mud-rich floodplain facies (3- 21). In a fluvial channel, the proportion of bed load (sand and gravel) to suspended load (silt and clay) influences channel morphology and resulting sand-body geometry (Schumm, 1977). Bed-load channel systems form broad belts of sandstone with good lateral connectivity, whereas mixed- and suspended-load channel systems are more lenticular and isolated in mud-rich floodplain facies (Galloway, 1981). Superposition of channel systems in extrabasinal rivers results in sand bodies that are thicker than original channel depths.

Quaternary alluvial aprons grade basinward into deltaic and shore-zone depositional systems. On the modern Texas Coastal Plain, sand-rich deltaic headlands are constructed by major extrabasinal rivers in the Rio Grande and Houston embayments, while basin-fringe and intrabasinal rivers feed bay-head deltas on the San Marcos arch (Figure 2-21). This pattern persisted throughout the Neogene with some important exceptions (see Section 2.4, Depositional History). Bay, lagoon, barrier island, and shelf depositional systems fringe the onshore and near-offshore parts of the northwest GOM coastal zone. Most transported sediment bypasses these coastal plain systems to be stored permanently in shelf-margin and continental slope depositional systems (Galloway and others, 2000). Neogene shelf-margin and slope systems, however, are located offshore under the modern continental shelf and thus are not part of the Gulf Coast Aquifer.

## **2.4 Depositional History**

Cenozoic sediments of the northwest GOM are monotonous sequences of interbedded sandstones and shales that lack distinctive lithostratigraphic units of regional extent (Galloway and others, 1991). Stratigraphic subdivision relies on a combination of: 1) biostratigraphic zonation; 2) depositional models based on Quaternary examples; and 3) regionally cyclic depositional

episodes (Galloway and others, 2000). Biostratigraphic zonation is based primarily on extinction points of foraminifera (fossil protozoa) and other marine microfossils (Galloway and others, 1991; Lawless and others, 1997; Fillon and Lawless, 2000). Because marine fossils are not available in alluvial sediments, stratigraphic subdivision typically is extended updip to outcrop using lithologic boundaries, well log correlation techniques, and limited nonmarine (vertebrate faunas) biostratigraphy (Tedford and Hunter, 1984; Baskin and Hulbert, 2008; Lundelius, 1972).

A depositional episode is a period of focused deposition and progradation of the shoreline followed by nondeposition and transgression (marine flooding) of the coastal plain (Galloway and others, 1991, 2000). The physical product of a depositional episode is a genetic stratigraphic sequence (Galloway, 1989a). At any one time, active deposition is localized, while adjacent areas receive little or no sediment. Thus, a genetic stratigraphic sequence forms a stratigraphically and geographically distinct body of sediment bounded by surfaces of transgression or nondeposition (Frazier, 1974; Galloway, 1989a). The location of deposition (depocenter) shifts through time owing to geographic variations in sediment supply, which are controlled by tectonic events in the sediment source area (Winker, 1982). The timing and cyclicity of progradational and transgressive events depends upon the interplay of sediment supply, subsidence, and sea-level change (Galloway, 1989b). In the northwest GOM, genetic stratigraphic sequences typically consist of one or more major extrabasinal fluvial systems that supply progradational deltaic systems. Smaller intrabasinal fluvial systems and interdeltic shore-zone systems separate deltaic headlands (Galloway and others, 1991) (Figure 2-21).

Early Cenozoic (Paleogene, Table 2-1) depositional episodes in the northwest GOM were responses first to mountain building in the southern Rocky Mountains and later to explosive volcanism in West Texas and Mexico (Winker, 1982; Morton and Galloway, 1991; Galloway, 2005). Large volumes of sand, silt, and clay were delivered to the northwest GOM. In response, extrabasinal fluvial-deltaic systems developed first in the Houston embayment and then in the Rio Grande embayment (Figure 2-22). Abundant sediment supply in the Paleogene overwhelmed sea-level fluctuations and controlled sequence development (Morton and Galloway, 1991). In the Neogene (Miocene-Pliocene), however, continental glaciers began forming in Antarctica (Fillon and Lawless, 2000), and the resulting high-amplitude sea-level fluctuations began exerting greater influence on sequence formation (Galloway and others, 1986;

Morton and others, 1988) (Figure 2-23). Miocene genetic stratigraphic sequences are bounded by transgressive surfaces that can usually be related to glacio-eustatic highstands (global sea-level rises attributable to melting glaciers), but tectonic activity in the source areas was still controlling locations of sediment input into the northwest GOM. Tectonic development of the Rio Grande Rift in New Mexico disrupted drainage systems feeding the Rio Grande and Houston embayments so that large extrabasinal fluvial systems began shifting northeast into the Mississippi embayment (Winker, 1982) (Figure 2-22). Uplift of the Edwards Plateau along the Balcones Fault Zone in Central Texas supplied abundant Cretaceous calcareous detritus to smaller Miocene fluvial systems on the Texas Coastal Plain (Galloway and others, 1986; Morton and others, 1988). The principal middle-late Miocene fluvial-deltaic system in Texas was located on the San Marcos Arch (Figure 2-22). During the Plio-Pleistocene (Table 2-1), tectonic quiescence and high-frequency glacio-eustatic fluctuations (this time from northern hemisphere glaciation) resulted in multiple cross-cutting and superimposed alluvial valley fills and preservation of thin sequences on the Texas Coastal Plain (Blum and Price, 1998).

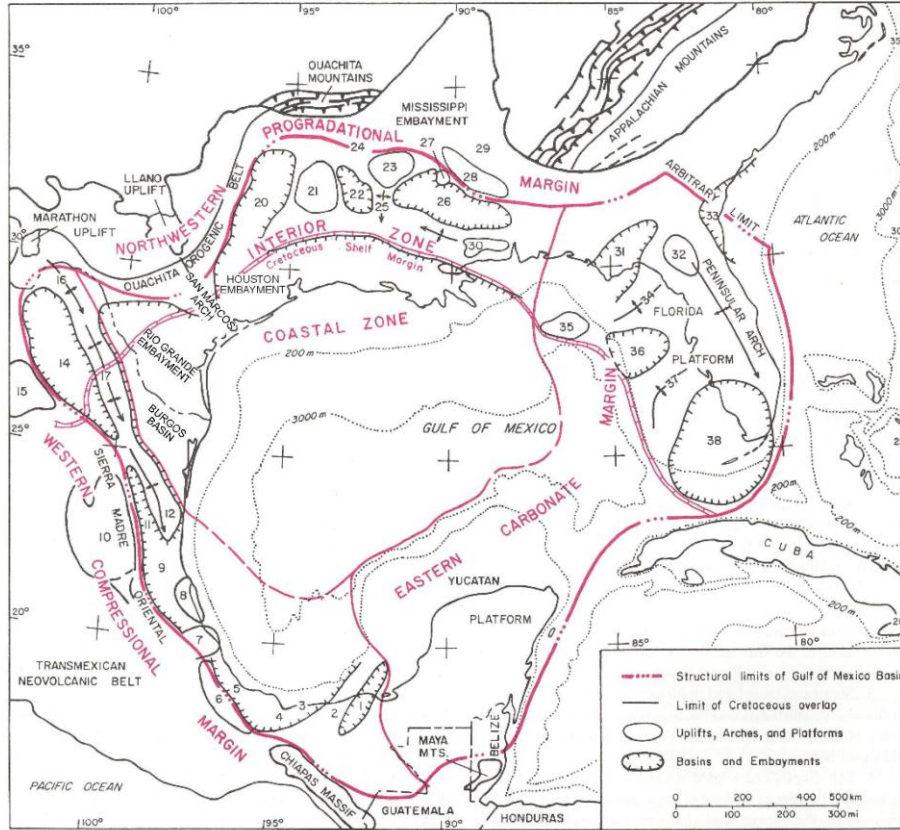


**Figure 2-1** Map of the Gulf of Mexico basin showing major structural elements and stratigraphic provinces. Modified from Ewing (1991).

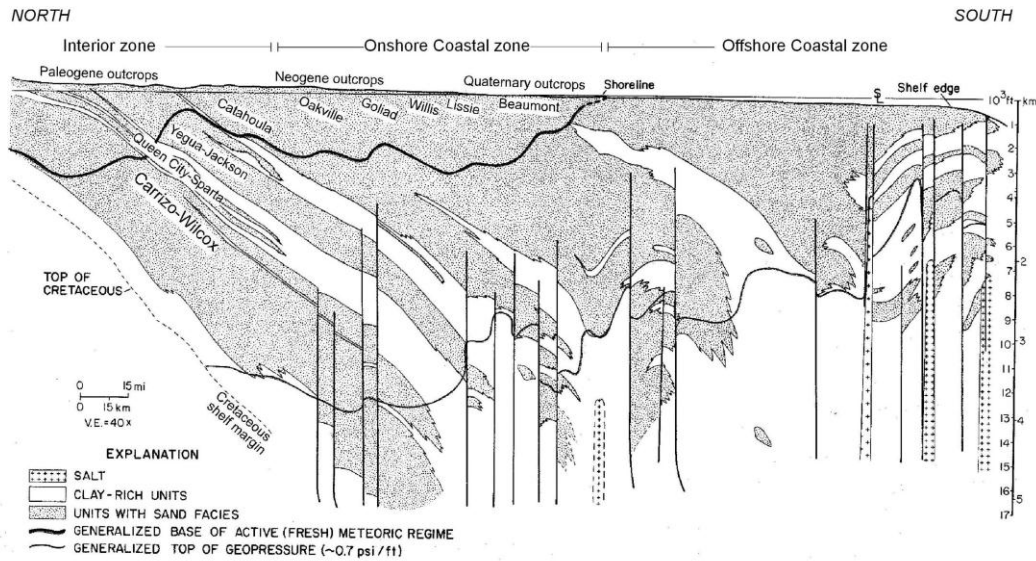


**Figure 2-2** Regional dip-oriented cross section of Cenozoic strata on the northwestern margin of the Gulf of Mexico basin. Modified from Galloway and others (1991) and Sharp and others (1991).

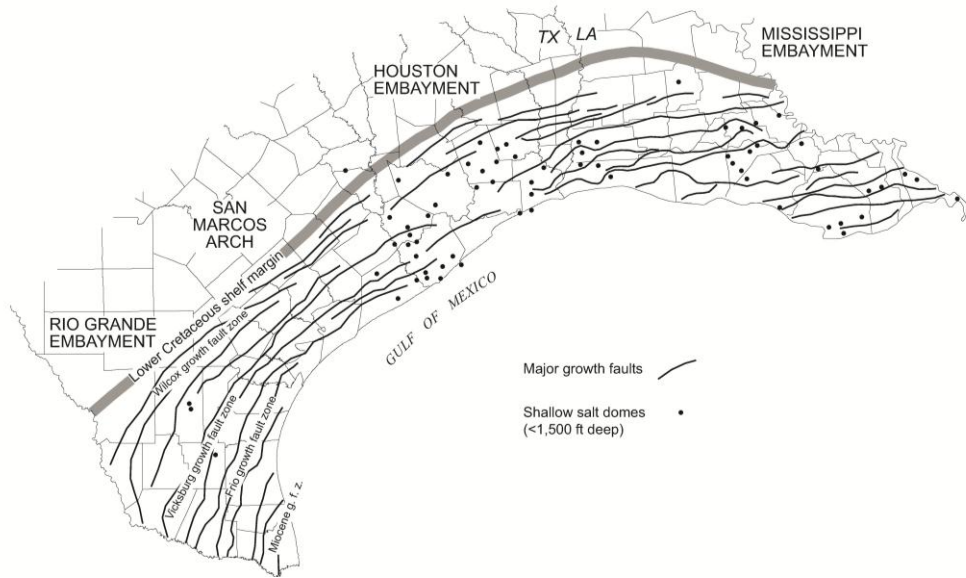


**Figure 2-3** Map showing major growth fault zones and shallow salt domes in the onshore part of the Texas coastal zone. Modified from Ewing (1990) and Hamlin (2006).

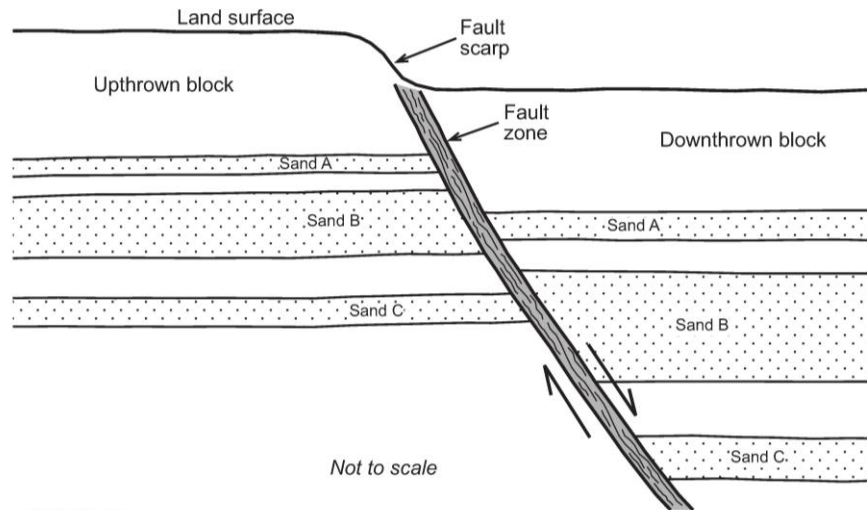


**FIGURE 1**

**Figure 2-4** Schematic cross section showing active surface fault. The fault zone is composed of deformed sediment having high vertical hydraulic conductivity locally. Aquifer sands are offset across the fault and commonly are thicker on the downthrown side owing to greater subsidence and sedimentation there. Modified from Verbeek and Clanton (1979).

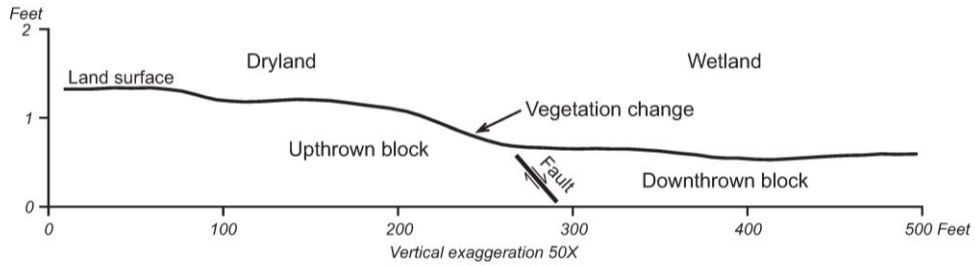


**Figure 2-5** Cross section showing typical surface expression of an active fault. The fault scarp is generally modified by erosion into a subtle topographic step. Vegetation changes near the fault line mark the boundary between dryland on the upthrown block and wetland on the downthrown block. Modified from Verbeek and Clanton (1979).

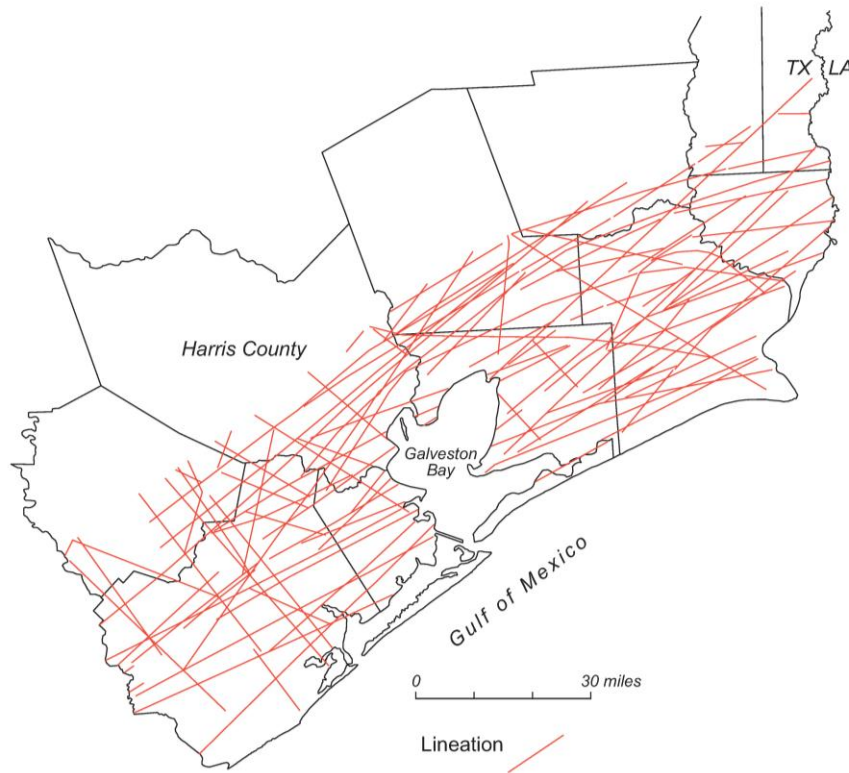


**Figure 2-6** Lination map of the Texas coastal zone in the Houston Embayment area. Lineations are the surface expressions of faults or fractures (Kreitler, 1976). The entire Texas coastal plain is covered by lineations, although only the more coastward lineations are mapped here. Modified from Fisher and others (1972, 1973) and McGowen and others (1976).

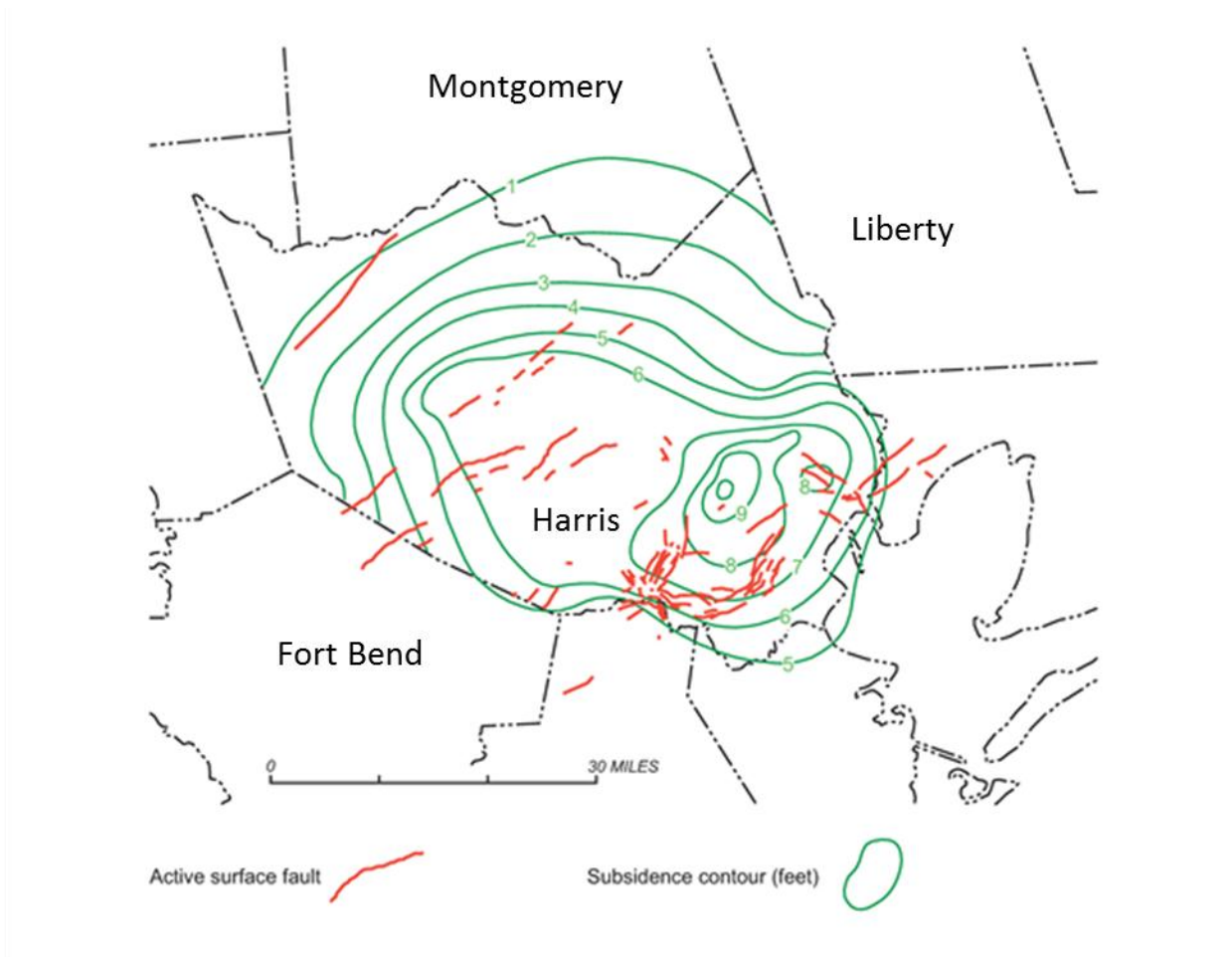


**Figure 2-7** Map of subsidence and active surface faults in the Houston metropolitan area. Modified from Holzer (1984) and Shah and Lanning-Rush (2005).

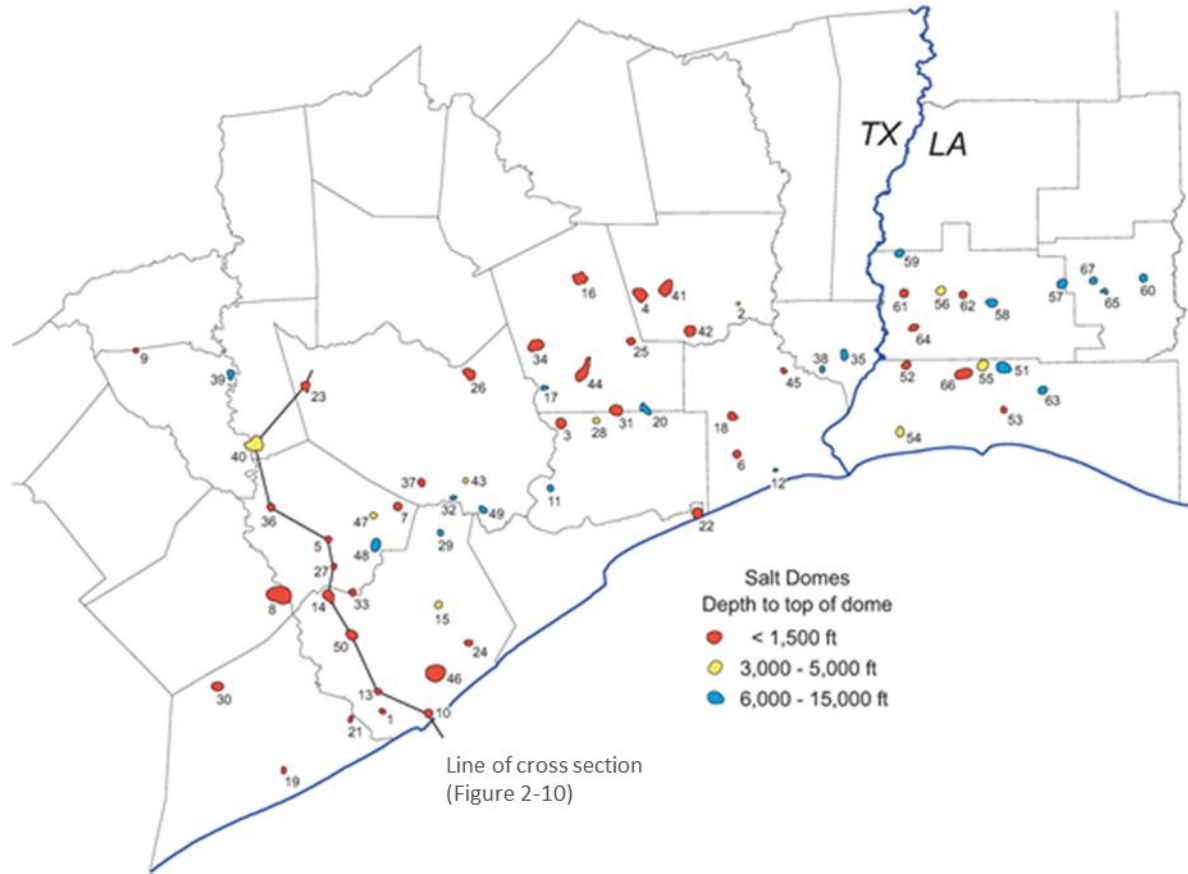


**Figure 2-8** Map showing locations of salt domes in southeast Texas and southwest Louisiana. Approximate dome sizes, shapes, and depths are shown. Individual salt domes identified by number (Table 1).



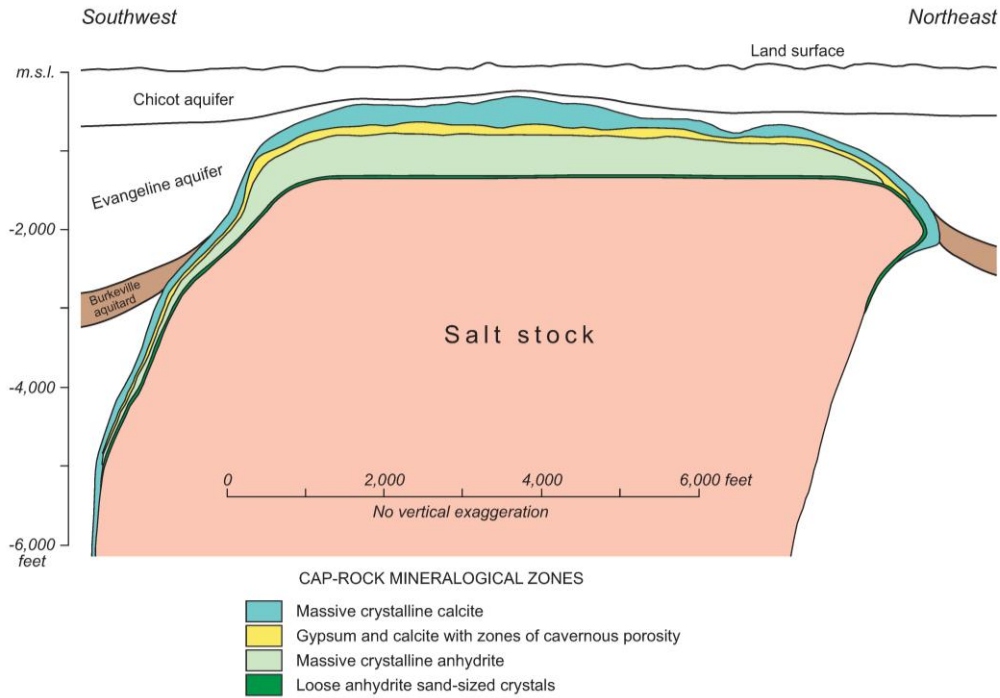


**Figure 2-9** Cross section of Barbers Hill salt dome in Chambers County showing the salt stock, cap rock mineralogical zones, and enclosing hydrostratigraphic intervals (modified from Hamlin and others, 1988). This cross section has no vertical exaggeration (vertical and horizontal scales are equal). Cap-rock layering is generally more complicated than shown here and varies widely among domes.

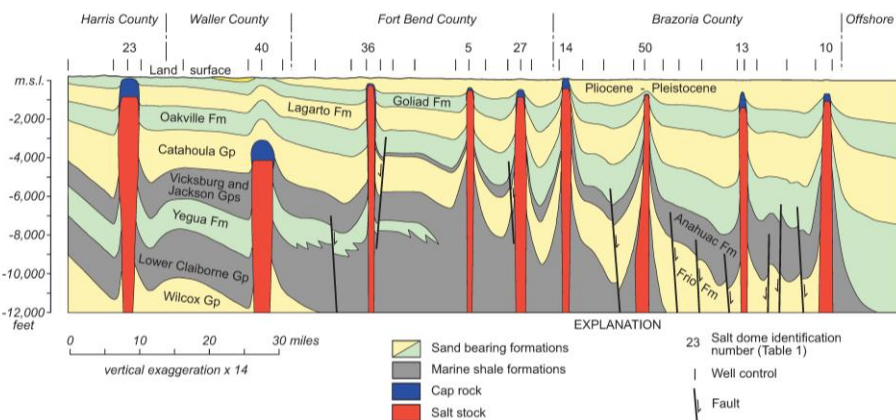


**Figure 2-10** Regional dip-oriented cross section of the upper Texas Gulf Coast showing salt domes and enclosing strata (modified from Hamlin, 1986). Line of section located in Figure 2-8.

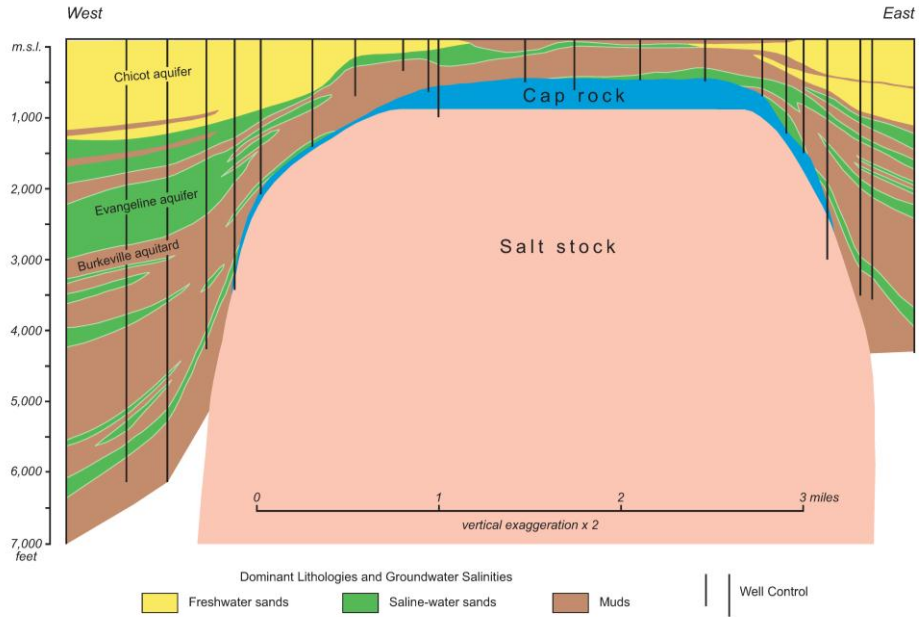


**Figure 2-11** Cross section of Boling salt dome in Wharton County showing salt stock, cap rock, and surrounding sediments (modified from Seni and others, 1985). Freshwater sands surround the dome, but muds and thin saline-water sands overlie the dome. Groundwater salinities are interpreted from resistivity logs (freshwater sands have >20 ohm-m resistivity).

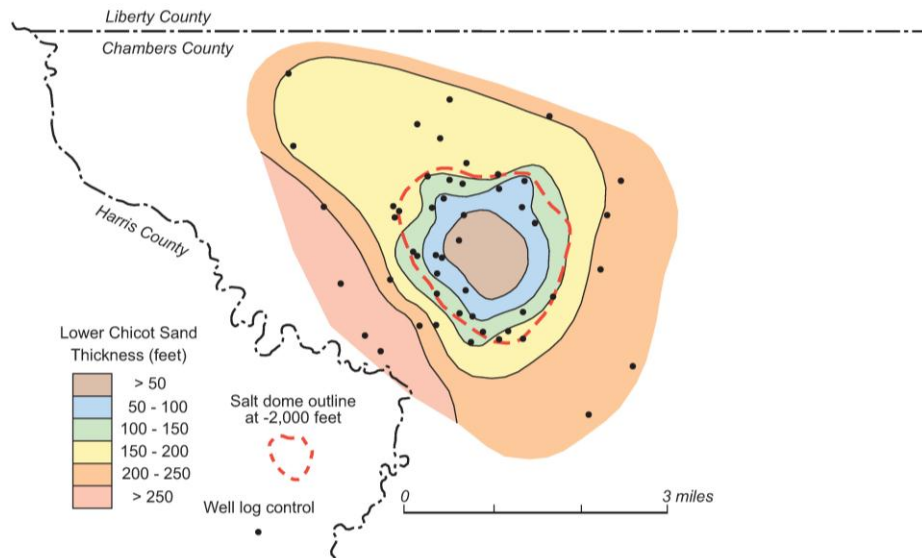


**Figure 2-12** Map of lower Chicot sand thickness around Barbers Hill salt dome (modified from Hamlin and others, 1988). The lower Chicot sand is widespread in the Houston area (Wesselman, 1971, 1972; Baker, 1979).

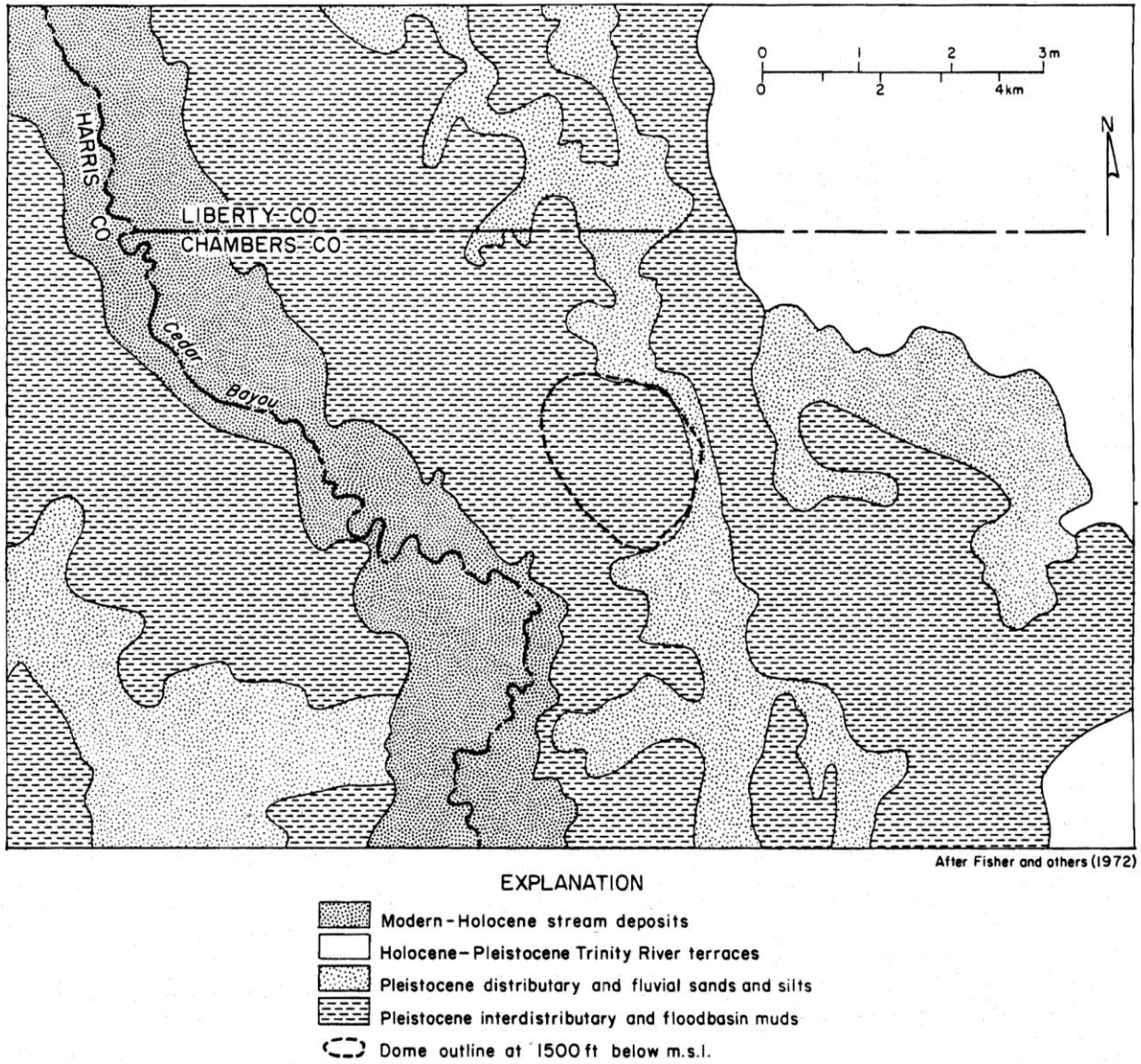


**Figure 2-13** Map of surficial sediments and depositional facies around Barbers Hill salt dome (from Fisher and others, 1972). Pleistocene channel sand follows peripheral low area east of the dome, whereas fine-grained interchannel facies cover the dome crest.



**Figure 2-14** Photograph showing catastrophic collapse and sinkhole that formed over Hull salt dome in 2008 in the town of Daisetta, Liberty County, Texas (from Horswell, 2009).

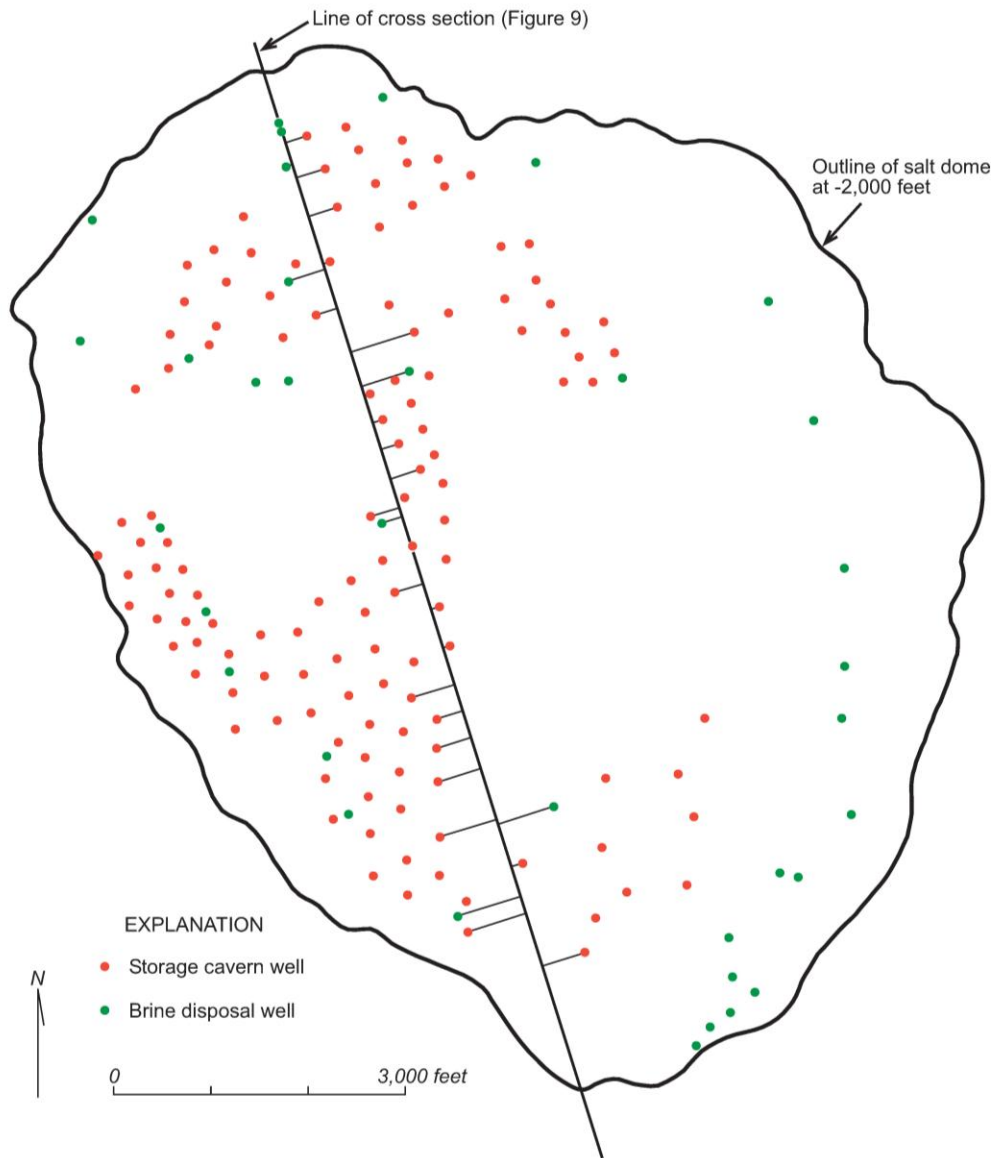


**Figure 2-15** Map of Barbers Hill salt dome showing locations of storage caverns in the salt stock and brine disposal wells in the cap rock as they existed in 1984 (modified from Seni and others, 1984c).

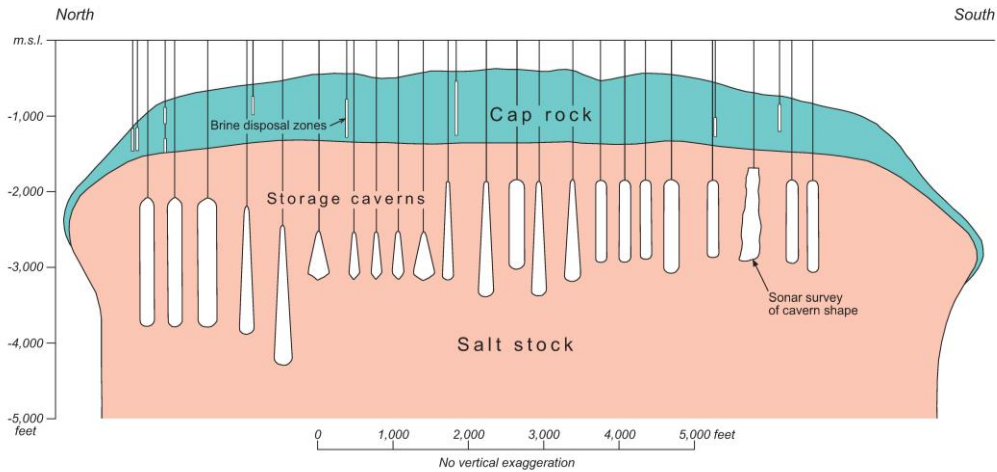


**Figure 2-16** Cross section showing storage caverns and brine disposal wells at Barbers Hill salt dome (modified from Seni and others, 1984c). Line of section located in Figure 8. Storage cavern locations, depths, and dimensions are accurate, but geometric details are generalized. Storage cavern geometries are commonly delineated using sonar, and a sonar survey was available for one cavern on this section (third cavern from the right).

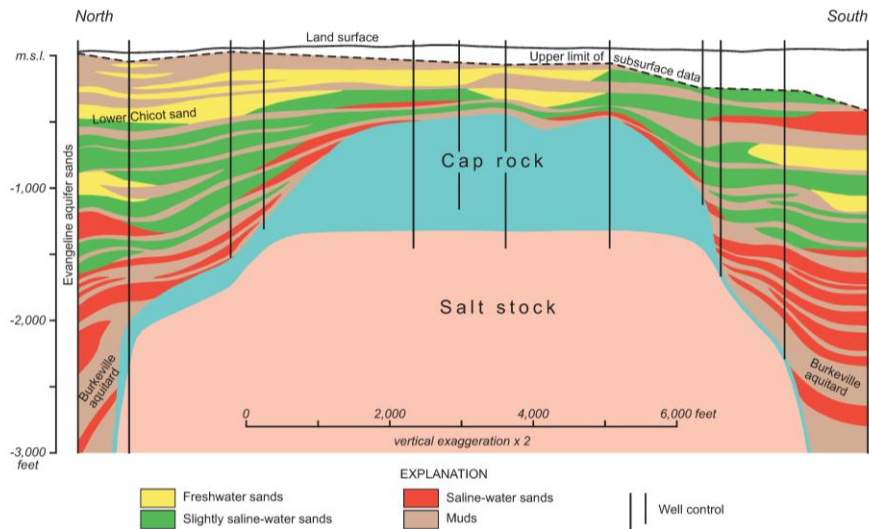


**Figure 2-17** Cross section of Barbers Hill salt dome showing salt stock, cap rock, and surrounding sediments (modified from Hamlin and others, 1988). Groundwater salinities are interpreted from resistivity logs. Sands become thinner and more saline with proximity to the dome. Sand thickness of the lower Chicot sand is shown in Figure 2-12.

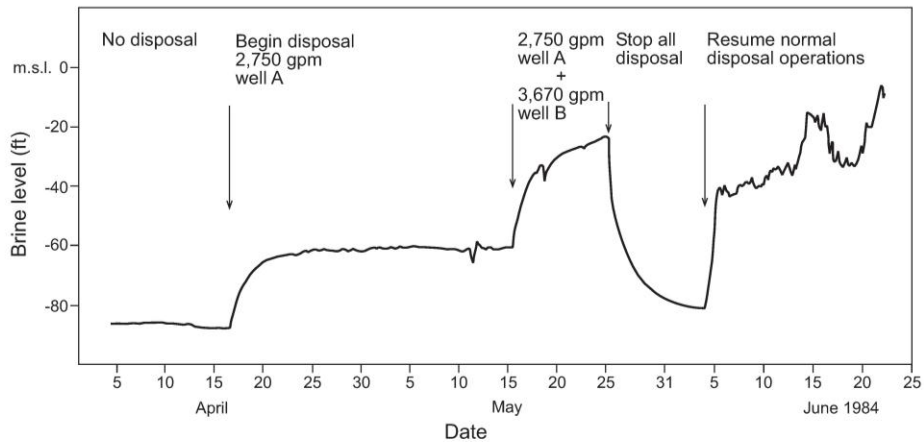


**Figure 2-18** Hydrograph of a long-term cap rock injection test at Barbers Hill salt dome showing brine-level changes in a cap rock observation well during controlled brine disposal in two other cap rock wells (from Hamlin and others, 1988). Water levels in nearby Chicot aquifer and Evangeline aquifer water wells are around 100 feet below sea level or similar to cap rock brine levels when no disposal is occurring. However, water levels in nearby water wells were not monitored during the injection test.

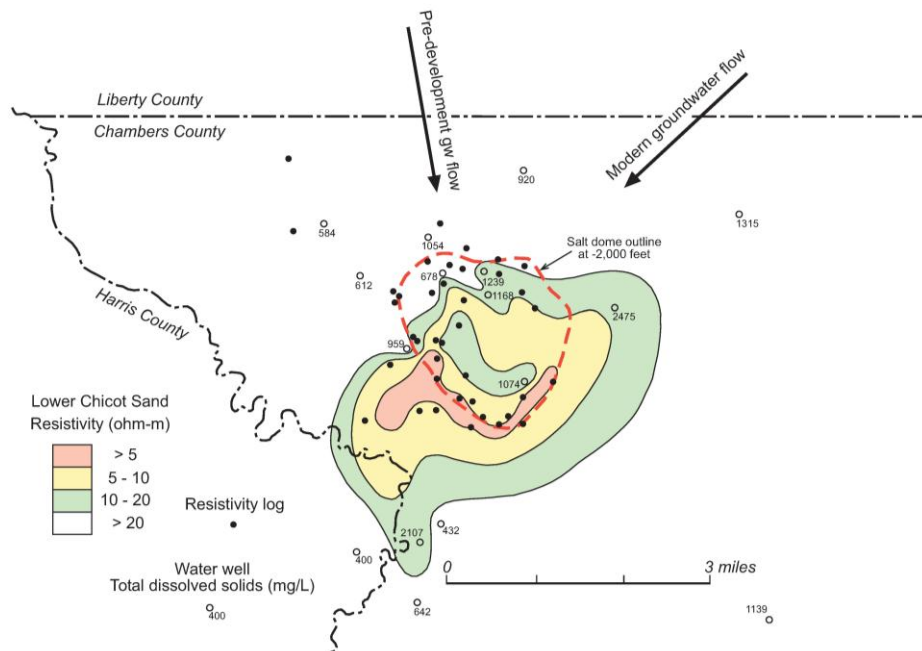


**Figure 2-19** Resistivity map of the lower Chicot aquifer at Barbers Hill salt dome (modified from Hamlin and others, 1988). Water wells completed in this lower Chicot sand are also shown along with total dissolved solids measurements. Low resistivities around the southern and southwestern dome flanks delineate a high-salinity plume extending away from the salt dome in the down-flow direction.

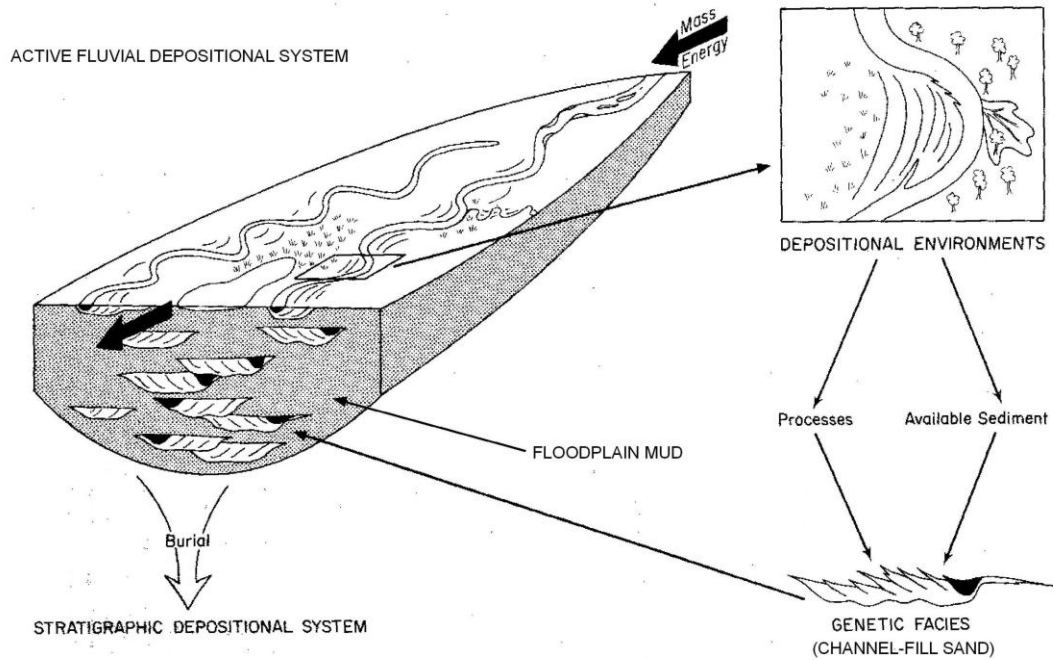


**Figure 2-20** Schematic diagram showing a fluvial depositional system with its component depositional environments and resulting genetic facies. Modified from Galloway and others (1979).

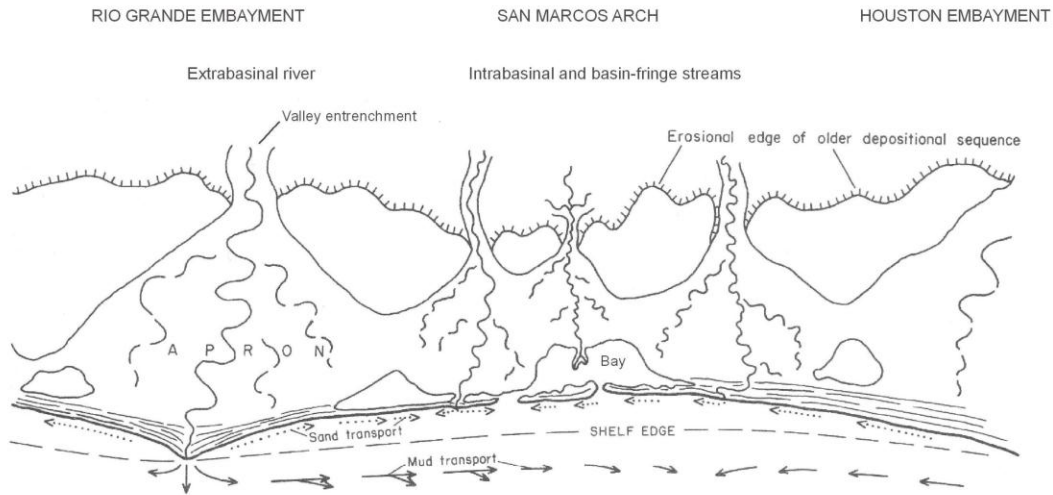


**Figure 2-21** Schematic drawing of Quaternary depositional systems of the Texas Coastal Plain. Modified from Winker (1979) and Galloway and others (1986).



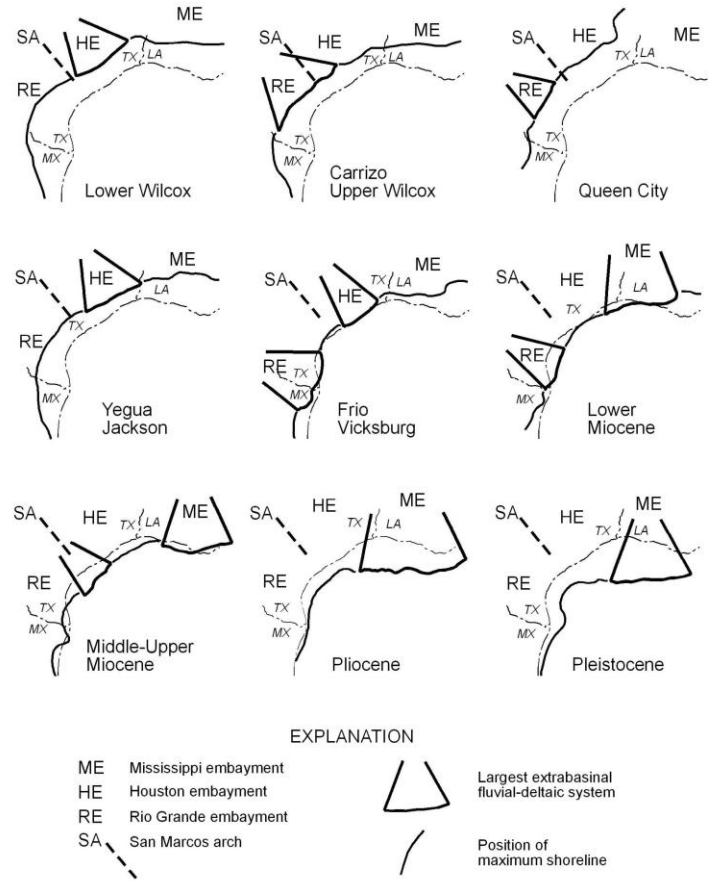


**Figure 2-22** Positions of principal fluvial-deltaic depocenters and interdeltic shorelines for selected depositional episodes, northwest GOM. Modified from Galloway (1989b) and Galloway and others (2000).

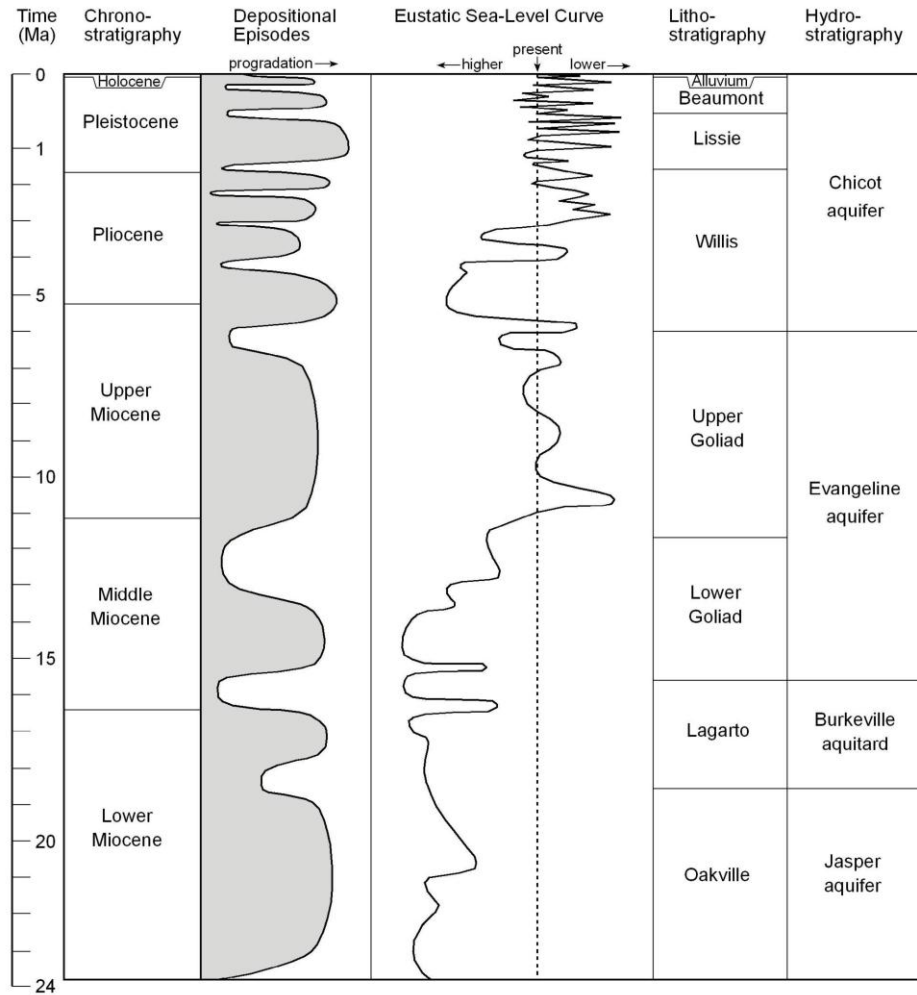


**Figure 2-23** Chronostratigraphic chart of Miocene to Holocene depositional episodes, northwest GOM. Lithostratigraphic and hydrostratigraphic boundaries are approximate. Depositional episodes from Galloway and others (2000) and sea-level curve from Haq and others (1987). Geologic ages in millions of years ago (Ma) from Berggren and others (1995).

*This page intentionally left blank.*

### **3.0 Stratigraphic and Hydrogeologic Framework**

The Gulf Coast Aquifer in Texas encompasses all stratigraphic units above the Vicksburg Formation (Ashworth and Hopkins, 1995; George and others, 2011) (Table 2-1). The lowermost stratigraphic unit is the Catahoula Formation (including the Frio and Anahuac in the deep subsurface), which is an aquitard everywhere except near the outcrop (Wood and others, 1963). In the overlying Fleming Group, the Oakville Sandstone is approximately equivalent to the Jasper Aquifer and the Lagarto Clay to the Burkeville Aquitard (Wesselman, 1967; Baker, 1979) (Figure 2-23). The Goliad, Willis, and Lissie Formations, which contain most of the fresh-water resources in the Gulf Coast Aquifer (Wood and others, 1963), are the focus of this description. The Goliad Formation is approximately equivalent to the Evangeline Aquifer, although the Evangeline includes some underlying Fleming sands locally (Baker, 1979). The Chicot Aquifer comprises all sands between the top of the Evangeline and the land surface (Baker, 1979) (Figure 2-23). Although Pliocene-Pleistocene stratigraphy in the shallow subsurface of the Texas Coastal Plain is complex, the primary components of the Chicot Aquifer are the Willis, Lissie, and Beaumont Formations (Ashworth and Hopkins, 1995; George and others, 2011). In southeast Texas, the Montgomery and Bentley Formations are approximately equivalent to the Lissie Formation (Baker, 1979; Dutton and Richter, 1990).

#### **3.1 Previous Studies**

The earliest geologic studies focused on outcrop description and correlation (Deussen, 1914, 1924; Barton, 1930; Trowbridge, 1932; Plummer, 1932; Price, 1933, 1934; Weeks, 1933, 1945; Doering, 1935, 1956; Bernard and LeBlanc, 1965). Outcrop mapping culminated in the publication by the Bureau of Economic Geology (BEG) of the *Geologic Atlas of Texas (GAT)* (Aronow and Barnes, 1968; Shelby and others, 1968; Proctor and others, 1974; Aronow and Barnes, 1975; Aronow and others, 1975; Brewton and others, 1976a; Brewton and others, 1976b) (Figure 3-1) and the *Environmental Geologic Atlas of the Texas Coastal Zone* (Brown and others, 1976, 1977, 1980; McGowen and others, 1976a,b). These studies demonstrated that outcropping Miocene to Holocene Formations are composed of unconformity-bounded, seaward dipping, nonmarine clastic wedges. In updip areas, each formation erosionally truncates and onlaps the underlying formation (Figure 3-2). Thin erosional remnants, isolated terraces,

onlapping veneers, and Holocene alluvial cover make it difficult to establish regional correlations between outcropping and subsurface stratigraphic intervals (Winker, 1979; DuBar and others, 1991).

Subsurface stratigraphic analysis of the Texas Gulf Coast was originally developed for petroleum exploration but became an essential tool for characterization of aquifer composition, correlation, and structure. Subsurface mapping was initially based on analysis of rock cuttings and fossils produced during the well drilling process. However, by the 1930s, geophysical (electrical) well logs provided a major source of data for formation identification and correlation. Early subsurface studies focused on the stratigraphic and structural framework of Gulf Coast Formations (e.g., Applin and others, 1925; Barton and others, 1933; Bornhauser, 1947, 1958; Williamson, 1959; Murray, 1961). Subsequent studies developed the concepts of depositional systems and facies (e.g., Boyd and Dyer, 1964; Rainwater, 1964; Fisher and McGowen, 1967). More recently, the concepts and techniques of sequence stratigraphy and chronostratigraphic correlation have been used to refine the stratigraphic framework and depositional history of the GOM (Galloway, 1989b; Lawless and others, 1997; Fillon and Lawless, 2000; Galloway and others, 2000; Hernandez-Mendoza and others, 2008). Gulf Coast subsurface stratigraphy, depositional systems, and structure are summarized in a series of well log cross sections published by BEG (Dodge and Posey, 1981; Morton and others, 1985; Galloway and others, 1994).

Subsurface analysis in Texas groundwater studies began early and has been an equal partner with petroleum studies in the development of our understanding of Gulf Coast stratigraphy. Early publications by the Texas Board of Water Engineers and the U.S. Geological Survey (USGS) used well logs to delineate aquifer boundaries and sand distribution in the subsurface (e.g., Rose, 1943; Lang and others, 1950; Jones, 1956). Numerous countywide and regional studies of geology and groundwater resources by the Texas Water Commission (later the Texas Water Development Board) refined aquifer stratigraphy (e.g., Baker, 1964; Wesselman, 1967). Building on stratigraphic interpretations from both petroleum and groundwater resources, Baker (1979) published a series of well log cross sections covering the entire Texas Gulf Coast, which became the standard reference for aquifer stratigraphy in the region.

The USGS conducts regional studies of major aquifer systems for resource evaluation and management. As part of their Regional Aquifer-System Analysis (RASA) Program, the USGS published a series of reports on major aquifer systems across the Gulf Coastal Plain from Texas to Florida (Grubb, 1984, 1987; Ryder, 1988; Weiss, 1992; Hosman, 1996; Williamson and Grubb, 2001; Ryder and Ardis, 2002). These reports assemble hydrogeologic data and interpretations and present the results of numerical simulations. The hydrostratigraphic units developed for the RASA Program, however, have generally not been adopted in recent Texas-based studies. Instead, the Chicot and Evangeline Aquifer designations that were established regionally by Baker (1979) have been retained (e.g., Chowdhury and Turco, 2006; Knox and others., 2006; Young and others, 2010).

A second USGS program, the Source Water Assessment and Protection (SWAP) Program, developed a computer-based data set of surfaces (stratigraphic boundaries) for the Chicot and Evangeline Aquifers. The primary source data set to generate the SWAP surfaces consist of digitized points taken from the surface contours for the Chicot and Evangeline Aquifers found in Carr and others (1985). Carr and others (1985) do not provide control points for these contours, nor do they explain the method used to develop the contours. Thus, the uncertainty associated with the original contours is largely unknown. In developing its SWAP data set, the USGS blended the information from Carr and others (1985) with information from Jorgensen (1975), Baker (1979, 1986), and geologic outcrops mapped on BEG's GAT sheets. The outcrop information provided by the GAT sheets was used to estimate the updip region of the aquifers. The information from Baker (1979, 1986) was used to smoothly transition between the more detailed works of Jorgensen (1975) in the Houston area with the general framework established by Carr and others (1985). The SWAP aquifer surfaces were used in developing conceptual models for TWDB groundwater availability models (GAMs) of the Gulf Coast Aquifer (Chowdhury and Mace, 2003; Chowdhury and others, 2004; Kasmarek and Robinson, 2004). The SWAP data, however, are based on stratigraphic studies conducted in the 1970s and 1980s, which are being superseded by more recent studies using sequence stratigraphic techniques and ties to offshore chronostratigraphy (Knox and others., 2006; Young and others., 2010).

### **3.2 Fleming Group: Oakville and Lagarto Formations**

The Fleming Group of the Texas Coastal Plain is early Miocene in age and comprises the Oakville and Lagarto Formations (Galloway and others, 1986) (Figure 2-23, Table 2-1). The Fleming Group is bounded by regional marine shales in downdip areas and by the bases of massive fluvial sandstones updip. Fleming boundaries were traced updip through the nonmarine interval to outcrop using correlation, projection, lithology, and minor datum changes (Galloway and others, 1986) (Figure 3-3). The lower boundary was delineated by correlating between the Anahuac Shale downdip and the base of massive Oakville sandstone updip and in outcrop, and the upper boundary was delineated by similarly connecting the Amphistegina B Shale downdip with the base of massive Goliad sandstone updip. The Oakville and Lagarto Formations together compose a major fluvial-deltaic depositional episode in which the Oakville forms the lower progradational part, and the Lagarto forms the upper retrogradational part. In the onshore area, the Oakville is generally sand-rich, whereas the Lagarto is relatively more mud-rich. The Oakville and Lagarto Formations are separated by a marine transgressive shale downdip and a lithologic boundary updip (Figure 3-3).

The Fleming Group crops out across the entire Texas coastal plain except in South Texas where it is overlapped by a thin interval of Goliad gravel and caliche (Galloway and others, 1986) (Figure 3-3). The Oakville Formation ranges from 300 to 700 feet thick at outcrop to 1,000 to 2,000 feet thick near the modern shoreline, whereas the Lagarto Formation ranges from 700 to 1,400 feet thick at outcrop to 2,000 to 3,000 feet thick near the coast (Baker, 1979; Galloway and others, 1982, 1986). The Fleming Group dips coastward 50 to 60 feet per mile (Wood and others, 1963). Oakville sandstone is thickest (>900 feet) across a broad area in South Texas (Figure 3-4). The Lagarto Formation also contains thick sandstone in South Texas but in a more restricted area (Figure 3-5). Both formations contain thick sandstone in the far northeast part of the Texas coast, and both contain thick sandstone in the near offshore area (Figures 3-4 and 3-5). Across the broad middle coast from Nueces County in the southwest to Chambers County in the northeast, both formations contain relatively less sandstone, and several large regions in and near outcrop are marked by low sandstone (<200 feet) in both formations (Figures 3-4 and 3-5). Although net sandstone is low locally near outcrop in the Oakville Formation, sandstone percent is high because the gross Oakville interval is thin (Galloway and others, 1986). Across much of

the outcrop and near outcrop area, the Oakville forms a thinner high-sand interval, and the overlying Lagarto forms a thicker low-sand interval.

The Fleming Group comprises several large fluvial systems that grade downdip into equally large delta and shore-zone systems (Rainwater, 1964; Doyle, 1979; Spradlin, 1980; DuBar, 1983; Galloway and others, 1982, 1986). The fluvial systems include conglomeratic bed-load channel-fill sandstones and finer-grained mixed-load channel-fill sandstones (Table 3-1). Channel-fill sandstones range from 500 feet to 5 miles wide and 3 to 30 feet thick. Broad, dip-oriented, sand-rich belts near outcrop and in mid-dip areas are composed of superposed and laterally amalgamated channel-fill and channel-margin splay facies (Figures 3-4 and 3-5). Channel belts are encased in mud-dominated floodplain facies. Downdip near the modern shoreline, coastal-barrier and beach-ridge facies form thick sequences of strike-aligned, massive sandstone in both formations.

**Table 3-1 Fleming Group depositional facies (Galloway and others, 1982, 1986).**

Facies	Composition grain size	Sedimentary structures	Thickness	Width	Vertical trend (log pattern)	Depositional systems
Conglomeratic bed-load channel	Medium to coarse sand, gravel up to pebble size, mud clasts	Planar bedding, low-angle tabular cross-bedding, trough cross-bedding	3–15 ft	1,000–5,000 ft	Blocky, irregular	Santa Cruz fluvial system, southwest part of Moulton/Point Blank streamplain system
Sandy bed-load channel	Fine to coarse sand, local gravel, mud clasts	Planar bedding, trough and tabular cross-bedding	10–20 ft	1–5 mi	Blocky, irregular	Santa Cruz fluvial system
Mixed-load channel	Fine to coarse sand, silt, mud, mud clasts	Trough cross-bedding, planar bedding, ripple and wavy lamination	15–30 ft	500–2,500 ft	Fining upward	Moulton/Point Blank streamplain system
Amalgamated small channel and splay	Very fine to coarse sand, silt	Trough cross-bedding, planar bedding, ripple and wavy lamination	10-25 ft	1–3 mi	Irregular to fining upward	Moulton/Point Blank streamplain system
Crevasse splay and sheet splay	Fine to coarse sand, silt, sandy mud, mud clasts	Planar lamination, ripples, small-scale cross bedding	3–15 ft	1,000–5,000 ft	Interbedded fine and coarse	All fluvial systems



**Table 3-1, continued**

<b>Facies</b>	<b>Composition grain size</b>	<b>Sedimentary structures</b>	<b>Thickness</b>	<b>Width</b>	<b>Vertical trend (log pattern)</b>	<b>Depositional systems</b>
Floodplain, coastal bays and lagoons	Silt, clay, sandy mud, caliche	Massive, horizontal lamination, roots, burrows	Variable	Fill inter-channel areas (miles)	No trend (shale baseline)	All fluvial systems
Coastal barrier and beach ridge	Fine to coarse sand	Not reported	Individual units not reported	Several miles wide, tens of miles long	Blocky, massive	North Padre delta system, Matagorda barrier/strandplain system, Calcasieu delta system

Major extrabasinal fluvial channel belts in the Fleming Group are located in South Texas and in the northeast near the Louisiana border (Figures 3-4 and 3-5). In South Texas, the Santa Cruz fluvial system (Table 3-2) is composed of coarse sand and gravel and is partly covered at outcrop by similarly coarse facies in the Goliad Formation (Galloway and others, 1982, 1986). Most Santa Cruz fluvial sandstones occur in the Oakville Formation; except for a few areas, the Lagarto Formation is dominated by mud-rich interchannel (floodplain) facies. In the northeast corner of the Texas coastal plain, the Newton fluvial system (Table 3-2) is just a small part of a large, lower Miocene fluvial-deltaic depocenter in Louisiana (Figure 2-22). Across the broad middle coast, the Moulton/Point Blank streamplain system (Table 3-2) comprises numerous small fluvial channel and splay sandstones encased in floodplain mudstones (Spradlin, 1980; Galloway and others, 1986).

**Table 3-2 Fleming Group depositional systems (Spradlin, 1980; Galloway, and others, 1982, 1986).**

<b>Depositional system</b>	<b>Location (Gulf Coast GAMs)</b>	<b>Principal facies</b>	<b>Sandstone geometry</b>	<b>Oakville sand content</b>	<b>Lagarto sand content</b>
Santa Cruz fluvial	southern GC GAM, southwest part of central GC GAM	bed-load channel fill, sheet splay, floodplain	multiple dip-oriented low-sinuosity channel belts	200–900 ft, 40–80 %	mostly <500 ft, 20–40 %
Moulton/Point Blank streamplain	central GC GAM, southwest part northern GC GAM	amalgamated small channel and splay, floodplain, bed-load channel (Oakville)	thin sinuous channel and splay belts encased in floodplain mudstone	mostly <300 ft, local pockets of >500 ft, 20–60 %, increasing southwest	<300 ft, <40 %, increasing northeast

**Table 3-2, continued**

Depositional system	Location (Gulf Coast GAMs)	Principal facies	Sandstone geometry	Oakville sand content	Lagarto sand content
Newton fluvial	northeast part northern GC GAM	mixed-load channel, crevasse splay, floodplain	coalesced channel and splay belts, minor floodplain	300–900 ft, 40–80 %	300–900 ft, 40–80 %
North Padre delta (onshore part)	southern GC GAM, southwest part of central GC GAM	coastal barrier and beach ridge, coastal bays and lagoons	strike-aligned, vertically stacked	500–1000 ft, 20–50 %	200–900 ft, 10–40 %
Matagorda barrier/strandplain (onshore part)	central GC GAM, southwest part northern GC GAM	coastal barrier and beach ridge, coastal bays and lagoons	strike-aligned, vertically stacked	300–900 ft, 20–40 %	300–500 ft (10–40 %) updip, >900 ft (40–60 %) along present shoreline
Calcasieu delta	northeast part northern GC GAM	coastal barrier and beach ridge, coastal bays and lagoons	strike-aligned, vertically stacked	300–700 ft, 20–40 %	900–1100 ft, 40–60 %

Delta systems in the Fleming Group display strongly strike-aligned sandstone orientations (Figures 3-4 and 3-5). Redistribution of sand along strike away from deltaic headlands by shore-zone waves and currents resulted in strike-elongate stacks of massive sandstone in downdip areas (Galloway and others, 1986) (Figure 2-21). The North Padre delta system (Table 3-2) is the seaward extension of the Santa Cruz fluvial system in South Texas. Much of the sand delivered to the North Padre delta system was redistributed to the northeast into the Matagorda barrier/strandplain system (Table 3-2), especially in near offshore areas (Figures 3-4 and 3-5). The Calcasieu delta system (Table 3-2) is the seaward extension of the Newton fluvial system in the northeast. Calcasieu deltaic sandstones are thickest in the Lagarto Formation.

Fleming Group depositional systems constructed a framework of dip-oriented fluvial sandstone belts updip to middip and strike-oriented shore-zone sandstone belts downdip. Fluvial and shore-zone sandstones are well interconnected only in South Texas and far northeast coastal Texas. Across the broad middle coast, shore-zone sandstones are more isolated, grading updip into mud-dominated lagoonal and floodplain facies (Figures 3-4 and 3-5). Furthermore, much of Fleming shore-zone sandstone lies seaward of the modern shoreline. In South Texas, Lagarto sandstones generally thin downdip, whereas Oakville sandstones thicken downdip. The Oakville is distinctly sandier than the Lagarto in South Texas. Along the middle coast, thick Lagarto

sandstones form a strike-aligned belt in coastal areas of Matagorda and Brazoria Counties, but this sandstone belt grades landward into low-sandstone areas (Figure 3-5). The Oakville is relatively sand-poor along the coast in Matagorda and Brazoria Counties but is somewhat sandier than the Lagarto in adjacent mid-dip areas (Figure 3-4). The Lagarto is generally sandier than the Oakville along the upper coast.

### **3.3 Goliad Formation**

The Goliad Formation of the Texas Coastal Plain is primarily middle-to-late Miocene in age (Morton and others, 1988) (Figure 2-23, Table 2-1). The Goliad includes vertebrate fossils ranging in age from middle Miocene to earliest Pliocene (Baskin and Hulbert, 2008). At outcrop and in the shallow subsurface, the Goliad Formation is bounded by regional unconformities at the base of massive fluvial sandstones, but downdip, the Goliad is bounded by marine transgressive shales (Figure 3-6). A minor datum change is required to tie downdip marine paleontologic markers to updip lithologic markers (Morton and others, 1988). The lithostratigraphic Goliad Formation occurs only in the onshore part of the Texas Coastal Plain, where it is defined by nonmarine depositional systems and facies (Solis, 1981; Hoel, 1982). In extreme South Texas and northeastern Mexico (Burgos basin), however, the Goliad-equivalent interval is composed of shore-zone and marine depositional systems (Morton and others, 1988). In the modern offshore area, middle-upper Miocene sequences include fluvial, deltaic, and marine depositional systems (Doyle, 1979; Morton and others, 1988; Galloway and others, 2000).

The Goliad Formation ranges in thickness from 200 feet at outcrop to about 1,400 feet near the modern shoreline. The Goliad does not display significant thickness changes attributable to differential subsidence across the San Marcos arch and into adjacent embayments but does thicken (15–20%) locally across the major growth fault zones shown in Figure 3-3 (Hoel, 1982). Goliad strata dip coastward about 10 to 20 feet per mile. Net sandstone thicknesses range from 100 to 800 feet, and sandstone content decreases regionally to the southwest (Morton and others, 1988). Sandstones in the upper Goliad typically are less conglomeratic and thinner bedded than are those in the lower Goliad (Hoel, 1982; Morton and others, 1988).

Goliad fluvial depositional systems comprise channel-fill and interchannel facies (Hoel, 1982) (Table 4-1). Fluvial channel-fill facies are composed mainly of medium- to coarse-grained sand and gravel, displaying large-scale cross-bedding. Hoel (1982) recognized both bed-load and mixed-load channel-fill facies in Goliad outcrops (Table 4-1). Gravelly coarse sand, sandy gravel, and pebble-to-cobble-sized gravel dominate bed-load channel-fill facies. Vertical stratigraphic successions in bed-load channel-fill facies are irregular, and grain size and sorting vary greatly. Mixed-load channel-fill facies, however, commonly display fining-upwards vertical grain-size trends. Coarse sand and sandy gravel are overlain by medium-to-fine sand, and very fine sand and silt cap the mixed-load channel-fill succession. Electric log responses reflect vertical grain-size trends: bed-load channel-fill facies cause blocky log patterns whereas mixed-load channel-fill facies cause fining-upwards log patterns.

Interchannel facies include sandy crevasse splays, and muddy floodplain and playa lake facies. Crevasse-splay facies formed where flood waters breached channel levees and deposited broad aprons of sandy sediment on the floodplain (Table 3-1). Crevasse splays associated with mixed-load channels are finer grained than those associated with bed-load channels (Hoel, 1982). Floodplain facies surround channel-fill and crevasse-splay facies and were deposited across interchannel areas during floods. Mottled red clays dominate floodplain successions, and secondary calichification and pedogenesis are pervasive (Hoel, 1982). Playa facies have been identified only in Brooks and San Patricio Counties (Hoel, 1982). In playa facies, gypsum occurs as interbeds and interstitial precipitates. The environment of deposition of playa facies was probably an arid-region evaporitic lake (inland sabkha facies of Hoel [1982]).

**Table 3-3 Goliad Formation depositional facies (Hoel, 1982).**

<b>Facies</b>	<b>Composition grain size</b>	<b>Sedimentary structures</b>	<b>Thickness</b>	<b>Width</b>	<b>Vertical trend (log pattern)</b>	<b>Fluvial systems</b>
Bed-load channel	Coarse sand, gravel up to cobble size, mud clastics	Large planar and trough cross-bedding	25–60 ft	~103 ft	Blocky, irregular	Realitos, Tomball
Mixed-load channel	Medium-coarse sand, gravelly sand, mud clasts	Large and small trough cross-bedding, low-angle planar bedding	30–60 ft	~103–104 ft	Fining upward	Eagle Lake

**Table 3-3, continued**

<b>Facies</b>	<b>Composition grain size</b>	<b>Sedimentary structures</b>	<b>Thickness</b>	<b>Width</b>	<b>Vertical trend (log pattern)</b>	<b>Fluvial systems</b>
Crevasse splay	Medium-fine sand, silt, gravel lags	Ripple, wavy and parallel lamination	10–30 ft	~103–104 ft	Fining upward	All
Floodplain	Silt, clay, caliche	Massive, horizontal lamination, roots, burrows	Variable	Fill interchannel areas (miles)	No trend (shale baseline)	All
Playa lake	Gypsum, sand, silt, clay	Horizontal lamination, ripples, chaotic	30–60 ft	Miles	Thin fining upward cycles	Realitos

The Goliad Formation includes three large extrabasinal fluvial systems listed in Table 3-4. (Hoel, 1982; Morton and others, 1988). Each Goliad fluvial system contained multiple channel axes that formed an integrated drainage network. Channels preferentially reoccupied the same locations on the coastal plain, resulting in vertical stacking of sand bodies (Morton and others, 1988). Owing to an arid paleoclimate and lack of bank-stabilizing vegetation, Goliad fluvial channels had poorly developed levees, channel migration was relatively unconstrained, and channel-fill deposits tended to coalesce laterally (Hoel, 1982). Thus, Goliad channel-fill sand bodies form broad belts that are much thicker and wider than the river channels in which they were deposited.

Goliad fluvial systems vary in overall composition and sandstone development, and generally become sandier to the northeast (Table 3-3, Figure 3-7). The Realitos fluvial system occupies the Rio Grande embayment. This fluvial system includes spectacular pebble- and cobble-sized gravels in outcrop (Plummer, 1932; Hoel, 1982), but in mid-dip positions, Realitos channel belts are narrow and include relatively less aggregate net sand than the other Goliad fluvial systems (Figure 3-7, Table 3-4). Realitos gravels include volcanic rock fragments, Permian limestone, and other compositions reflecting extrabasinal source areas in West Texas and beyond (Hoel, 1982). The Realitos fluvial system feeds small deltaic and barrier-lagoon depositional systems that are located under the modern South Texas shoreline and adjacent offshore area.

The Eagle Lake fluvial system is located (atypically) on the San Marcos arch and the adjacent southwestern part of the Houston embayment. Fluvial axes of the Eagle Lake system are broader and sandier than those of the Realitos system (Figure 3-7, Table 3-4). Individual channel-fill

sand bodies in the Eagle Lake system are slightly thicker than those in the other Goliad fluvial systems. Eagle Lake sand bodies are most developed in the upper part of the Goliad Formation (Hoel, 1982; Knox and others, 2006). The Eagle Lake fluvial system was the primary middle-late Miocene drainage conduit for the Texas part of the northwest GOM and supplied sediment to the South Brazos delta system located well offshore (Morton and others, 1988). The largest northwest GOM fluvial-deltaic drainage system in the middle-late Miocene was located in the Mississippi embayment (Figure 2-22).

**Table 3-4 The Goliad Formation fluvial depositional systems (Hoel, 1982; Morton and others, 1988).**

Depositional system	Location	Channel-belt composition	Channel-belt width	Stratigraphic position of maximum sand	Interchannel composition	Source area	Overall sand content (rank)
Realitos bed-load fluvial	Rio Grande embayment	≤400 ft sand, 40–50% sand	5–15 miles	lower and upper Goliad	calcareous mudstone, <20% sand	West Texas, northern Mexico	third (lowest sand content)
Eagle Lake mixed-load fluvial	North flank San Marcos arch	≤500 ft sand, 40–60% sand	10–20 miles	upper Goliad	calcareous mudstone, <20% sand	Central Texas	second
Tomball bed-load fluvial	Houston embayment	≤600 ft sand, 40–60% sand	10–30 miles	lower and upper Goliad	mudstone and sandstone, >25% sand	East Texas	first (highest sand content)

The Tomball fluvial system is located in the Houston embayment. Even though it was not the primary extrabasinal drainage conduit in Texas, the Tomball system is the sandiest of the three Goliad fluvial systems (Figure 3-7, Table 3-4). Tomball channel belts are broad and sand-rich, but interchannel areas are unusually sandy as well because of the abundance of crevasse-splay facies (Morton and others, 1988). During the middle Miocene, tectonic activity in the source areas disrupted drainage networks and shifted the axis of sedimentation northward from the Rio Grande embayment to the Houston and Mississippi embayments (Morton and others, 1988). For this reason, Tomball rivers transported larger volumes of sediment than more southerly rivers, and this large sediment influx was sustained though both middle and late Miocene depositional episodes. Tomball rivers supplied sediment to form the thick sand-rich, shore-zone facies of the Galveston Strandplain system in the southeast Texas offshore area (Morton and others, 1988).

### 3.4 Willis Formation

The Willis Formation is approximately Pliocene in age (Galloway, 1989b). At outcrop, the Willis erosionally downcuts and locally truncates the underlying Goliad Formation and is in turn eroded and locally overlapped by the overlying Lissie Formation (Doering, 1935) (Figure 3-2). The Willis outcrop consists of cuesta-forming erosional remnants in the Houston Embayment and on the San Marcos Arch (Figure 3-1). The Willis does not outcrop in the Rio Grande Embayment, although Pliocene-age deposits are present there in the subsurface. Along the south and central Texas coast, Willis-equivalent strata have been mapped with the Lissie (Doering, 1956) or with the Goliad (Solis, 1981). Similar to the Goliad, the Willis is dominated by nonmarine, fluvial depositional systems in the onshore part of the Texas Coastal Plain (Guevara-Sanchez, 1974; Solis, 1981; Galloway and others, 2000). At outcrop, the Willis is composed of gravelly coarse sand in several upward-fining successions that are interpreted as incised valley fills overlain by transgressive deposits (Morton and Galloway, 1991). Near the modern shoreline and offshore, Willis deltaic and marine systems record four cyclic depositional episodes bounded by transgressive shales (Galloway and others, 2000) (Figure 2-23). The paleo Red River extended across the upper Texas Coastal Plain. This major Pliocene extrabasinal river for deltaic and continental margin progradation extends offshore from Houston. The ancestral Mississippi River in Louisiana was the second main source of sediment input during the Pliocene. Although the ancestral Mississippi River in Louisiana was the main source of sediment input during the Pliocene, the onshore part of the Willis is more sand-dominated in the Houston Embayment than it is in southwest Louisiana (Figure 3-8).

The Willis Formation ranges in thickness from about 100 feet at outcrop to 500 feet near the coast and also thickens northeastward (Knox and others, 2006). The Willis dips coastward about 15 to 20 feet per mile and is 1,000 to 2,000 feet deep at the modern shoreline (Doering 1935; Knox and others, 2006). Willis fluvial systems include dip-oriented sand-rich channel-fill facies and sand-poor interchannel areas, which grade toward the coast into shore-parallel deltaic and shore-zone sands and interdeltic muddy bay deposits. Individual Willis sands vary widely in thickness from about 20 to 200 feet and are separated by muds of similar thickness (Knox and others, 2006). The abundance of sand in the Willis Formation is greater than 60% across most of the Houston Embayment but decreases downdip to around 40% along the coast (Figure 3-8).

### **3.5 Lissie Formation**

The Lissie Formation is approximately early Pleistocene in age (DuBar and others, 1991). Pleistocene fossils have been found in the Lissie at several locations on the Texas coastal plain (Plummer, 1933). In Texas and southwest Louisiana, the Lissie outcrop is continuous except where cut by modern river valleys or where covered by Holocene windblown deposits in South Texas (Figure 3-1). North of the Brazos River, the Lissie Formation has been mapped at the surface as the Montgomery and Bentley formations (Barnes, 1992). At outcrop the Lissie is composed of fine-grained sand and sandy clay and unconformably overlies and onlaps the Willis (Morton and others, 1991). In the subsurface the Lissie is defined as the interval between the Willis and the Beaumont (Figure 3-2). The Lissie is dominated by nonmarine depositional systems in the onshore part of the Texas and Louisiana coastal plains, although shore-zone facies are prominent in some coastal counties (Guevara-Sanchez, 1974; Solis, 1981). Lissie deposition was strongly influenced by glacial-interglacial cycles on the North American continent. High-frequency glacio-eustatic sea-level fluctuations resulted in shorter depositional episodes, thinner genetic sequences, and greater erosional downcutting (Figures 2-23, 3-2).

The Lissie Formation ranges in thickness from about 100 feet at outcrop to greater than 700 feet at the coast (Knox and others, 2006). The Lissie dips coastward about 5 to 20 feet per mile and is 500 to 1000 feet deep at the modern shoreline (Doering, 1935; Knox and others, 2006). Lissie depositional facies patterns are similar to those of the Willis: dip-oriented fluvial channel sands separated by interchannel muds and grading downdip into shore-parallel sands and muds. In Lissie fluvial systems, individual sand bodies are 20 to 100 feet thick, whereas interbedded muds are generally less than 20 feet thick (Knox and others, 2006). Shore-zone and marine systems downdip, however, include much thicker muddy intervals. The Lissie Formation is >60% sand in updip fluvial systems and 20 to 60% sand in downdip shore-zone systems (Figure 3-9). Along the northeastern Texas coast, the Lissie is less sandy than is the Willis (Figures 3-8, 3-9). The sandiest part of the Lissie is located in southern Louisiana (Figure 3-9).

### **3.6 Beaumont Formation**

The Beaumont Formation is late Pleistocene in age (DuBar and others, 1991). Pleistocene-age fossils have been found in the Beaumont at numerous locations on the Texas Coastal Plain



(Maury, 1920, 1922; Plummer, 1933; Price, 1934). The Beaumont outcrop covers a large part of the lower coastal plain except where cut by modern river valleys or covered by Holocene wind-blown sand in south Texas (Figure 3-1). The Beaumont is composed of clay-rich sediments transected by sandy fluvial and deltaic-distributary channels. The Beaumont also includes isolated segments of coast-parallel, sandy beach ridges known as the Ingleside barrier/strandplain system (Price, 1958) (Figure 3-10). The Beaumont depositional episode records a continuation of patterns that developed during deposition of the Lissie: high-frequency, glacio-eustatic, sea-level fluctuations (Figure 2-23) and dominant fluvial sediment input located in Louisiana (Galloway and others, 2000). Much of the original depositional morphology of Beaumont fluvial, deltaic, and marginal-marine systems, such as abandoned channels and relict beach ridges, can be seen at the surface in aerial photographs. At sea-level highstand, the position of the Beaumont shoreline approximately coincided with that of the modern shoreline (Solis, 1981; Knox and others, 2006). During sea-level lowstand, Beaumont-incised valleys extended many miles seaward of the present shoreline (Morton and others, 1991).

North of the Brazos River, the Beaumont Formation ranges in thickness from a thin veneer in updip areas to about 500 feet near the modern coast and thickens to the northeast (Guevara-Sanchez, 1974). The Beaumont dips coastward from 1 to 10 feet per mile (Guevara-Sanchez, 1974). Individual sands range from 20 to 50 feet thick, stacking locally to reach 150 feet in thickness (Knox and others, 2006). Interbedded muddy intervals are generally of similar thickness to the sands. Thicknesses of individual sands increase updip, whereas thicknesses of individual shales increase downdip. Fluvial channels display dip-oriented, meandering and distributary patterns at the surface. Within the channel belts, the Beaumont is 50 to 65% sand (Guevara-Sanchez, 1974). Channel belts are separated by sand-poor floodplain, delta-plain, and bay-lagoon systems.

### **3.7 Holocene Deposits**

Holocene sediments were deposited within the last 18,000 years. In Texas Holocene sediments consist mainly of isolated river valley fills that merge coastward with bays, lagoons, and barrier islands (Fisher and others, 1972, 1973; McGowen and others, 1976a,b; DuBar and others, 1991) (Figure 3-10), whereas in south Louisiana, Holocene fluvial-deltaic sediments are widespread (Autin and others, 1991). Holocene depositional systems record the final period of sea-level rise

following the last North American glaciation, a rise that was punctuated by numerous stillstands and small reversals (McGowen and others, 1976). The base of the Holocene is an erosional surface that formed during sea-level lowstand at the end of the Pleistocene. River valleys were deeply incised into the preexisting Beaumont coastal plain and filled slowly with bay-estuary muds as sea-level rose. Subsequently, fluvial-deltaic systems prograded seaward filling the updip parts of the valleys with sandy alluvial deposits, but only the Colorado River, Brazos River, Mississippi River, and the Rio Grande have completely filled their valleys to the coast. The other Texas coastal river valleys are still partly occupied by bays and lagoons. In southeastern Texas, the sandiest parts of the Holocene are located in the Colorado and Brazos river valleys (Figure 3-10). In Louisiana, broad areas along the coast and in the wide Mississippi River valley are covered by Holocene sediments up to 400 ft thick (Autin and others, 1991) (Figure 3-1).

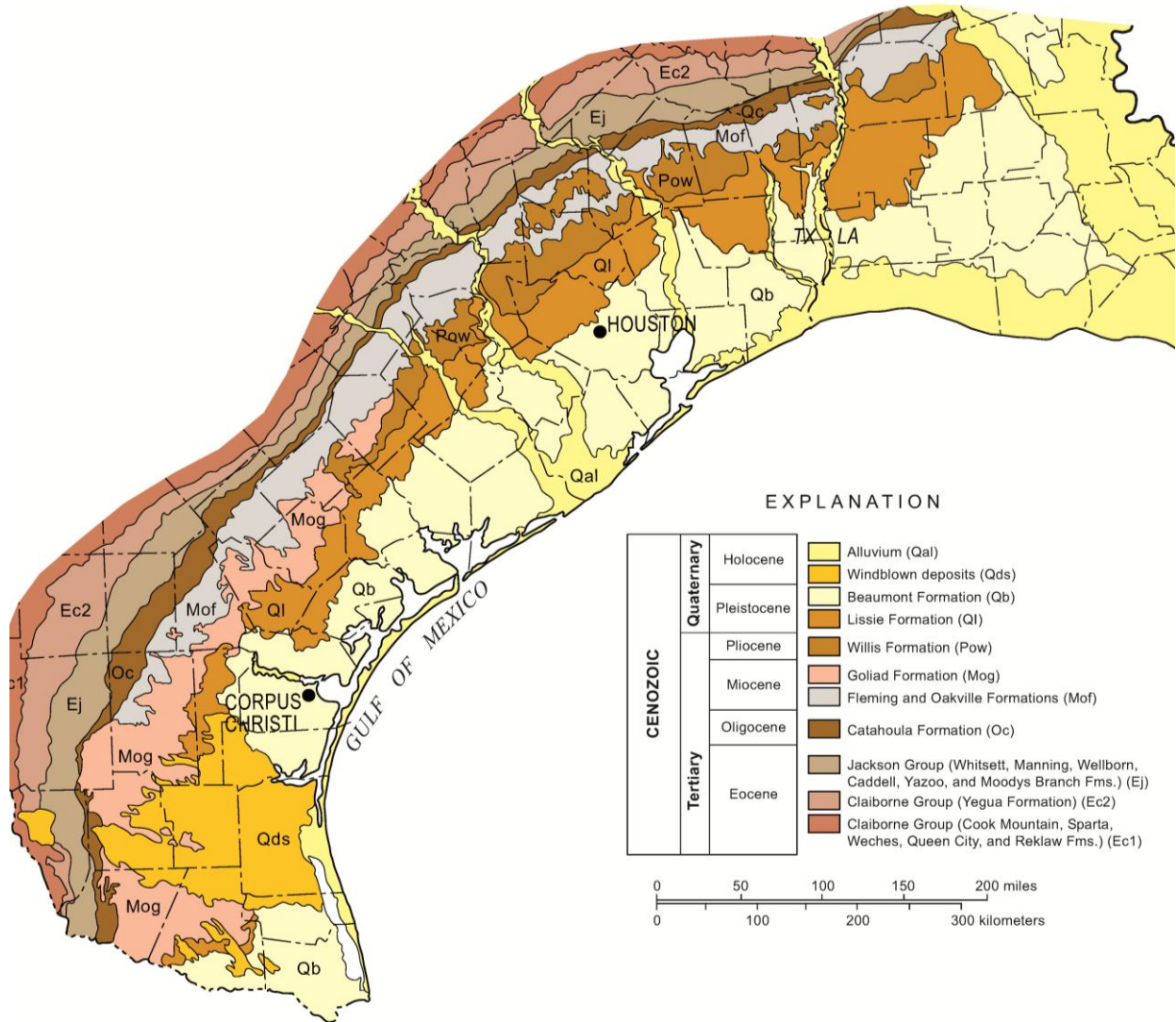
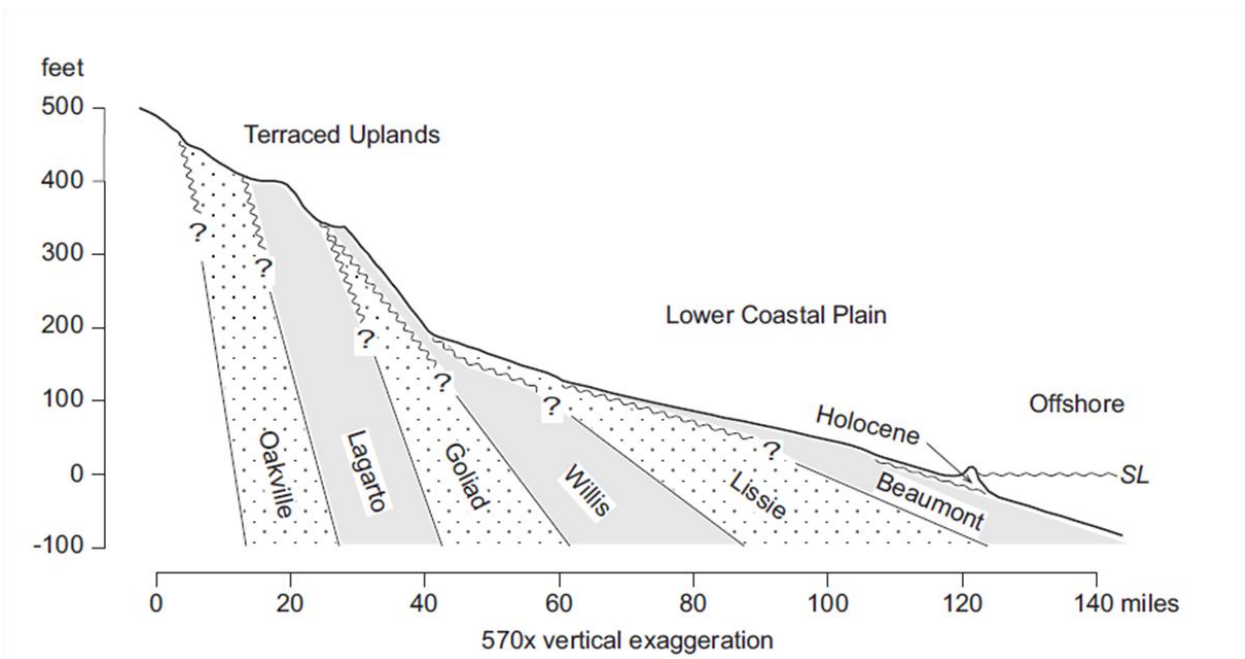
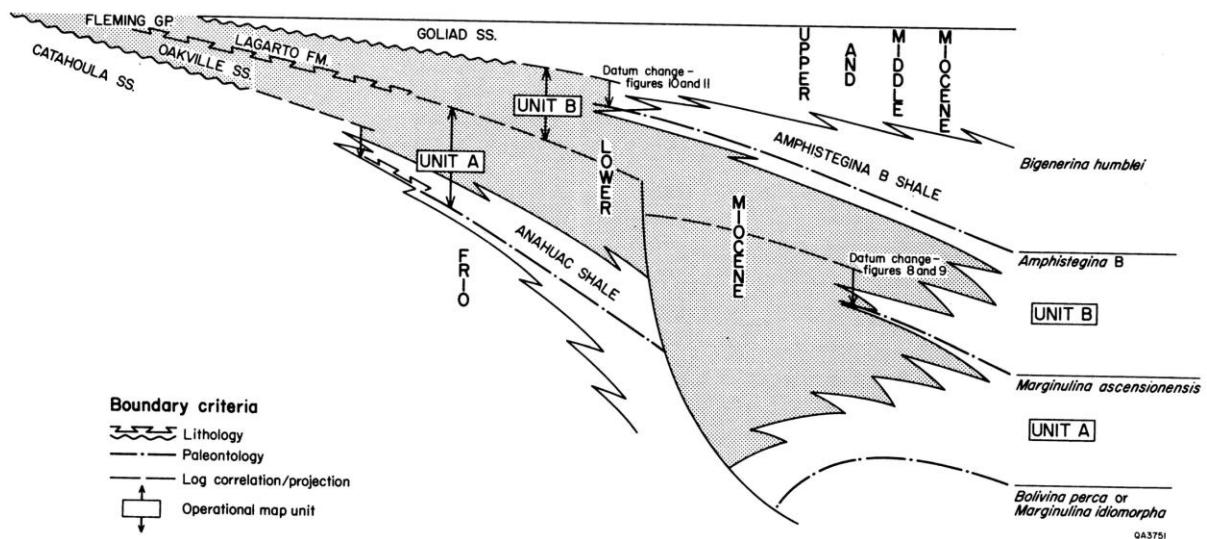


Figure 3-1 Geologic map of the Texas Coastal Plain. Source: Barnes (1992).



**Figure 3-2** Schematic dip cross section showing relationships between outcropping formations and subsurface stratigraphy, central coastal plain, Texas. Modified from Doering (1956).



**Figure 3-3** Schematic cross section of lower Miocene stratigraphy showing depositional sequences and lithostratigraphic and biostratigraphic boundaries. Source: Galloway and others. (1986).

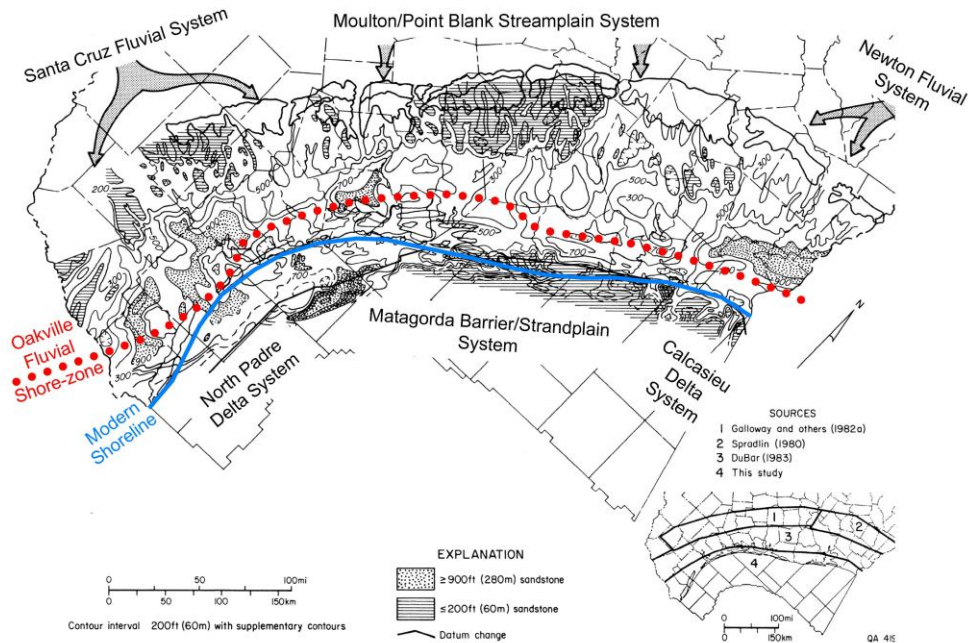


**Figure 3-4** Net-sandstone isopach map of the Oakville Formation also showing depositional systems. Red dotted line separates updip fluvial systems from downdip delta and shore-zone systems. Modified from Galloway and others. (1986).

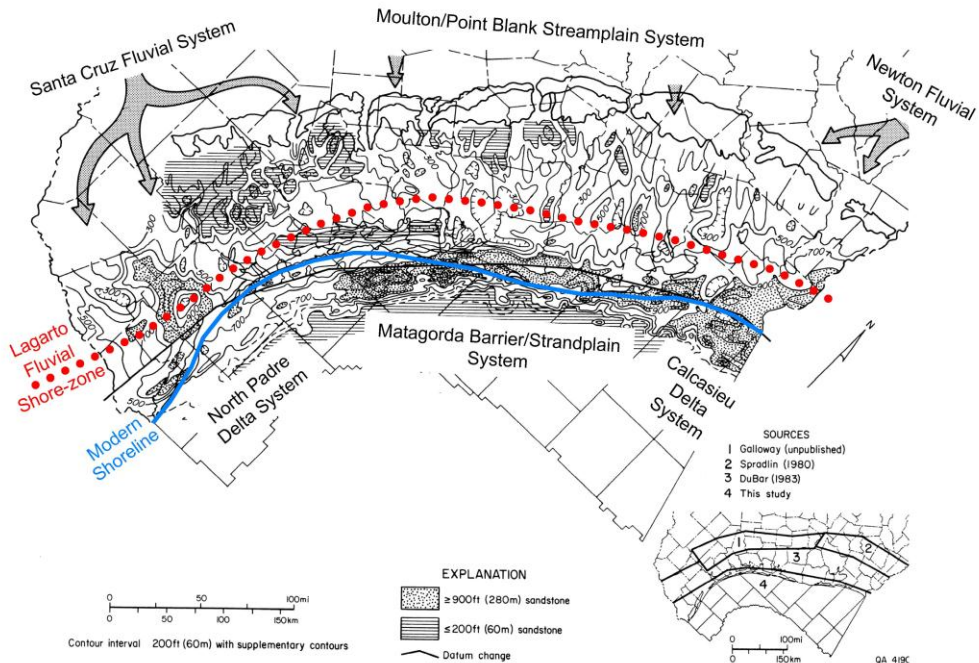


**Figure 3-5** Net-sandstone isopach map of the Lagarto Formation also showing depositional systems. Red dotted line separates updip fluvial systems from downdip delta and shore-zone systems. Modified from Galloway and others. (1986).

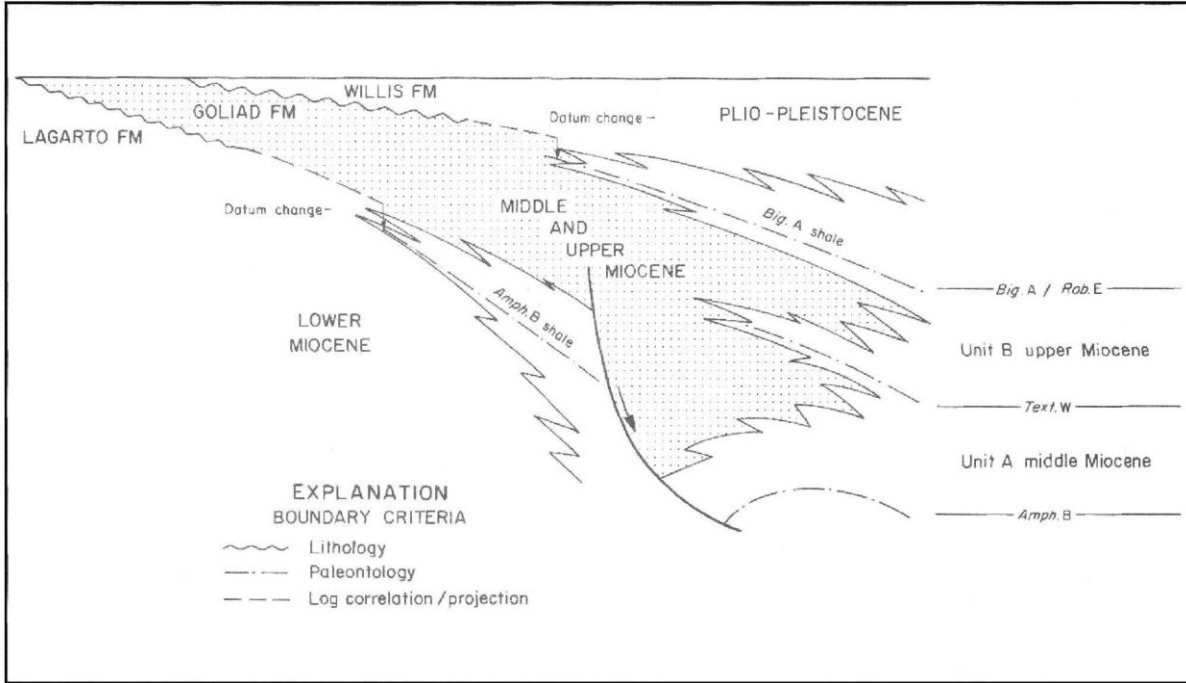


**Figure 3-6** Schematic cross section of middle-upper Miocene stratigraphy showing depositional sequences and lithostratigraphic and biostratigraphic boundaries. From Morton and others. (1988).

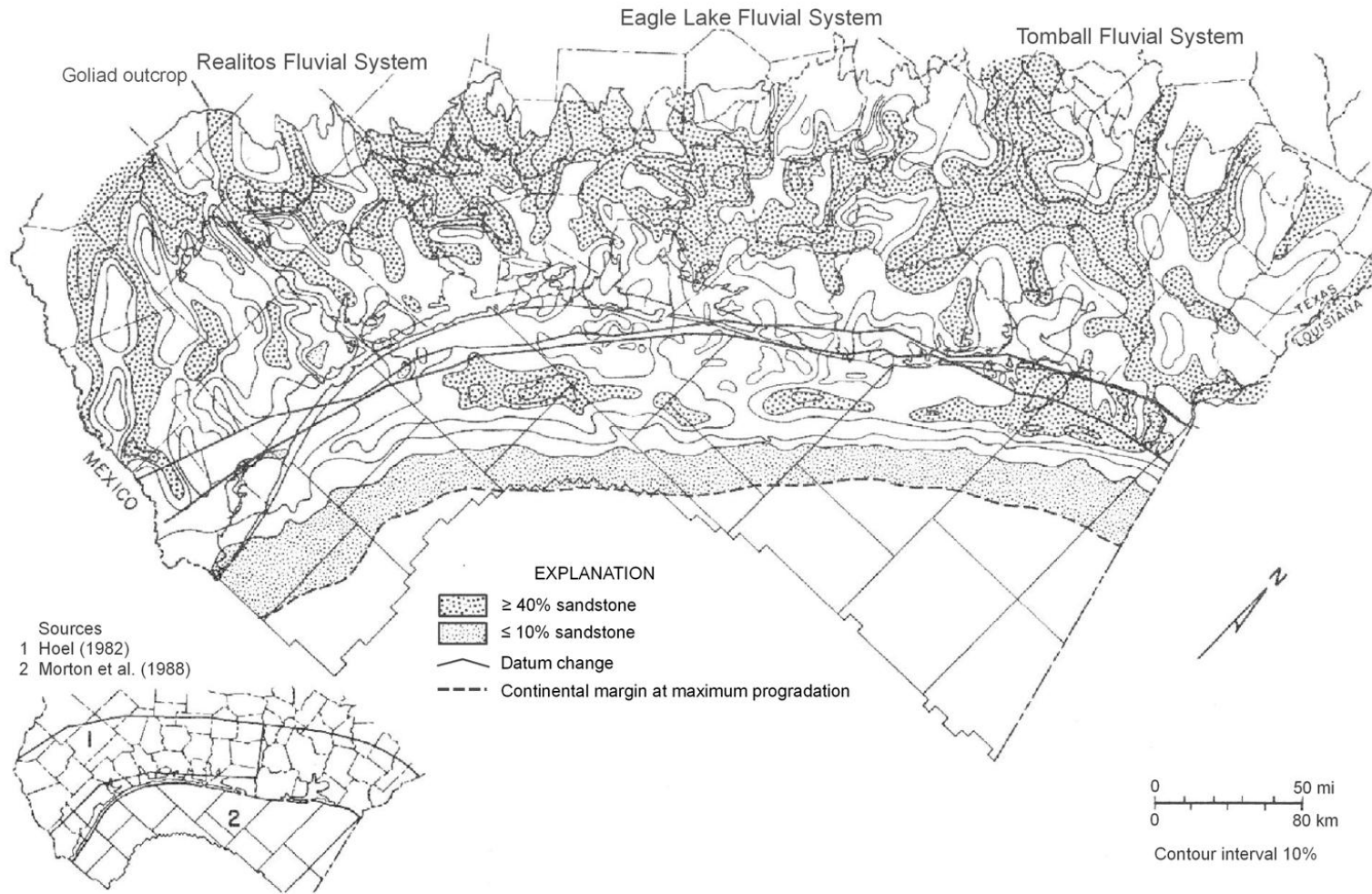


**Figure 3-7** Percent sandstone maps of Goliad and equivalent middle-upper Miocene sequences. From Hoel (1982) and Morton and others, (1988).

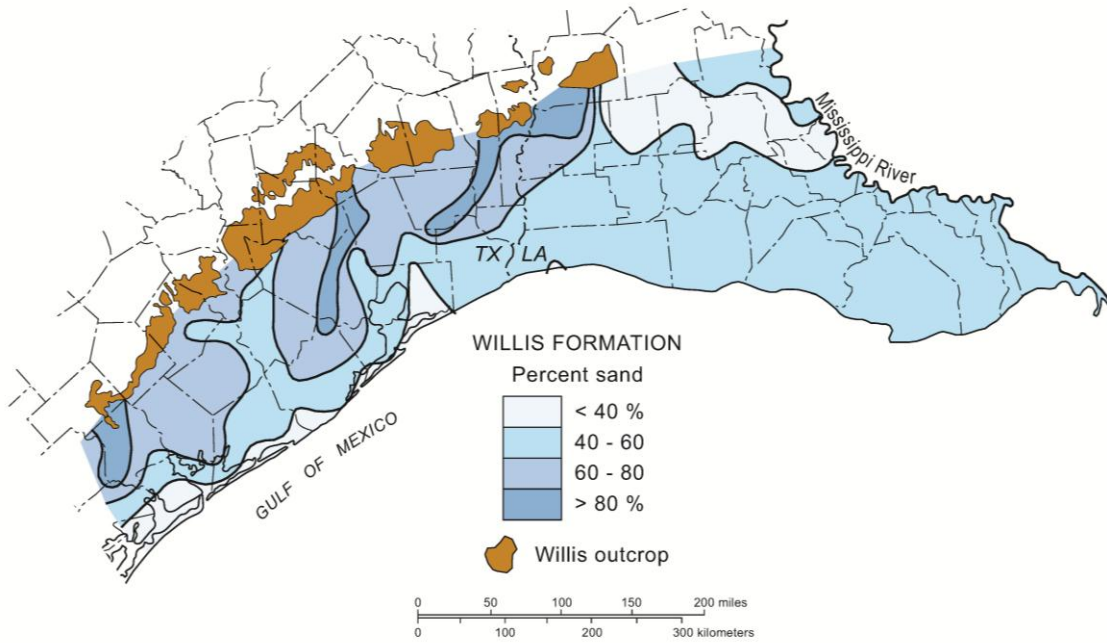


**Figure 3-8 Sand percent map of the Willis Formation, southeast Texas and south Louisiana. Modified from Weiss (1992).**

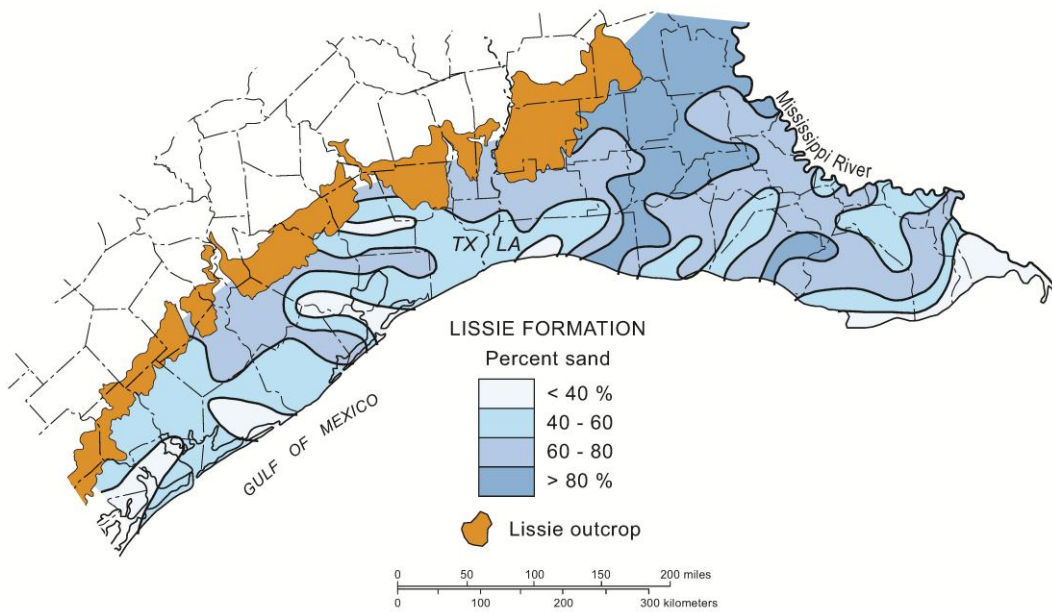


**Figure 3-9 Sand percent map of the Lissie Formation, southeast Texas and south Louisiana. Modified from Weiss (1992).**



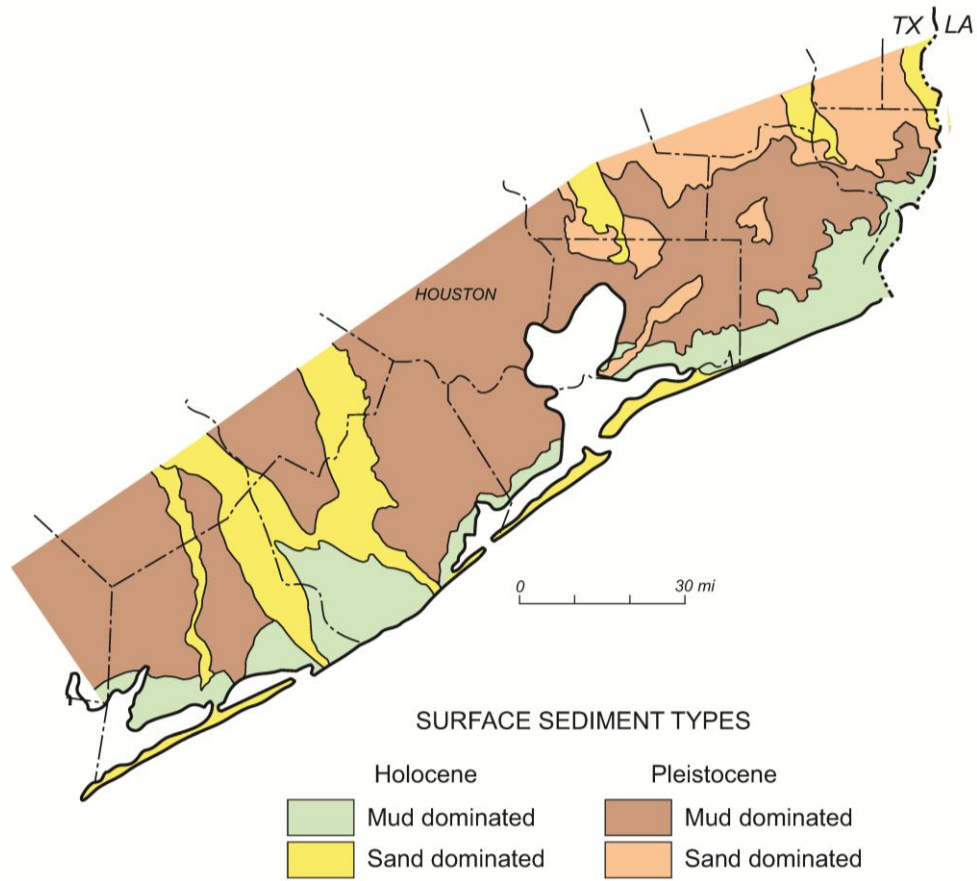


**Figure 3-10** Simplified map of surface sediment types covering Matagorda County to the Louisiana border showing Pleistocene (Beaumont Formation) and Holocene deposits. Modified from Fisher and others (1972, 1973) and McGowen and others (1976a,b).

## **4.0 Information sources**

The information used to develop the hydrostratigraphy of the Gulf Coast Aquifer can be divided into two data groups. One group consists of geophysical logs, and the other consists of the information used to help guide the analysis of the geophysical logs. This section describes the type of information associated with each data group used to characterize the chronostratigraphy and lithology of the Gulf Coast Aquifer.

### **4.1 Geophysical Logs**

Extensive investigation of the subsurface conducted by the petroleum industry in the state of Texas has yielded a considerable number of geophysical logs that can be used to characterize the subsurface deposits. At the time of this writing, the Texas Railroad Commission was monitoring approximately 400,000 oil and gas wells in the state of Texas. The Texas Gulf Coast, particularly within the upper Cenozoic stratigraphy that includes the Gulf Coast Aquifer system, contains one of the largest concentrations of petroleum in the world (Nehring, 1991).

Geophysical logs are generated by lowering a measuring device into a borehole and taking a series of continuous measurements of the physical properties of the wellbore environment. A geophysical log typically contains a number of different curves acquired prior to completion of the well. Common geophysical logs include caliper, gamma, single-point resistance, normal resistivity, spontaneous potential, electromagnetic induction, fluid resistivity, temperature, flowmeter, television, and acoustic televiewer. The combination of a resistivity log and a spontaneous potential log are often referred to as an electrical log.

For this study, electrical logs were used extensively in the study because of their widespread use on the Gulf Coast for over 70 years and because they are particular well suited for developing sequences of clastic sediments. One of the limitation with using electrical logs for developing stratigraphy that most of the wells drilled after the 1970s do not record readings from the first several hundred feet of borehole. However, for developing groundwater availability models, data from as shallow as 100 ft below the ground surface can be important.

### ***4.1.1 Resistivity Logs***

Resistivity logs record an apparent electrical resistance in and within the vicinity of the borehole at different depths. The unit of resistivity measurement is the ohm-meter<sup>2</sup> per meter. The reciprocal of resistivity is conductivity, which is measured in mhos per meter.

To generate a resistivity log, one or more electrodes are suspended on a cable and lowered into a borehole. An electric current is then forced to flow between an electrode at the surface and one or more electrodes that are downhole. The changes in the current losses are then recorded as the locations of the electrodes are moved up and down the borehole. The variations in the resistivity with depth are caused primarily by differences in the porosity and composition of the subsurface deposits and by the mineral content of the water contained in the strata and in the borehole.

The resistivity logs that were most commonly analyzed for this study consist of two electrodes downhole. When the separation of the electrodes is 16 inches or less, the configuration is called a short normal. If the two electrodes are separated by 64 inches, the configuration is called a long normal. The larger the spacing between the two downhole electrodes, the deeper the penetration of the measurement into the formation.

Dry formations will have very high resistivities because they are poor conductors of electricity. Saturation of a deposit reduces its resistivity because water is an electrical conductor. In general, saturated subsurface materials with low resistivity include silts, clays, and shales. Fresh water deposits composed of sands and gravel tend to have high resistivities. The resistivity of a formation will vary inversely with the total dissolved solids concentrations in its pore water. One of the reasons that clays tend to have low apparent resistivities is because their interstitial waters are often highly mineralized. On the other hand, sands and gravels saturated with fresh water tend to have high apparent resistivities because their surfaces are relatively inert and tend to release few minerals into solution.

Figure 4-1 illustrates how apparent resistivity can vary with differences in subsurface material and total dissolved solid concentrations in groundwater. In fresh water, the difference in the apparent resistivity between sandy and clayey deposits is considerably greater than in very brackish water. In fact, in salt water, the difference in apparent resistivity between a clay and a sand is subtle. In situations that involve heterogeneous deposit types and vertical variations in

water quality, analysis of the resistivity logs should be performed in concert with the analysis of other logs that provide independent information on either the characteristics of the deposits or the water quality.

Because the borehole fluids affect the resistivity measurement, the borehole diameters should be kept as small as possible. In a large-diameter hole or with short spacings between the electrodes, the resistivity will be heavily influenced by the drilling fluid. This is because the "zone of influence" of the electrodes may not extend very far into the formation (Driscoll, 1986). If the drilling fluid is quite clayey or salty (highly conductive), the formation resistivity may serve to partially mask the resistance of relatively thin sandy aquifers.

#### ***4.1.2 Spontaneous Potential Logs***

Spontaneous potential (SP) logs record naturally occurring electrical potentials (voltages) that occur in the borehole at different depths. The SP log primarily measures the electrochemical potential between a stationary reference at the surface and a moving electrode in the borehole.

The circuitry between the surface and the downhole electrode does not include an external source for an electric current. The electrochemical potential is generated by ions moving between the borehole fluid and the formation water. If there is no contrast in the ionic concentrations of the borehole fluid and the formation water, there is no electrochemical potential, and the SP potential is zero. The downhole electrode usually has a lower (more negative) potential than the surface electrode. SP logs only record relative values rather than the absolute values of resistivity tools.

The examples in Figure 4-1 illustrate the type of SP responses that can be expected in formations containing fresh water, brackish water, and salt water when the drilling fluid is composed of fresh water. As shown in Figure 4-1, at shallow depths where there may be little difference in the concentration of ions between the drilling fluids and the aquifer, the analysis of the SP log may be difficult because of the lack of deflections. However, at deeper depths where the formation waters are more mineralized than the drilling fluids, the leftward deflections (more negative values) in the SP logs are useful for identifying permeable strata. Despite the fact that the SP logs can provide potentially useful information on the location of permeable zones, there is no direct relationship between the magnitude of the SP deflection and either permeability or porosity because just a fraction of a millidarcy of permeability is sufficient to support the ionic

movement required to generate a SP deflection. The deflections associated with sands and gravels are more associated with their mineralogical differences than their permeability difference with clays and shales.

The analysis of an SP log begins with developing a "baseline" by connecting the potentials associated with the impermeable beds such as clays and shales. Deflections to the left of this baseline are usually associated with beds of coarse-grained deposits such as sands and gravels. If no clay layers are present in the lithologic profile, the SP log may not provide much useful information.

### 4.1.3 American Petroleum Institute Format

The standard format for geophysical logs used by the petroleum industry is set by the American Petroleum Institute (API). The API format includes a header file and a set of log curves.

Table 4-1 summarizes categories of data contained in the API headers.

**Table 4-1 Types of log header data.**

<b>Data Categories</b>	<b>Description</b>	<b>Use</b>
Measurement Datum / Log Datum	Elevation from which logged depths are measured	Allows referencing of curve measurements to a selected datum such as sea level
Kelly Bushing (KB)	An oil rig design component, specifically the device that transfers the torque of the rotary table to the drill stem	Elevation of KB is commonly used as the measurement datum by the logging engineer. Often given as height above GL.
Ground Level (GL)	Elevation of surface of ground at the well head	Allows measured depths to be converted to absolute depths
Top of Logged Interval (TLI)	Shallowest measured depth	Determines whether the log covers the relevant stratigraphic interval
Bottom of Logged Interval (BLI)	Deepest measured depth	Determines whether the log covers the relevant stratigraphic interval
Operator / Company	The person or company, either proprietor lessee, actually operating an oil well or lease	A searchable term used to identify and locate wells
Lease	A parcel of land on which mineral exploration rights have been granted by the landowner to a lessee	A searchable term used to identify and locate wells
Well Number	A numbering system within a lease or other unit	A searchable term used to identify and locate wells
Well Field	A region encompassing several leases in which proven reserves exist	A searchable term used to identify and locate wells
Permit Date or Completion Date	Date after which well installation is permitted, date of complete of well construction for production	A searchable term used to identify and locate wells

The Kelly Bushing is an adapter that connects the drilling rig rotary table to the drill string. As shown in Figure 4-2, the Kelly Bushing exists near the elevation of the drill rig floor. The elevation of the Kelly Bushing is important because it is used as the measurement datum referenced by the log curves. Accurate datums for well log records are important because they establish the relationship between depths of stratigraphic events in the well and a universal datum – sea level. The well log header usually contains both the elevation of the Kelly Bushing and the ground level at the wellbore. Often, the height of the datum above ground level is provided.

For some of the log headers, no elevation information is available for either the ground level or the Kelly Bushing. To estimate the elevation of the Kelly Bushing in those instances, a computer script was written to estimate the ground elevation at the well bore location from the USGS Digital Elevation Model (DEM) of the Gulf Coast and then to add an additional 16 ft, which is the average height of the Kelly Bushing above ground level based on the headers of logs used in this study having completed elevation data.

Beneath the header, the main body of the geophysical log contains the log curves. Figure 4-3 shows an example header and set of log curves for a geophysical log used for this study. The logs are plotted on three tracks with a depth column dividing tracks 1 and 2. The vertical-scale plotting depth is always linear and is usually scaled as 1, 2, or 5 inches per 100 feet of depth. The three tracks for the logs can have different scales and are reserved for specific types of logs. Among the logs that are plotted on track 1 are SP, gamma ray, and caliper. Track 1 always uses a linear scale, whereas the other two tracks can use either a linear or logarithmic scale. Porosity and resistivity logs are always shown in track 2 or 3. At the top of each track, the scale and log types are shown.

## **4.2 Approach for Obtaining Geophysical Logs**

The approach for obtaining geophysical logs focused on gathering information along a series of dip- and strike-oriented lines to develop stratigraphic cross-sections. Where appropriate, we used the same logs as previous stratigraphic studies. Key information gathered from previous studies included analysis of paleontology data, estimates of age of deposition, mapping of depositional systems, identification of flooding surfaces (explained in Section 6), and delineation

of geologic formations. As the logs were being collected along the dip-oriented and strike-oriented lines, additional logs were collected between the lines to fill in areas to benefit the generation of sand and facies maps and the correlation of stratigraphic surfaces across the study area.

A primary consideration in our log selection was a starting depth above 300 feet below ground surface. This consideration significantly reduced the number of candidate well logs because many drilling operations are not interested in characterizing the zone of fresh water that is cased off during the construction of an oil well.

#### ***4.2.1 Geophysical logs' Sources***

At the beginning of the project, the initial search for suitable logs focused on the logs that had been used as part of four previous aquifer studies. Two of these studies are considered to be among the landmark studies of the Texas Gulf Coast Cenozoic. These studies were performed by Dodge and Posey (1981), whose study focused on the Tertiary-age deposits, and by Morton and others (1985), whose study focused on Miocene-age deposits. A third study provided a detailed chronostratigraphic analysis of the Yegua and Jackson Aquifers (Knox and others, 2006). A fourth study was a detailed chronostratigraphic analysis of the southern Gulf Coast Aquifer by Young and others (2010).

All of the logs selected from the four previous studies were combined with additional logs from our generalized search through the professional literature. Our search for logs included a review of maps and databases from the BEG, TWDB, the Texas Commission on Environmental Quality (TCEQ), the Texas Railroad Commission, and the Bureau of Ocean Energy Management, Regulation and Enforcement (BOEMRE), which was formerly known as the U.S. Mineral Management Service (MMS). Additional logs were also assembled from the USGS offices in Austin and several private companies including The Subsurface Library.

#### ***4.2.2 Geophysical Logs Selected for the Study***

Figure 4-4 shows the locations for approximately 800 logs that were used for our study. Out of the 800 logs, approximately 125 logs were analyzed as part of the TWDB study of the southern Gulf Coast (Young and others, 2010). Appendix A provides the information listed in Table 4-2

for the 666 logs for which lithologic or stratigraphic picks were made as part of this study.

Appendix B provides the stratigraphic contacts made by Dr. Ewing for this study.

**Table 4-2 Selected tables and fields from the Microsoft Access database used to manage information on the 665 well logs analyzed for the study.**

<b>Field Name</b>	<b>Description</b>
API number	American Petroleum Institute (API) identification number.
NAD27 latitude	Latitude based on North American Datum 1927.
NAD27 longitude	Longitude based on North American Datum 1927.
Dip section/position	If blank, the log is not associated with a dip cross-section. Otherwise, the dip number is listed, and the position of the log is counted from a northwest-to-southeast sequence.
Strike section/position	If blank, the log is not associated with a strike cross-section. Otherwise, the strike number is listed, and the position of the log is counted from a southwest-to-northeast sequence.
Company	Company operating the oil or gas lease.
Lease	Land parcel being leased for use of the oil or gas well.
County	County (Texas) or Parish (Louisiana) in which the lease is located.
State	Texas or Louisiana
Lithology and water quality data	Indicates whether lithology picks and water quality interpretations were performed on the well log.
Paleo data	Indicates whether paleo data are associated with the log.

### 4.3 Literature Review

A review of existing literature uncovered some key studies important to this investigation. The GAT maps, compiled as the Geologic Map of Texas (Barnes, 1992) provided surface outcrop data. Stratigraphic unit geometries and approximate depths were obtained from the cross-section sets of Dodge and Posey (1981) and Morton and others (1985). General structural features for the Gulf coast were obtained from the Tectonic Map of Texas (Ewing, 1991) and from papers within Jones and Freed (1996). More specific structural information was obtained from Galloway and others (1982; 1986). Numerous stratigraphic studies were valuable in assessing depositional setting, facies, and systems, including Galloway and others (1986), Morton and others (1988), Hoel (1982), Coleman (1990), Solis (1981), Knox and others (2006), Hernández-Mendoza (2008), and Galloway and others (2000). Aquifer studies that were reviewed included Baker (1979) and county water resource studies by USGS and TWDB, including Rogers (1967), Shafer (1960, 1965, 1968, 1970, 1974), Loshkot and others (1982), Hammond (1969), Marvin and others (1962), Harris (1965), Thompson (1966), Peckham (1965), Anders and Baker (1961),



Anders (1957), Dale (1952), Mason (1963), Myers and Dale (1961, 1966), Shafer and Baker (1973), Reeves (1967), Myers and Dale (1967), Baker, R.C., and Dale (1961), McCoy (1990), and Chowdhury and Mace (2007). Paleontological and chronological data from Paleo-Data, Inc. (2009) and from Galloway and others (2000) were referenced to establish the chronostratigraphic framework for this study.

#### **4.4 Paleontology Data**

Paleontologic data are critical for defining geologic ages of stratigraphic intervals and surfaces. These data are collected during the drilling of oil and gas wells, and are more commonly associated with exploration drilling. Because the stratigraphic interval of the Gulf Coast Aquifer only produces hydrocarbons in the area beyond the current shoreline, the most useful data come from wells near the Texas shore and beyond. A collection of paleontologic data in digital form was obtained from the BEG, The University of Texas at Austin. The data are from wells drilled before 1980 either on land or within Texas submerged lands, which includes bays and the offshore area within 3 miles of the shoreline. For wells drilled beyond this area, data were collected from the MMS. These data are available digitally from the Bureau of Ocean Energy Management, Regulation and Enforcement website (<http://boemre.gov>).

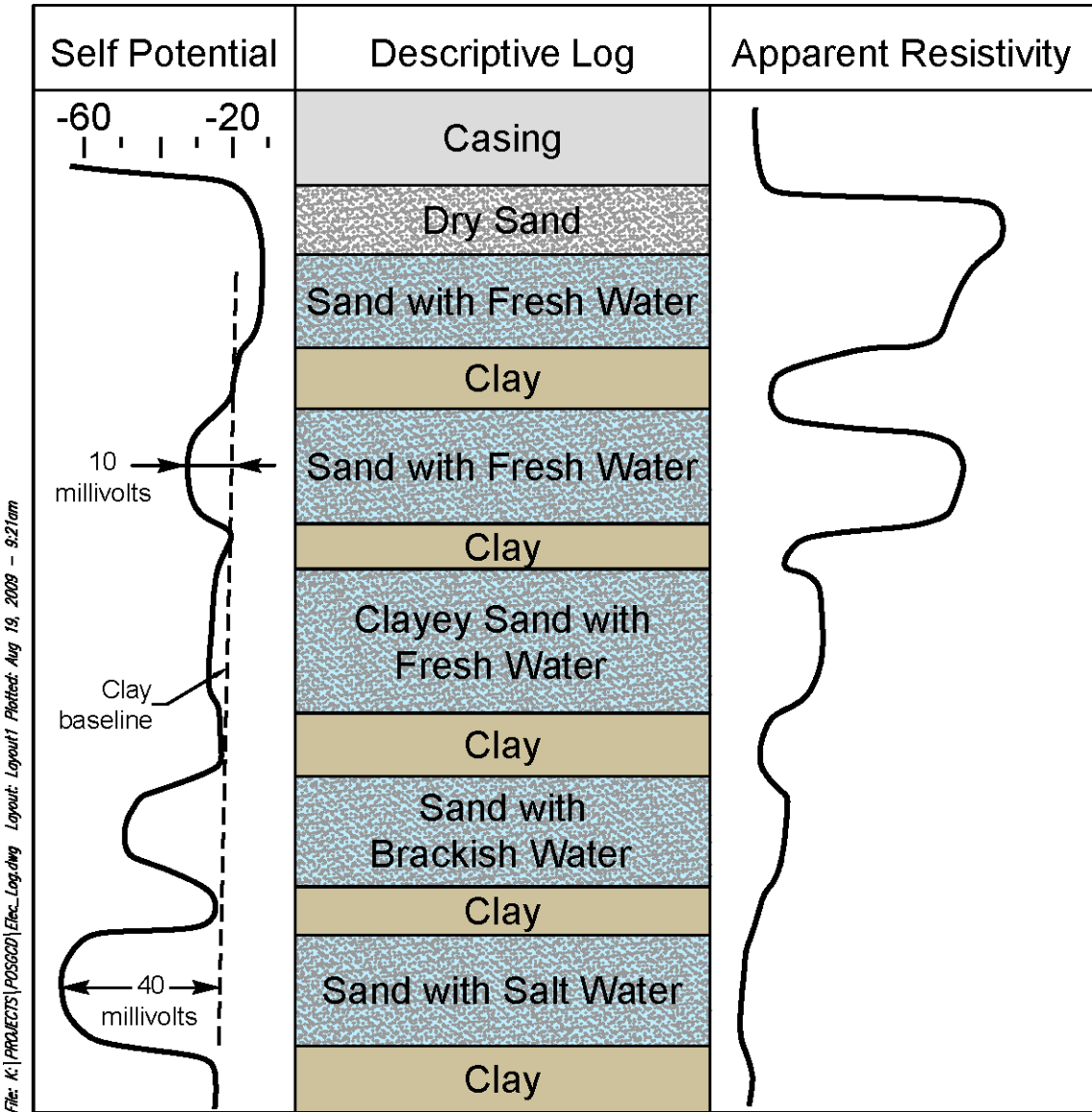


**Figure 4-1** Idealized SP and resistivity curve showing the responses corresponding to alternating sand and clay strata that are saturated with groundwater that has significant increases in total dissolved concentrations with depth. Modified from Driscoll (1986).

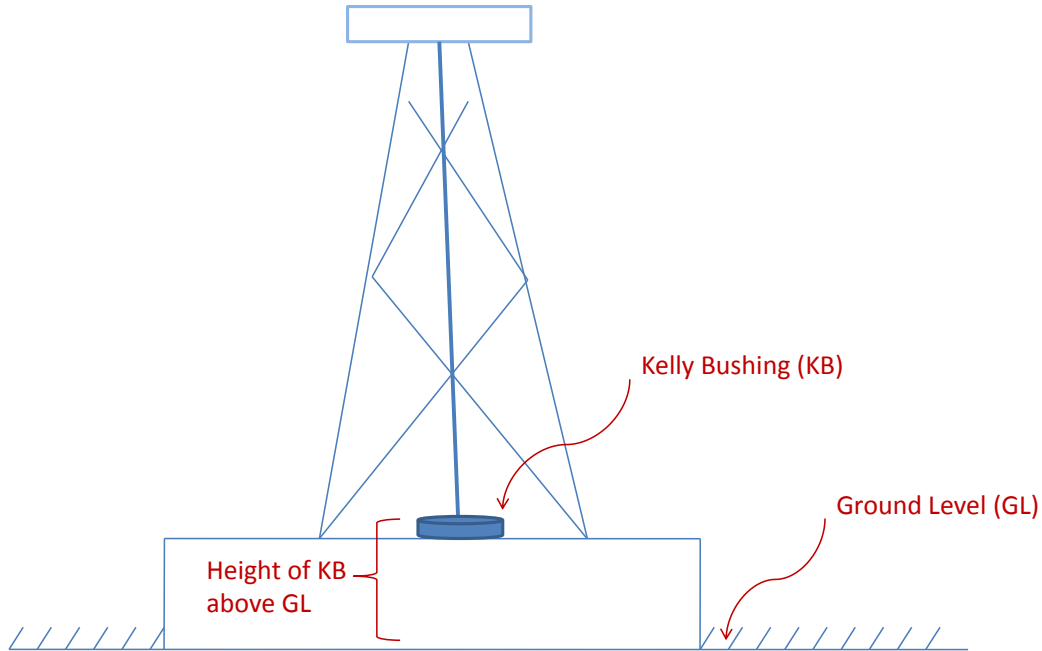


Figure 4-2 Schematic showing the location of the Kelly Bushing relative to the ground level and the oil rig.

FINAL LOG		DUAL INDUCTION-SFL	
Schlumberger		WITH LINEAR CORRELATION LOG	
COUNTY: HIDALGO	WEST JEFFRESS	COMPANY: COASTAL OIL & GAS CORPORATION	WELL: YTURRIA
LOCATION: YTURRIA LAND & CATTLE CO. #3	FIELD: W. JEFFRESS, W. (Vicksburg V)	WELL: NFD-L (2" - 100') API # 215-31708	WELL: YTURRIA #3
LOCALITY: 5825' ENCL & 660' ENCL OF THE ANTONIO M. CANO SURVEY, A-81, PORC. 44	STATE: TEXAS	LOGGERS: YOUNG, WAVEFORM, CYBERLOOK, HDT, CBL/VDL	
Permeation Datum: G.L.	Elev. 320.9	Elev.: K.B. 348.6	D.P. 342.6
Log Measured From: K.B.	22.7 Ft. Above Perm. Datum		G.L. 320.9
Drilling Measured From: K.B.			
Date	13-SEPT-86	27-SEPT-86	10-OCT-86
Run No.	ONE	TWO	THREE
Depth-Driller	6446	10906	12506
Depth-Logger (Sckl.)	6452	10442	12501
Run Log Interval	6446	10436	12501
Top Log Interval	3024	6430	10553
Casing-Driller	13-3/8 3025	8-62 6446	7-5/8 @ 10553
Casing-Logger	3024	6450	10553
Bit Size	12-1/8	8-7/8	6-3/4
Type Fluid In Hole	CLS	OIL BASE	OIL
Dens. Visc.	12.8 39.0	16.3 46.0	17.0 52.0
pH	10.5	6.2	ml
Source of Sample	CIRC PIT		OIL BASE
Km @ Mass Temp.	4.63 @ 120°		
Km @ Mass Temp.	1.31 @ 75°		
Source: Knt / Mass	PRESS CHART		
Km @ BHT	311 @ 182°		NOT AVAIL
Circulation Stopped	12:00 9/13	01:00 9/27	15:30 10/10
Logger on Bottom	16:30 9/13	10:00 9/27	21:00 10/10
Max. Rec. Temp.	204	252	299
Equip. Location	8406 EDIN	8246 EDIN	8406 EDIN
Recorded by	P. BERRIE	RUGG	BERRIE
Witnessed by	G. SANDEFUR	SANDEFUR / ZOMEN	SANDEFUR / ZOMEN

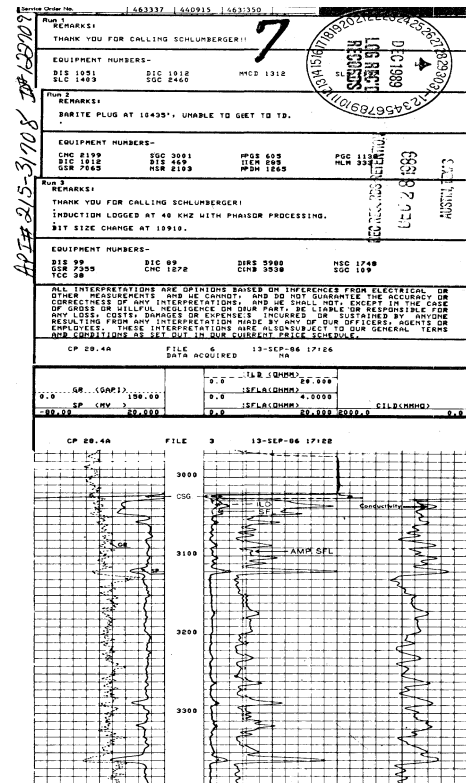
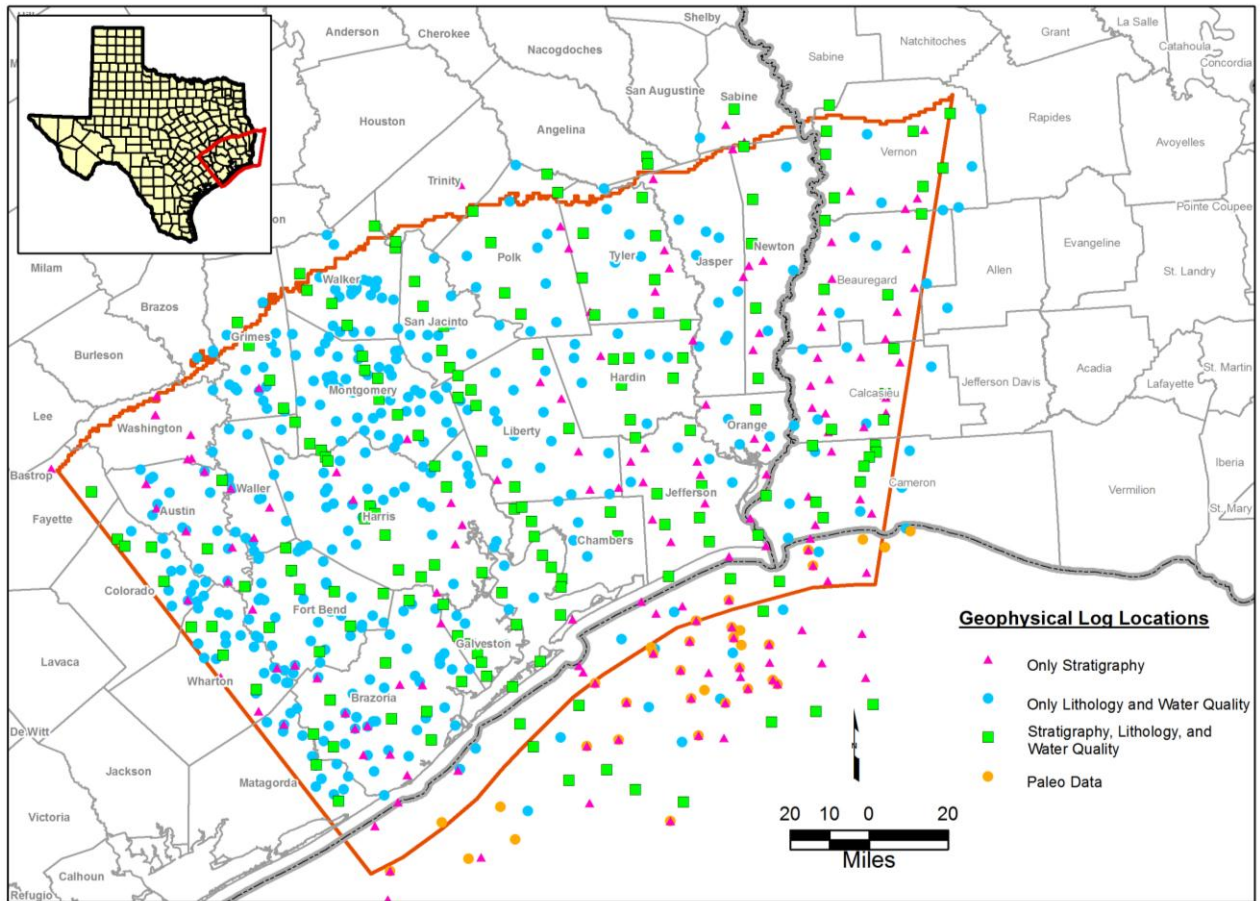


Figure 4-3 Example of a geophysical well log that uses the American Petroleum Institute format.



**Figure 4-4** Location of the approximately 800 logs used to characterize the stratigraphy and lithology of the northern portion of the Gulf Coast Aquifer System.

*This page intentionally left blank.*

## **5.0 Approach for Stratigraphic Interpretation**

This section identifies the geologic units that comprise the Chicot, Evangeline, and Jasper Aquifers and the Burkeville confining unit. For each of these units the maps of the base elevations and total thickness is provided.

### **5.1 Chronostratigraphic Conceptual Framework**

Modern techniques for stratigraphic correlation and mapping are based on the principles of sequence stratigraphy, which integrate depositional systems with chronostratigraphically significant surfaces (Van Wagoner and others, 1990). Chronostratigraphy (time-stratigraphy) deals with the age relationships of stratigraphic layers and surfaces. Sequence stratigraphy emphasizes surfaces of widespread extent that bound sedimentary packages (sequences) formed during a specific time period in related depositional environments. An example of related depositional environments would be a fluvial system connected to a delta with flanking bay-lagoon systems (e.g., Figure 2-21). Chronostratigraphic surfaces typically are not precisely synchronous throughout their extents, but they do separate layers of differing ages and depositional environments. Within the discipline of sequence stratigraphy, there are various interpretive models, but the fundamental components – related depositional facies bounded by chronostratigraphic surfaces – are determined objectively and are common to all models (Catuneanu and others, 2009).

For the purpose of defining layers in the Gulf Coast Aquifer, there are two key chronostratigraphic surfaces: erosional unconformities and marine flooding surfaces. In sequence stratigraphy, unconformities are surfaces separating younger from older strata along which there is evidence of erosional truncation or down cutting (Van Wagoner and others, 1990). In the Gulf Coast Aquifer, most unconformities are formed where fluvial systems have eroded valleys into older sediments (incised valleys). Marine flooding surfaces are created by relative sea-level rise and transgression of the coastal plain. Marine transgressions, which may also be erosive, are generally accompanied by interruption in the supply of sandy sediment and formation of muddy marine facies (Galloway and Hobday, 1996). The maximum flooding surface is a special type of marine flooding surface that marks the most widespread extent of coastal transgression (Figure 5-1).

Marine flooding surfaces make good boundaries for aquifer layers. Flooding surfaces are enclosed in mud-dominated layers (marine facies), are laterally extensive, and produce distinctive signatures on well logs. Marine facies associated with flooding surfaces commonly contain fossils with well-documented extinction times, which are useful for global chronostratigraphic correlation (biostratigraphic zonation). Flooding surfaces bound genetic stratigraphic sequences formed during progradational depositional episodes (see Section 2.4, Depositional history). In the Gulf Coast Aquifer, progradational systems are dominated by fluvial sand and related nonmarine facies (Figure 5-1). Thus, flooding surfaces lie within regionally correlative, mud-dominated layers that enclose sand-prone layers. Sand bodies may be interconnected within these layers but are rarely interconnected across flooding-surface boundaries. Marine flooding surfaces, however, are not perfect aquifer layer boundaries. Transgression and marine flooding often do not extend across the entire coastal plain. Fluvial depositional systems may persist uninterrupted in one area while marine transgression is occurring in another area. Furthermore, all marine flooding surfaces have limits to their landward extents (Figure 5-1).

Although marine flooding surfaces are useful for tracing aquifer layer boundaries, depositional facies modeling and mapping are needed to characterize hydrogeologic properties within layers. The depositional environment controls intrinsic aquifer-matrix properties – porosity, permeability, and mineral composition – as well as larger-scale aquifer storage and flow properties related to sand-body size, shape, orientation, and interconnectivity. In a fluvial depositional system, for example, channel-fill sand bodies are elongated in the direction of depositional dip (coastward) (Figure 2-20). In the Gulf Coast Aquifer, regional structural dip and hydraulic gradient parallel fluvial sand-body elongation, enhancing the potential for coastward groundwater flow. In sand-dominated fluvial systems, such in some regions of the Lissie Formation, sand bodies are highly interconnected, whereas in sand-poor fluvial systems, such in some regions of the Beaumont Formation, sand bodies are more isolated in floodplain muds. In marine shore-zone depositional systems, strand-plain and barrier-island sand bodies are elongated perpendicular to the regional hydraulic gradient and are located at the interface between meteoric fresh waters and marine saline waters. Thus, shore-zone sand bodies are commonly sites of groundwater mixing and saltwater intrusion. Post-depositional controls – compaction and intergranular cementation – modify aquifer properties inherited from the

depositional environment. The Gulf Coast Aquifer, however, which is relatively young geologically and not deeply buried, has not been affected significantly by post-depositional processes.

Within sequence stratigraphy, the concept of depositional cyclicity provides a framework for regional stratigraphic correlation and layer definition. Deposition is inherently episodic, periods of coastal plain progradation alternating with relative sea-level rise and marine transgression (see Section 2.4, Depositional history). Depositional cyclicity is controlled by the interplay of varying sediment supply, sea-level fluctuation, climate, and subsidence. In the Gulf Coast Aquifer, a relatively constant rate of coastward increasing subsidence provided space for younger sediments to accumulate above older sediments without major interruption. The climate of the Texas Coastal Plain also has not varied greatly during the depositional history of the Gulf Coast Aquifer. Uplift of the Rocky Mountains and other tectonic events provided a relatively continuous supply of sediment for rivers to transport to the coast, although the location of sediment input onto the coastal plain varied (Figure 2-22). Sea-level fluctuation, on the other hand, has been cyclic, rising and falling at rates in response to the formation and melting of glaciers. For the Gulf Coast Aquifer, the combination of localized sediment input and sea-level fluctuation has created systematic depositional cycles of sand-prone progradational facies alternating with mud-dominated transgressive facies (Figure 5-1).

Depositional cycles occur at various scales. A geologically brief depositional cycle, commonly called a parasequence, records a single, usually localized, progradational event followed by transgression (Van Wagoner and others, 1990; Galloway and Hobday, 1996). Parasequences range in thickness from about 10 to 200 feet and in lateral extent from about 10 to 2,000 square miles (Van Wagoner and others, 1990). A parasequence is composed of beds of sand or mud, each a few feet to a few tens of feet thick, which record single depositional events produced by storms or floods. Sandy beds within a parasequence extend progressively farther seaward as the fluvial-deltaic system progrades the shoreline. Rising sea level and diminished sediment supply combine to halt shoreline progradation and drown the coastal plain, capping the parasequence with a veneer of transgressive mud. Commonly, parasequence deposition is terminated when the fluvial-deltaic system moves to an adjacent part of the coastal plain. The process of lateral



migration of fluvial-deltaic systems eventually creates a regionally continuous wedge of coastal plain sediments composed of amalgamated parasequences.

Parasequences stack to form sequences of increasing scale and duration. Large, long-term sequences record the entire GOM Tertiary fill, but the most commonly described sequences span 1 to 5 million years, range widely in thickness from about 30 to 5,000 feet, and cover 500 to 30,000 square miles (Van Wagoner and others, 1990). The Gulf Coast Aquifer encompasses about 10 such sequences, corresponding to major depositional episodes and covering a time span of about 24 million years (Galloway and others, 2000) (Figure 2-23). The duration of Gulf Coast sequences generally decreases through time in response to increasingly high-frequency sea-level fluctuations (Figure 2-23). As defined by Galloway and others (Galloway, 1989b; Galloway and others, 2000), Gulf Coast sequences are bounded by maximum flooding surfaces and are composed of sets of parasequences displaying alternating progradational and retrogradational (transgressive) stacking patterns (Figure 5-1). Sequences are hierarchical – shorter, more localized sequences group to form longer more widespread sequences – and the conceptual framework of sequence stratigraphy can be adapted to fit the scale of resolution allowed by the available data (Catuneanu and others, 2009). The upper Goliad sequence, for example, may be further subdivided based on distinctive parasequence stacking patterns, similarity of depositional systems, and/or areal extents of flooding surfaces.

## **5.2 Methodology**

The methodology that we used to define and characterize layers in the Gulf Coast Aquifer is based on chronostratigraphic correlation and well log lithologic determination and has been developed and refined in similar studies of Texas coastal aquifer systems (Knox and others, 2006, 2007; Young and Kelley, 2006; Young and others, 2010). The basic work flow involves: 1) identification and correlation of flooding surfaces; 2) ranking of flooding surfaces and selection of aquifer layer boundaries; 3) systematic correlation of layers throughout the study area using a grid of cross sections; and 4) facies-based sand mapping within aquifer layers.

The task of identification and correlation of flooding surfaces started with the large scale and progressed toward smaller scales and higher resolutions (more numerous and thinner layers). Geophysical well logs were the basic data for stratigraphic correlation and lithologic

interpretation. First we reviewed previous studies in the geologic literature (see Section 3, Stratigraphic and Hydrogeologic Framework) and used their correlations and sequence interpretations as a starting point. Then we identified and correlated the most laterally extensive flooding surfaces, such as those that bound the major depositional episodes (Figure 2-23). Using well log pattern recognition and trial and error, we searched out additional flooding surfaces to further subdivide the sequences into aquifer layers. To systematize and control the quality of this process, we constructed a grid of dip- and strike-oriented cross sections across the study area (Figure 1-1). A goal was to develop chronostratigraphic surfaces for the same geologic units delineated by Young and others (2010) for the southern portion of the Gulf Coast Aquifer System.

Marine flooding surfaces, as previously discussed, are rarely as continuous as we would like, and so techniques must be applied to extend correlations beyond their limits. Near the coast and offshore, Miocene to Holocene sequences contain abundant marine facies and flooding surfaces, in which biostratigraphic zonation is well defined (Lawless and others, 1997; Fillon and Lawless, 2000). As we correlate these flooding surfaces landward, however, they grade into nonmarine facies and lose their distinctive well log signatures as well as marine biostratigraphic age control (Figure 5-2). In fluvial systems updip, depositional episodes commonly begin with erosion, followed by deposition of amalgamated channel sands (Galloway and others, 1986). Following the technique of Galloway and Morton (Galloway and others, 1986; Morton and others, 1988), we correlated the basal flooding surfaces updip as far as possible and then extended correlations toward the outcrop along the bases of major channel sands. In the Gulf Coast Aquifer, basal channel sands represent the initial pulse of a progradational sequence following marine transgression, even though no record of the transgression remains in updip areas.

The final step in the correlation process was to trace boundaries to outcrop. As we discussed in Section 3.1, previous studies, subsurface-to-surface correlations are difficult and still uncertain after many decades of geologic investigation (DuBar and others, 1991). Outcrop mapping is based on lithologic changes, soil characteristics, and topographic expression, whereas our subsurface correlations are based on chronostratigraphy and depositional systems. Nevertheless, we tied layer boundaries from the subsurface to outcrop contacts by: 1) referring to previous studies that established the general correspondence between outcrop and subsurface;

2) projecting correlations updip from the wells closest to the outcrop while maintaining inclinations (dips) established in the subsurface; and 3) projecting outcrop contacts downdip using dips measured at the surface (Figure 5-2).

A discussion of the differences between chronostratigraphic and lithostratigraphic correlation techniques is in order. Until the 1980s, most well log correlation was lithostratigraphic, but with the advent of sequence stratigraphy, new conceptual tools became available to correlate layers that may display varying lithologies but were deposited during a specific time interval under distinct environmental conditions. Such chronostratigraphic layers are more likely to be internally integrated, hydrogeologic systems. Lithostratigraphic correlation relies on the interpretation from well logs of formation lithologies and boundaries between different lithologies (mud on sand, for example) and then correlating those boundaries between wells. A thick marine shore-zone sand, for example, would be correlated to other thick marine sands based on lithology and position within the vertical profile (Figure 5-3). It is now known that, owing to depositional cyclicity and the offlapping nature of many facies, sands that apparently form a continuous sheet are actually separated laterally by thin fine-grained layers or veneers (Figure 5-3). Thus, lithostratigraphic correlation may result in overestimation of sand-body or clay-body continuity and/or miscorrelation of sand or clay bodies of differing ages. In general and in practice, however, the differences between the two techniques are more subtle than the extreme case illustrated in Figure 5-3, and in some cases lithologic boundaries coincide with chronostratigraphic surfaces. Pioneering work by Baker (1979) and others (see Section 3.1, Previous Studies) established accurate stratigraphic frameworks using lithostratigraphic correlation combined with a good understanding of geologic processes.

As part of this project, the software package called PETRA (IHS, 2009) was used to organize and help analyze the geophysical logs. PETRA was used to associate geophysical logs to the dip-oriented and strike-oriented cross-sections show in Figure 1-1 and to large print-out of cross-sections. The cross-sections include profiles of the geophysical logs and were used to help identify new stratigraphic picks, confirm previous stratigraphic picks, and to check the stratigraphic surfaces for consistency. Checking of the stratigraphic surfaces included assessing impacts of nearby salt features (domes and pillars) and faults, calculating the thicknesses of the

marked geologic units, placing paleomarkers into the stratigraphic chronologic column, and checking the dip angle between log picks.

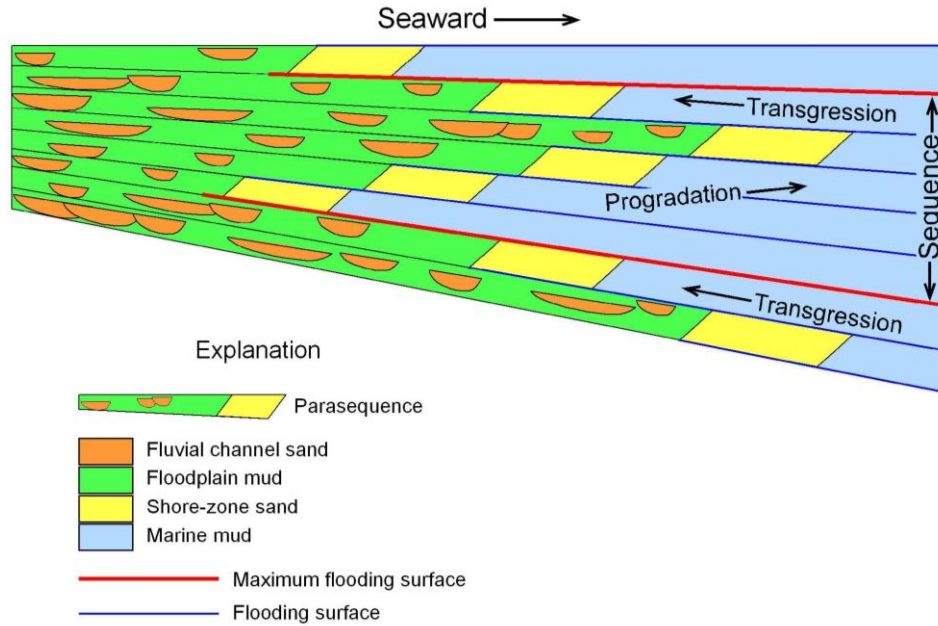


**Figure 5-1 Schematic cross section showing small-scale depositional cycles (parasequences) and larger-scale sequence bounded by maximum flooding surfaces.**

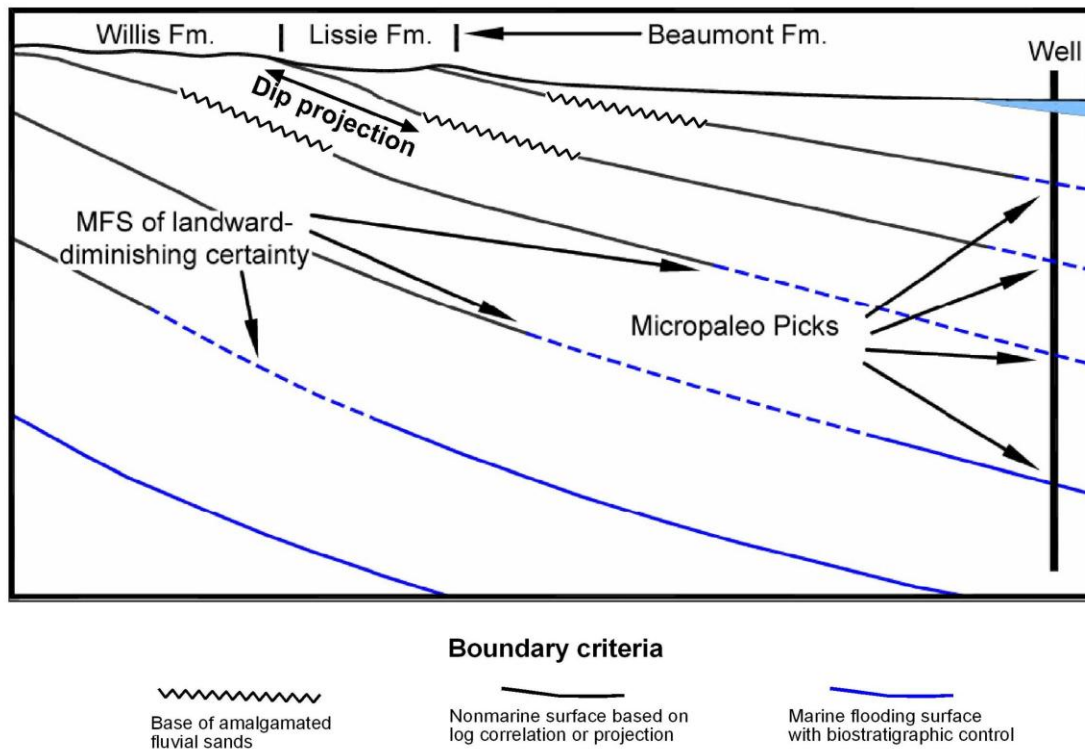


**Figure 5-2 Schematic cross section showing correlation strategies.** Maximum flooding surfaces (MFS) are the correlation boundaries of choice in the marine region but must be replaced in the nonmarine region with well log correlation, tracing channel bases, and dip projection. Modified from Knox and others (2006).

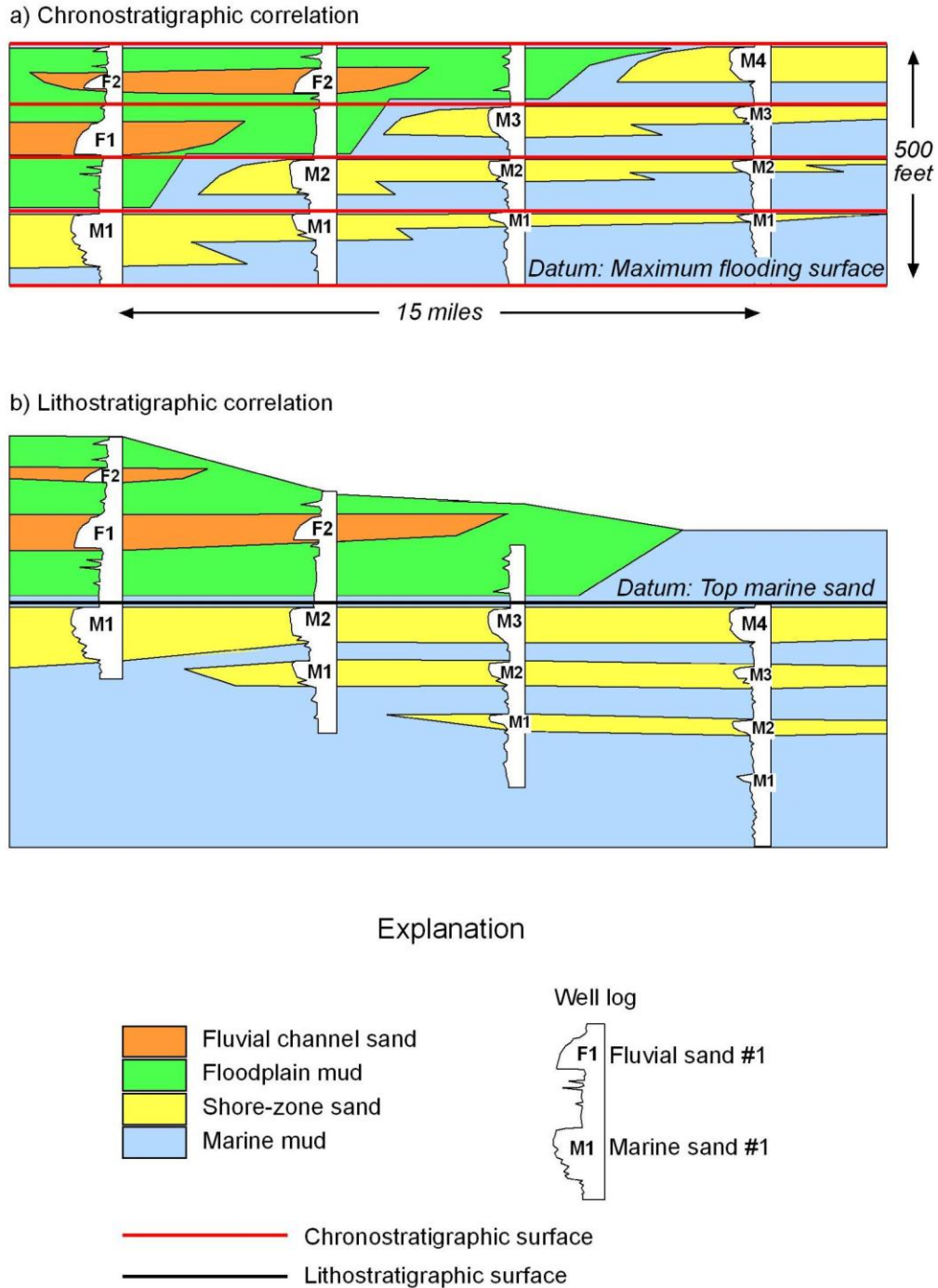


**Figure 5-3 Schematic cross section comparing (a) chronostratigraphic correlation to (b) lithostratigraphic correlation.** Identical (hypothetical) well logs are used in both sections, but their vertical positions are shifted to line up correlated sands. Sands are numbered to show the correct correlations. Using lithostratigraphic correlation, the top of the thickest marine sand is incorrectly assumed to be a continuous surface, whereas chronostratigraphic correlation uses marine flooding surfaces in a progradational context to correctly correlate the sands. Modified from Van Wagoner and others (1990).

*This page intentionally left blank.*

## **6.0 Gulf Coast Aquifer Stratigraphy**

This section presents the geologic units that comprise the Chicot, Evangeline, and Jasper Aquifers and the Burkeville confining unit. For each of these units the maps of the base elevations and total thickness is provided.

### **6.1 Chronostratigraphic Surfaces and Aquifer Boundaries**

The Gulf Coast Aquifer is comprised of, from shallowest to deepest, the Chicot Aquifer, the Evangeline Aquifer, the Burkeville Confining System, and the Jasper Aquifer. In this study, aquifer units have been further subdivided on the basis of chronostratigraphic correlation to yield subaquifer layers. These layers are bounded by clay-dominated facies deposited during a sequence or parasequence flooding event. The layers consist of formations or parts of formations that have been historically considered part of a given aquifer. Formation boundaries were traced from outcrop boundaries provided by Barnes (1992) to identifiable flooding surfaces in the deeper subsurface, where paleontologic control constrained geologic ages of surfaces.

Figure 6-1 shows the relationship of chronostratigraphic units used in this study with respect to aquifer boundaries, paleontologic markers, geologic age, and epoch. The Chicot Aquifer includes, from the shallowest to deepest, the Beaumont and Lissie Formations of Pleistocene age and the Pliocene-age Willis Formation.

The Evangeline Aquifer includes the upper Goliad Formation of earliest Pliocene and late Miocene age, the lower Goliad Formation of middle Miocene age, and the upper unit of the Lagarto Formation (a member of the Fleming Group) of middle Miocene age.

The Burkeville unit historically has been defined by lithology. As noted by Baker (1979) the Burkeville unit transverses several geological formations and represents the low permeability deposits that lie between the Jasper and the Evangeline Aquifers. This definition is difficult to apply objectively to this study because the unit is not defined such that it could be comprised of deposits from one or more chronostratigraphic unit. For this study, the Burkeville unit is associated with the middle unit of the Lagarto Formation of middle and early Miocene age. The middle Lagarto Formation was identified by Young and others (2010) as having the lower sand content than either the lower and upper Lagarto Formations.



The Jasper Aquifer, as defined by Baker (1979) and reiterated by Chowdhury and Mace (2007), includes a sandy clay section below the highly clayey section of the Burkeville Confining System, the Oakville Sandstone of the Fleming Group, and sandy sections of the Catahoula Tuff and Catahoula Sandstone. For this study, the Jasper Aquifer is defined as including the lower Lagarto unit of early Miocene age, the early Miocene Oakville sandstone member of the Fleming Group, and the sandy intervals of the Oligocene-age Catahoula Formation. Elevations from the established base Jasper surface in the SWAP dataset were used close to the outcrop and were merged with the chronostratigraphic base of the Oakville Sandstone defined in this study.

The lowermost clayey unit of the Catahoula Formation, sometimes mapped in outcrop as the Frio Clay and equivalent in age to the Vicksburg Formation of the subsurface (Galloway, personal communication, 2009), is treated in this report as part of the Catahoula Confining System and is therefore not part of the Jasper Aquifer.

## **6.2 Structural Configuration of Surfaces**

Our primary study area was from the Brazos River eastward to westernmost Louisiana. Within this area we constructed 12 regional Gulf Coast dip sections at roughly 12-mile intervals, using logs that cover as much of the post-Jackson section as possible. Average control spacing was approximately one well every 3-4 miles along each dip section. Correlations were performed using both hardcopy log comparisons and examination of the computer-drafted uncorrelated section of the top 8,000 ft of section.

Geologic units in the Gulf Coast Aquifer system dip east or southeast toward the coast at a direction roughly perpendicular to the local shoreline. Consequently, the strike of geologic units is approximately parallel to the shoreline. Units also thicken toward the coast. Older units dip more steeply because of the accumulated subsidence and tilting since their deposition. Growth faults occur frequently in Gulf Coast geologic units and are most pronounced near the paleo-shelf margin of a geologic unit (the geomorphic shelf edge as the unit was being deposited). The shelf margin has grown toward the center of the Gulf of Mexico over time, so that growth faults of older units are well inland, and growth faults in units being deposited today are several tens of miles offshore (see Figures 2-2 and 3-2). Growth faults do not significantly impact the freshwater portions of the Gulf Coast Aquifer but may offset deeper parts of the Evangeline

Aquifer, Burkeville Unit, and Jasper Aquifer. Some older growth faults have continued to move slightly, and units within the Gulf Coast Aquifer may be impacted by localized changes in dip angle. Salt and shale movement and diapirism also modify structure under the Gulf Coast Aquifer system (see section 2.2.2 Salt Domes in Southeast Texas and Southwest Louisiana).

Figure 2-8 shows the locations of 67 salt domes in the study area. Based on our literature review, there is a wide-range of potential impacts from the salt dome activity on stratigraphic surfaces and groundwater flow. Some salt and shale activity has had no effect on Gulf Coast Aquifer layers, while other activities may have created localized areas of higher elevations in the lower layers of the aquifer. Still other salt and shale movement significantly impacts localized areas of the aquifer to a very shallow depth (Hamlin, 2006).

Figure 2-10 illustrates the type of impacts that salt domes can have on the stratigraphy in the northern Gulf Coast Aquifer system. The figure shows in Fort Bend and Brazoria counties the stratigraphy near salt domes is warped and distorted. Near the salt domes the stratigraphic surfaces are several hundreds of feet higher than the corresponding surfaces several miles away. In Figure 2-10, the salt dome's impact on the stratigraphy is usually greater with an increase in depth with some stratigraphic offsets reaching values up to thousands of feet in the deeper formations.

Because the stratigraphy near salt domes is not reflective of regional stratigraphy, geophysical signatures that appeared to have been impacted by salt-tectonic effects were not used to create the final surfaces. During the process of developing stratigraphic surfaces from the picks in Appendix B, we compared localized differences in surface elevations to maps of salt dome locations to help highlight areas of concern. Where salt activity appeared to have impacted our stratigraphic picks, we removed the picks from those locations prior to developing the regional surfaces for this study.

The development of the stratigraphy surfaces began by developing surfaces for dip section 6 and working southwest to develop surfaces for dip sections 7, 8, 9, 10, and 11 (see Figure 1-1). The process provided us with surfaces that overlapped and could be compared to surfaces developed by Young and others (2010) for dip sections 8 through 11. Because the two sets of picks were not identical in the overlapping area, difference preferences were assigned to picks made by Mr.

Knox for the southern study and to picks made by Dr. Ewing for this study. To develop the surfaces for this study we used Mr. Knox's picks for dip sections 10 and 11 and gave Mr. Knox's picks preference for dip section 9. For dip sections 7 through -1 we used Dr. Ewing's picks and gave Dr. Ewing's picks preference for dip section 8. These preferences were given so that stratigraphic surfaces generated from this study would be consistent and match with the stratigraphic surfaces provided by Young and others (2010) at dip section 10. Thus, for the purposes of producing a comprehensive chronostratigraphic structure for entire Gulf Coast, the surfaces from Young and others (2010) should be used south of dip section 10 and surfaces from this study should be used north of dip section 10.

Our analysis at each dip section began with identifying the Anahuac shale wedge near the downdip extent of a dip section. To help identify the Anahuac shale, the paleomarker *Marginulina idiomorpha* was used to identify the top of Frio and paleomarkers *Heterostegina* sp. and *Bolivina perca* were used to help identify the maximum flooding surface. Above the Anahuac Shale additional marine shale wedges were identified with some assistance from paleomarkers and log patterns and correlated throughout their zone of development. These paleomarkers included the following:

- *Siphonina davisi* (within Oakville)
- *Marginulina* A (base of lower Lagarto)
- Lower extent of *Amphistegina* B (base of middle Lagarto as identified by a maximum flooding surface)
- Upper extent of *Amphistegina* B (base of upper Lagarto)
- *Cibicides opima* ( base of lower Goliad)
- *Textularia W stapperi* (base of upper Goliad)
- *Buliminella* 1 (Based of Willis as identified by a Pliocene marine shale )

Above the Goliad formation, the base of Willis was picked immediately above the Pliocene shale. This elevation was followed updip to the base along a surface that connect thick sand packages and then extrapolated landward following knowledge of regional dips (correcting for salt tectonic effects) to the Willis outcrop. The Lissie and Beaumont formations were picked in

the mostly continental sequence by projection down from outcrop, following the base of major sandy valley-fill packages where possible.

Figure 6-2 shows the structural contours on the base and the thickness of the Oakville Formation. The structural contours indicate a relatively consistent dip of 70 to 80 feet per mile from the updip extent to the coastline. Figures 6-3 through 6-8 provide a better view of the dip of the Oakville Formation across the study area. These figures show that despite the consistency among the dip angle in the figures there the Oakville does dip slightly more toward Louisiana than it does toward the mid-section of the Texas Gulf Coast. Figures 6-3 through 6-8 also show that the dip angles for each geological above the Oakville generally decreasing with age. For instance, the dip angle for the Willis formation, which is the base of the Chicot Aquifer has a relatively consistent dip of 15 to 20 feet per mile from it updip extent to the coast.

An important feature of the cross-sections in Figures 6-3 through 6-8 is that across most of the northern Gulf Coast the two uppermost units ( the upper Goliad and lower Goliad Formations) of the Evangeline Aquifer do not outcrop. Instead, the updip boundary of these units terminate and pinch out into the Willis Formation. These pinch outs as well as pinch outs for other geologic units occur because of changes in subsidence rates (both through time and across the study area), eustatic sea level, and sediment supply, deposition of the various stratigraphic units of the Gulf Coast Aquifer deposits over time. In general terms, a geologic unit outcrops if it reaches ground surface and a geologic unit subcrops it if terminates and pinches out into a younger unit above itself. Bates and Jackson (1983) define a "subcrop" and an "outcrop" as:

*Outcrop* – that part of a geological formation or structure that appears at the surface of the earth; also, bedrock that is covered only by surficial deposits such as alluvium.

*Subcrop* – An occurrence of strata in contact with the undersurface of an inclusive stratigraphic unit that succeeds an important unconformity on which overstep is conspicuous; a "subsurface outcrop" that describes the areal limit of a truncated rock unit at a buried surface of unconformity. (b) An area within which a formation occurs directly beneath an unconformity.

The most pronounced areas in Figures 6-3 through 6-8 where subcrops occur are below the Willis Formation. These figures show that the erosional truncation of the units beneath the Willis generally becomes greater moving north from dip section 9 (Figure 6-3) toward dip section -1 (Figure 6-8). In dip section 9 (see Figure 6-3), the Willis Formation prevents the outcropping of the upper and lower Goliad formations whereas in dip section -1 (see Figure 6-8) the Willis Formation prevents the outcropping of five formations (the upper and lower Goliad formations and the upper, middle, and lower Lagarto formations).

Figure 6-9 shows the variations in the base elevation and thickness of the geologic units along strike section B-B' shown in Figure 1-1. The figure shows that, along the strike, the base elevation of the Chicot Aquifer remains near -1100 ft msl but the base elevations of the Jasper and Evangeline Aquifer deepen toward the east. The base elevation of the Jasper Aquifer changes from about -5000 ft msl in the west to about -8000 ft msl in the east. In the west, the Evangeline Aquifer has a base elevation of about -3000 ft msl but has a base elevation of about -4800 ft msl in the east. In reviewing Figure 6-9, the reader should be aware of several issues regarding the irregular surfaces in the eastern portion of the Evangeline and Jasper Aquifer. These oscillations are not a result of well control but rather an artifact of how the raster surfaces have been sampled to by the strike sections. The oscillations occur at the resolution of the rasters, which is 4000 ft, and are an artifact of the stair-step manner at which elevations are picked off the raster to match the strike section.

In combination with Figure 6-2, Figures 6-10 through 6-20 provide the structural surfaces and thicknesses for the geologic formation and aquifers that comprise the Gulf Coast Aquifer system. Figures 6-2, 6-10, and 6-11 shows that pattern in the structural contours and total thicknesses of the Oakville Formation, the lower Lagarto Formation, and the Jasper Aquifer are very similar. For the purpose of this study, the updip boundary of the Jasper Aquifer is defined by the updip boundary for Jasper Aquifer as defined by the Source Water Aquifer Program for the Jasper Aquifer (Strom and others, 2003). As a result of this delineation, the Jasper Aquifer extends beyond the Oakville Formation and includes a portion of the Catahoula formation.

Figure 6-12 provides the structural contours and thicknesses for the middle Lagarto Formation, which is associated with the Burkeville confining unit. These structure contours have a similar

pattern to underlying units with a dip from 65 to 80 feet per mile. Across most of the formation, its total thickness is between 400 and 800 feet.

Structural contours and total thicknesses of the three formations of the Evangeline Aquifer – the upper Lagarto, lower Goliad, and the upper Goliad – are shown in Figures 6-13, 6-14, and 6-15, respectively. The base of the Evangeline Aquifer, which corresponds to the base of the upper unit of the Lagarto Formation, as well as the total thickness of the Evangeline are shown in Figure 6-16. These structural features are similar to those in underlying units but the thickness and updip extents exhibit considerable more variability than the deeper units. This variability is caused by the significant erosion of the Evangeline formations by the Willis formation. As shown in Figure 6-16, the erosion truncation of the upper Goliad Formation is greatest in Harris County and is associated with deposition associated with the Houston Embayment (see Figure 2-22). Because of the significant erosion of the Goliad units, the updip boundary of these units are difficult to locate accurately because they are subcrops.

Figures 6-17, 6-18, and 6-19 show the structural contours and thickness of the geologic unit that comprise the Chicot – the Willis, Lissie, and Beaumont Formations. Figure 6-20 provides structural contours on the base of the Chicot Aquifer as well as the total thickness of the aquifer. The structure contours for both the Willis and the Lisse Formations show indications of possible fluvial axes where concave contours exit. In the Willis Formation, sets of concave axes exist in Hardin and Chambers Counties. In the Lissie Formation, sets of concave axes exist in Cameron Parish.

Among the concerns with delineating the structural contours in the outcrops areas of all the formations is the scarcity of geophysical logs with coverage to within 200 feet of the ground surface and the lack of thickness information associated with the mapped outcrop locations (Barnes, 1992). These two concerns become most acute where the geological units flatten and are suspected of becoming relatively thin near the surface and where thin veneers of alluvium or reworked deposits exist at ground surface. Because of the unknown thicknesses and accuracy of the mapped surface geology, we did not match our outcrop boundaries to the farthest updip boundary of the formation shown in a surface geology map. Rather, we used the surface geology map to guide our placement of the updip boundary. As a rule, we tried to place the updip boundary within the most updip regions of a formation's mapped outcrop.

Placement of the updip boundary of formations that subcrop is based on interpretations of the surface geology map and where the base of the geological formation intersect the geological surface above it based on the extrapolation of the stratigraphic picks in Appendix B. Figure 6-21 illustrates the occurrence of a single subcrop. In this situation the subcrop pinches out to a zero thickness below an overlying unit directly above it. This occurs because an updip portion of the second youngest unit was eroded, truncated, then covered by the deposition of an overlying geologic unit. Figure 6-21a shows vertical cross-sections where a light brown geological strata pinches out in to a yellowish upper strata. Figure 6-21b shows the updip boundaries as either outcrop or subcrop boundaries for all of the colored strata shown in Figure 6-21a. In map view (looking downward upon the surface), a solid line and a dashed line in Figure 6-21b mark the locations where the updip boundary of the brown strata occurs as an outcrop and as a subcrop, respectively. The subcrop situation shown in Figure 6-21 is analogous to the upper Goliad formation pinching out beneath the Willis formation. Figure 6-22 shows the locations of updip extend estimated for the geological formations that comprise the Gulf Coast Aquifer. These locations were used as the updip boundaries for all of the structural contours and thickness plots generated in this study.

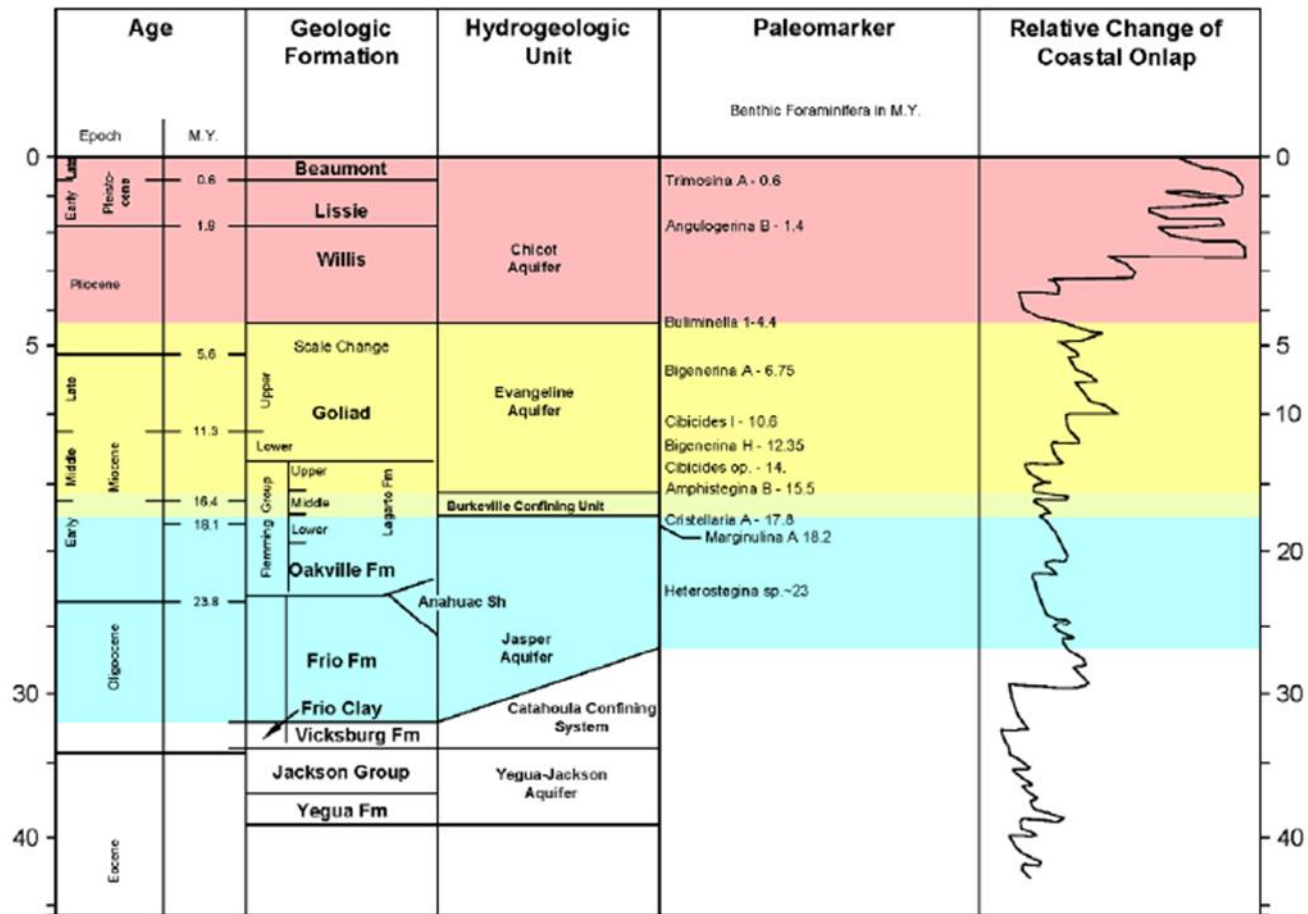
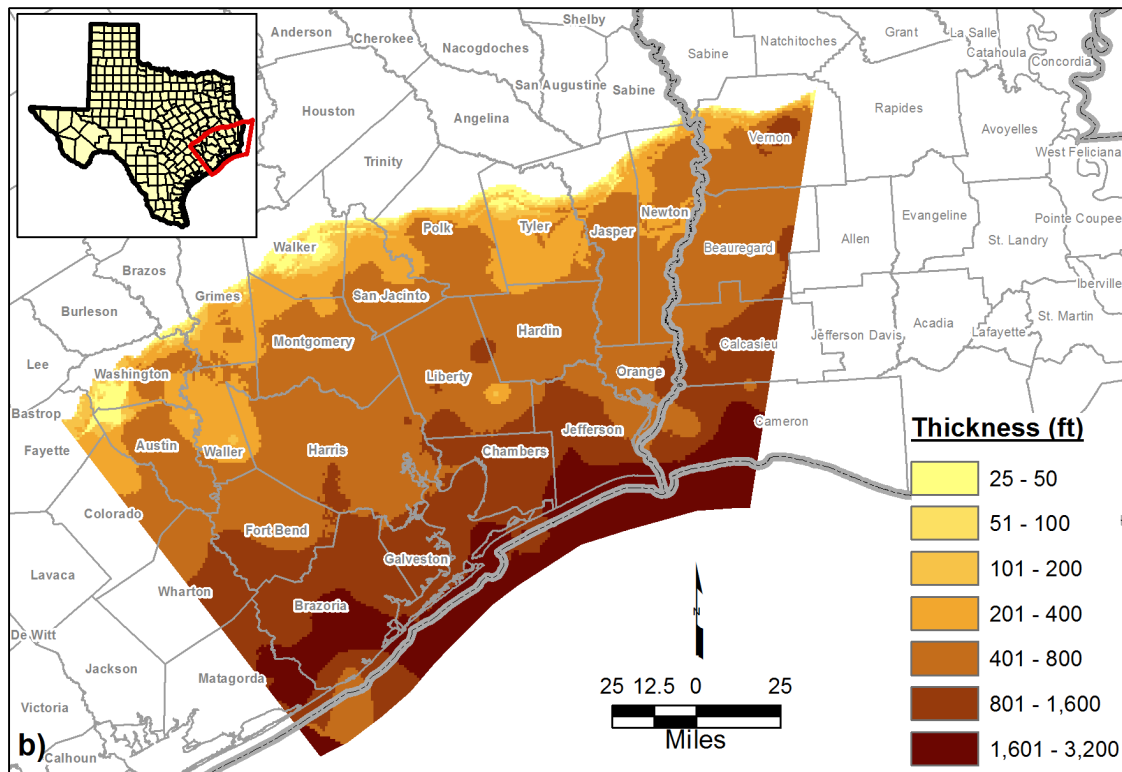
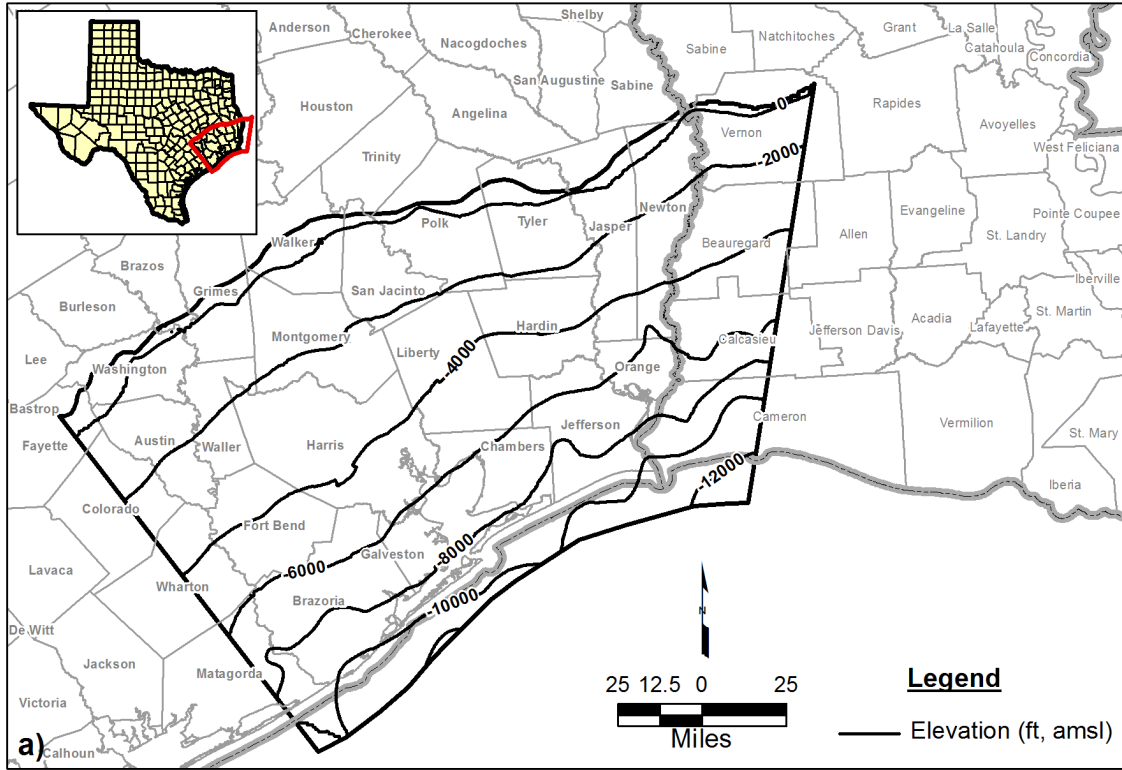


Figure 6-1 Stratigraphic column showing correlations among age, geologic formations, hydrogeologic units, paleomarkers, and relative change of coastal onlap.





**Figure 6-2** Contours for the Oakville geologic unit showing: (a) base elevation and (b) thickness.

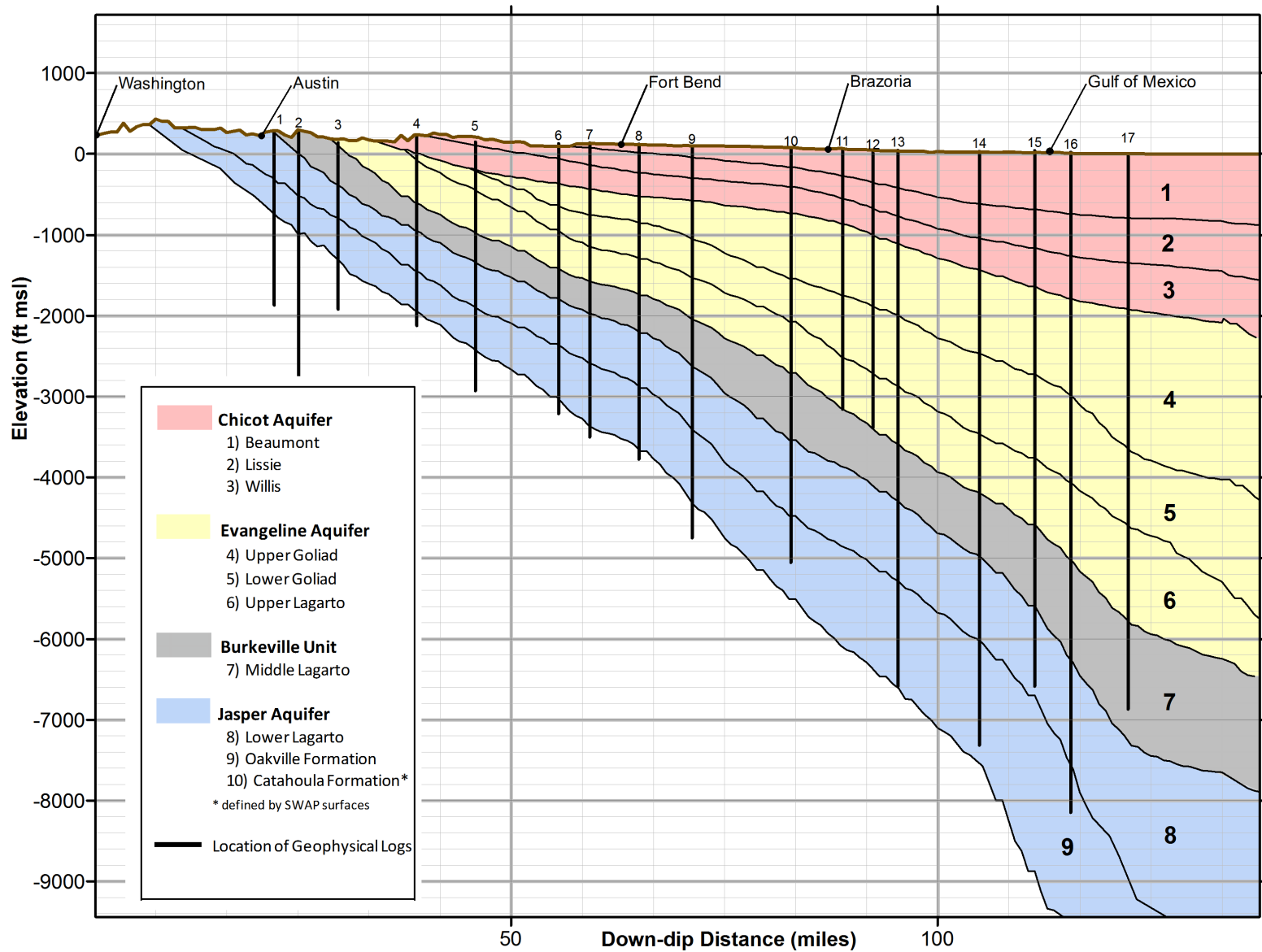


Figure 6-3 Vertical cross-section of the geological units near dip section 9 in Figure 1-1.

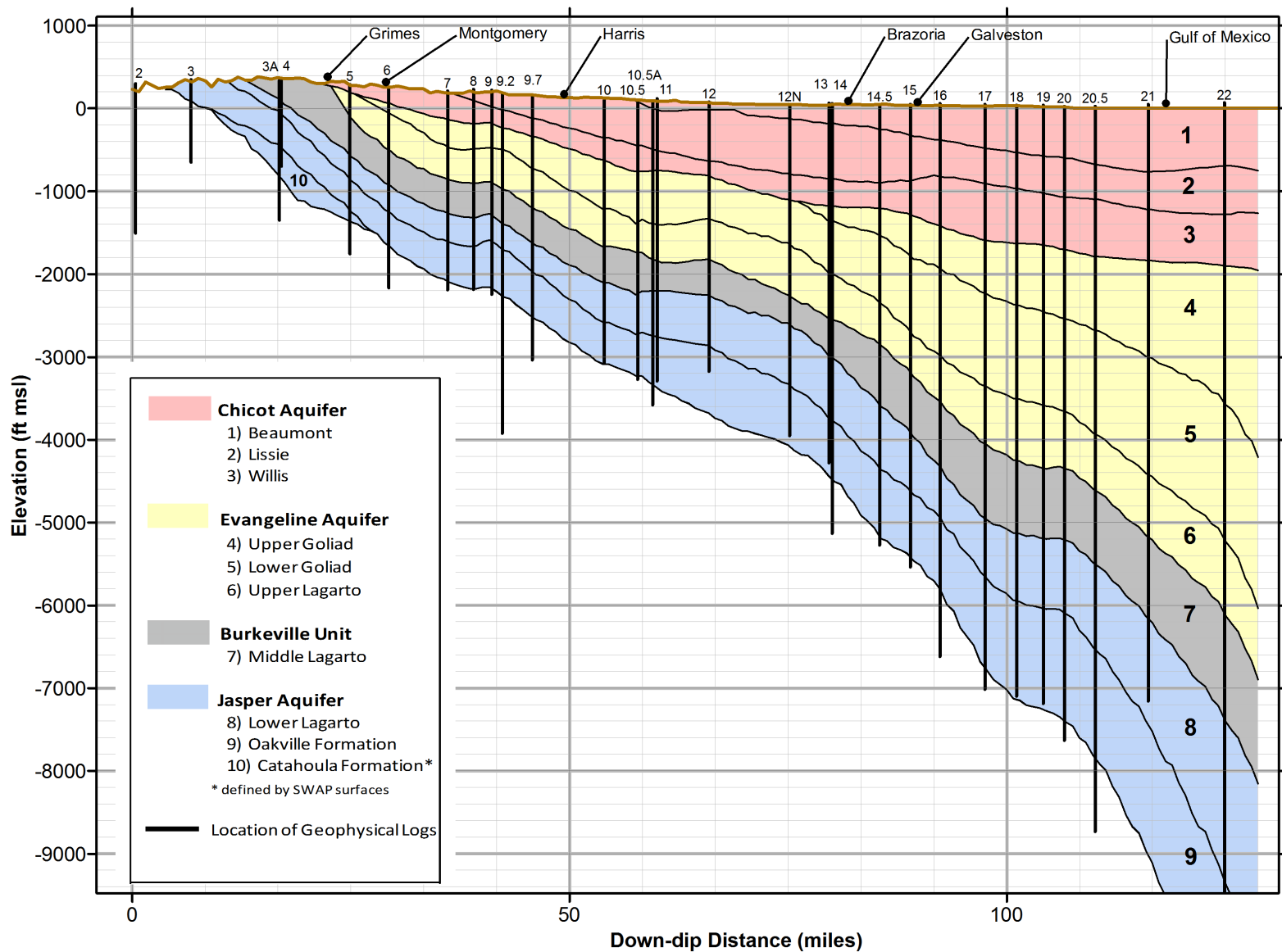


Figure 6-4 Vertical cross-section of the geological units near dip section 7 in Figure 1-1.

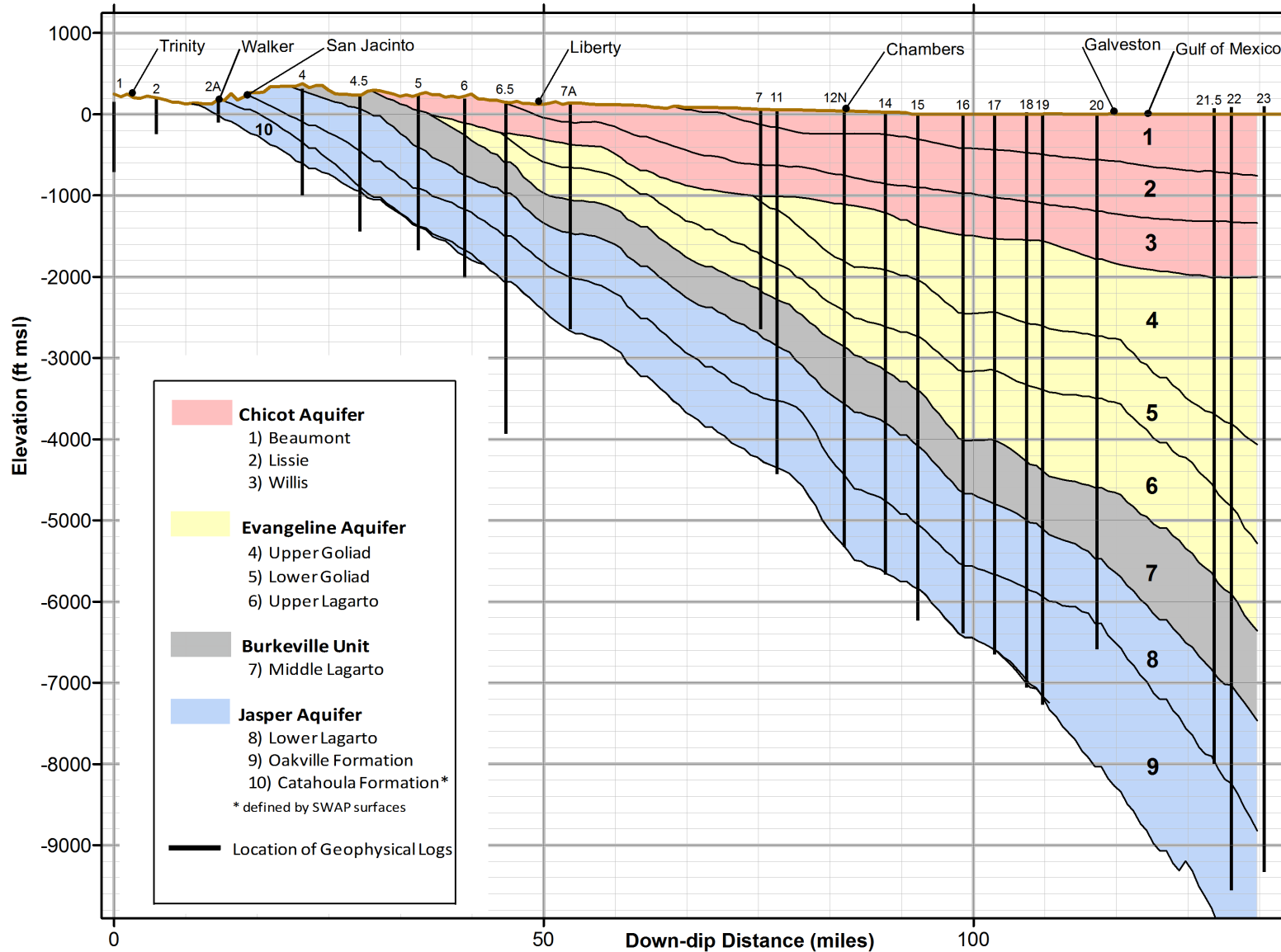


Figure 6-5 Vertical cross-section of the geological units near dip section 5 in Figure 1-1.

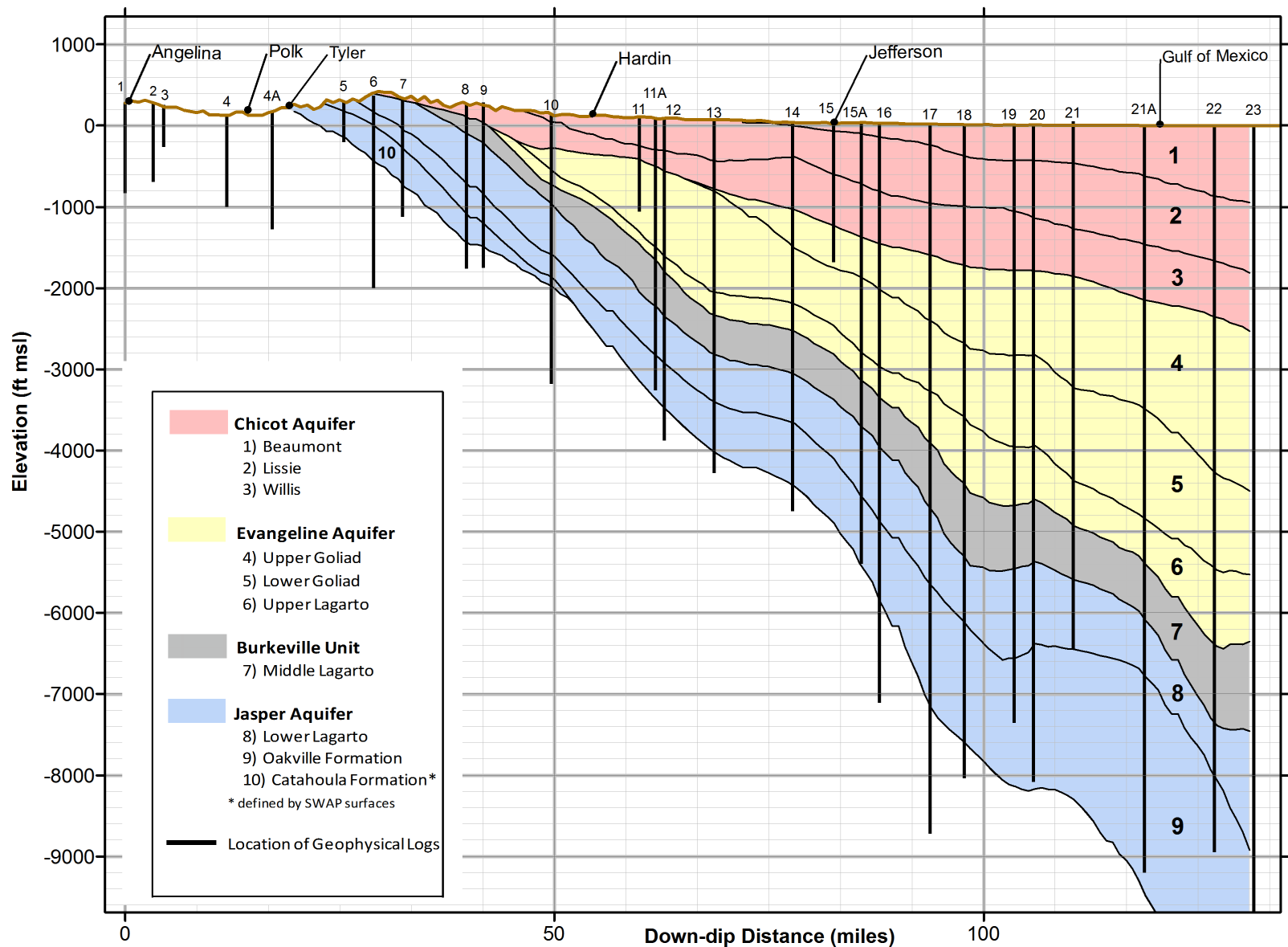


Figure 6-6 Vertical cross-section of the geological units near dip section 3 in Figure 1-1.

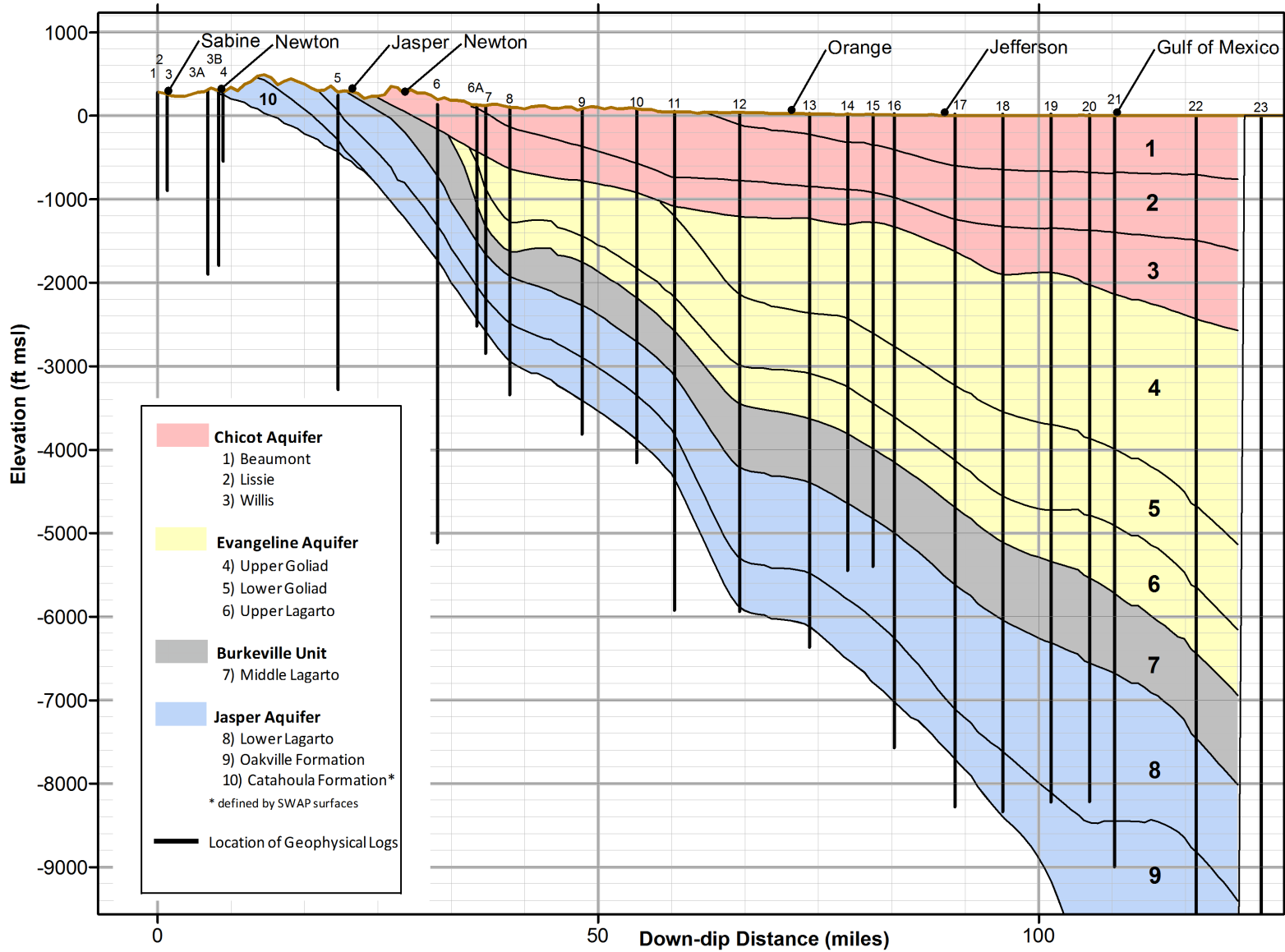


Figure 6-7 Vertical cross-section of the geological units near dip section 1 in Figure 1-1.

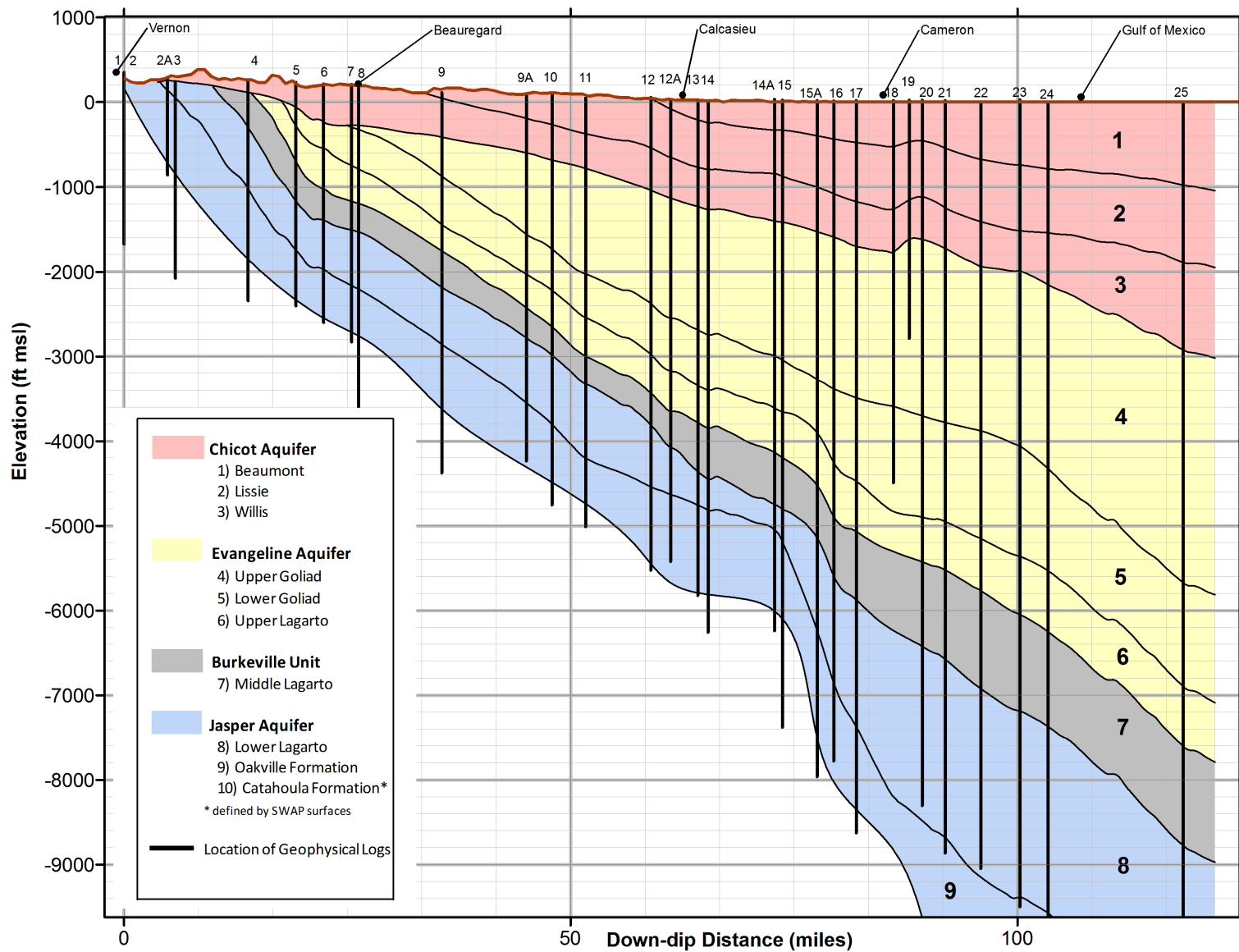


Figure 6-8 Vertical cross-section of the geological units near dip section -1 in Figure 1-1.

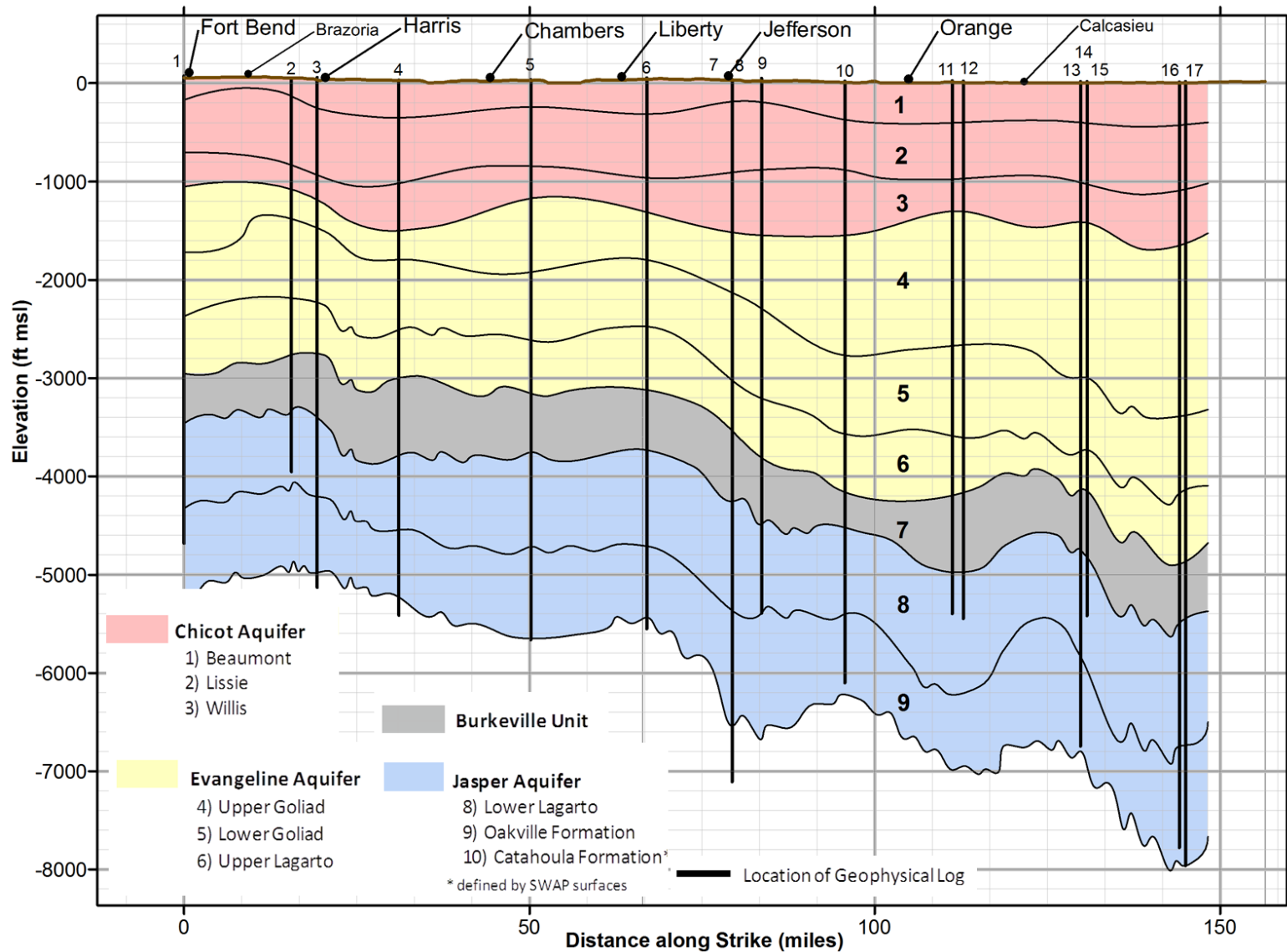


Figure 6-9 Vertical cross-section of the geological units near strike section B-B'.



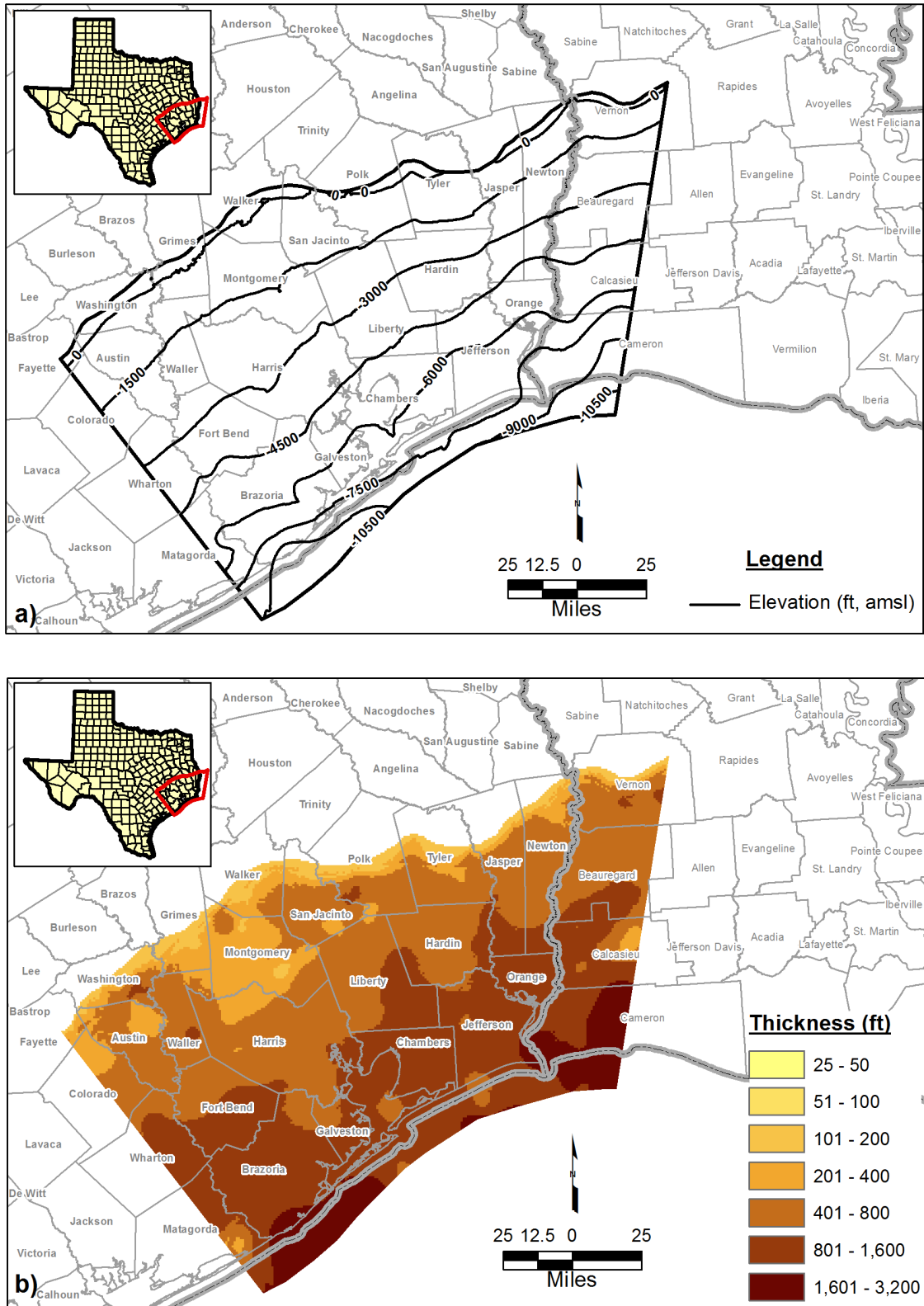


Figure 6-10 Contours for the lower Lagarto geologic unit showing: (a) base elevation and (b) thickness.

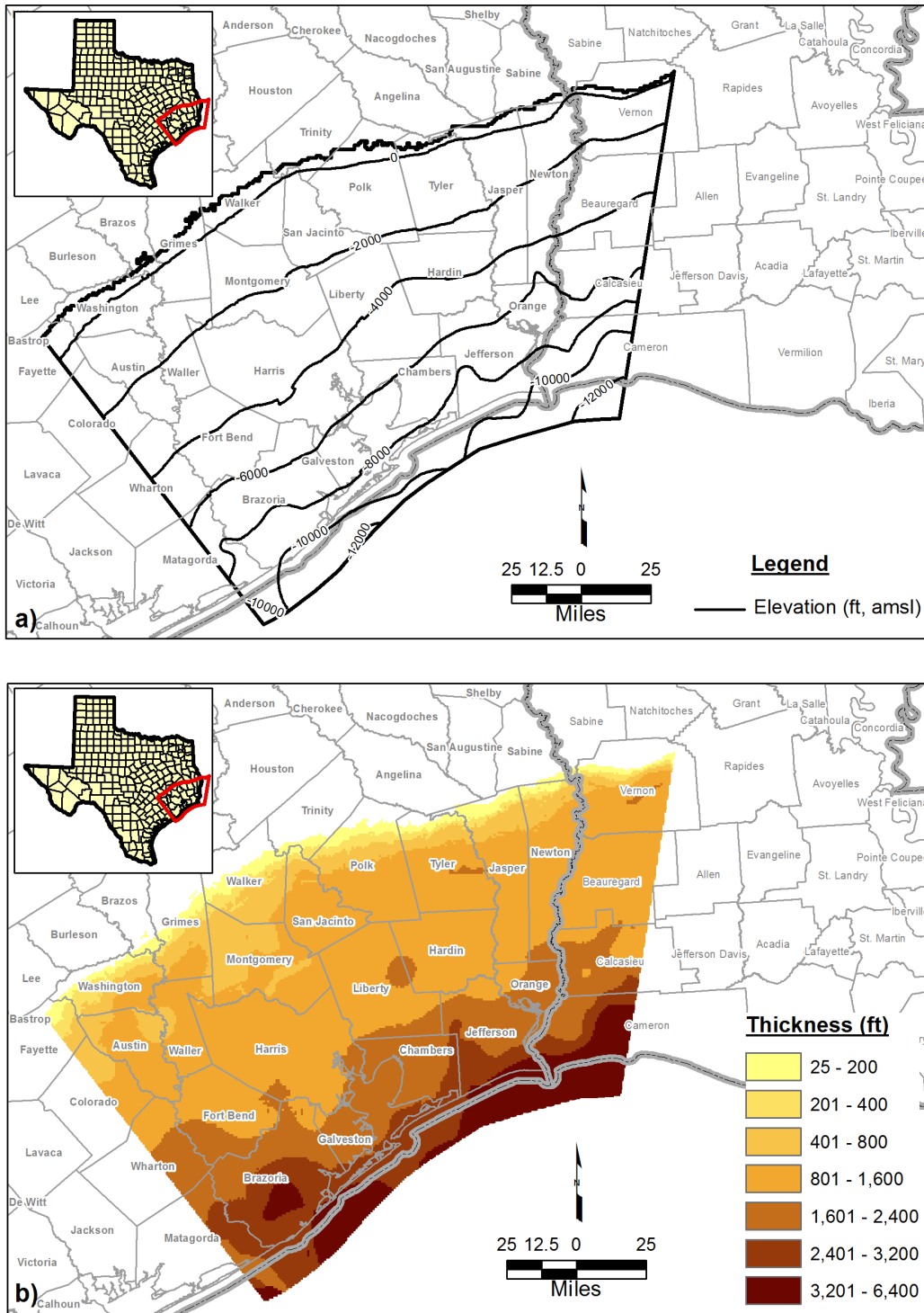
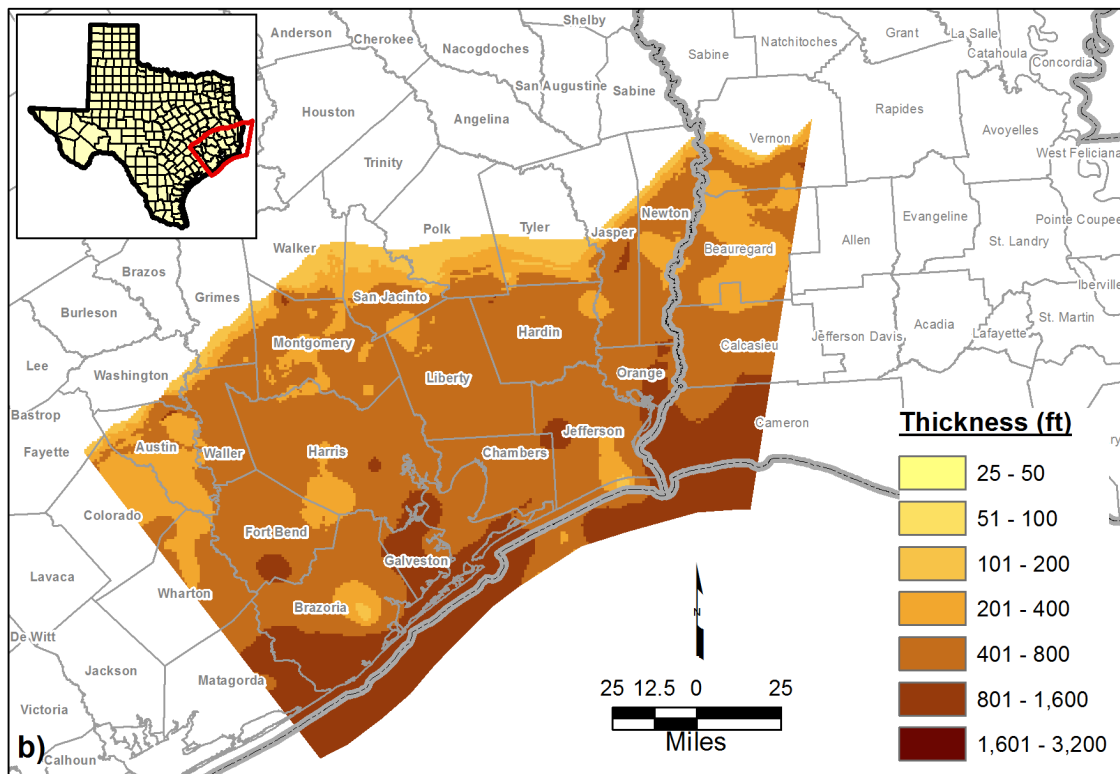
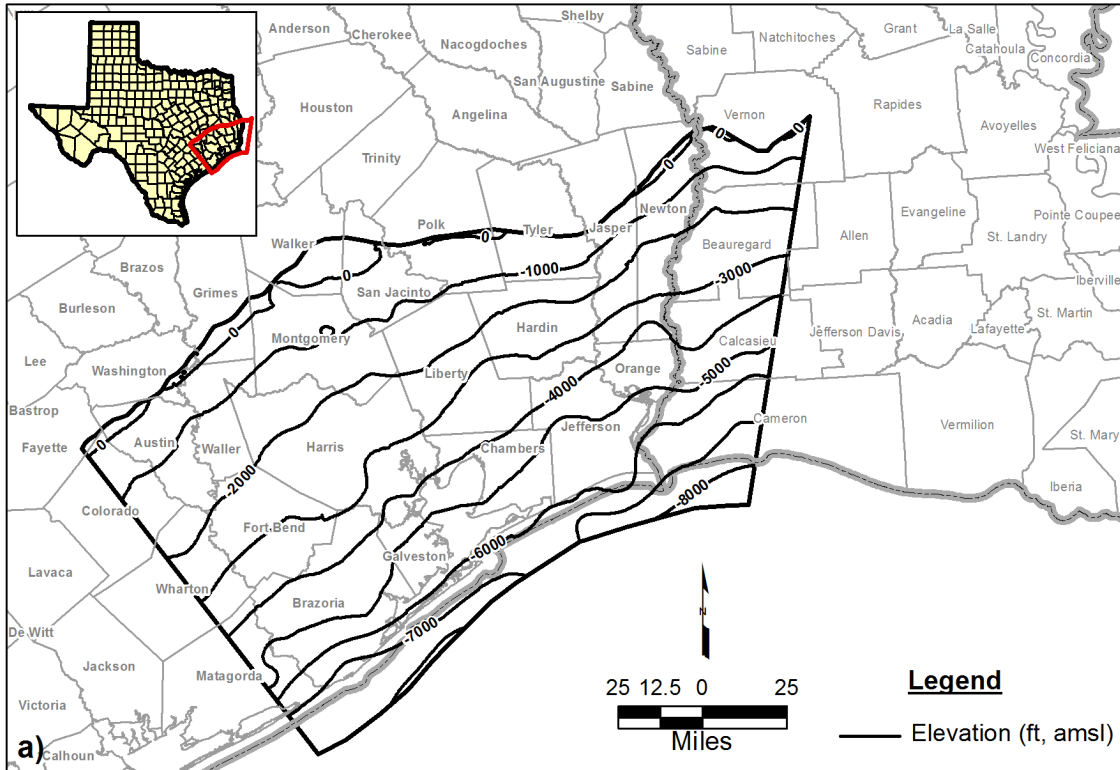
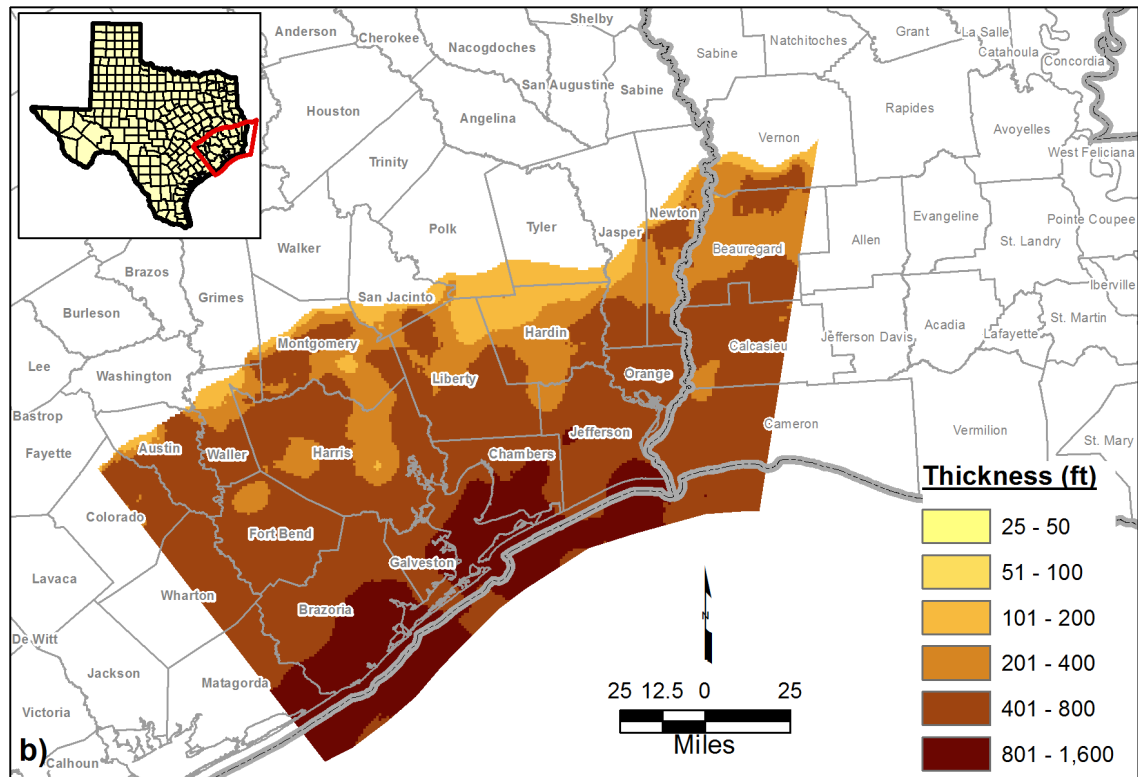
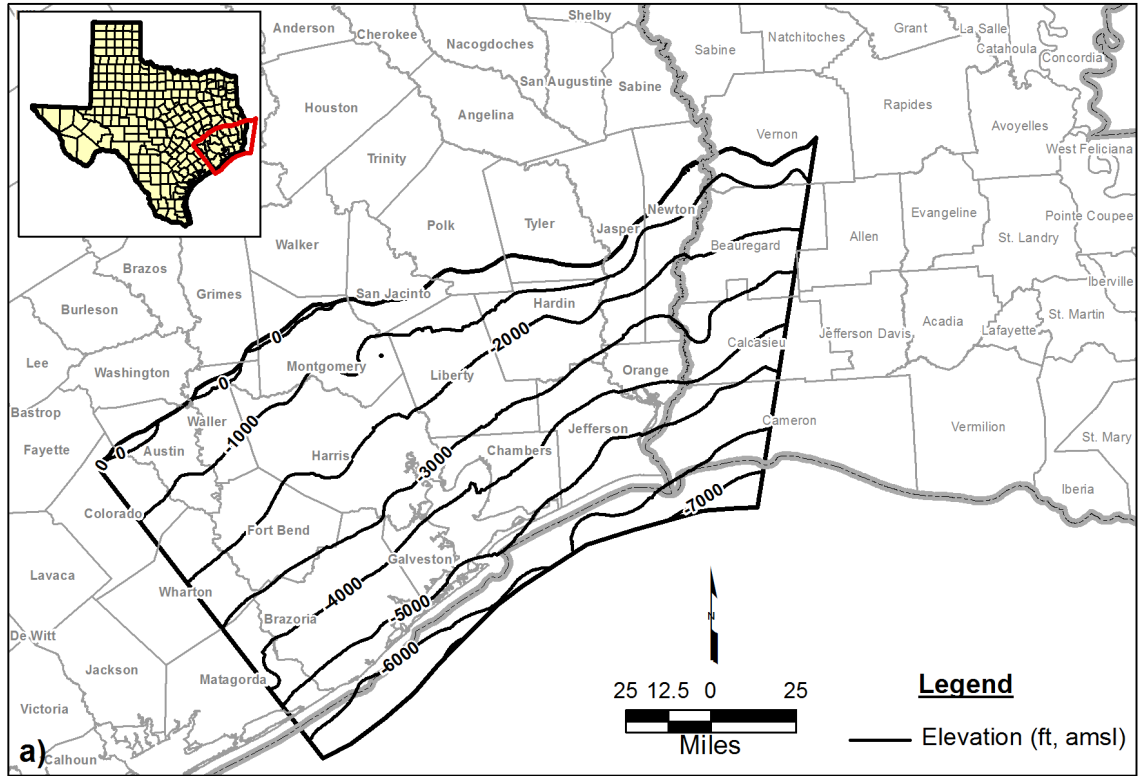


Figure 6-11 Contours for the Jasper Aquifer showing: (a) base elevation and (b) thickness.



**Figure 6-12** Contours for the middle Lagarto Formation, which is associated with the Burkeville Unit, showing: (a) base elevation and (b) thickness.



**Figure 6-13** Contours for the upper Lagarto geologic unit showing: (a) base elevation and (b) thickness.

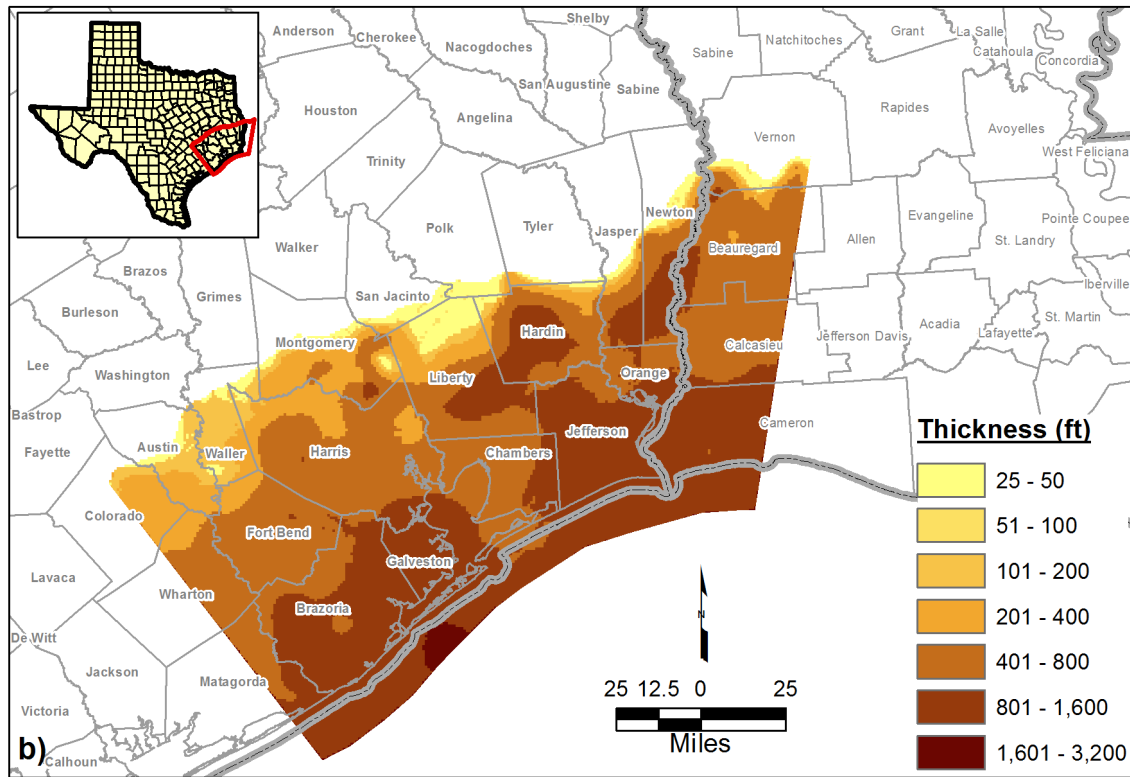
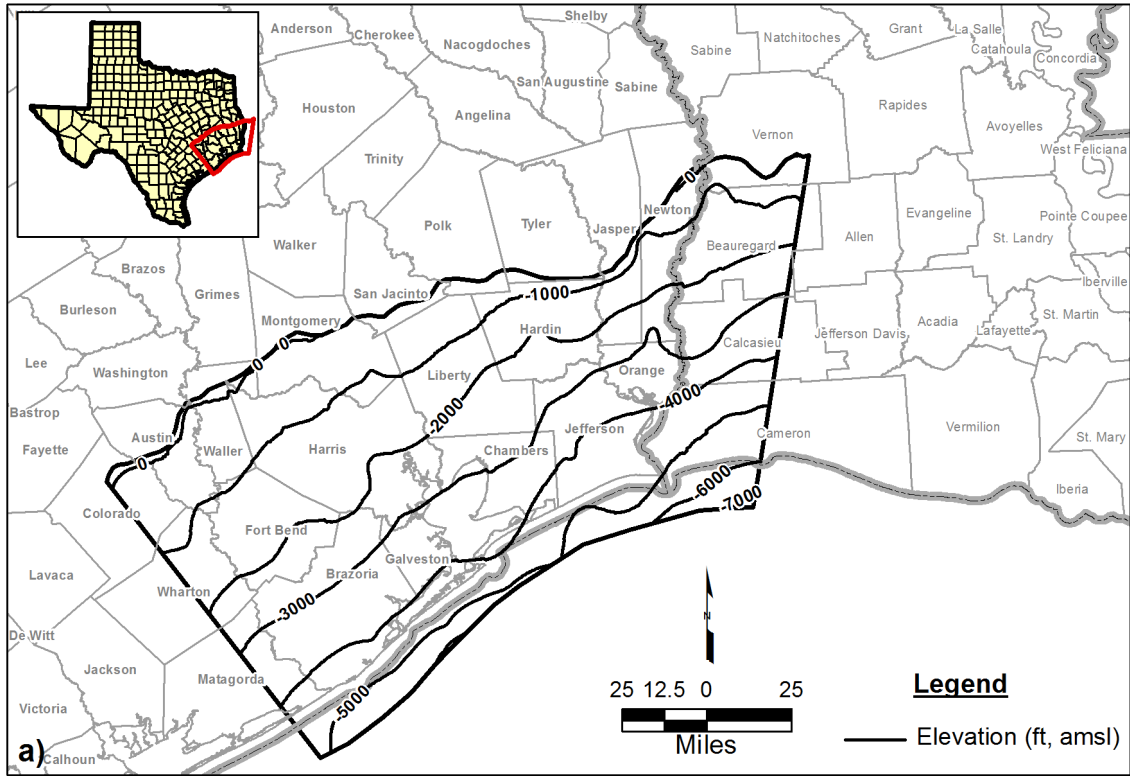


**Figure 6-14** Contours for the lower Goliad geologic unit showing: (a) base elevation and (b) thickness.

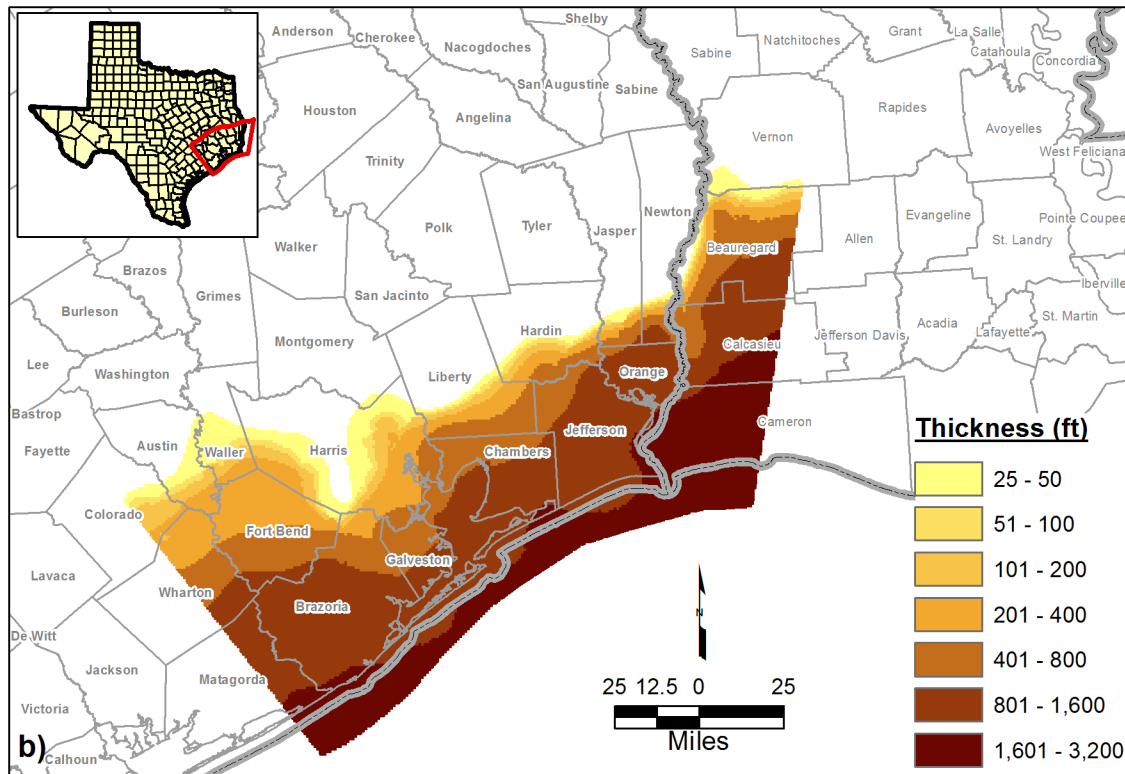
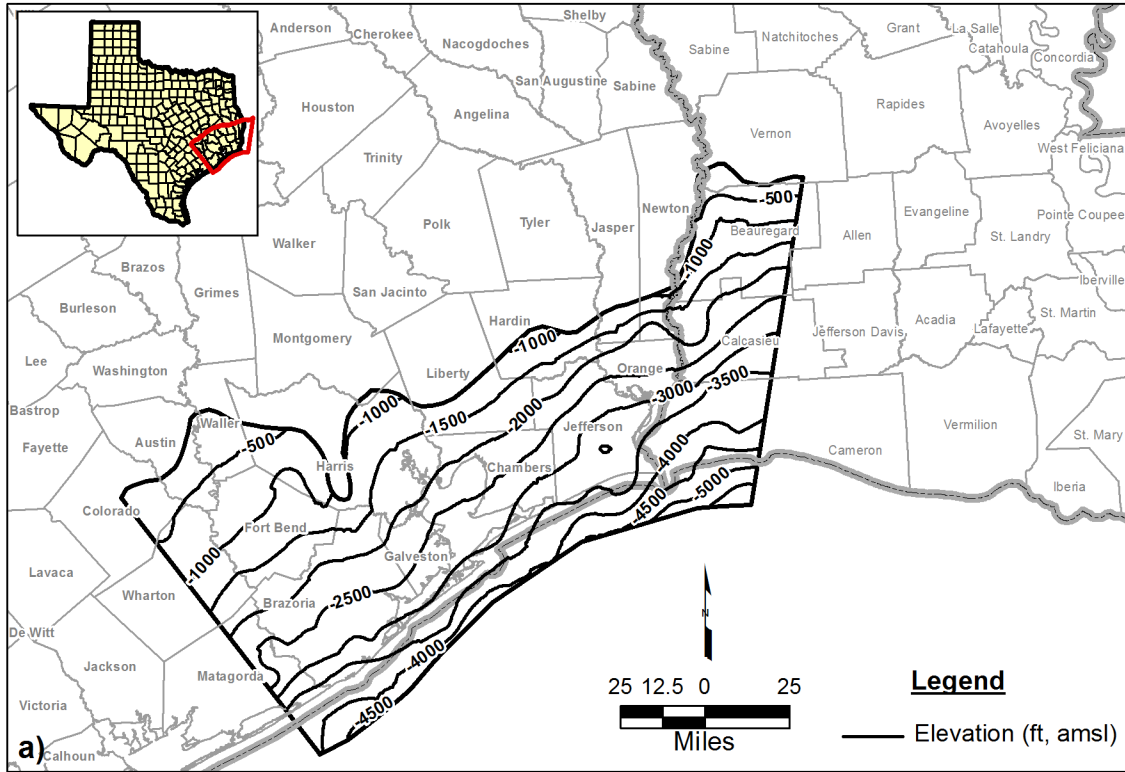


**Figure 6-15** Contours for the upper Goliad geologic unit showing: (a) base elevation and (b) thickness.

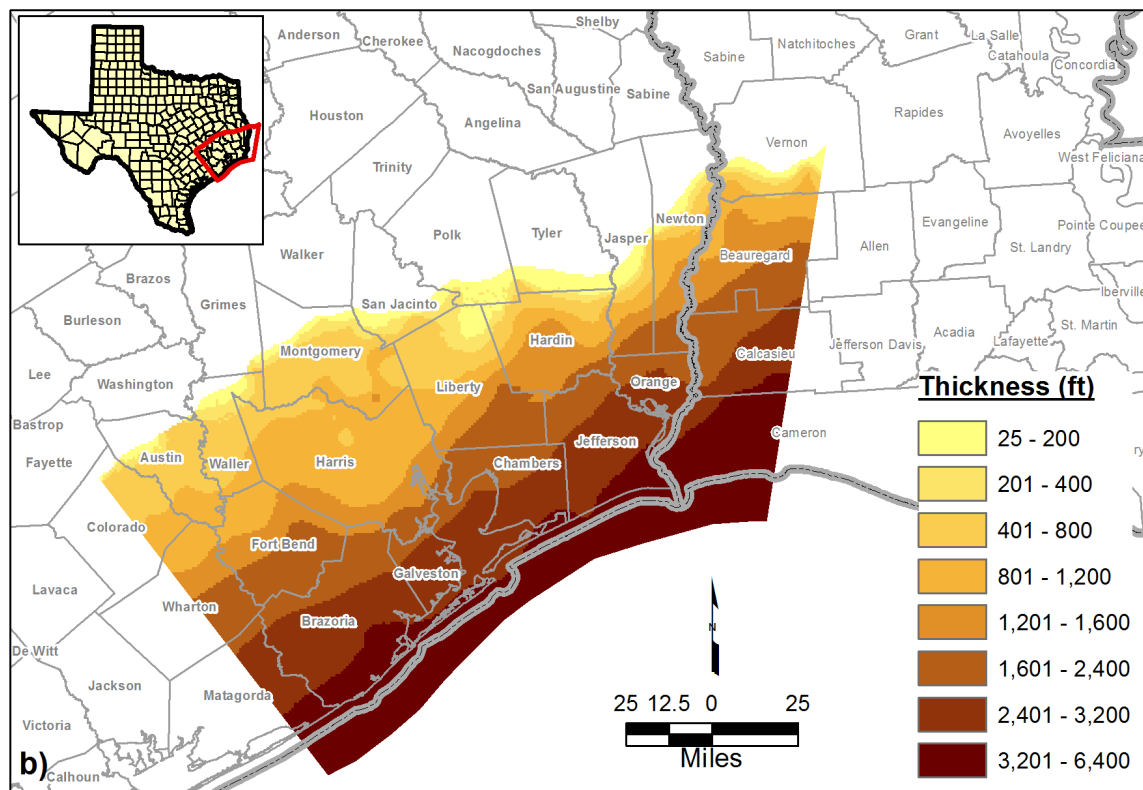
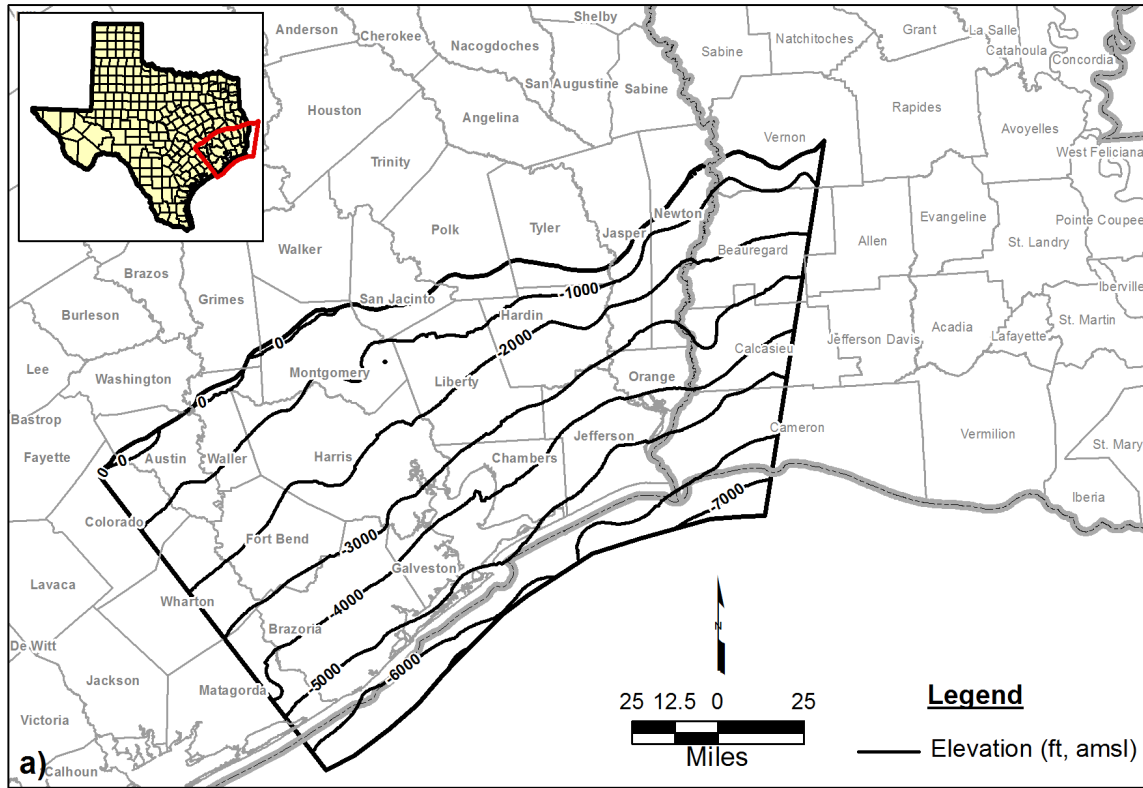


Figure 6-16 Contours for the Evangeline Aquifer showing: (a) base elevation and (b) thickness.

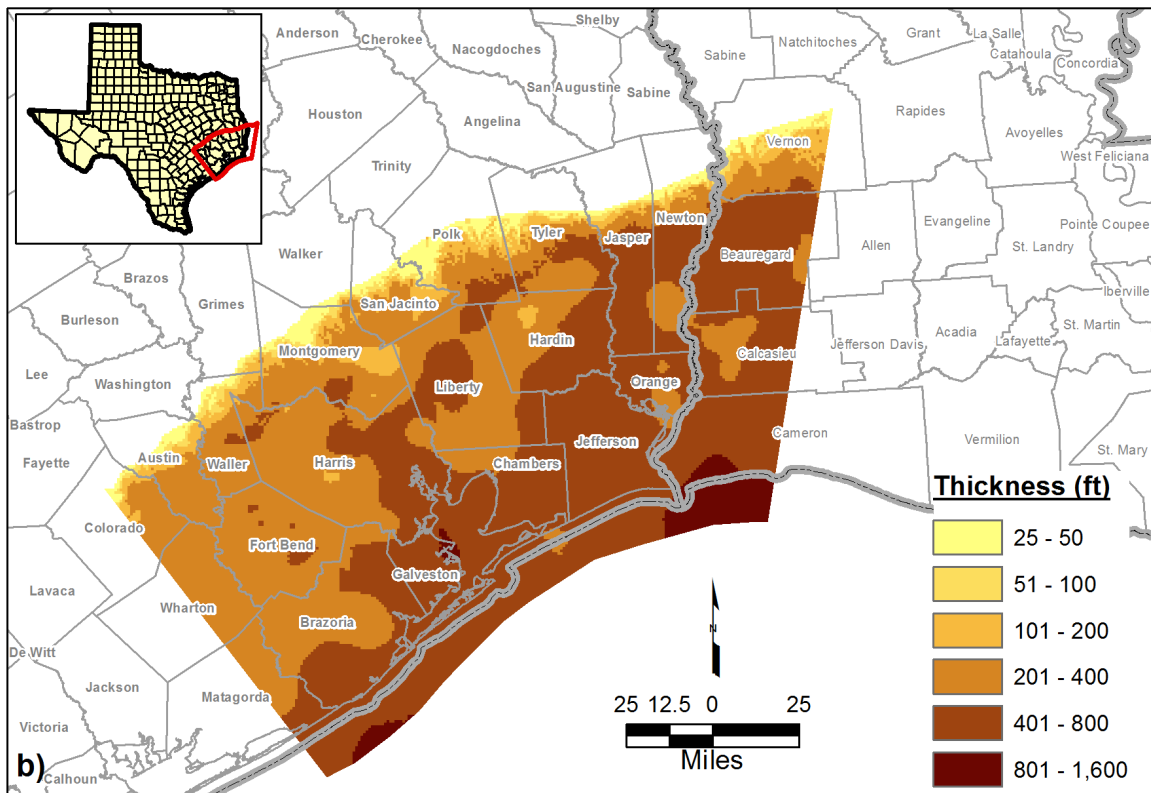
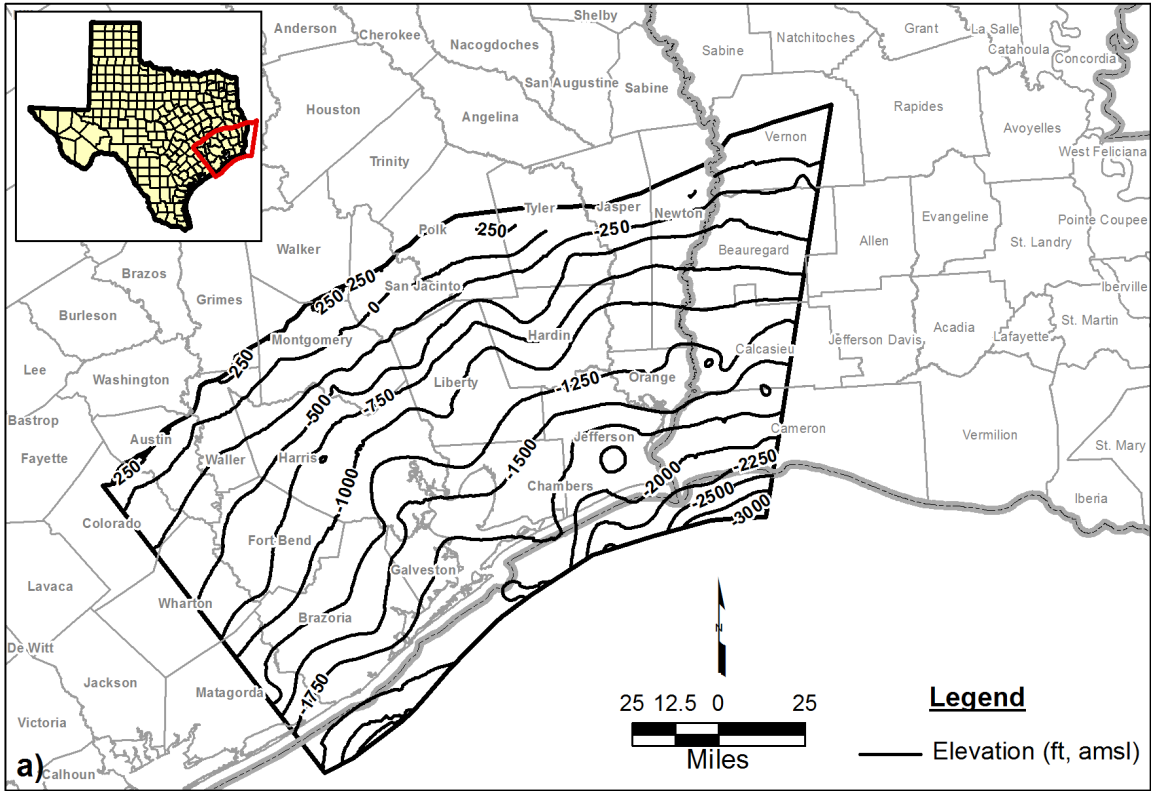
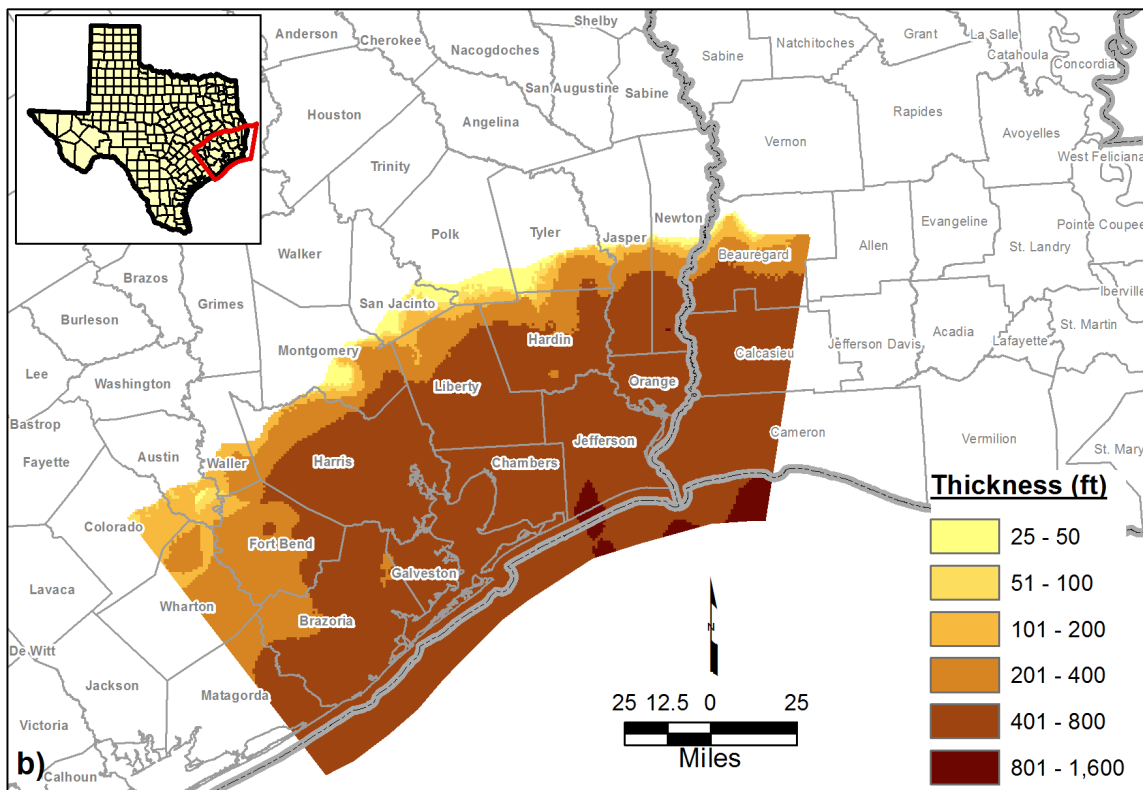
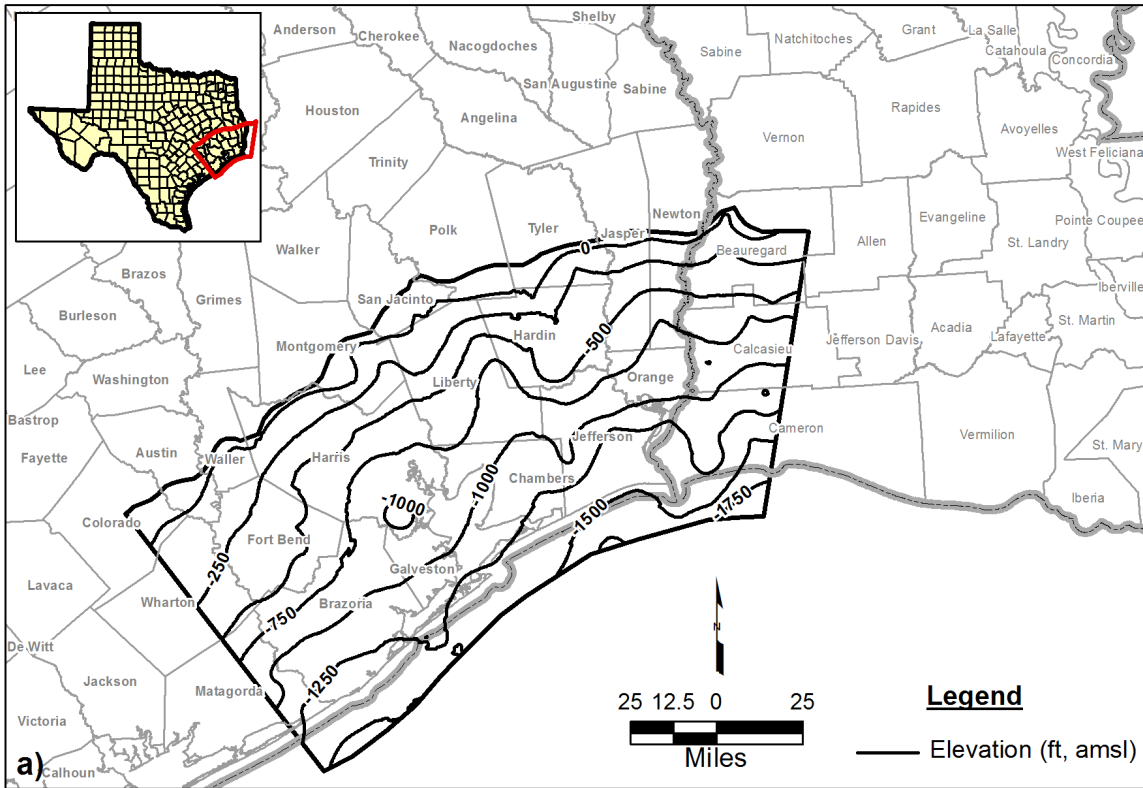
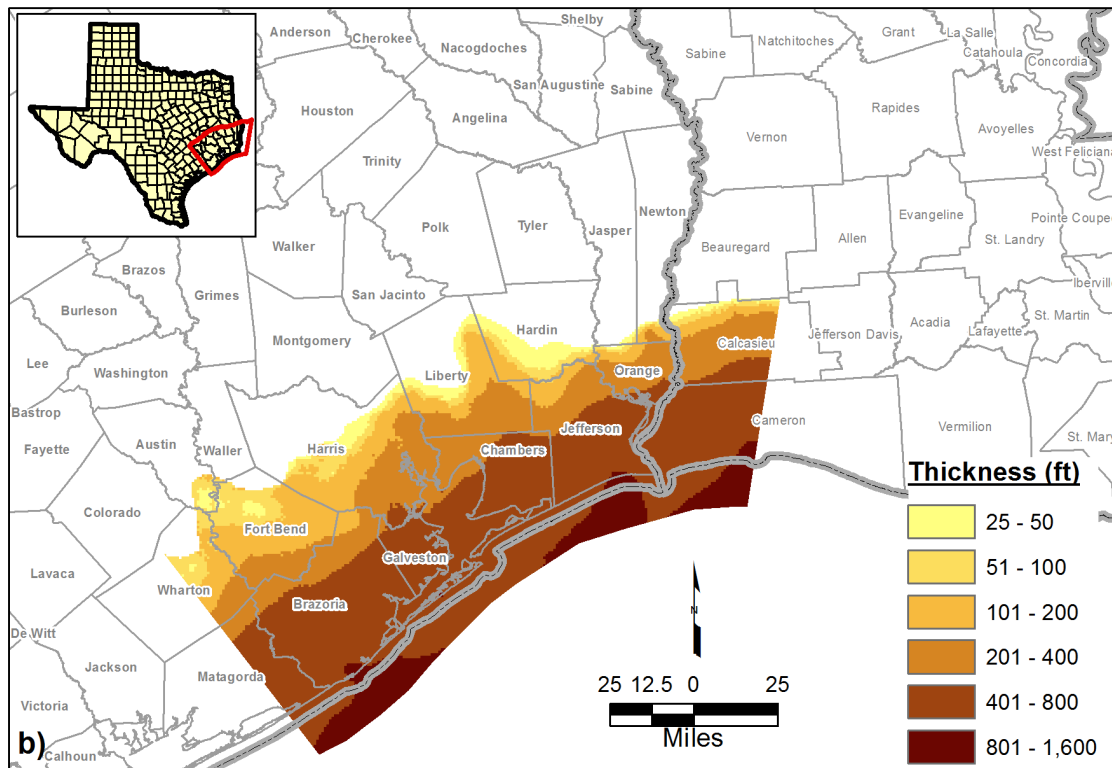
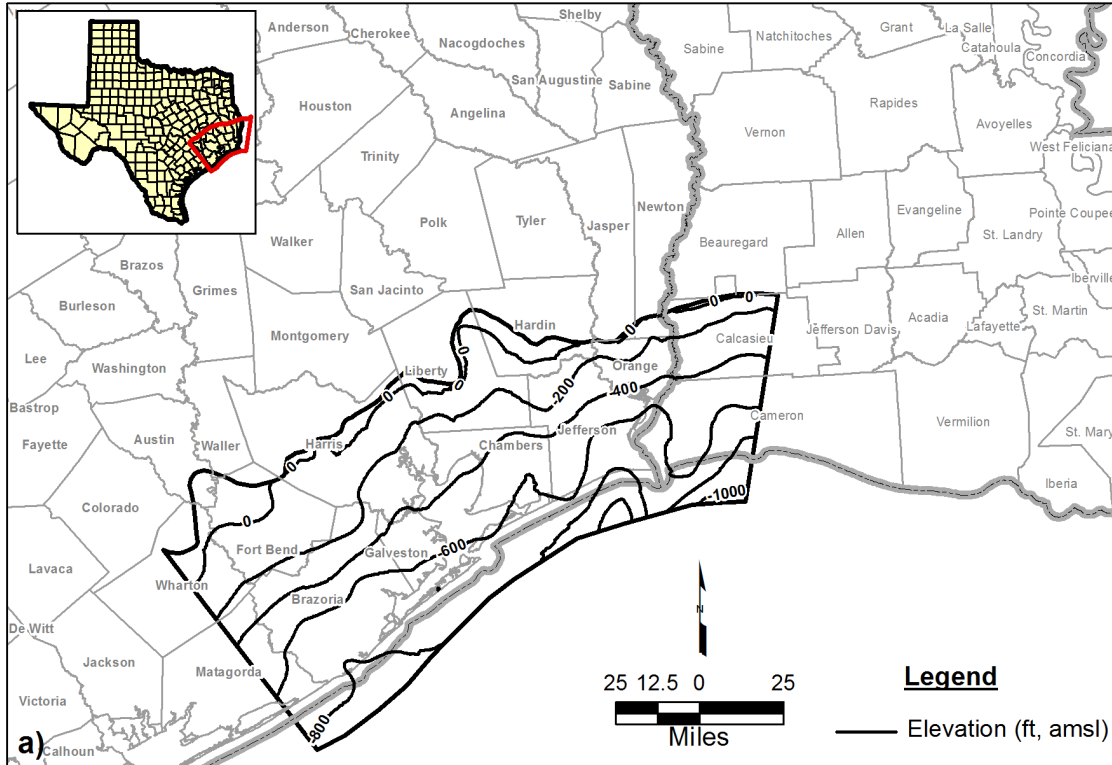


Figure 6-17 Contours for the Willis geologic unit showing: (a) base elevation and (b) thickness.





**Figure 6-18** Contours for the Lissie geologic unit showing: (a) base elevation and (b) thickness.



**Figure 6-19** Contours for the Beaumont geologic unit showing: (a) base elevation and (b) thickness.

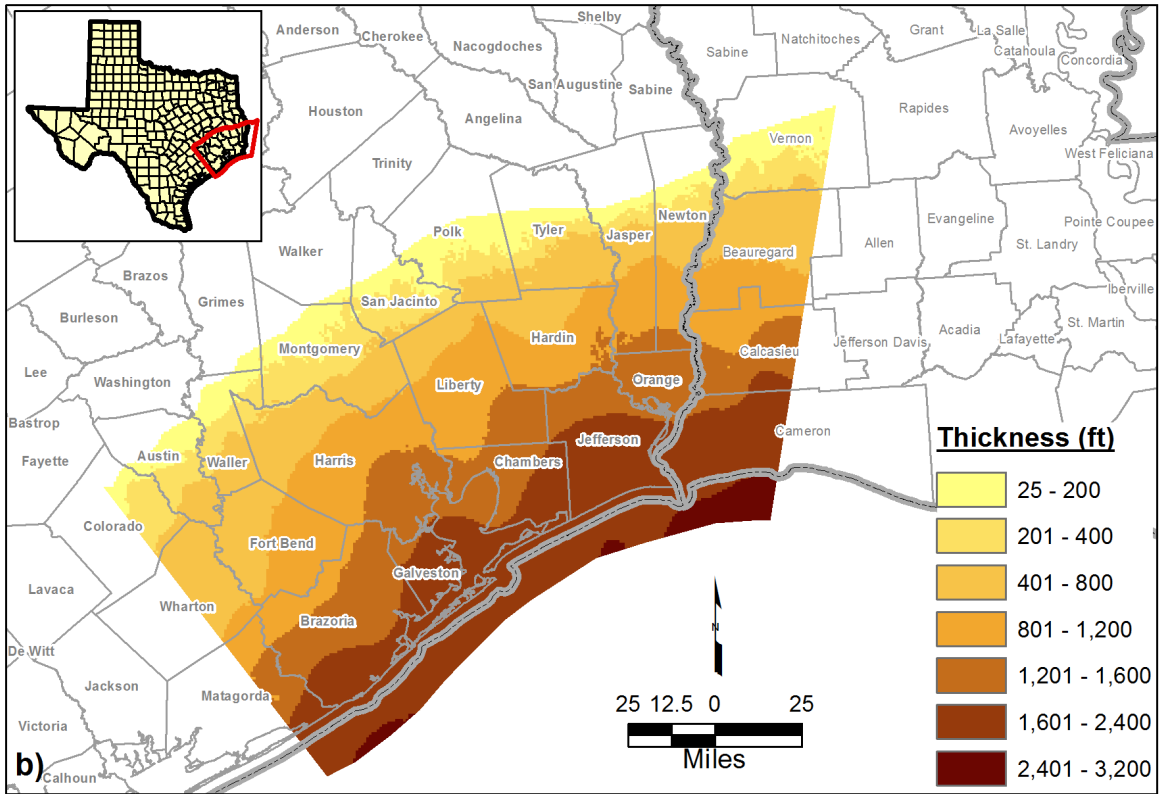
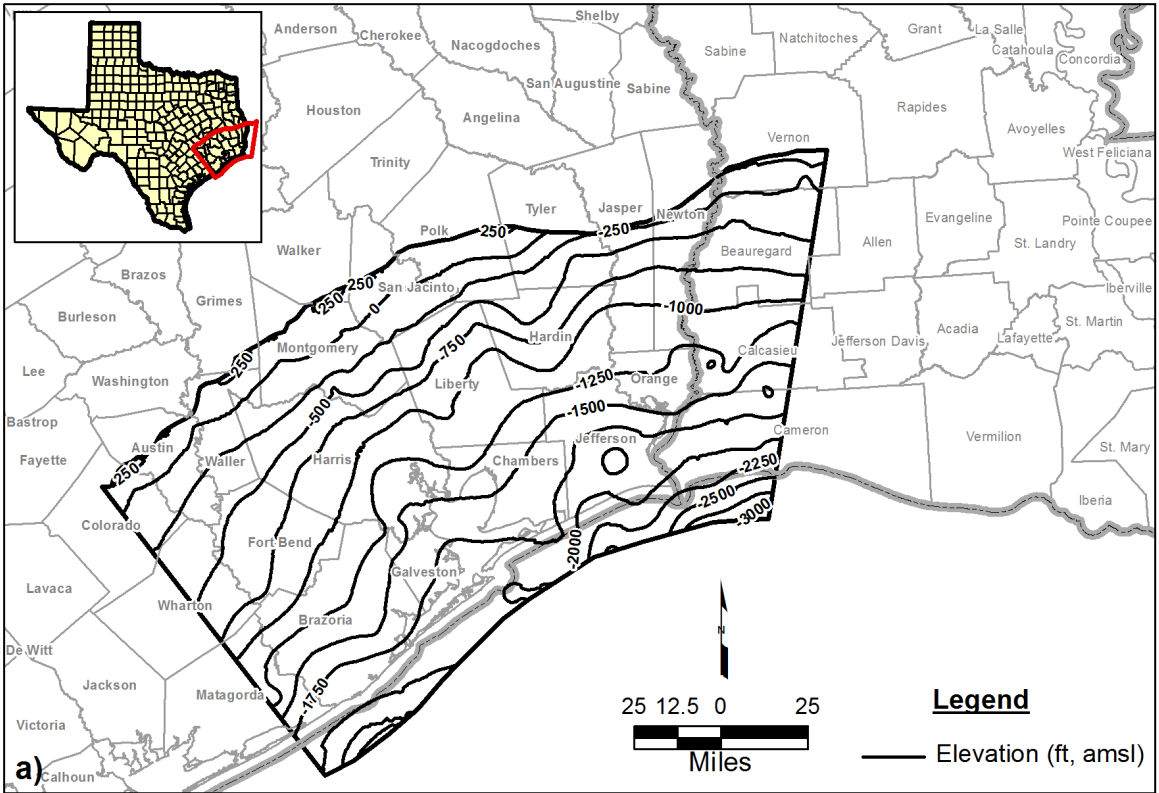


**Figure 6-20** Contours for the Chicot Aquifer showing: (a) base elevation and (b) thickness.

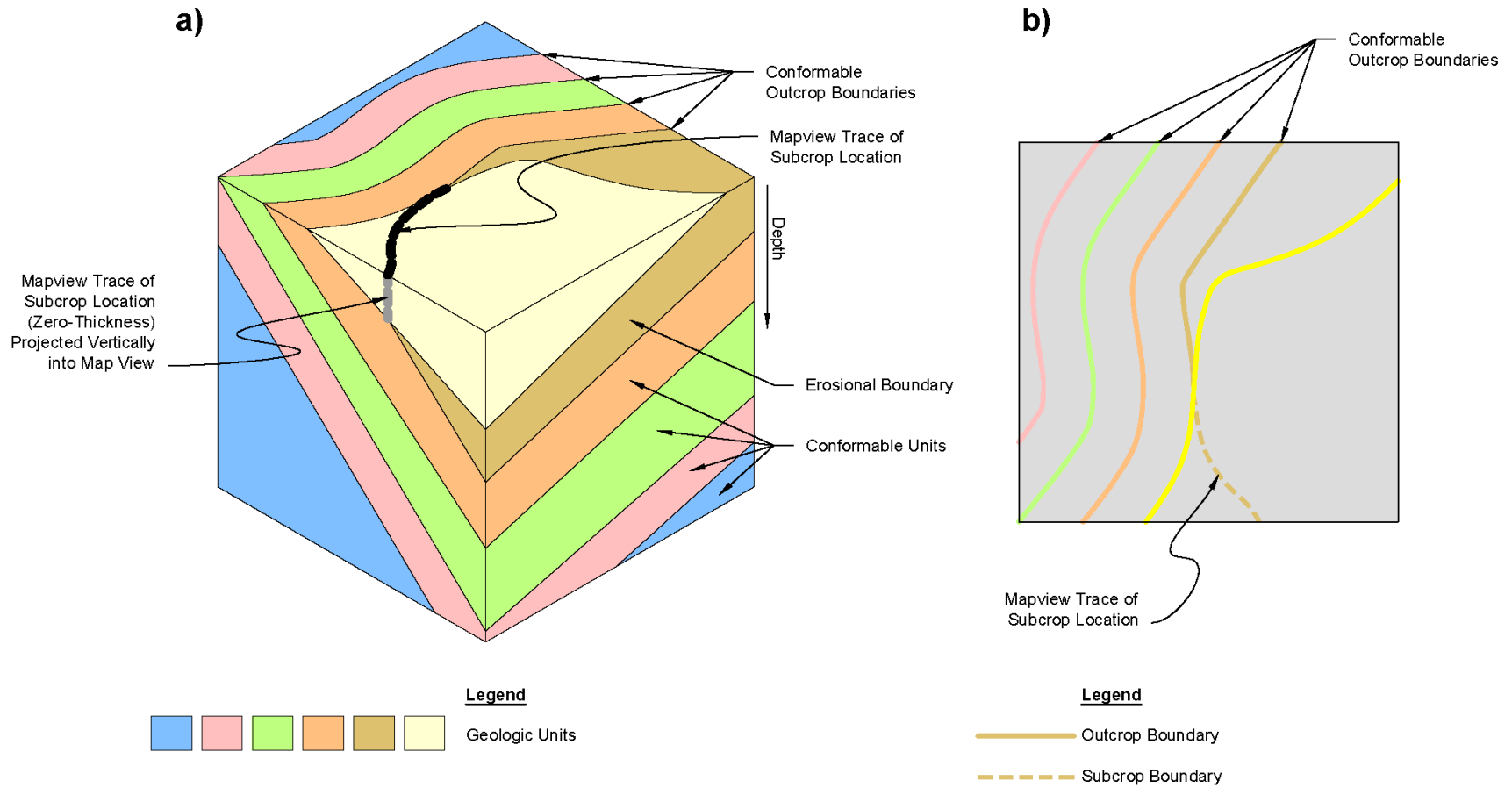


Figure 6-21 Schematic showing outcrop and subcrop locations of geologic units in a three-dimensional block (a) and in a map view (b).

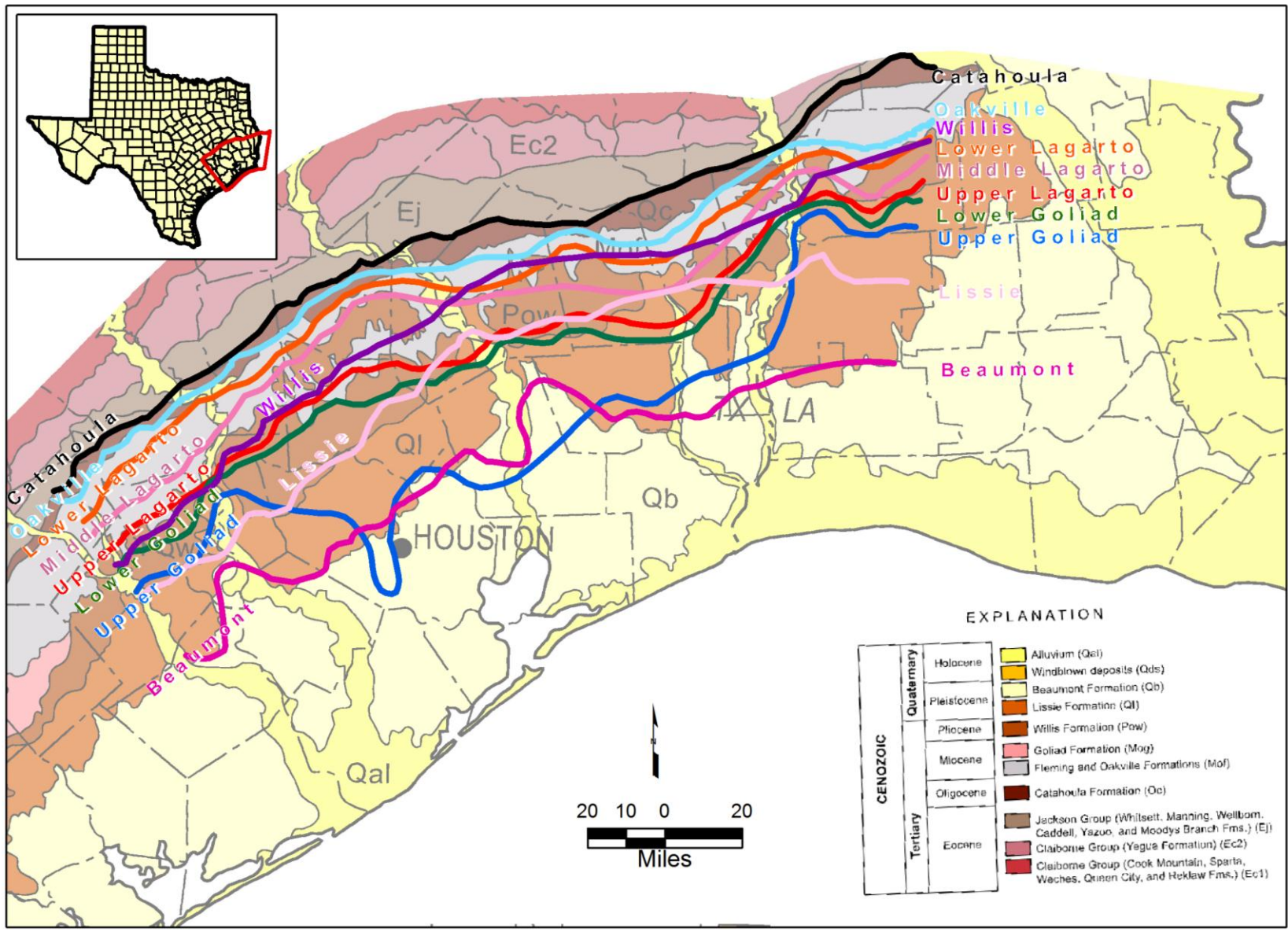


Figure 6-22 Surface geology map from Barnes (1992) showing the estimated locations of the subcrop of selected geologic units.

## **7.0 Approach for Lithologic Interpretation**

This section explains the approaches used to classify the deposits into groups related to their sand percentages and their depositional environments. These approaches are important because they indirectly determine the type of analysis that can be used to estimate spatial distribution of aquifer properties.

### **7.1 Lithology Classification**

The geophysical logs were interpreted to develop a continuous lithology profile with depth. The traditional approach for this interpretation is to use a binary classification system. The "binary" system, namely aggregating or restricting the sediment beds (as shown on electric logs) into only two classes, either basically sand beds or clay beds, has been traditional through decades of Federal/State investigative studies of county or regional groundwater projects. Figure 7-1 provides an example using an SP log to determine lithology based on a binary system. The interpretation requires that a cutoff value (which is shown in Figure 7-1) be used to determine whether the deposit is classified as either a sand or a clay. For this project, Mr. Ernest Baker performed all of the lithologic interpretations visually.

Among the obstacles associated with interpreting a log for lithology is how to interpret relatively thin beds of sands and clays, which can be very time-consuming to track at a scale of less than a few feet. A common approach that Mr. Baker and many other log analysts have used is to ignore lithology changes that occur below a designated vertical interval. For this project, another approach was used, which involved using a four-class system. This system was first discussed by Young and Kelley (2006) and was used by Mr. Baker for the Gulf Coast Aquifer and then used for the study of the southern Gulf Coast (Young and others, 2010). The four-class system uses the four textural classes described in Table 7-1. Figure 7-2 compares the results from using the binary and four-class systems to interpret lithology from a log.

The reason for using the four-class system is to more precisely characterize the nature of the sand-clay relationship without having to expend the resources to define small-scale changes in the lithologic profile. With the commonly used approach of ignoring alternating sand and clay layers to implement the binary system, vertical intervals of intermixed sands and clays that

extend more than 20 or 30 feet are represented as either a sand or a clay. With the four-class system, there is less chance of falsely indicating too much sand or clay, and a greater chance of more accurately representing the thicker beds of sands. The increased level of specificity with the four-class system provides a lithologic description that better supports characterizing the aquifers' permeability and storage properties. For instance, a sand bed consisting of primarily sands typically will be more permeable than an equally thick bed of a sand mixed with clays. Similarly, a clay bed consisting primarily of clay typically will have a lower vertical permeability than does an equally thick bed of clay mixture with appreciable amounts of sand.

**Table 7-1 Description of the four textural classes used to characterize the lithology of the LCRA-SAWS Water Project (LSWP) wells.**

Class	Description
Sand	A vertical interval of 20 feet or more, composed of 50% to 95% sand-size grains or gravel
Clay	A vertical interval of 20 feet or more, composed of less than 20% sand-size grains
Sand-with-clay	A vertical interval, composed of individual sand and clay beds less than 20 feet thick and composed of more sand than clay
Clay-with-sand	A vertical interval of 20 feet or more, composed of less than 20% sand-size grains

## 7.2 Depositional Facies Classification

Depositional facies can be viewed as how different environments arrange and pack sand beds. The basis for understanding deposition is that sediments are transported by well-understood processes that carry them from the hills from which they are eroded to a lower-energy resting place, such as the ocean or a floodplain. The environmental factors that govern the nature of the deposits include climate, ocean level, sediment sources, and chemistry. As these factors change over time, the composition of the deposits change, and cycles of repeating sequences of sand and clay occur. Based on a detailed study of depositional cycles from cores and geophysical logs, geologists have defined facies that characterize deposition in the fluvial and coastal environments of the Gulf Coast.

The depositional facies of aquifer layers provide information on factors that affect groundwater flow such as the sorting, arrangement, and sizes of the particles in a deposit and how the deposit is or is not interconnected to similar and different deposits. For this project, we have selected depositional facies based on the work of Galloway (2000) that have also been used by Young and Kelley (2006) and Young and others (2010). These facies can be divided into fluvial facies,

coastal facies, and shelf facies. Fluvial facies are associated with deposition in rivers and on the floodplains of rivers. Coastal facies are associated with depositions in coastal and shoreline environments. Shelf facies are associated with off-shore environments.

Galloway (2000) describes the deposition across a coastal plain of the Gulf Coast that was located updip of the shoreline during highstands of sea level and in an area between major axes of fluvial input, with the exception of the Corsair system of the middle and Late Miocene. As modified from Young and others (2010), the lithologies and depositional facies in this study included:

- Floodplain clays deposited during flooding of coastal streams and, less frequently, major rivers;
- Fluvial channel sands deposited within or immediately adjacent to coastal streams or major rivers;
- Coastal or deltaic bayfill clays, silts, and, rarely, sands deposited behind barrier islands, away from channels on alluvial aprons, or between deltaic distributary channels;
- Lower coastal plain fluvial or coastal sands deposited on alluvial aprons fed by streamplain systems or on delta plains of major extrabasinal rivers;
- Delta front sands, most likely deposited as narrow strike-elongated bodies of a wave-dominated delta;
- Coastal sands deposited as barrier bars, strandplains, or delta fronts where local fluvial input is minor and sand is transported and deposited primarily by along-shore currents; and
- Shallow marine shelf clays and minor silts and sands deposited seaward of the highstand shoreline, which may include interbedded muddy floodplain, bayfill, or lagoonal lowstand deposits.

Based on the information from Galloway and others (2000), Young and others (2010) constructed the facies categories and descriptions listed in Table 7-2. Each facies in Table 7-2 has a different range of hydrologic flow characteristics as a consequence of varying grain size,



sorting, mineralogy, sedimentary features, and the degree to which contrasting lithologies are intimately interbedded. Also because of the long time period and large area associated with the project, there may be a large range in the hydraulic properties among deposits with the same facies because of the differences in environmental conditions and sediments that formed them. The flow characteristics ascribed to the different facies in Table 7-2 are generalized estimations and should be used as a relative measure for at the dimensions of typical bed deposit, which may be a foot to tens of feet thick. The effective hydraulic conductivity of the facies deposits are ultimately controlled by their site-specific conditions and measurement scale.

**Table 7-2 Depositional Facies Definition and Predicted Flow Characteristics [modified from Table 3.1.3 in Young and Kelley (2006)].**

Code	Facies	Definition	Flow Character	Log Profile
FP	Floodplain	Clay-dominated interval of floodplain and overbank clay, mud, and silt, with rare interbedded fluvial channel, levee, or splay sands less than 20-ft thick.	<b>Sand:</b> relative Kh rating of 2 (1 being lowest K, 7 being highest), Kv rating of 2. $K_v/K_h \sim 0.3$ . <b>Clay:</b> Kh rating of 1, Kv rating of 2. $K_v/K_h \sim 0.1$ .	See Figures 7-3 and 7-4
F	Fluvial Meanderbelt	Sand-dominated interval containing fluvial channel (rarely levee and splay) sands. Bankfull fluvial channel depths or combinations of channel sand thickness and other facies exceed 30 ft in thickness. Interbedded clays can include channel abandonment and floodplain with potential for development of soil profiles or calichification.	<b>Sand:</b> relative Kh rating of 7 (1 being lowest K, 7 being highest), Kv rating of 5. $K_v/K_h \sim 0.5$ . <b>Clay:</b> Kh rating of 2, Kv rating of 3. $K_v/K_h \sim 0.05$ .	
FD	Lower-Coastal Plain Fluvial and Coastal	Sand-dominated interval containing fluvial and, rarely, distributary channel, levee, splay, and coastal sands often exceeding 30 ft in thickness. Channel sands are commonly stacked. Coastal sands may include wave-networked terminal fluvial deposits, minor shorezone and tidal channel, and localized incised-valley deposits. Interbedded muds are most often silty floodplain, bayfill, or lagoonal deposits. Upward-coarsening silty profiles occur far more frequently than in F facies.	<b>Sand:</b> relative Kh rating of 4 (1 being lowest K, 7 being highest), Kv rating of 4. $K_v/K_h \sim 0.4$ . <b>Clay:</b> Kh rating of 5, Kv rating of 5. $K_v/K_h \sim 0.1$ .	

**Table 7-2, continued**

Code	Facies	Definition	Flow Character	Log Profile
BF	Bayfill/Lagoon	Mud-dominated interval containing interbedded bayfill, lagoonal, and coastal plain deposits. Sands are typically thin, spiky bayfill splay, overbank, or washover deposits.	<b>Sand:</b> relative Kh rating of 1 (1 being lowest K, 7 being highest), Kv rating of 1. <u>Kv/Kh ~ 0.5.</u> <b>Clay:</b> Kh rating of 3, Kv rating of 4. <u>Kv/Kh ~ 0.1.</u>	
WD	Wave-Dominated Delta	Sand-dominated intervals containing upward-coarsening to blocky mouth bar, delta front, strandplain, or barrier bar, and upward-fining distributary channel deposits where sand-component thicknesses of each deposit typically exceed 30 ft. Clays are prodelta, shelf, and bayfill / lagoonal deposits.	<b>Sand:</b> relative Kh rating of 6 (1 being lowest K, 7 being highest), Kv rating of 6. <u>Kv/Kh ~ 0.5.</u> <b>Clay:</b> Kh rating of 7, Kv rating of 6. <u>Kv/Kh ~ 0.1.</u>	
SF	Shoreface / Barrier Bar / Delta Front / Shorezone Coastal	Sand-dominated intervals with upward-coarsening to blocky (rarely upward-fining) sand bodies exceeding 30 ft in thickness. Clays are prodelta, shelf, or bayfill / lagoonal deposits.	<b>Sand:</b> relative Kh rating of 5 (1 being lowest K, 7 being highest), Kv rating of 7. <u>Kv/Kh ~ 0.7.</u> <b>Clay:</b> Kh rating of 6, Kv rating of 7. <u>Kv/Kh ~ 0.1.</u>	
SH	Shelf / Lagoonal / Bayfill / Floodplain	Mud-dominated intervals with rare sandy marine or non-marine scour or reworked deposits. Clays are commonly shelf deposits, with lowstand facies such as FP, BF, or lagoonal sediments.	<b>Sand:</b> relative Kh rating of 3 (1 being lowest K, 7 being highest), Kv rating of 2. <u>Kv/Kh ~ 0.2.</u> <b>Clay:</b> Kh rating of 4, Kv rating of 1. <u>Kv/Kh ~ 0.01.</u>	

No absolute values in terms of feet per day for hydraulic conductivity are provided in Table 7-2 because of the wide variety of sediment loads and range of energies associated with each depositional facies. The ranking of hydraulic conductivity values are intended to provide a relative measure of how hydraulic conductivity values vary among the sand and clay beds associated with different facies within a given depositional episode. The hydraulic conductivity rankings are based on the expected differences in the grain size, sorting, and packing characteristics associated with the sand and clay beds typically associated with each facies type. In general, Kh increases with increases with grain size and sorting and Kv/Kh decreases with increases in layering and stratification.

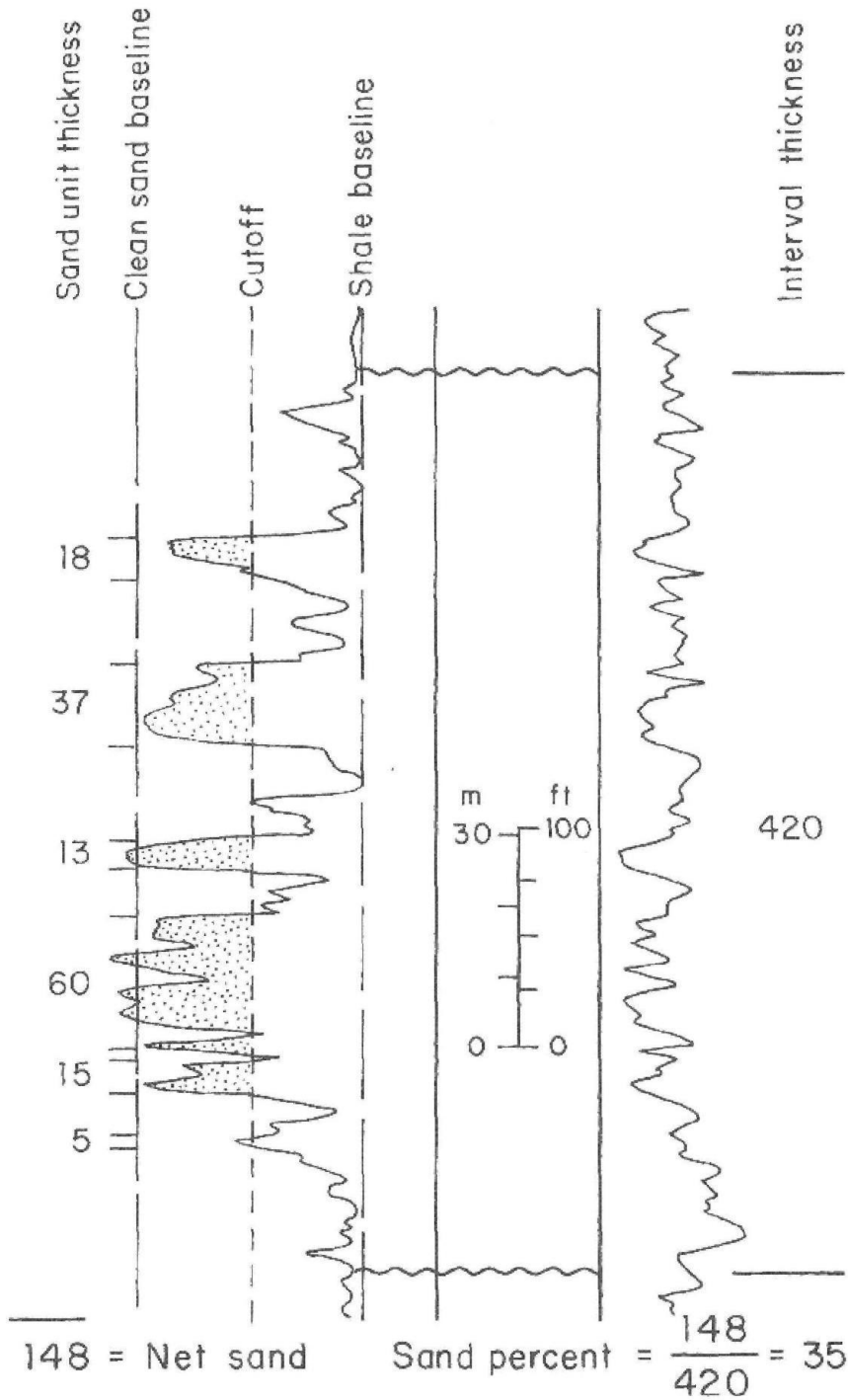


**Figure 7-1** Example calculation of net and percent sand from a spontaneous potential (SP) log curve. First baselines are established for the end member lithologies, and then a cutoff is picked for measuring sand thickness and sand/mud ratio (sand percent). Source: Galloway and Hobday (1996).

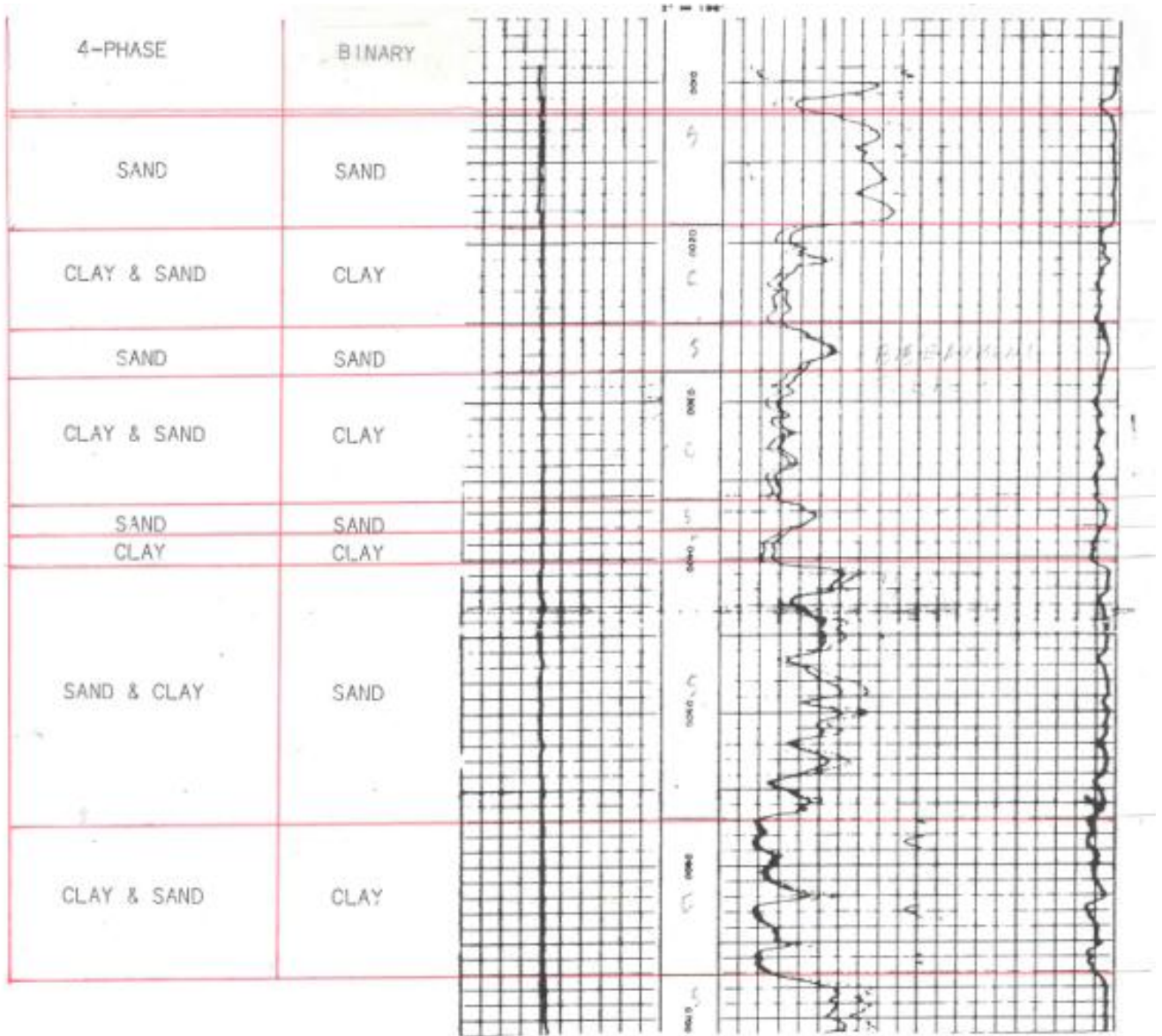
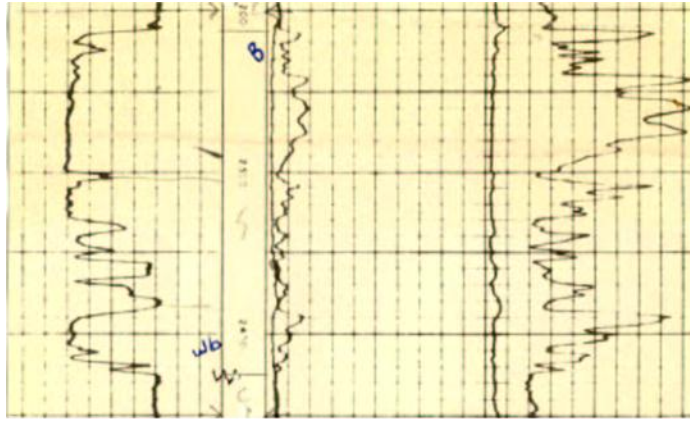
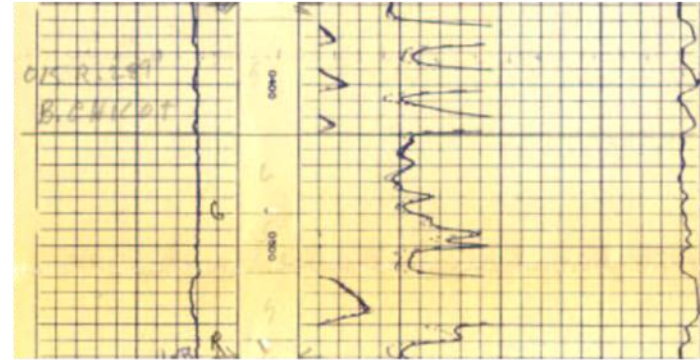


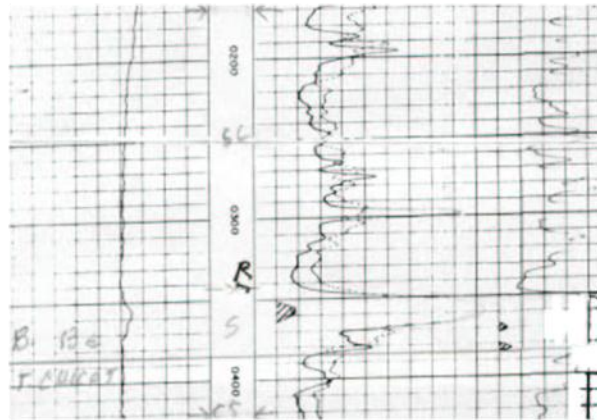
**Figure 7-2** Example analysis of a geophysical log showing a binary and four-phase classification of lithology (taken from Young and Kelley, 2006). Resistivity log is on the right-hand side, and spontaneous potential log is on the left-hand side. Each grid block has a height of 1 foot.



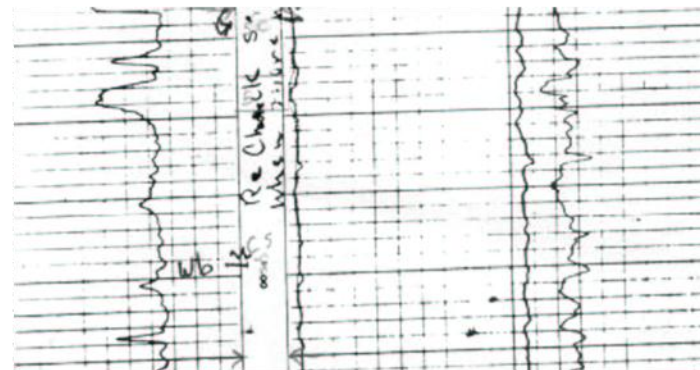
Log profile example of shorezone facies (SF)



Log profile example of fluvial facies (F)

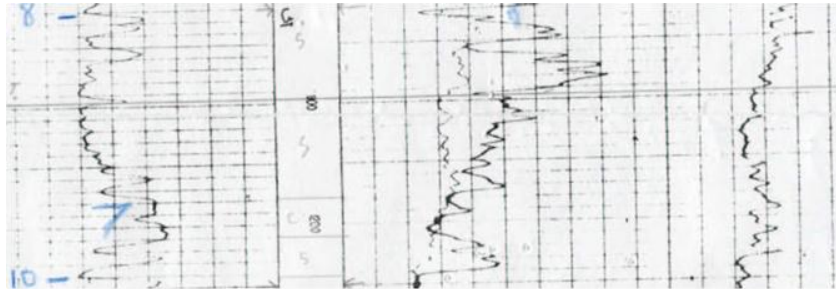


Log profile showing example of floodplain facies (FP)

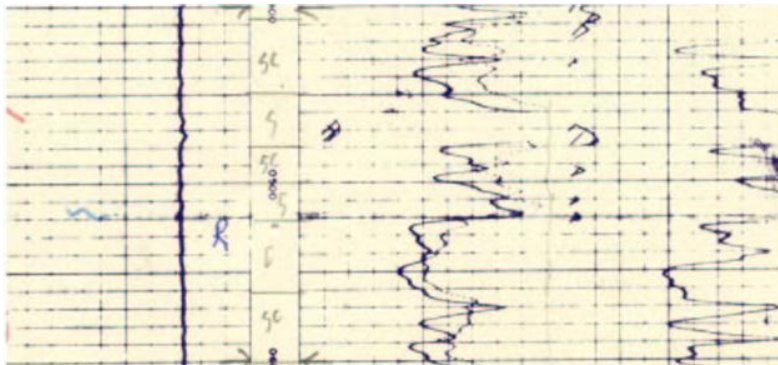


Log profile showing example of shelf/lagoon/  
coastal plain facies (SH)

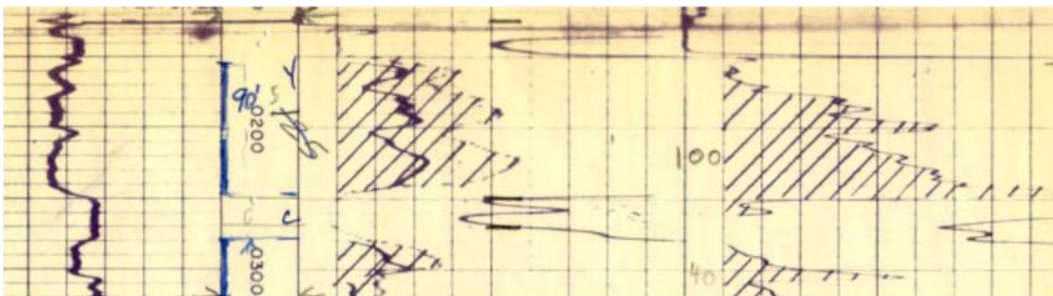
**Figure 7-3** Example analysis of a geophysical log showing a binary and four-phase classification of lithology (taken from Young and Kelley, 2006). Resistivity log is on the right-hand side and spontaneous potential log is on the left-hand side.



Log profile showing example of wave-dominated delta facies (WD)



Log profile showing example of bayfill facies (BF)



Log profile showing example of lower coastal plain fluvial and coastal facies (FD)

**Figure 7-4** Example analysis of a geophysical log showing a binary and four-phase classification of lithology (taken from Young and Kelley, 2006).

Resistivity log is on the right-hand side and spontaneous potential log is on the left-hand side.

*This page intentionally left blank.*

## **8.0 Gulf Coast Aquifer Lithology**

The Gulf Coast Aquifer system is a mixture of interbedded sands and clays of various physical properties, sizes, shapes, and dimensions. As a result of these variations, considerable spatial variability occurs in the hydraulic properties of the deposits. This section provides maps of sand percentage, total sand thickness, and depositional facies to identify spatial differences among and within the geologic units that may be useful to modelers who are developing transmissivity maps of the Gulf Coast Aquifer System.

### **8.1 Sand Thickness and Percent**

The factors that govern the transmissivity of an aquifer include a wide range of depositional characteristics that occur at a wide range of scale. These factors include different sizes and sorting of particles at the scale of less than 1 foot; the arrangement and orientation of beds at the scale of tens of feet, and the interconnection and distribution of different facies at the scale of hundreds of feet. Despite the complexities associated with these different factors, a simple approach commonly practiced in the groundwater industry is to estimate transmissivity based on sand fractions and total sand thickness.

The sand percentage for each geologic unit was calculated by summing the total sand amount across the thickness of the geologic unit and dividing by the amount of the thickness for which the lithology was characterized. Thus, if the geologic unit had a thickness of 100 feet but lithology was determined for only 85 feet and the total measured sand thickness was 75 feet, the sand percentage would be 88% ( $100 \times 75 / 85$ ) and not 75% ( $100 \times 75 / 100$ ). The total sand thickness was calculated by summing the sand amount associated with each of the four lithology groups identified by Mr. Baker. For the total sand thickness calculation, the sand class was assigned a sand percentage of 100%; the sand-with-clay class was assigned a sand percentage of 65%; the clay-with-sand class was assigned a sand percentage of 35%; and the clay class was assigned a sand percentage of 0%.

A continuous distribution of sand percentage for each geologic unit was constructed by interpolating the point values of sand percentages at locations where the geophysical log intersected at least 70% of the geologic unit. These distributions were then mapped onto a raster



grid using kriging algorithms provided in GSLIB (Deutsch and Journel, 1998). The raster grid had a resolution of 4,000 ft by 4,000 ft, and two-dimensional ordinary kriging was used for this process. These values were similar to those used in Young and others (2010) for mapping deposits in the Gulf Coast. The continuous distribution for the sand thickness was developed by multiplying the raster grid of total geologic unit thickness by the raster grid for the sand fraction. Appendix C provide the total sand thickness calculated for each geological unit for each geophysical log.

A recent study of the Chicot and Evangeline Aquifers in a 10-county area near Wharton County (Young and others, 2009; Young and Kelley, 2006) showed good correlations between sand fractions and hydraulic conductivity after different depositional environments had been considered. Based on these correlations, they were able to successfully calibrate a model using aquifer transmissivity values that were generated with relatively simple algorithms that relate transmissivity to sand fraction, total sand thickness, geologic unit, and facies type. An important component of these relationships is that they are sensitive to the unique conditions at the scale of the geologic unit and to the facies type within a geologic unit. This sensitivity is attributed to the fact that the geologic unit and the facies type can be indicators of the general nature, distribution, and interconnectivity of the sand beds that comprise the total sand thickness.

Figures 8-1 through 8-21 provide sand percentage and sand thickness maps for the Chicot Aquifer, Evangeline Aquifer, Burkeville confining unit, Jasper Aquifer, and the geologic units that compose the three aquifers. These figures show a wide range of sand percentages and sand thicknesses among the geologic units that comprise the Gulf Coast Aquifer system. Comparison of these maps to similar maps provided by Young and others (2010) may show differences in the areas where they overlap. The overlap areas occur between cross-sections 10 and the mid-point between cross-sections 7 and 8 (see Figure 1-1). Where differences occur between the two sets of sand maps, the mapped values in this study supersede the mapped values presented by Young and others (2010). There are three primary reasons for why differences may occur between the two sets of maps. One reason is that the contouring in the overlapping area is influenced by new information gather slightly outside of the overlapping area that was not available for contouring by Young and others (2010). A second reason is that addition sand information in the overlapping area is included in this study. A third reason is that there are

some adjustments to the top and bottom boundaries of the geology units north of dip-section 10, which affects the intervals over which sand thicknesses and sand percentages are tallied.

### ***8.1.1 Chicot Aquifer***

Figure 8-1 shows the sand thickness distribution for the Chicot Aquifer. The sand thicknesses increase toward the coast where it achieves values as high as about 1,500 ft. Among the three geologic units that comprise the Chicot Aquifer, the units all have distinctly different distributions of sand percentages. In the Beaumont unit (Figure 8-2), the sand percentages typically are between 40% and 60%. In both the Lissie unit (Figure 8-4) and the Willis unit (Figure 8-6), sand percentages greater than 60% are relatively common. In the Lissie unit, the higher sand percentages (60% to 100%) are found near Wharton, Fort Bend, and Waller Counties whereas the lower sand percentages (40% to 60%) are found near Liberty, Hardin, and Chambers counties. In the Willis unit (Figure 8-6), the sand percentage is highest in the eastern region near Fort Bend County where it is typically greater than 60% and frequently higher than 80%. Because the Beaumont, Lissie, and Willis Formations dip and thicken towards the coast, all of their maps for total sand thickness thicken toward the coast.

### ***8.1.2 Evangeline Aquifer***

Figure 8-8 shows the sand thickness distribution for the Evangeline Aquifer. The sand thickness increases toward the coast and approaches 3,000 feet near the coastline. In the upper Goliad (Figure 8-9), the sand percentages are typically between 40% and 60%. However, in the vicinity of Fort Bend County and Cameron Parish, sand percentages in the range between 60% and 80% are relatively common. The distribution of the sand percentages in the lower Goliad unit (Figure 8-11) mimic those for the upper Goliad unit except that the percentages tend to be about 10% lower and more spatially variable. Among the geologic units that comprise the Evangeline Aquifer, the upper Lagarto unit (Figure 8-13) has the lowest sand percentage with sand values usually between 20% and 60%. However, the upper Lagarto displays higher sand percentages that exceed 60% near the Louisiana/Texas boundary.

### ***8.1.3 Middle Lagarto (Burkeville confining unit)***

Figure 8-16 shows the sand thickness distribution for the middle Lagarto unit. Across most of the unit, the sand thicknesses vary between 100 and 200 feet and increase toward the coast. The

sand fraction distribution (Figure 8-15) shows that across most of the Burkeville unit, the sand percentages vary between 20% and 60%, have regions with less than 40% in the western part of the study area, and have regions with greater than 60% in the eastern part of the study area.

#### ***8.1.4 Jasper Aquifer***

Figure 8-17 shows the sand thickness distribution for the Jasper Aquifer. The sand thickness increases toward the coast where it exceeds 1,000 feet. In the lower Lagarto (Figure 8-18), the areas of high and low sand percentages are similar to the sand percent distribution across the middle Lagarto unit, except in some areas they are slightly higher. Across the Oakville unit (Figure 8-20), the sand percentages distribution is highly variable but is commonly between 40% and 60%. In its updip region, the Oakville unit has localized areas with sand percentages greater than 60% and in its downdip region, the Oakville has localized area with sand percentages less than 40%.

## **8.2 Depositional Facies**

The hydrological properties of the Gulf Coast Aquifer system and its component hydrogeologic units are governed strongly by the characteristics of the sediments laid down at the time of deposition. Sediment texture (grain size, sorting, etc.) and composition of framework grains and matrix material are dependent upon the influences of depositional energies, which vary with depositional setting. Sand body size, shape, orientation, and interconnection are similarly products of the depositional setting. Sediments and rocks deposited in a similar depositional setting can be grouped together as a "facies." Facies are in turn elements of a given "depositional system." Thus, sediments deposited in a fluvial depositional system can have relatively coarser grain size and good sorting when deposited in a high-energy river channel, and can be considered "fluvial" facies. In contrast, a fine-grained, often less well sorted sediment also deposited as part of a fluvial depositional system can be deposited in low-energy overbank and floodplain settings. The deposits would be considered "floodplain facies." Sediments in a floodplain facies will have substantially poorer hydrologic properties as a result. Table 7-2 provides a summary of facies types and brief descriptions of each type.

### ***8.2.1 Chicot Aquifer***

Depositional facies within the Chicot Aquifer are shown in Figures 8-2, 8-4, and 8-6. For the Willis, Lissie, and Beaumont units, the most prevalent facies in the updip areas are the Fluvial/Meanderbelt facies. Fluvial/Meanderbelt facies are characterized by zones of relatively high permeability associated with networks of sand beds with thicknesses greater than 30 feet. Along the eastern edge of all three formations, the Fluvial/Meanderbelt facies cover the entire width of each formation with the eastern coverage being the greatest for the Lisse and the least for the Beaumont. Within the matrix of the Fluvial/Meanderbelt facies, all of the units contain Floodplain facies. The most dominant coverage in the Lissie unit is from the Fluvial/Meanderbelt facies and the Floodplain facies. Floodplain facies include overbank sediments deposited from the major rivers responsible for the meanderbelt facies. Floodplain facies are characterized by zones of moderate to fair permeability associated with interbedded layers of clays, sands, and fine-grained deposits. In the central portion of the Lissie unit, the Fluvial/Meanderbelt facies are separated by a dip-oriented band of floodplain facies with a width of 30 miles and extending from the updip to the downdip boundary of the facies map. Across the western and central coastal regions of the Willis and the Beaumont units, the dominant facies is the lower Coastal Plain Fluvial/Coastal facies. These facies typically include mixtures of sands and clays deposited from fluvial channels and terminal fluvial deposits.

### ***8.2.2 Evangeline Aquifer***

Within the Evangeline Aquifer, the dominant facies are Lower Coastal Plain Fluvial/Coastal facies. The distribution pattern of facies for the upper Lagarto (Figure 8-13) and the lower Goliad (Figure 8-11) units are very similar. Both units are characterized by a coverage consisting of approximately 70% are Lower Coastal Plain Fluvial/Coastal facies and approximately 15% sand-poor Bayfill/Lagoonal facies in the western part of the study area. The primary difference between the two units is that the higher percentage of Fluvial/Meanderbelt facies in the updip region of the lower Goliad unit. The transition from the lower Goliad unit to the upper Goliad unit includes an expansion of the updip Fluvial/Meanderbelt facies and the occurrence of Shorezone facies along the coast. The Shorezone facies are characterized by sands primarily associated with barrier islands and delta fronts and contain clays associated with prodelta, bayfill, and lagoonal deposits.

### ***8.2.3 Middle Lagarto Unit (Burkeville confining unit)***

Figure 8-15 shows the depositional facies associated with the middle Lagarto unit. The distribution of facies across the middle Lagarto unit are similar to the facies distribution across the upper and lower Lagarto units. The majority of the coverage is Lower Coastal Plain Fluvial/Coastal facies but a significant part of the coverage in the eastern area are the Bayfill/Lagoonal facies. Bayfill/Lagoonal facies are characterized by mud-dominated deposits containing occasional layers of sands. Among the three Lagarto units, the middle Lagarto unit has the largest continuous zone and greatest overall coverage by the Bayfill/Lagoonal facies.

### ***8.2.4 Jasper Aquifer***

Figures 8-18 and 8-20 present the facies maps for the lower Lagarto and Oakville units that comprise the Jasper Aquifer. Whereas the coverage of the lower Lagarto unit is dominated by a Lower Coastal Plain Fluvial/Coastal plain facies, the coverage of the Oakville is dominated by a Wave Dominated Delta facies. The difference in the facies coverage occurs because although both the Lagarto and Oakville units were formed during a major fluvial deltaic depositional episode, the Oakville units forms the lower progradational part and the Lagarto forms the upper retro gradational part. The Bayfill/Lagoonal facies in the downdip regions of both units represents part of a marine transgressive shale that separates the two Jasper units.

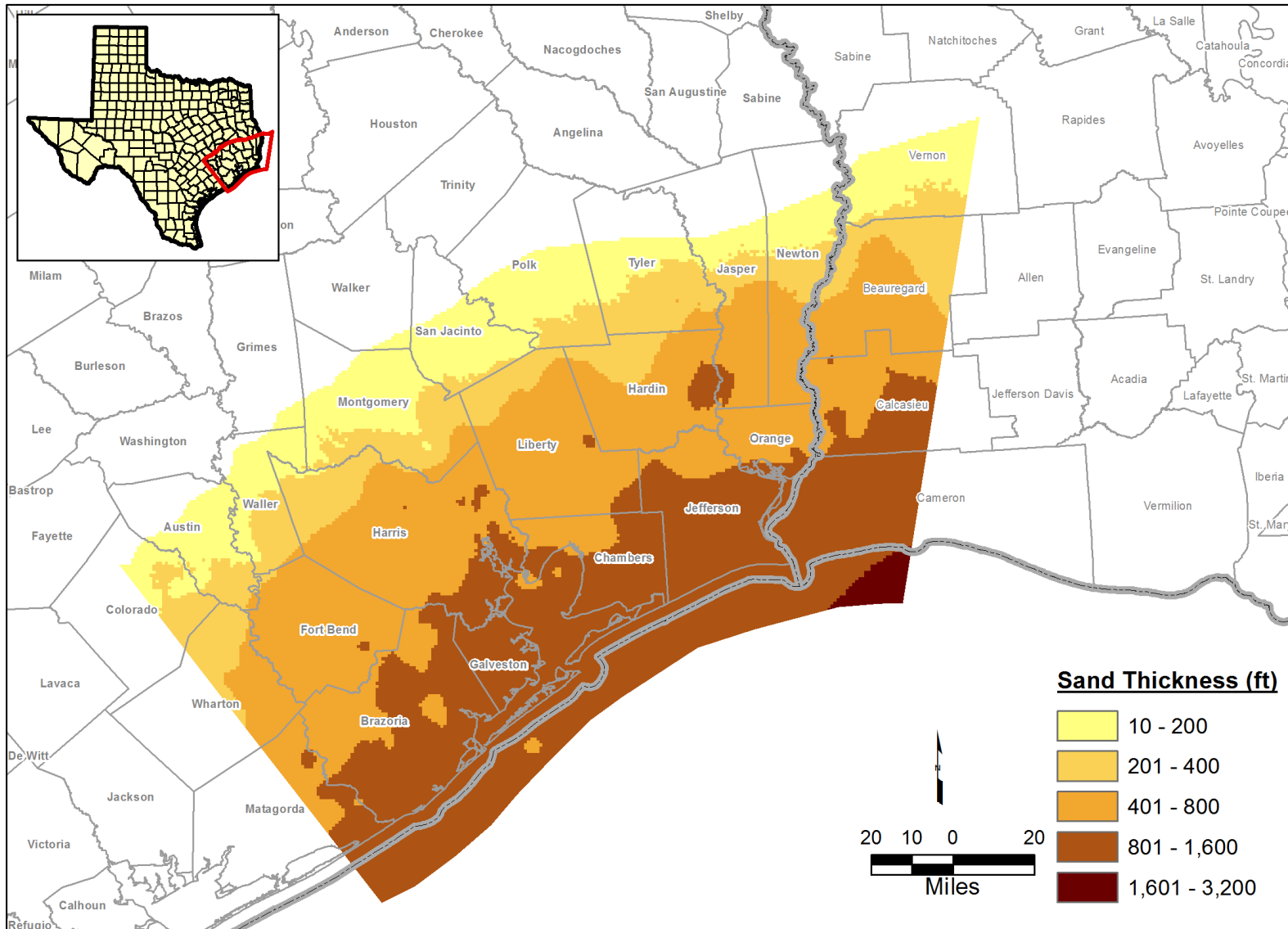
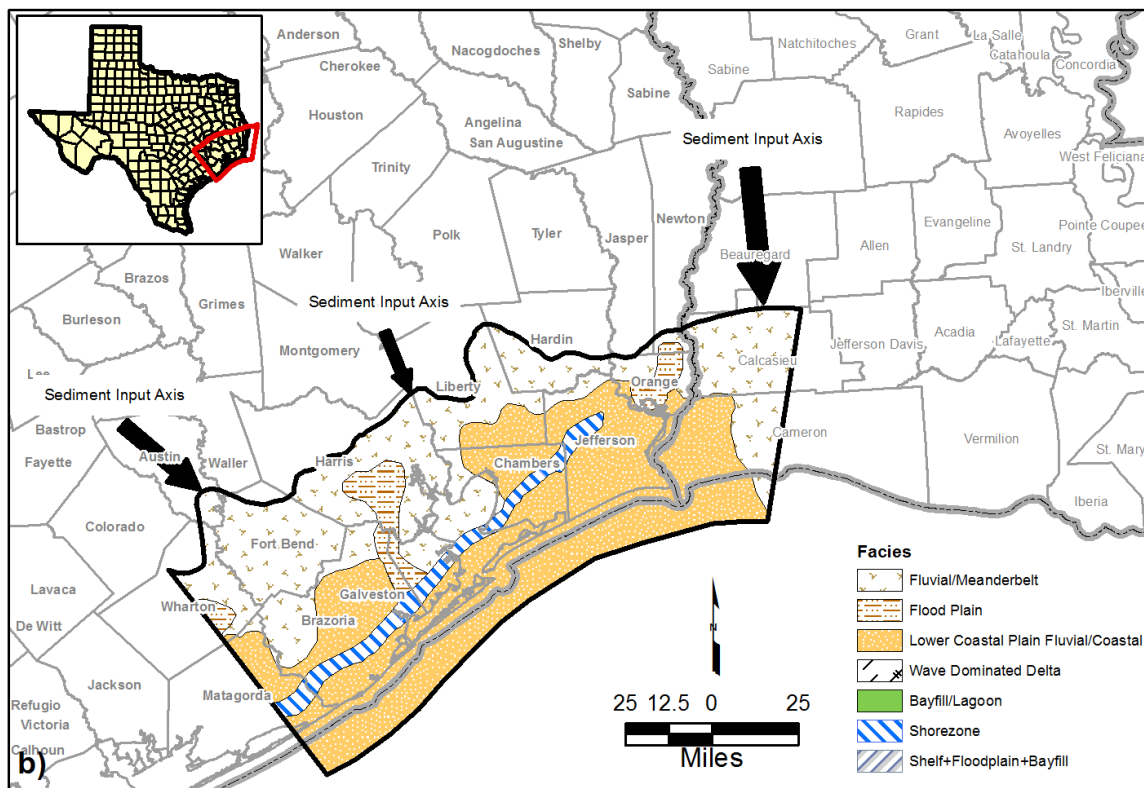
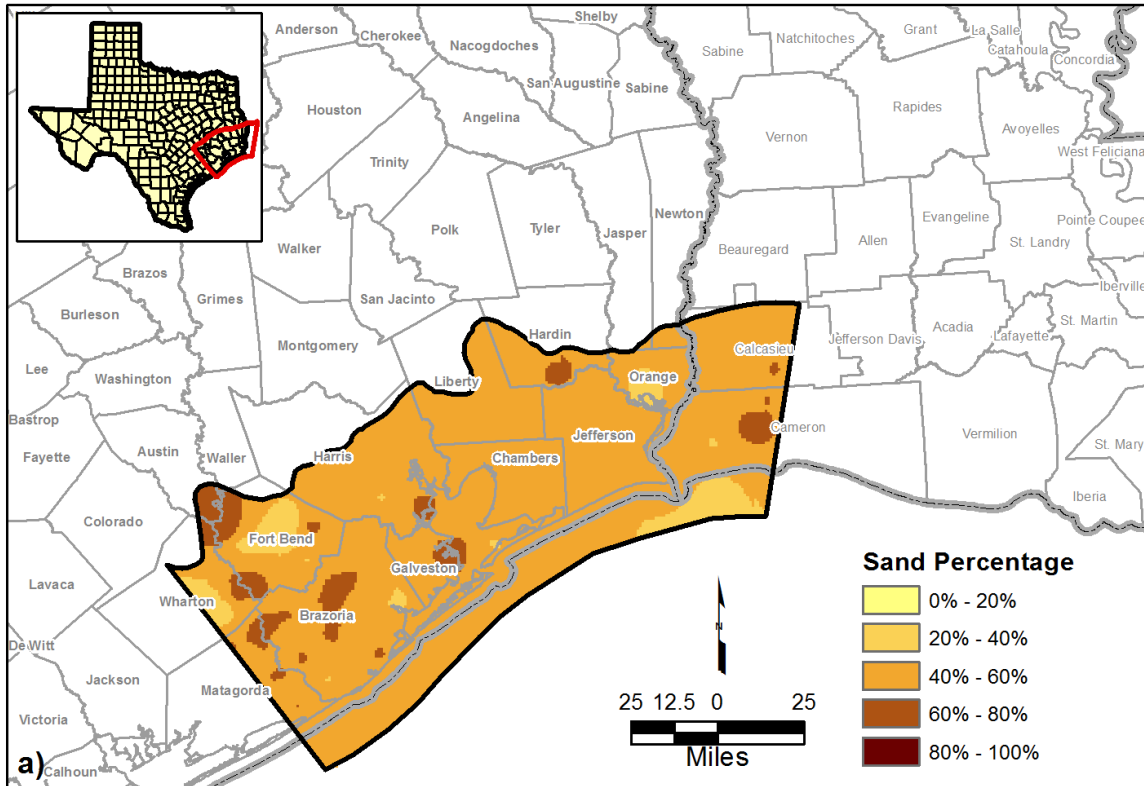


Figure 8-1 Map of the Chicot Aquifer showing total sand thickness.



**Figure 8-2** Map of the Beaumont geologic unit showing: (a) percentage sand coverage and (b) depositional facies.

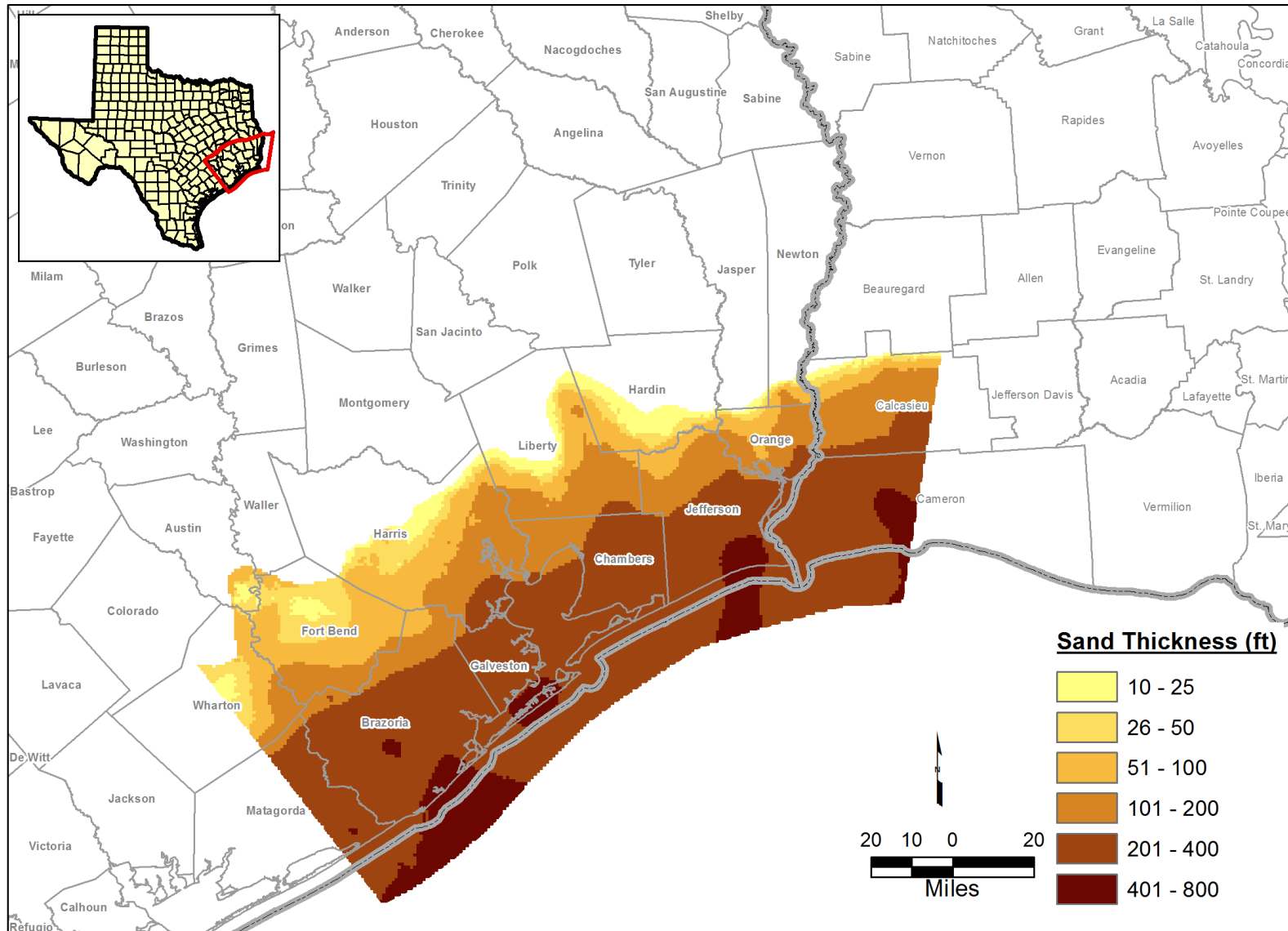
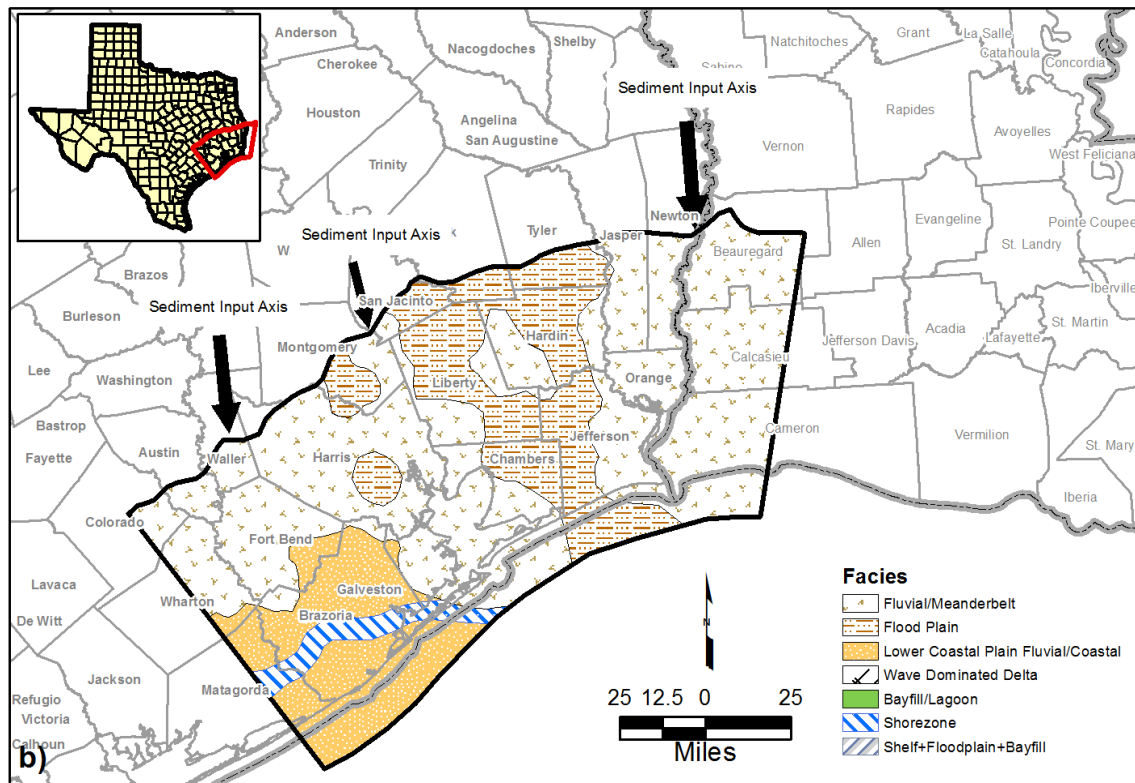
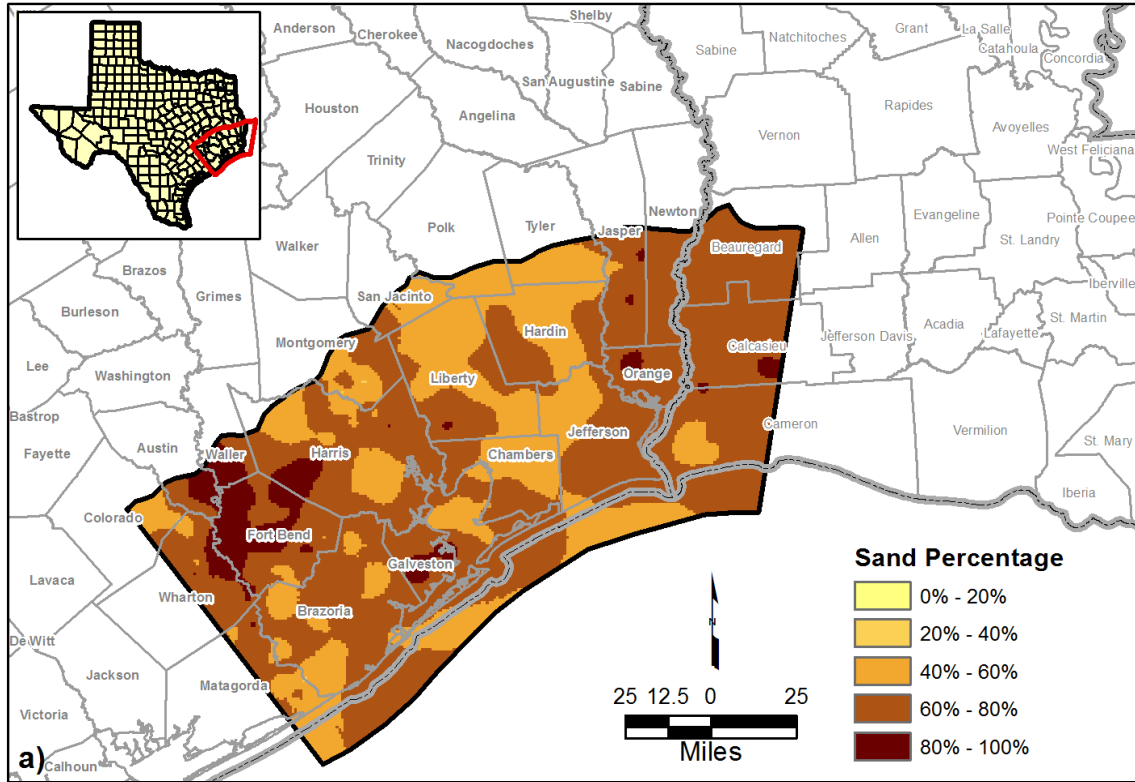


Figure 8-3 Map of the Beaumont geologic unit showing total sand thickness.





**Figure 8-4** Map of the Lissie geologic unit showing: (a) percentage sand coverage and (b) depositional facies.

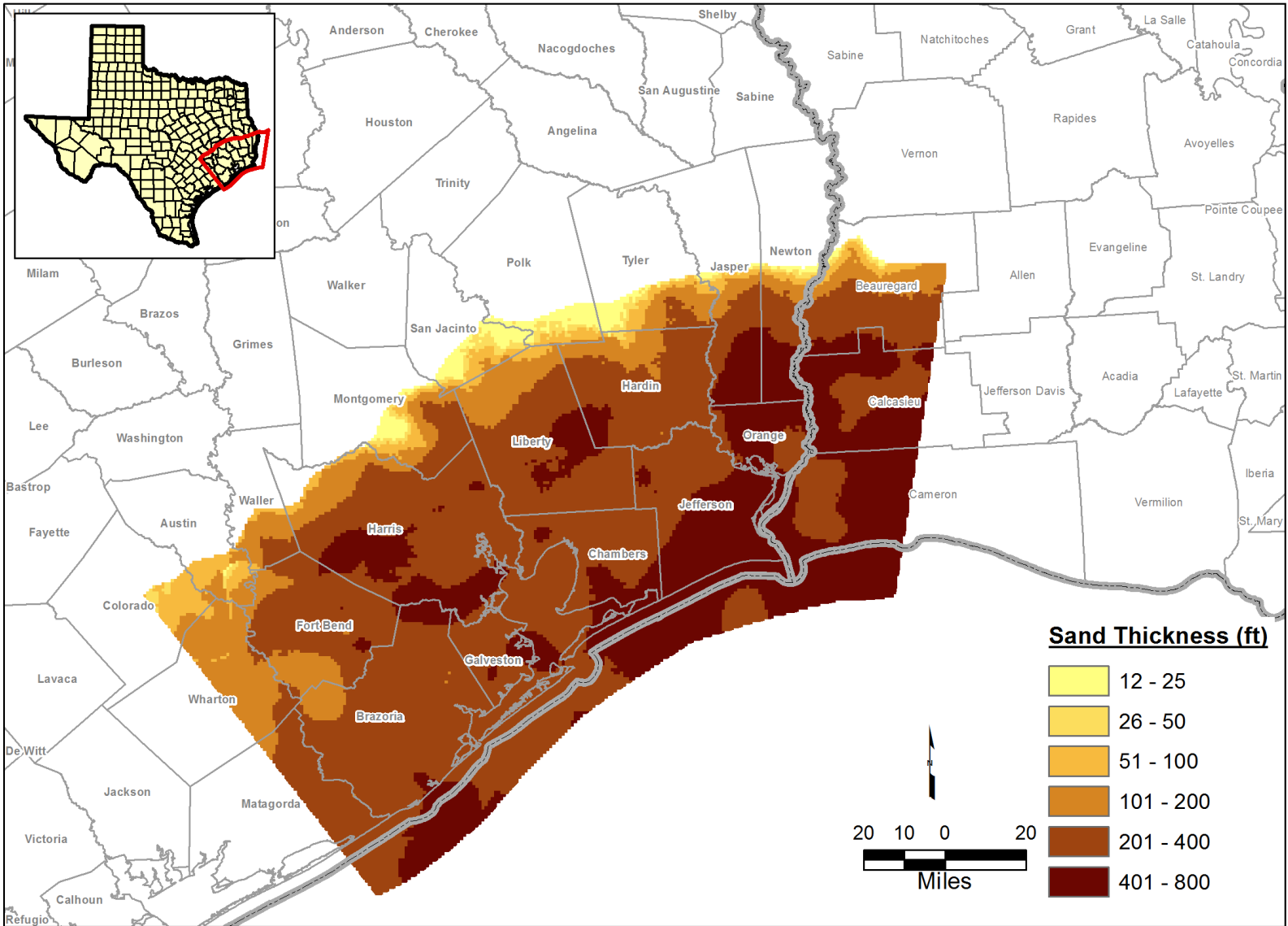
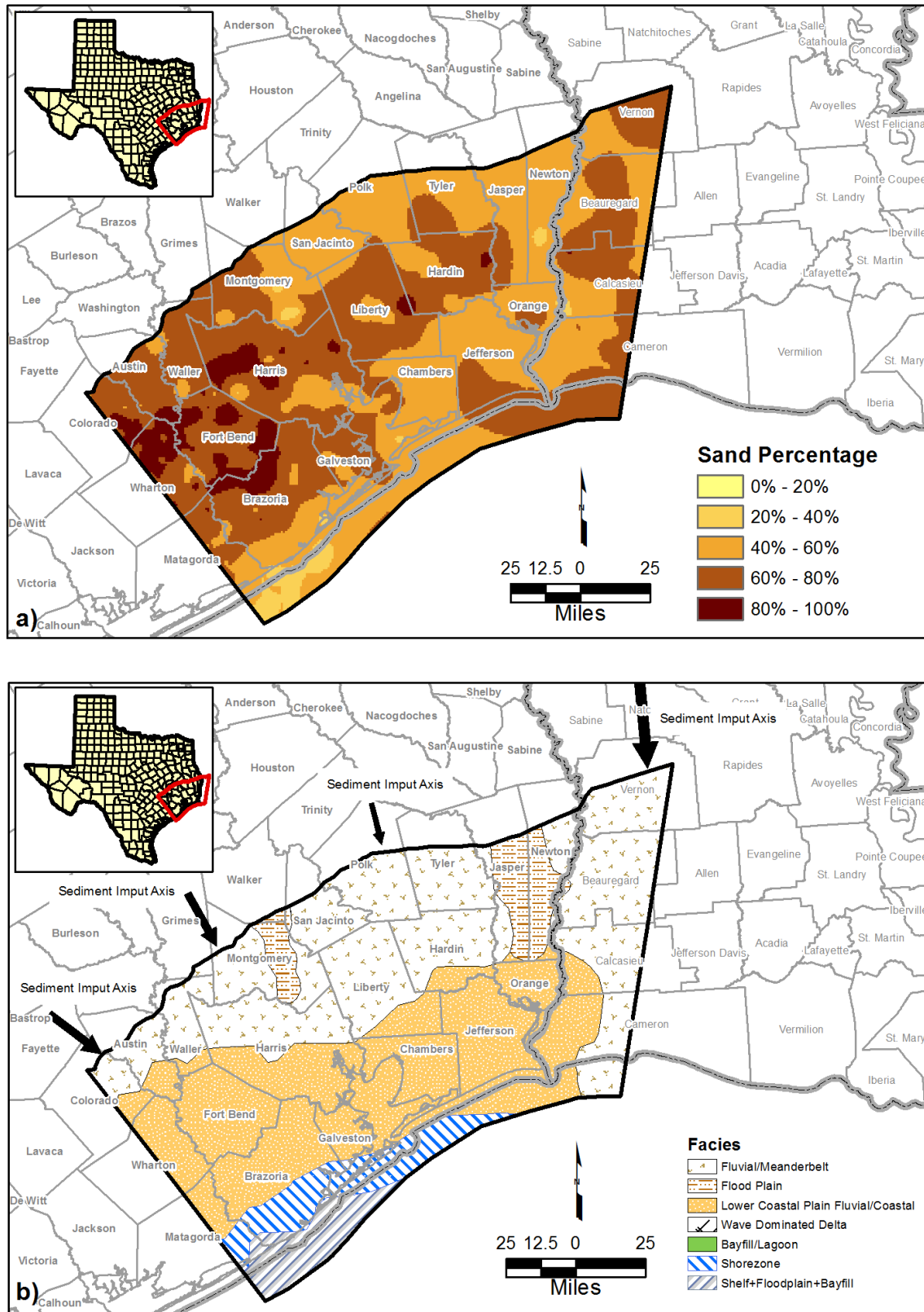


Figure 8-5 Map of the Lissie geologic unit showing total sand thickness.



**Figure 8-6** Map of the Willis geologic unit showing: (a) percentage sand coverage and (b) depositional facies.

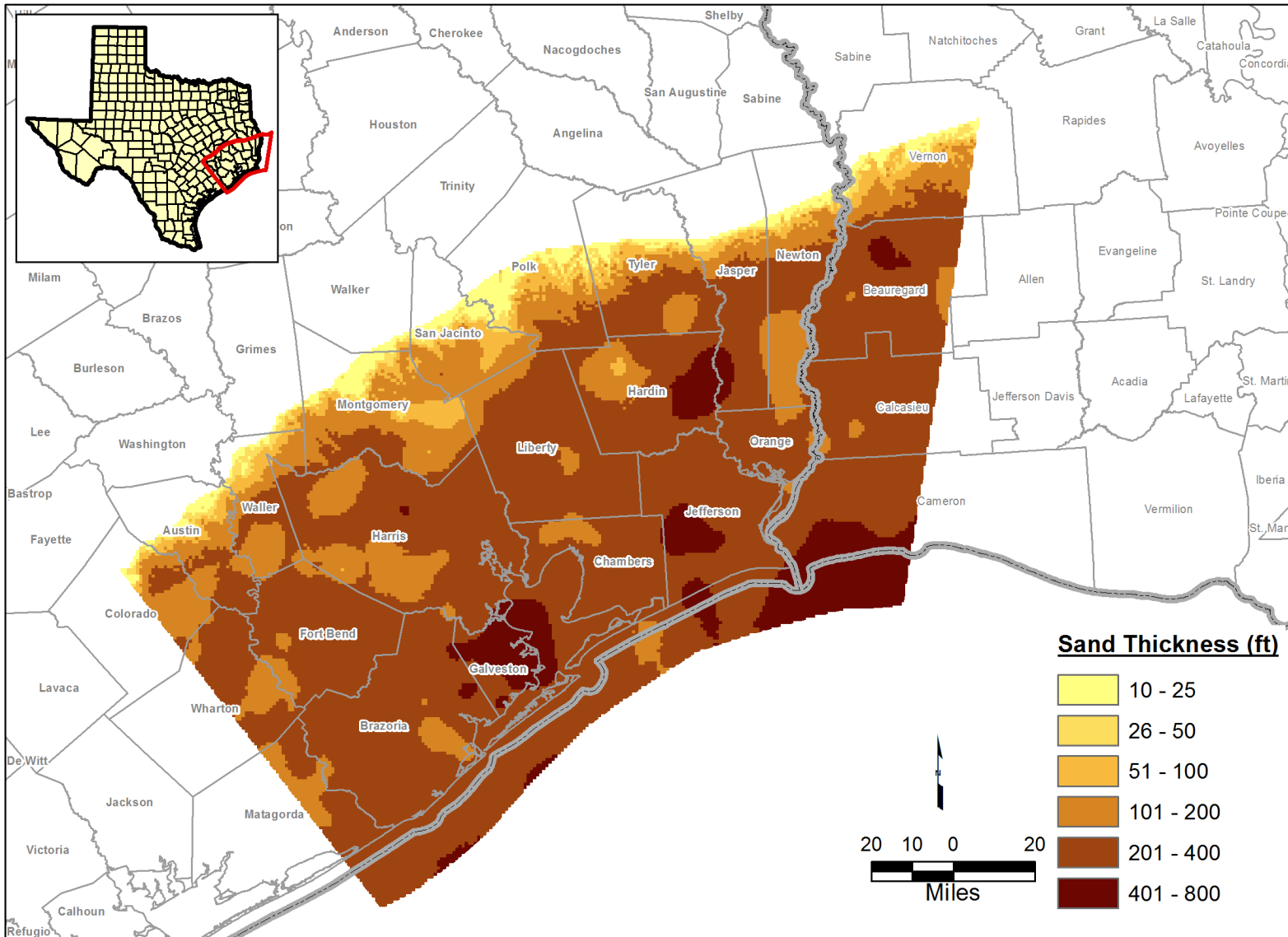


Figure 8-7 Map of the Willis geologic unit showing total sand thickness.

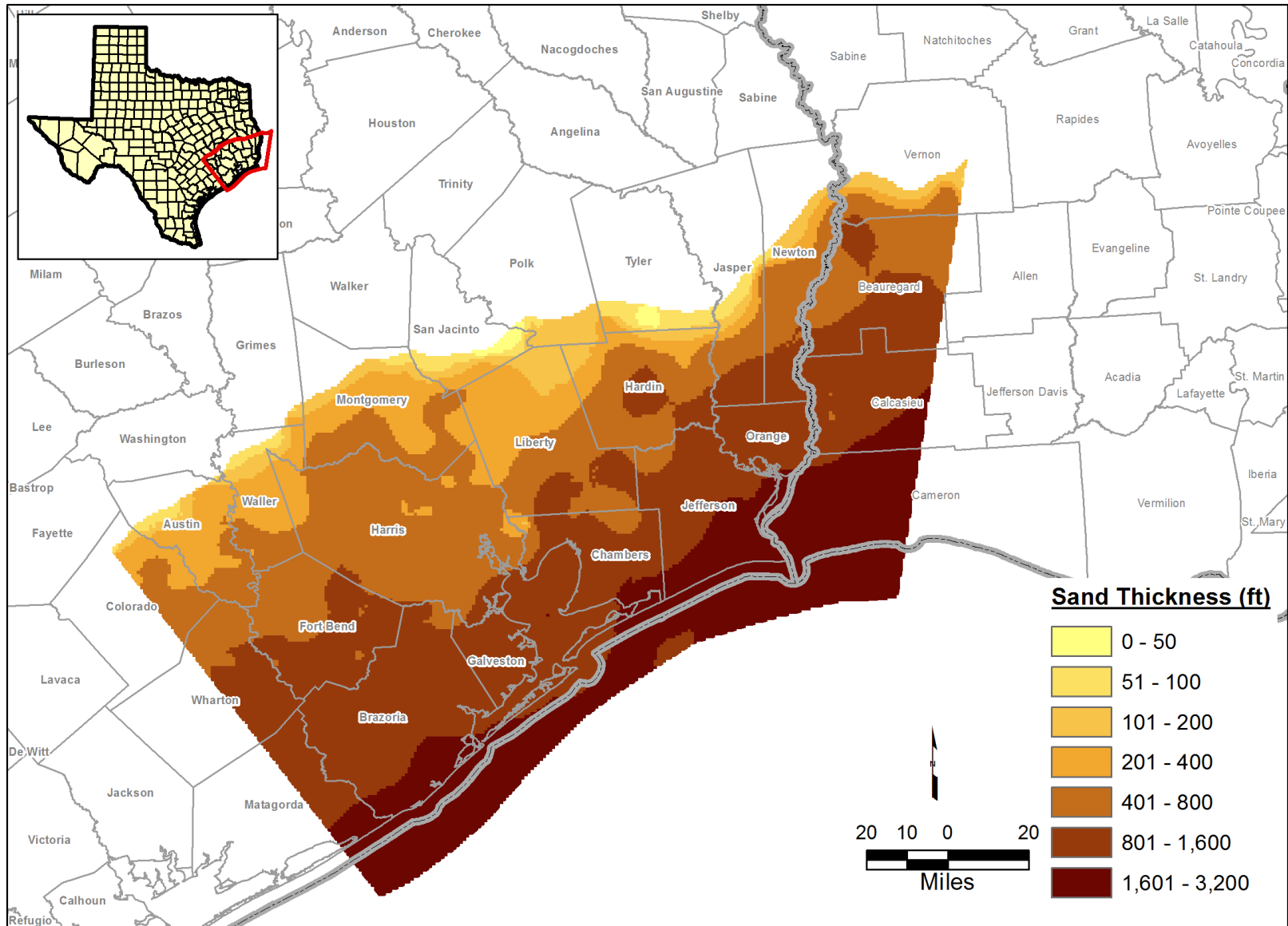
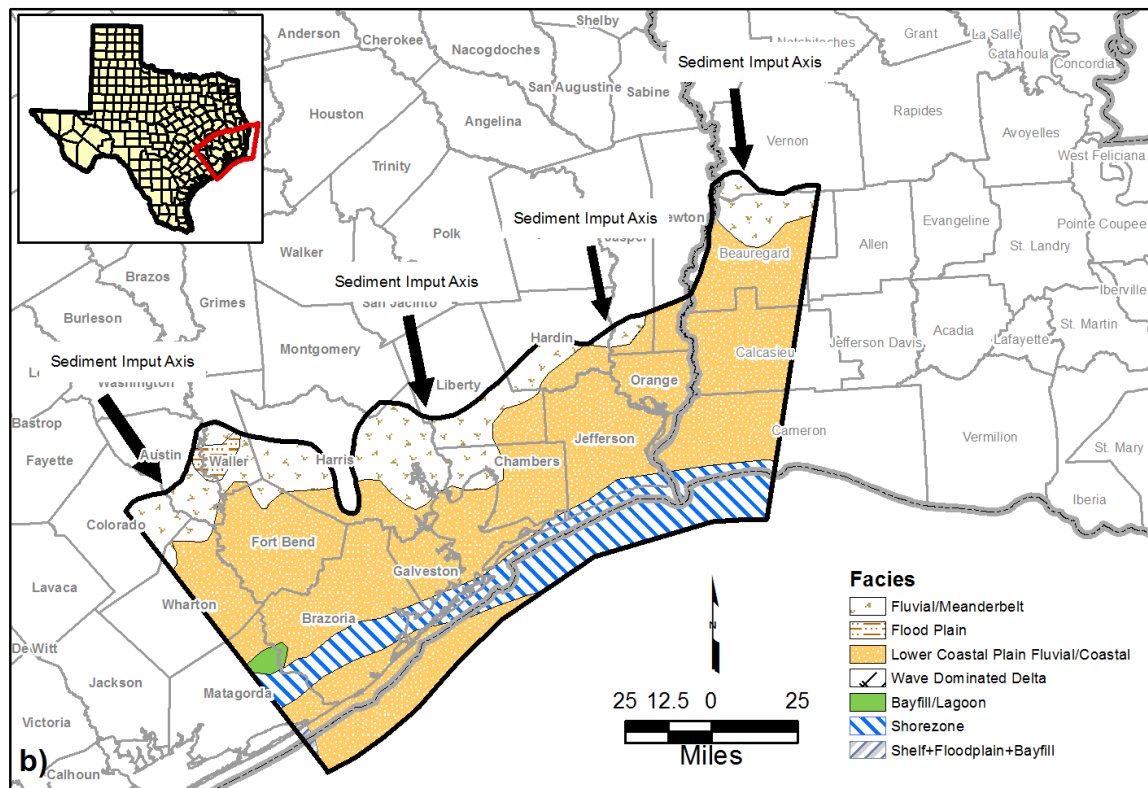
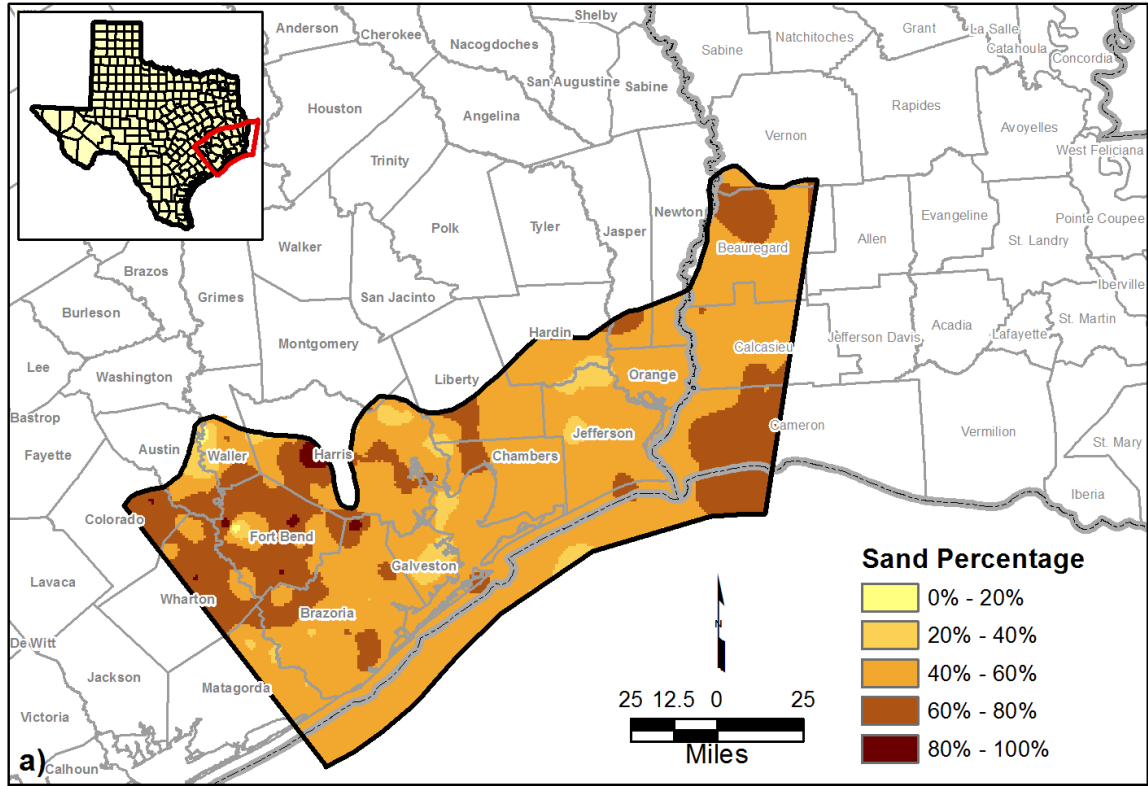


Figure 8-8 Map of the Evangeline Aquifer showing total sand thickness



**Figure 8-9** Map of the upper Goliad geologic unit showing: (a) percentage sand coverage and (b) depositional facies.

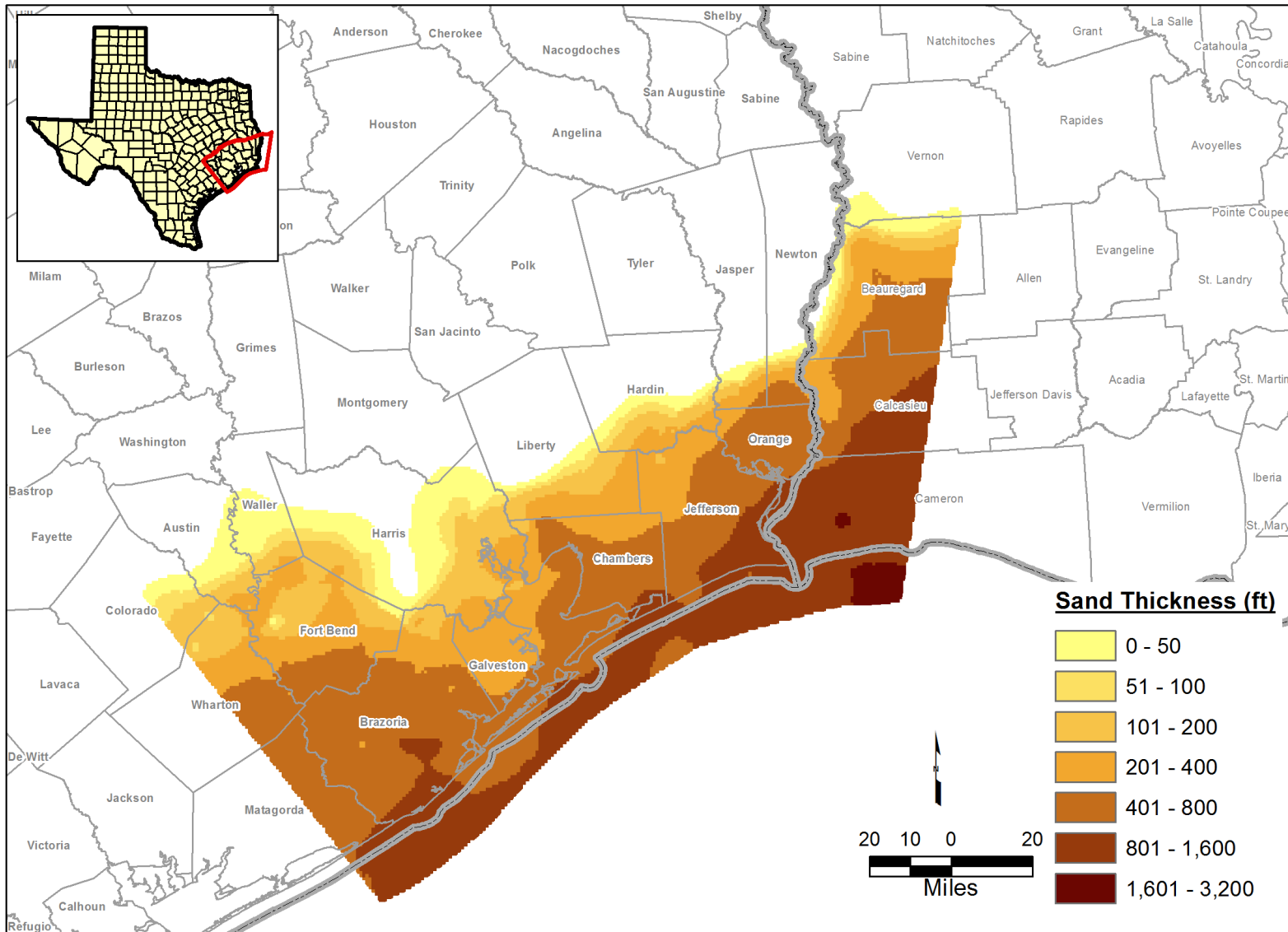
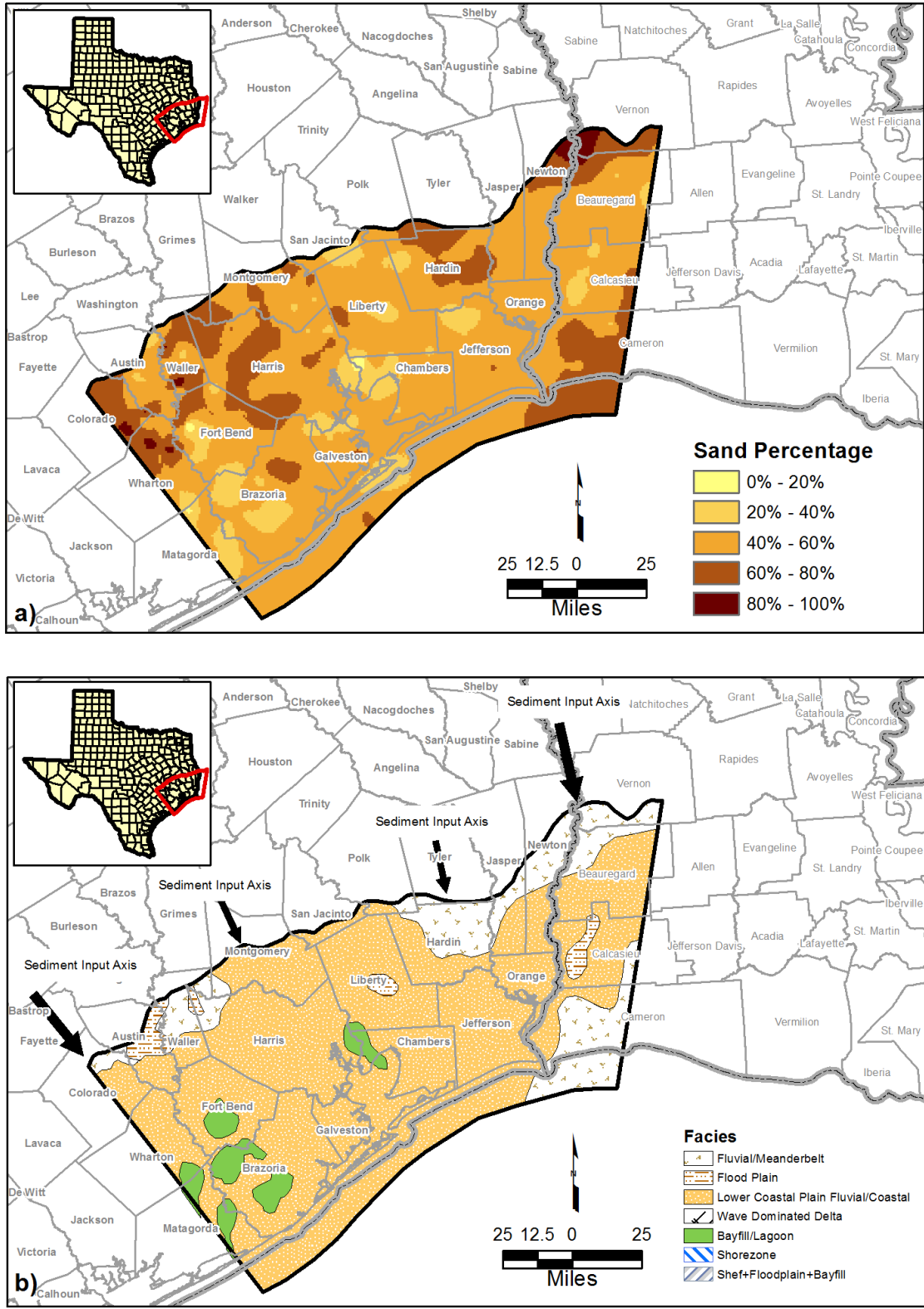


Figure 8-10 Map of the upper Goliad geologic unit showing total sand thickness.



**Figure 8-11** Map of the lower Goliad geologic unit showing: (a) percentage sand coverage and (b) depositional facies.



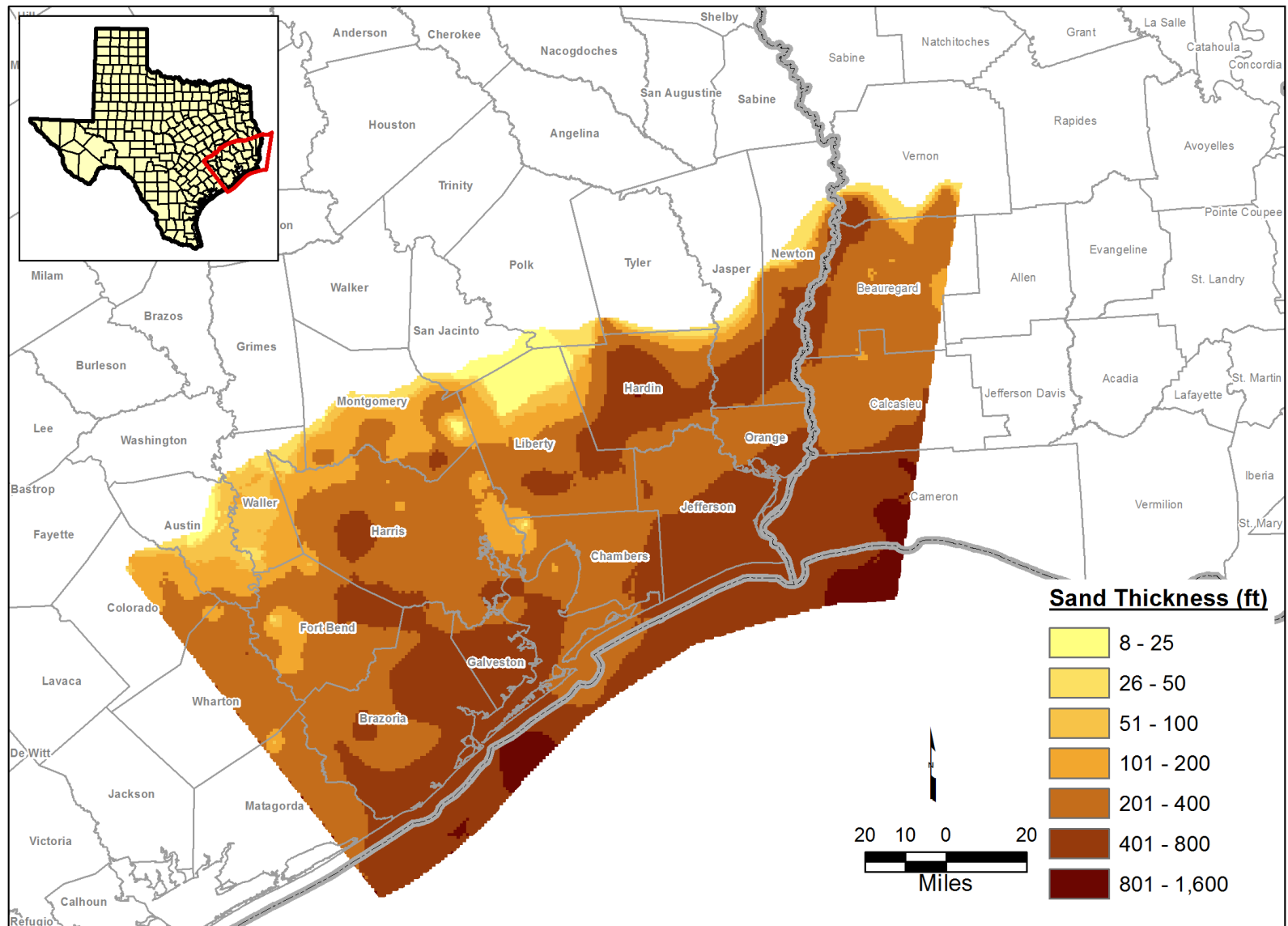
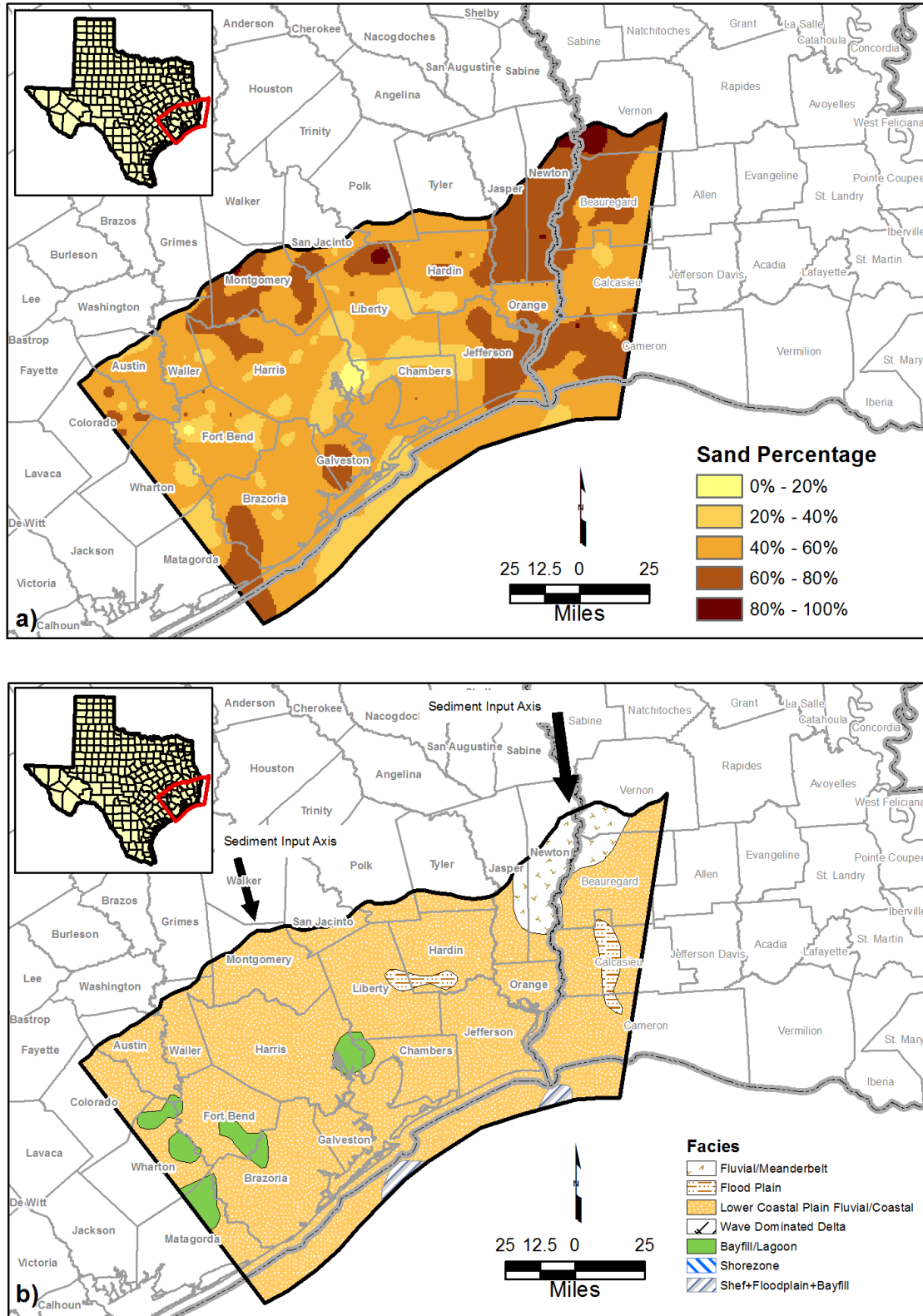


Figure 8-12 Map of the lower Goliad geologic unit showing total sand thickness.



**Figure 8-13** Map of the upper Lagarto geologic unit showing: (a) percentage sand coverage and (b) depositional facies.

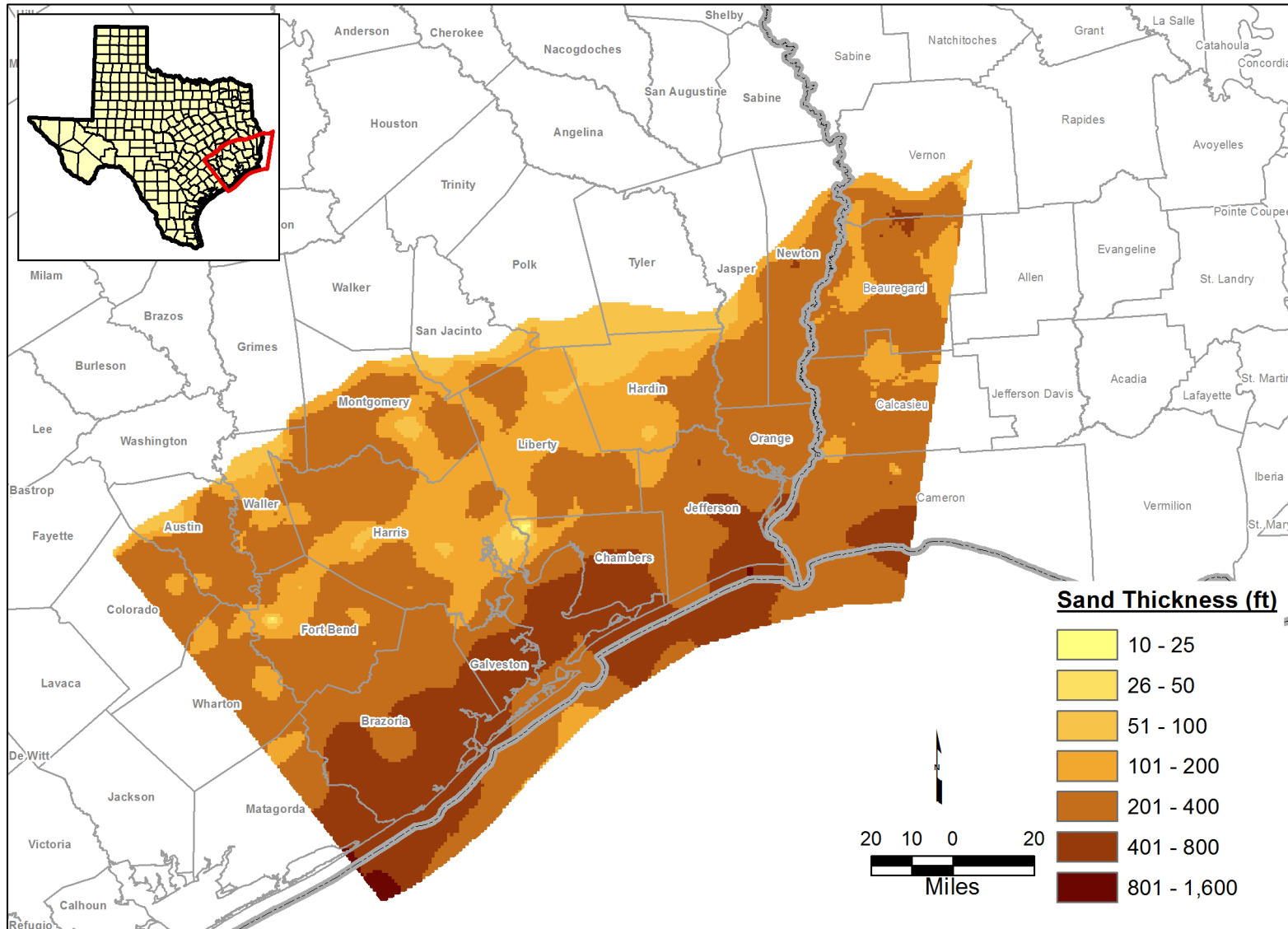
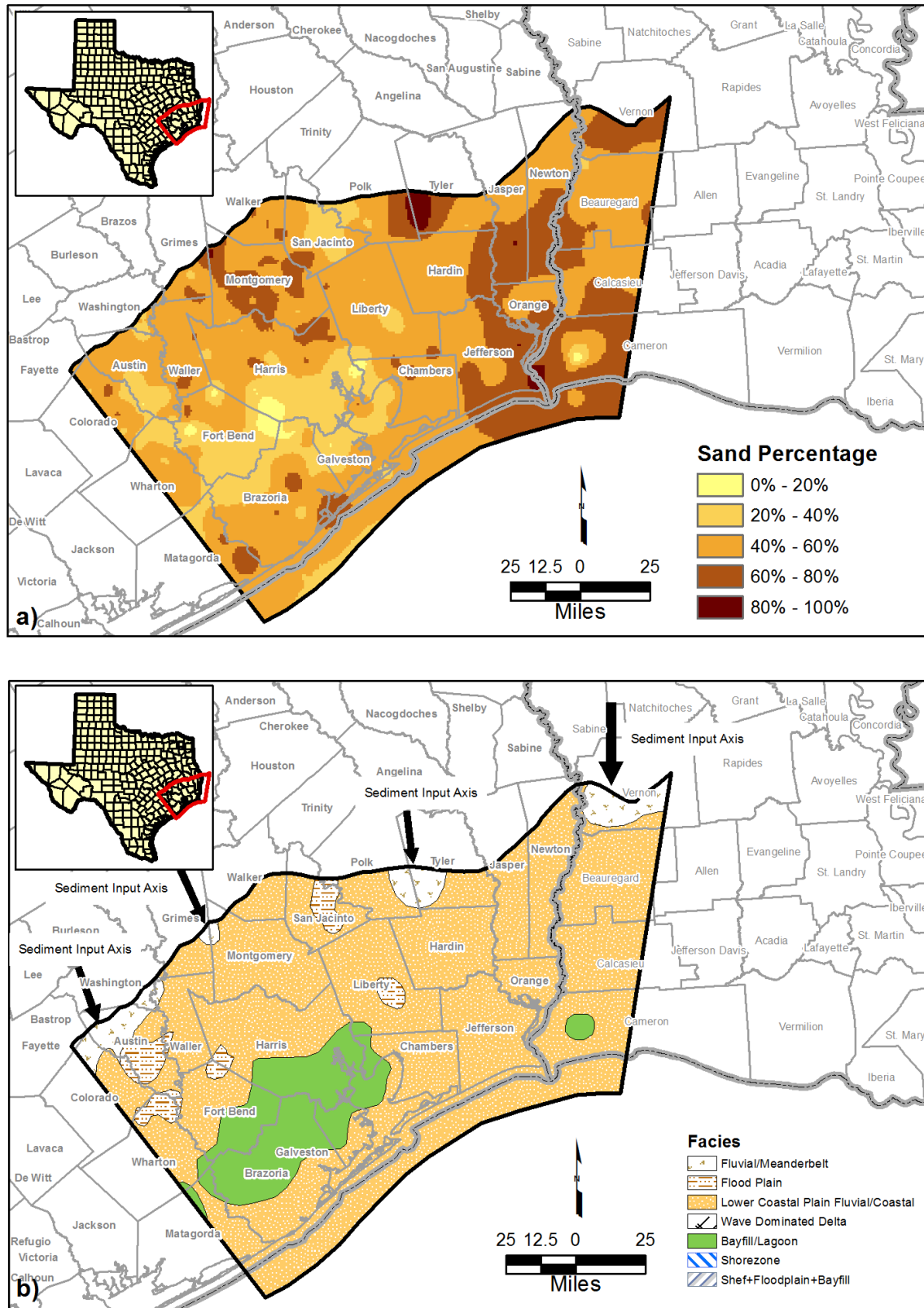


Figure 8-14 Map of the upper Lagarto geologic unit showing total sand thickness.



**Figure 8-15** Map of the Burkeville confining unit (middle Lagarto geologic unit) showing: (a) percentage sand coverage and (b) depositional facies.

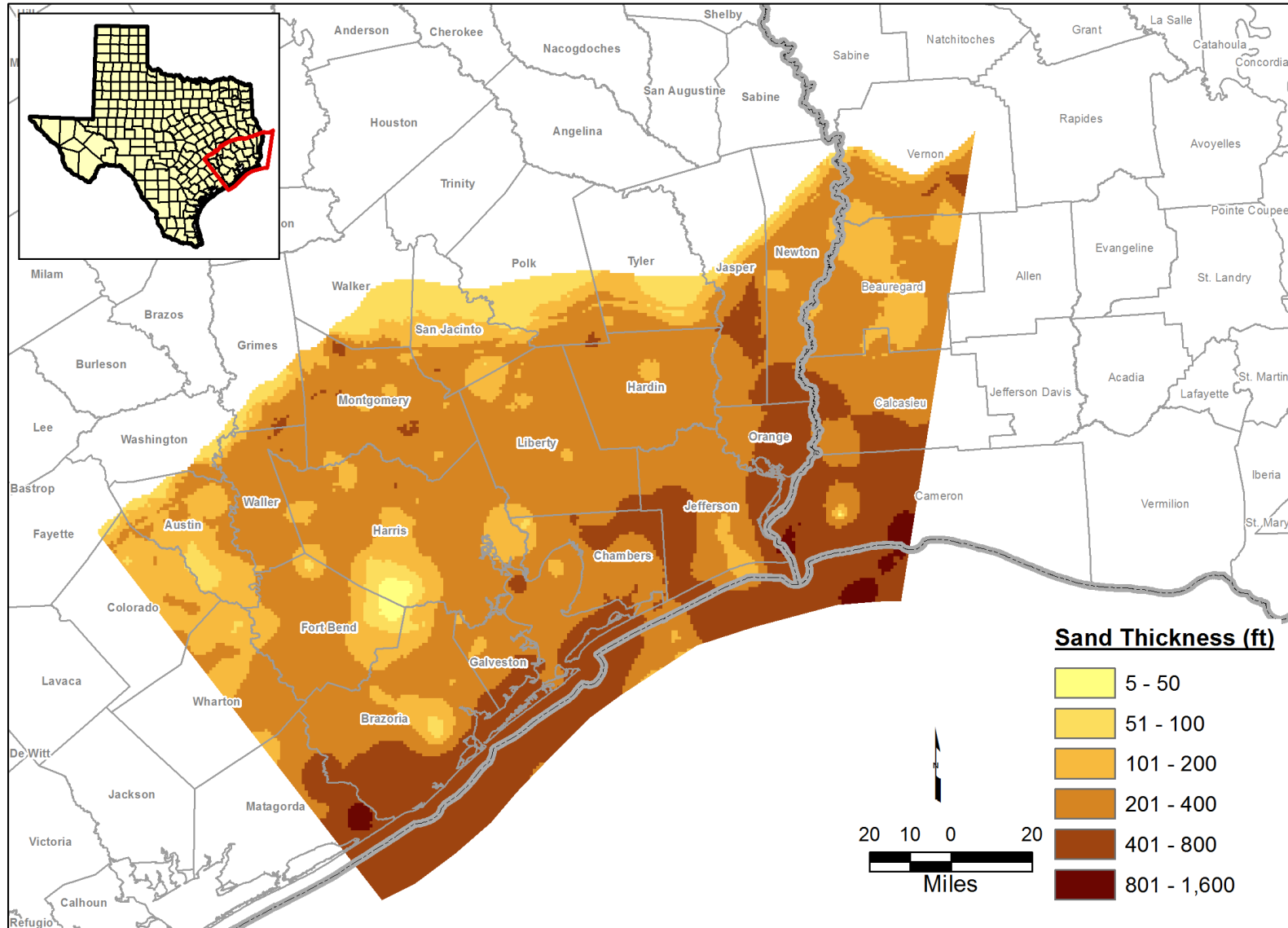


Figure 8-16 Map of the Burkeville confining unit (middle Lagarto geologic unit) showing total sand thickness.

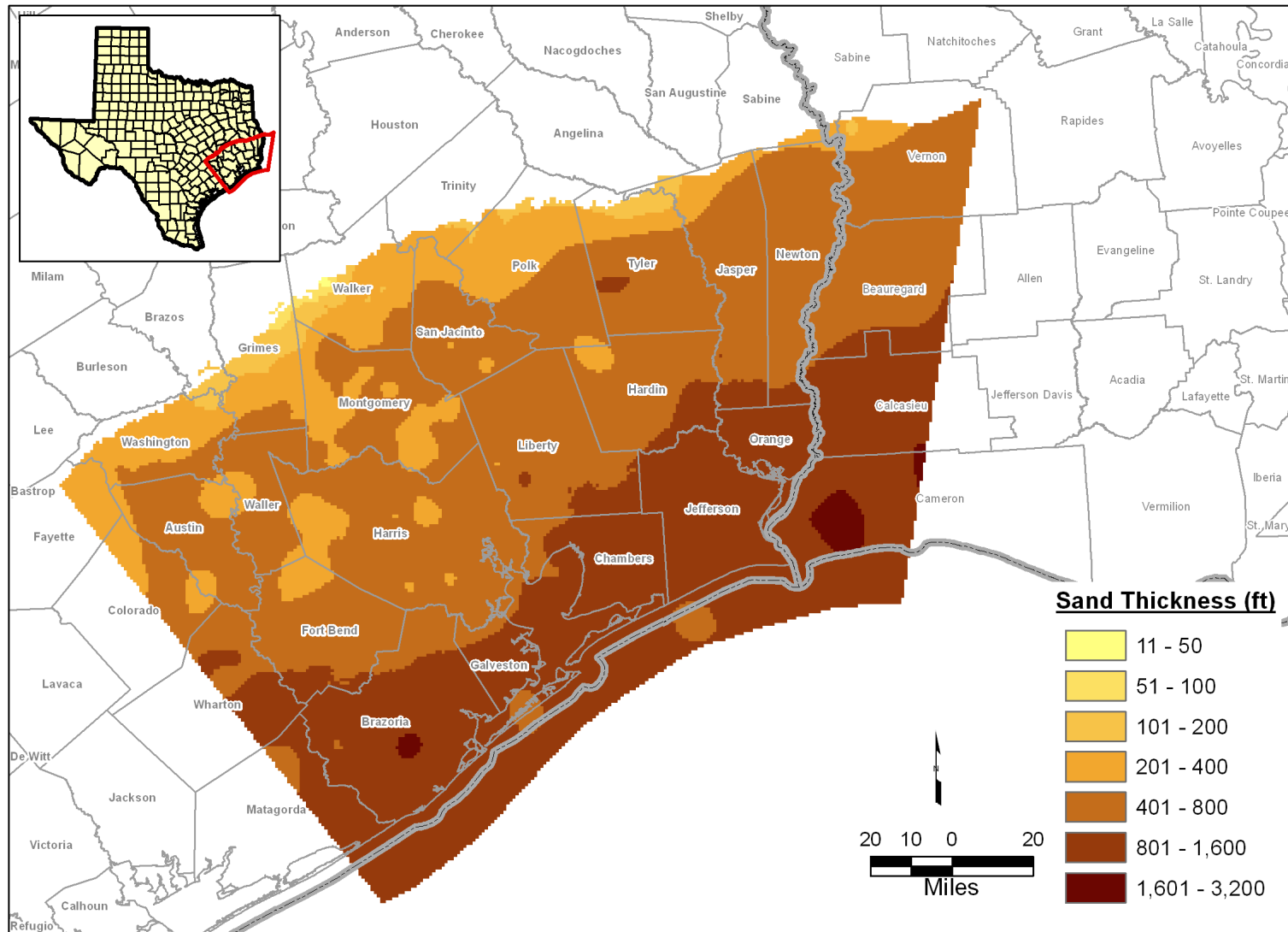


Figure 8-17 Map of the Jasper Aquifer showing total sand thickness.

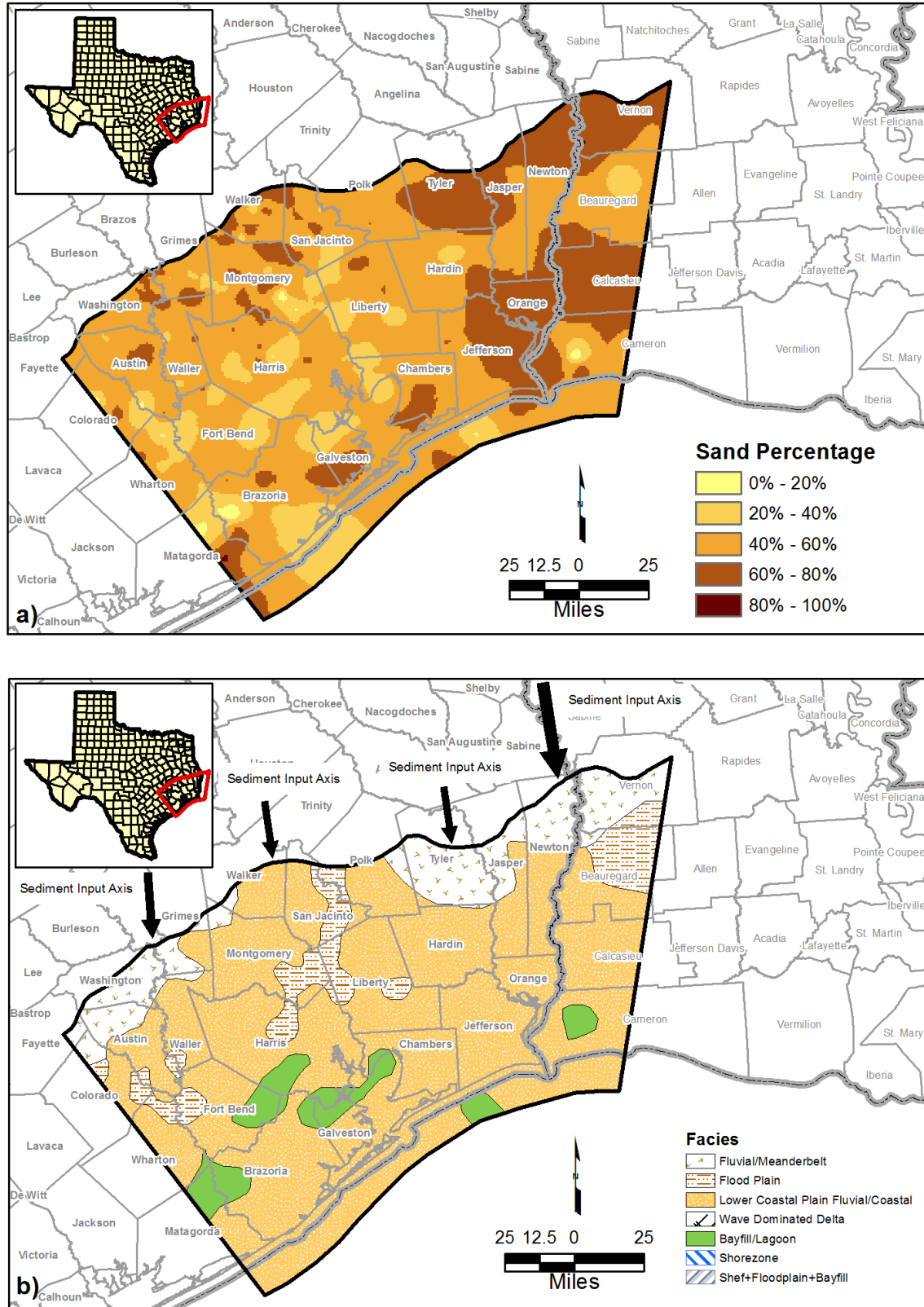


Figure 8-18 Map of the lower Lagarto geologic unit showing: (a) percentage sand coverage and (b) depositional facies.

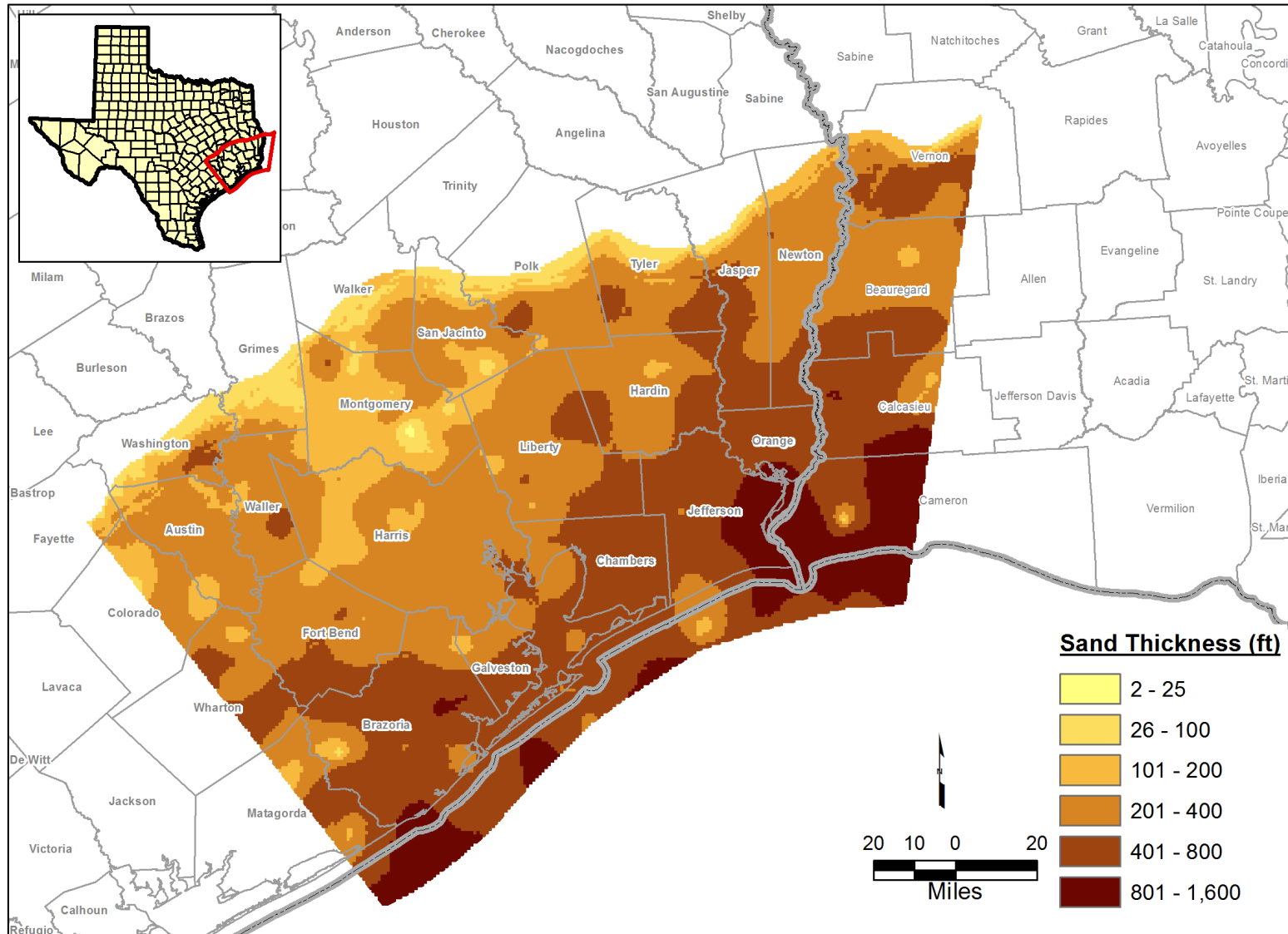
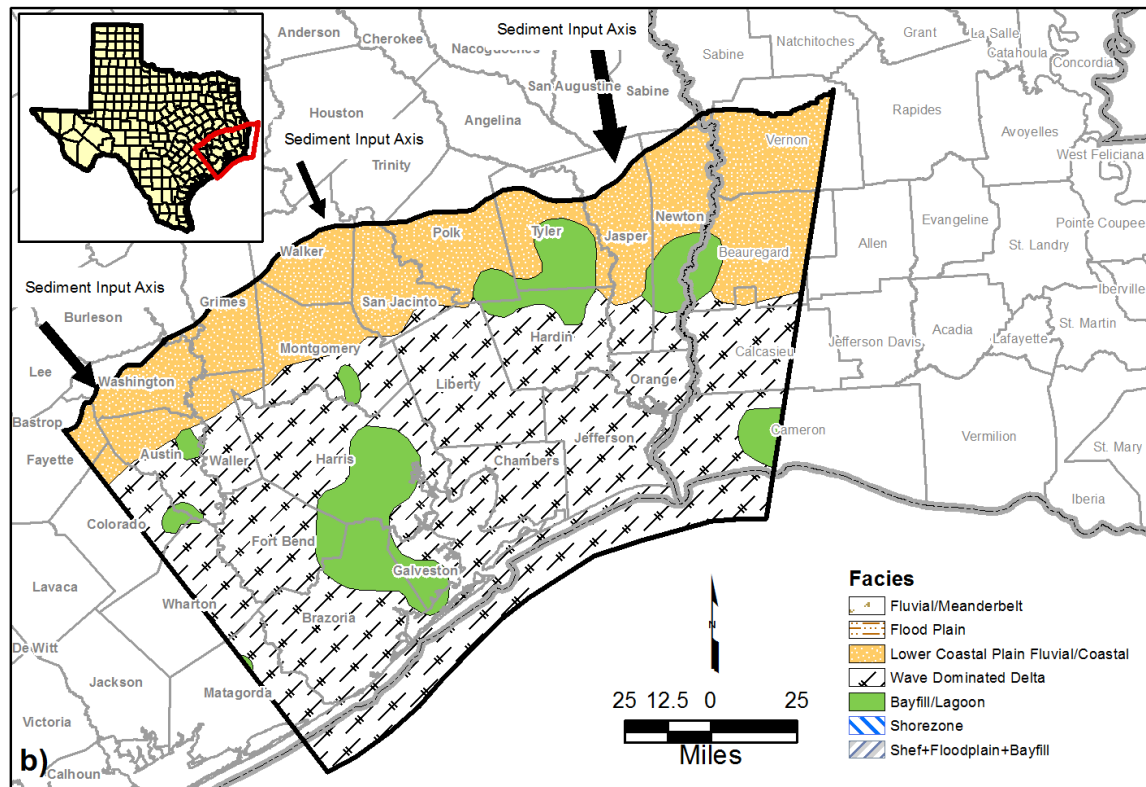
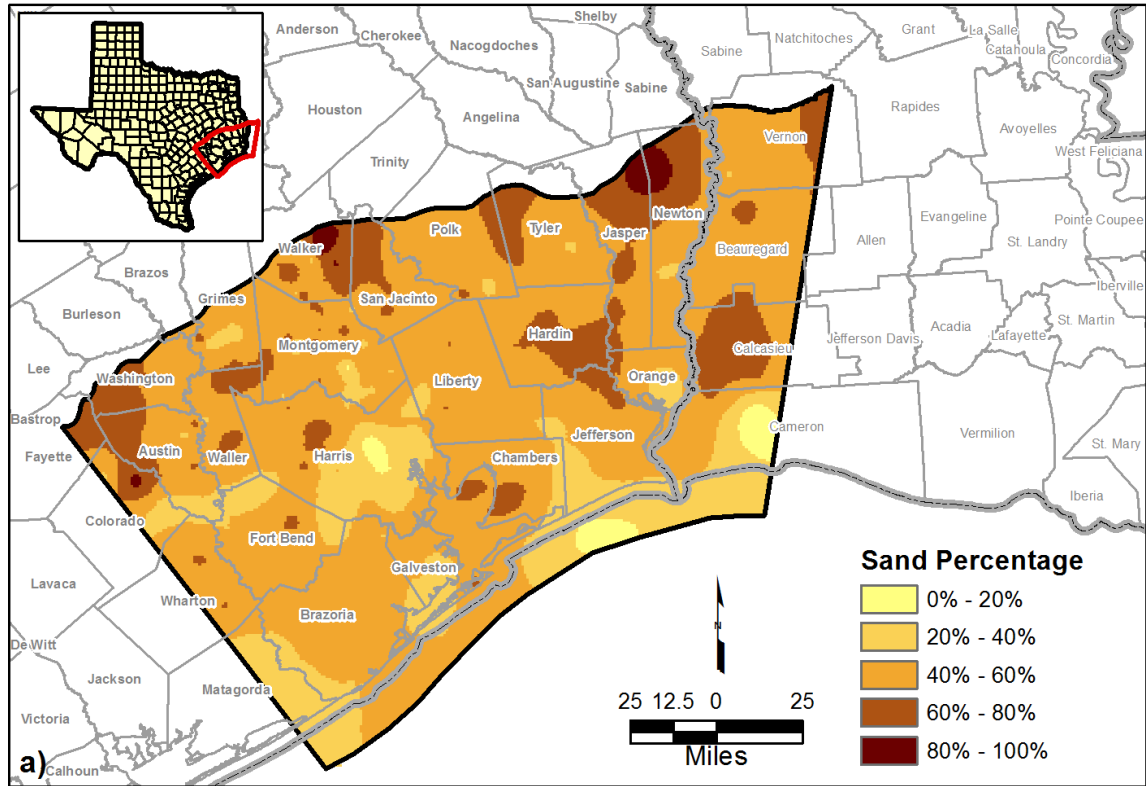


Figure 8-19 Map of the lower Lagarto showing total sand thickness.





**Figure 8-20** Map of the Oakville geologic unit showing: (a) percentage sand coverage and (b) depositional facies.

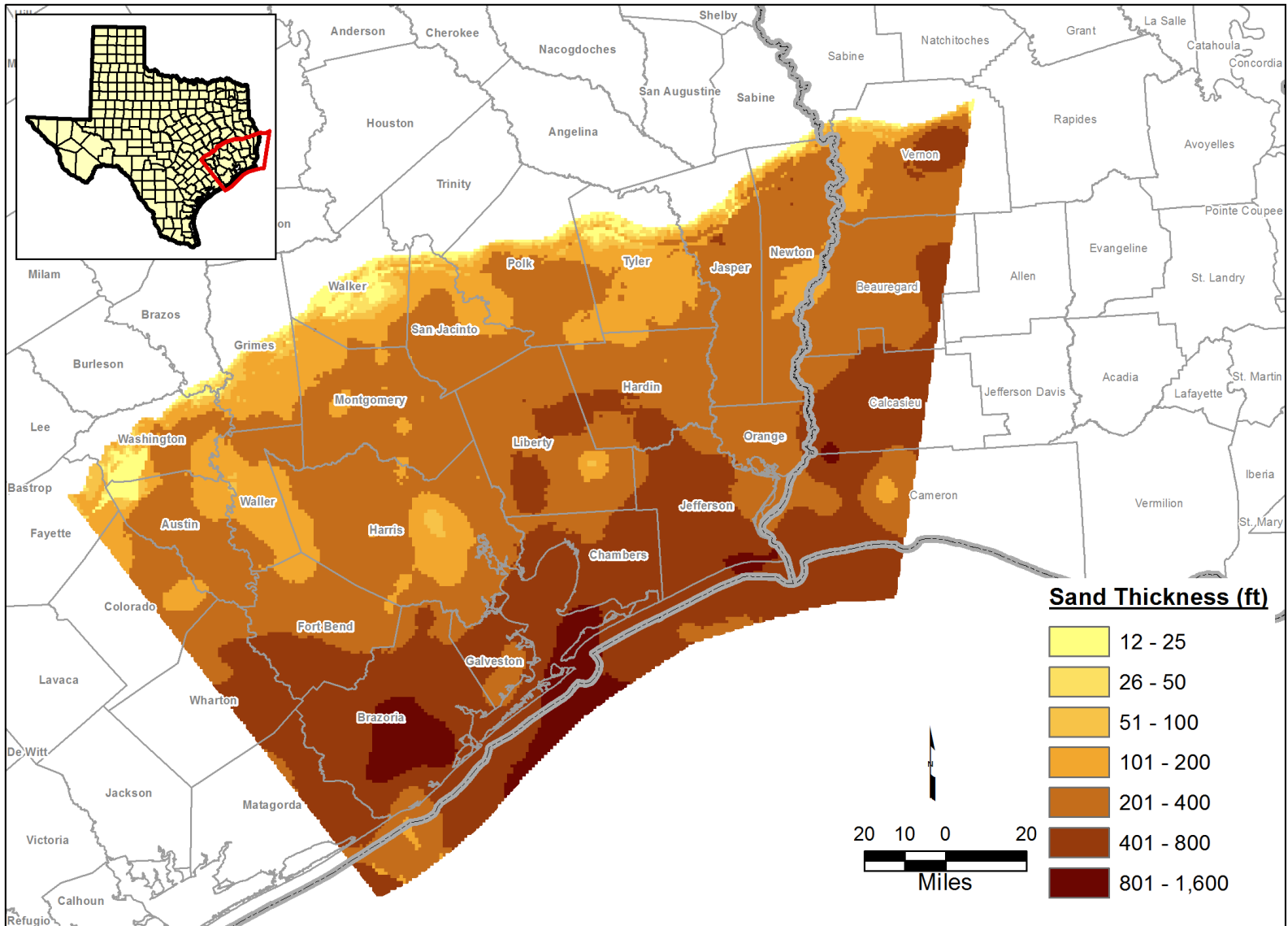


Figure 8-21 Map of the Oakville geologic unit showing total sand thickness.

*This page intentionally left blank.*

## 9.0 Gulf Coast Water Quality

The quality of the groundwater in the Gulf Coast Aquifer System varies significantly. From the water supply perspective, a useful metric for measuring water quality is concentration of total dissolved solids (TDS). Groundwater is categorized as fresh water and as brackish water based on its measured TDS. In this section, estimates of fresh water are provided based on analysis of geophysical logs and water well data.

### 9.1 Terminology

#### 9.1.1 Fresh and Brackish Groundwater

Total dissolved solids (TDS) is a measurement of all the dissolved solids in a specific water sample and is often used to classify groundwater based on water quality. Table 9-1 divides groundwater into five classes based on TDS. This project uses these five classes to characterize the groundwater of the Gulf Coast. LGB-Guyton and NRS Consulting (2003) have grouped the classes of slightly saline and moderately saline water under the general category of brackish groundwater. Thus, brackish groundwater by definition has a TDS between 1,000 ppm and 10,000 ppm, and fresh water has a TDS less than 1,000 ppm. Water with a TDS greater than 10,000 ppm is classified as being saline water (LGB-Guyton and NRS Consulting, 2003).

**Table 9-1 Groundwater classifications based on TDS (from Collier, 1993).**

Class	Total Dissolved Solids (mg/L)	Example of Use
Fresh water	0 to 1,000	Drinking and all other uses
Slightly saline water	More than 1,000 to 3,000	Drinking if fresh water is unavailable, irrigation, industrial, mineral extraction, oil and gas production
Moderately saline water	More than 3,000 to 10,000	Potential future drinking and limited livestock watering and irrigation if fresh or slightly saline water is unavailable; mineral extraction, oil and gas production
Very saline water	More than 10,000 to 100,000	Mineral extraction, oil and gas production
Brine water	More than 100,000	Mineral extraction, oil and gas production

#### 9.1.2 Total Dissolved Solids and Specific Conductivity

In the groundwater industry and for this report, TDS is used interchangeably with dissolved solids even though there is a real difference between the two measurements. Dissolved solids

refers to the sum of all the chemical constituents that were analyzed in a specific water sample. The practice of using TDS and dissolved solids interchangeably is generally acceptable as long as the water analysis has been designed and executed to account for 90% or more of the dissolved ions in solution. The major ions that comprise TDS for most groundwaters include silica, calcium, magnesium, sodium, chloride, bicarbonate, sulfate, and carbonate. Secondary ions that should be considered as part of the TDS measurement include fluoride, nitrate, potassium, manganese, iron, and aluminum.

Measurements of TDS usually are reported as parts per million by weight (ppm) or milligrams per liter (mg/L). For fresh and brackish water, the terms can be used interchangeably even though the two terms can differ because the weight of 1 liter of water depends on the solute concentrations. Hem (1985) estimates that for a typical groundwater sample, the analytical method is within  $\pm 5\%$  of the actual TDS value.

Specific conductivity is a measure of a water's ability to conduct electricity and therefore is a measure of a water's ionic activity. The standard unit of measure for specific conductance is microhms per centimeter ( $\mu\text{mhos/cm}$ ) at 25°Celsius (77°Fahrenheit). The specific conductivity is affected by the nature and movement of the ions in solution. Thus, the specific conductivity is affected by the concentration of the ions, the activity of the ions, the electric charge on ions, and water temperature. When adjusting for temperature, a general rule of thumb stated in the literature is that specific conductivity increases about 2% per degree Celsius increase in temperature (Hem, 1982). Figure 9-1 illustrates how the relationships between concentration and specific conductivity can vary among different salts and is concentration dependent.

The reciprocal of electrical conductivity is electrical resistivity. The unit of measure for resistivity is the mirror inverse of the conductivity unit of mho, or ohm. The relationship between conductivity and resistivity is important to a log analyst because resistivity is one of the measurements that comprise most geophysical logs. The relationship between resistivity and conductivity is as follows:

$$\text{Resistivity (ohm-m)} = 10,000 / \text{Specific Conductivity}(\mu\text{mhos/cm})$$

## 9.2 Analysis of Geophysical Logs

### 9.2.1 Approach

Any approach for estimating TDS from the geophysical logs involves three general steps. The first step is to estimate the resistivity of the formation water from a geophysical log. The second step is to convert the resistivity value into a specific conductivity value. The third step is to convert the specific conductivity into a TDS value. Thus, a TDS concentration estimated from the analysis of a geophysical log is dependent on the accuracy of the log analyst's ability to estimate the resistivity of the formation water and the relationship between the specific conductivity and TDS for the specific conditions at the borelog.

To illustrate the relationship among TDS, specific conductivity, and resistivity, we have created Table 9-2. In developing Table 9-2, we skipped the key step of interpreting the geophysical log to estimate the resistivity of the formation water. The conversion from resistivity to specific conductivity is performed by applying the equation discussed above. To calculate the TDS from specific conductivity, we used general relationships developed and reported by Collier (1993) in Table 3-1 for groundwater measurements taken in the Chicot, Evangeline, and Jasper Aquifers. For this example, we have selected resistivity values of 0.7, 2.5, 7.1, 15.4, and 30.8 and have calculated specific conductivities of 14000, 4000, 1400, 650, and 325  $\mu\text{mhos/cm}$ ., respectively, based on the above equation. For each of the five specific conductivities, Table 9-2 shows the TDS value calculated for the three aquifers using the relationships provided by Collier (1993) and shown in Table 9-2. The results in Table 9-2 show that the range in the calculated TDS values for the different aquifers increases with higher resistivity values because of the non-linearities in the TDS-specific conductivity relationships.

**Table 9-2 Relationship among TDS, specific conductivity, and resistivity (from Collier, 1993).**

Aquifer	Relationship between TDS (mg/L) and specific conductivity ( $\mu\text{mhos/cm}$ )	Specific conductivity of formation water ( $\mu\text{mhos/cm}$ )				
		14,000	4,000	1400	650	325
Chicot	$\text{TDS} = 1.283 * \text{SC} 0.922$	8,530	2,687	1,021	503	266
Evangeline	$\text{TDS} = 1.780 * \text{SC} 0.994$	10,312	2,969	1,046	488	245
Jasper	$\text{TDS} = 0.751 * \text{SC} 1.010$	11,567	3,264	1,130	521	259
Average TDS (mg/L) for three aquifers		10,136	2,973	1,066	504	256
Percent variation in predicted TDS among aquifers		30%	19%	8%	7%	5%

The specific approach we used to estimate TDS from geophysical logs is similar to the general approach discussed above with the additional step of estimating the resistivity of the aquifer formation water from the geophysical log signatures. Mr. Baker performed all of the TDS interpretations for this project at the same time that he performed the lithologic interpretations. For every lithologic interval identified, Mr. Baker assigned a classification of fresh, slightly saline, or moderately saline water. Table 9-3 provides a description of the general criteria and assumptions used by Mr. Baker. Where appropriate, Mr. Baker deviated from the general criteria to accommodate site-specific conditions and adjusted his criteria as needed based on his 40 years of log analyst experience. Mr. Baker's approach is based on numerous references that include Schlumberger (1972), Keys and McCary (1971), Whitman (1965), and Alger (1966).

**Table 9-3 General criteria used by Mr. Baker to estimate the TDS from the geophysical logs.**

Classification	Resistivity (ohms-m) of aquifer formation	Assumptions
Freshwater (<1,000 ppm TDS)	> 15-20 ohms	Assume water has major calcium ions
Slightly saline (1,000-3,000 ppm TDS)	8-15 ohms	Calcium ions decreasing, sodium ions gaining
Moderately saline (3,000 -10,000 ppm TDS)	< 8 ohms	Sodium and chloride ions predominate

### ***9.2.2 Results***

For each of the major aquifers and the Burkeville confining unit, maps of the three water quality classifications in Table 9-3 were calculated using a two-step process. The first step was to determine the percentage of each water quality classification for each aquifer/geologic unit at approximately 600 geophysical log locations shown in Figure 4-4 with water quality information. This was accomplished by summing the vertical intervals associated with each classification and dividing by the total thickness the aquifer/geologic unit. The second step was to generate a continuous distribution of percentage of the different water classification by interpolating the point values using a kriging algorithm with a rectangular grid consisting of nodes spaced 4,000 feet apart.

Figures 9-2 through 9-13 are maps showing the percentage of fresh, slightly saline, and moderately saline water in the Chicot, Evangeline, and Jasper Aquifers and the Burkeville confining unit. Because of several simplifying assumptions in each analysis, the results should

be used as a guide to water quality at a regional scale. At the scale of a few tens square miles and less, the results should not be used without additional information to validate the reasonableness of the approach at the specific location of interest. .

### **Chicot Aquifer**

As shown in Figure 9-2, fresh water occupies most of the Chicot Aquifer. The higher percentage (80% to 100%) of freshwater occurs along strike in the central region of the aquifer. The lower percentages (0 to 10%) of fresh water occurs approximately 30 miles from the coastline. As shown in Figure 9-3, slightly saline water occupies a volume considerably less than does the fresh water. The percentage of saline water greater than 40% are typically in the central region of the Chicot Aquifer but there are some areas with slightly saline water percent above 40% in the updip and downdip regions of the aquifer. The higher percentage (80% to 100%) of slightly saline water occurs in the vicinity of Chambers, Liberty, and Jefferson Counties. As shown in Figure 9-4, moderately saline water is most common near the downdip region of the Chicot Aquifer. The higher percentage (80% to 100%) of moderately saline water occurs along strike and is highest near and in Jefferson County.

### **Evangeline Aquifer**

As shown in Figure 9-5, the percentages of freshwater in the Evangeline Aquifer greater than 50% is limited to the updip region of the aquifer. Figure 9-5 does not show any freshwater percentages greater than 10% within about 40 miles of the shoreline. As with the Chicot Aquifer, the percentage of freshwater changes very quickly over short distances as the percent of freshwater drops below 40%. As shown in Figure 9-6, the highest percentage (80% to 100%) of slightly saline water generally occurs along strike within the central region of the aquifer in the vicinity of Harris County, Liberty County, Calcasieu Parish, and Beauregard Parish. The lower percentages (0 to 10%) occurs near the downdip extent of the Evangeline. As shown in Figure 9-7, the highest percentage (80% to 100%) of moderately saline water occurs along strike throughout the downdip region of the aquifer whereas the lower percentages (0 to 10%) occur in the updip extent of the Evangeline.



### **Burkeville Confining Unit**

As shown in Figure 9-8, the Burkeville confining unit has a footprint of freshwater percentage similar to the percentage footprint for Evangeline Aquifer except that it is smaller. The percentage of freshwater greater than 50% occurs across an updip region that covers between 10% and 30% of the aquifer. As with the previously mentioned aquifers, freshwater percentages for the Burkeville change quickly over short distances where the percent of freshwater drops below 40%. As shown in Figure 9-9, slightly saline water is predominant across the updip region that covers approximately 50% of the Burkeville confining unit. The spatial location of the slightly saline water is similar to that of the Evangeline, but contains the Burkeville has more areas with higher percentages (80% to 100%) of slightly saline water. The higher percentages generally occur along strike within the central and in the vicinity of Austin County, Fort Bend County, Harris County, Liberty County, Montgomery County, San Jacinto County, Waller County, Wharton County, and Beauregard Parish. As shown in Figure 9-10, moderately saline water occurs in approximately 60% to 75% of the Burkeville confining unit. The higher percentage (80% to 100%) of moderately saline water occurs near the downdip region of the aquifer.

### **Jasper Aquifer**

As shown in Figure 9-11, the Jasper Aquifer has a footprint of freshwater percentage similar to the freshwater percentage footprint for the Burkeville confining unit except that it is smaller. The percentages of freshwater greater than 50% occur in a small updip areas that only cover 10% to 20% of the aquifer. As with the previously mentioned aquifers, freshwater percentages for the Jasper change quickly over short distances where the percent of freshwater drops below 40%. As shown in Figure 9-12, slightly saline water is predominant across the updip portions of the Jasper Aquifer. The slightly saline percentage footprint is similar to that of the Evangeline and the Burkeville, but contains more regions with a higher percentage (80% to 100%) of slightly saline water. As shown in Figure 9-11, moderately saline water is predominant across the downdip region that covers approximately 60% to 75% of the Jasper. As with the Evangeline and the Burkeville, there is a sharp gradient along strike in which the percentage of moderately saline water rapidly changes from 80% to less than 10% over distances typically less than 10 miles.

### 9.3 Analysis of Water Well Measurements

#### 9.3.1 Approach

In July 2009, the TWDB database for water quality (GWDB.mdb) was queried for at least one TDS measurement in wells with the aquifer codes in Table 9-4 that are located north of dip section 10. The query produced 4,575 wells that had depths that are above the base of the Jasper. For wells that had multiple TDS measurements, the measurements were averaged to produce a single measurement. From this well population, 4,080 wells were assigned a TDS less than 1,000 ppm and 495 wells were assigned a TDS greater than 1,000 ppm.

**Table 9-4 Aquifer codes used in Gulf Coast query**

Aquifer_Name
Alluvium and Evangeline Aquifer
Burkeville Aquiclude
Chicot and Evangeline Aquifers
Chicot Aquifer
Chicot Aquifer, Lower
Chicot Aquifer, middle
Chicot Aquifer, upper
Evangeline and Jasper Aquifers
Evangeline Aquifer
Evangeline Aquifer and Burkeville Aquiclude
Evangeline Aquifer and upper Unit of Jasper Aquifer
Fleming Formation and Burkeville Aquiclude
Gulf Coast Aquifer
Jasper Aquifer
Jasper Aquifer and Burkeville Aquiclude
Jasper Aquifer and Catahoula Sandstone
Jasper Aquifer, upper Unit

#### 9.3.2 Results

Figure 9-14 shows 3,105 wells with TDS concentrations for wells with depths that terminate in the Chicot Aquifer. Out of the 3,105 wells, 2,556 and 449 wells had TDS concentrations below 1,000 ppm and above 1,000 ppm, respectively. Except for Chambers County, every county has more wells with TDS concentrations below 1,000 ppm than above 1,000 ppm. In Jefferson and Brazoria counties, there are considerable TDS measurements with concentrations above

1,000 ppm but these measurements are less than the number of TDS measurements of less than 1,000 ppm. Overall, the areas of fresh water shown in Figure 9-14 are consistent and supportive of the areas of fresh water estimated from geophysical logs in Figure 9-2.

Figure 9-15 shows 668 wells with TDS concentrations for wells with depths that terminate in the Evangeline Aquifer. Out of the 668 wells, 650 and 18 wells had TDS concentrations below 1,000 ppm and above 1,000 ppm, respectively. Except for Chambers County (which has only three wells where TDS has been measured), every county has more wells with TDS concentrations below 1,000 ppm than above 1,000 ppm. Figure 6-15 shows that except for the vicinity of Harris County there is significantly less wells with TDS measurements in the Evangeline than in Chicot Aquifer. As for Figure 9-14, the areas of fresh water shown in Figure 9-15 are consistent and supportive of the areas of fresh water estimated from geophysical logs in Figure 9-5.

Figure 9-16 shows 234 wells with TDS concentrations for wells with depths that terminate in the middle Lagarto Formation. Out of the 234 wells, 230 and 4 wells had TDS concentrations below 1,000 ppm and above 1,000 ppm, respectively. Except for a few wells in Harris and Jasper counties, the vast majority of the wells are located near the updip extent of the middle Lagarto Formation. Overall, the areas of fresh water shown in Figure 9-16 are consistent and supportive of the areas of fresh water estimated from geophysical logs in Figure 9-8.

Figure 9-17 shows 568 wells with TDS concentrations for wells with depths that terminate in the Jasper Aquifer. Out of the 568 wells, 544 and 24 wells had TDS concentrations below 1,000 ppm and above 1,000 ppm, respectively. The figure shows that except for about 20 wells, the wells are located within about a 30 mile of the updip extend of the Jasper Aquifer. Overall, the areas of fresh water shown in Figure 9-17 are consistent and supportive of the areas of fresh water estimated from geophysical logs in Figure 9-11.

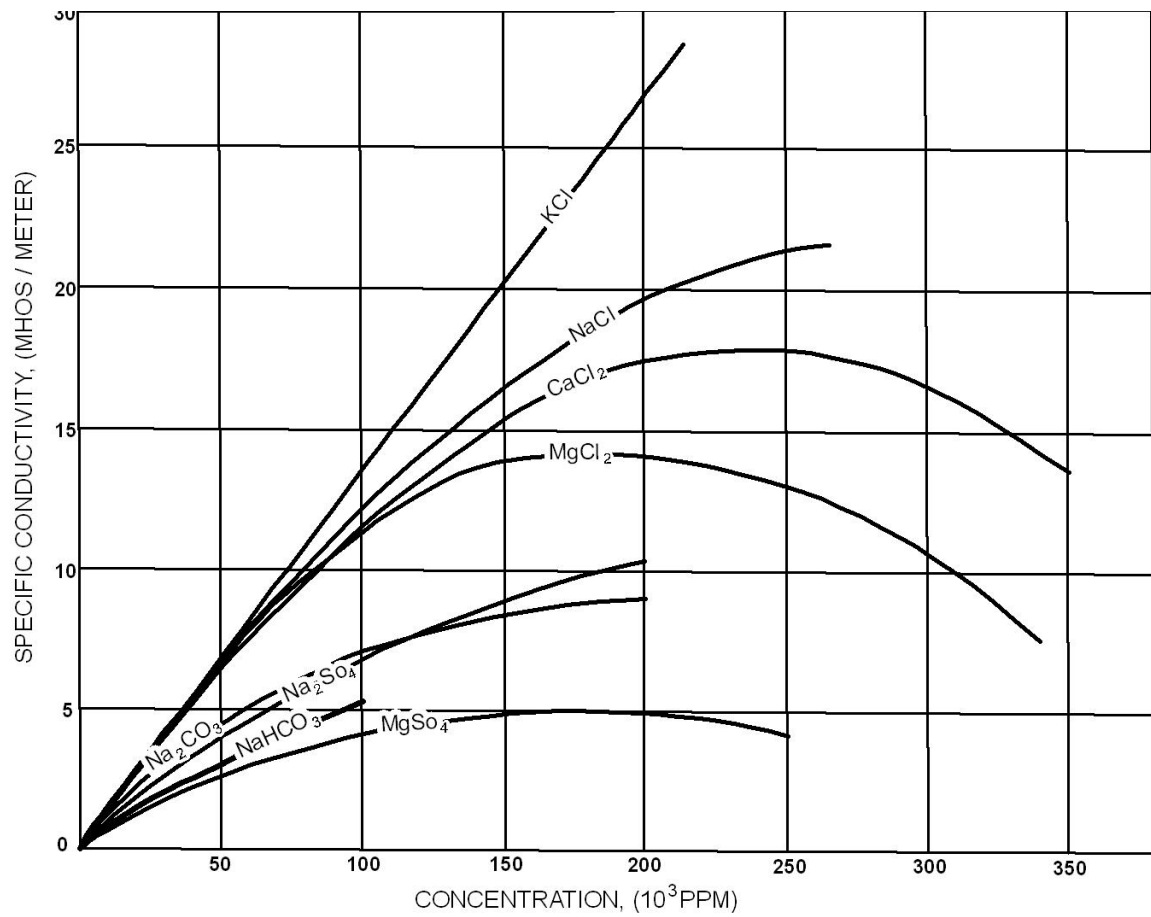
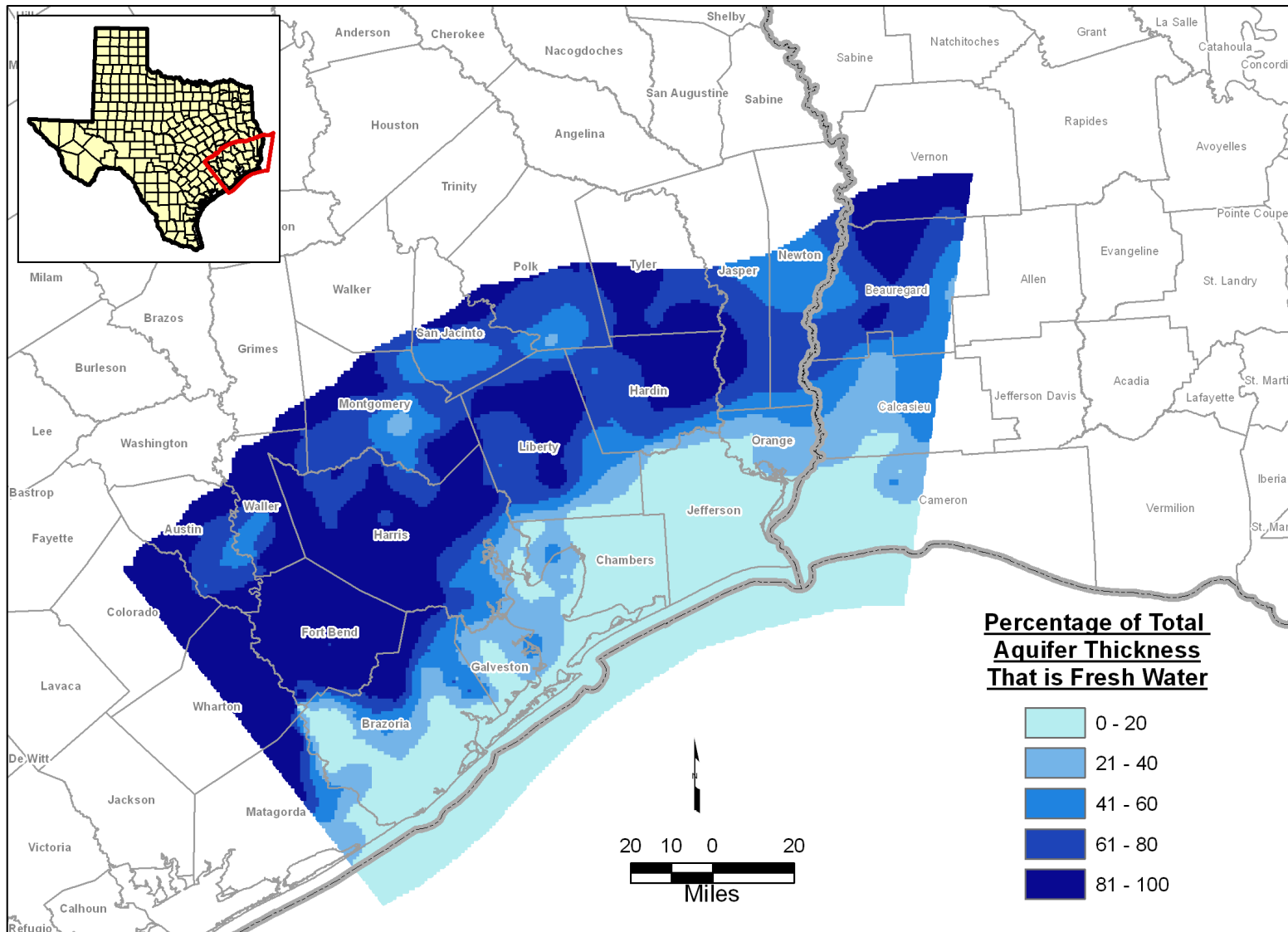
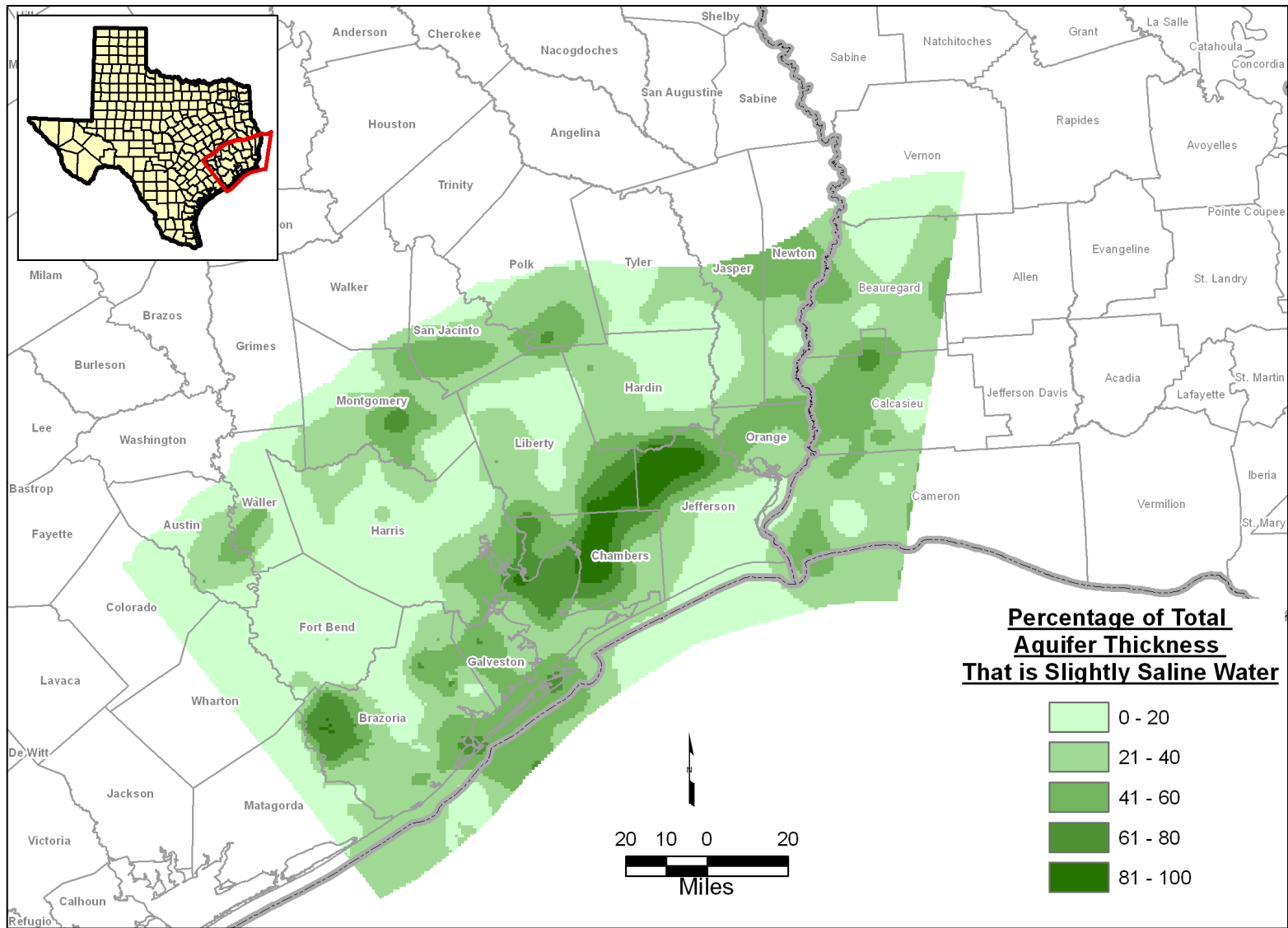


Figure 9-1 Specific conductivity of salt solutions (modified from Moore, 1966).



**Figure 9-2** Percentage of the Chicot Aquifer estimated to be fresh water with a TDS concentration less than 1,000 ppm, as determined by the analysis of geophysical logs.



**Figure 9-3** Percentage of the Chicot Aquifer estimated to be slightly saline water with a TDS concentration between 1,000 ppm and 3,000 ppm, as determined by the analysis of geophysical logs.

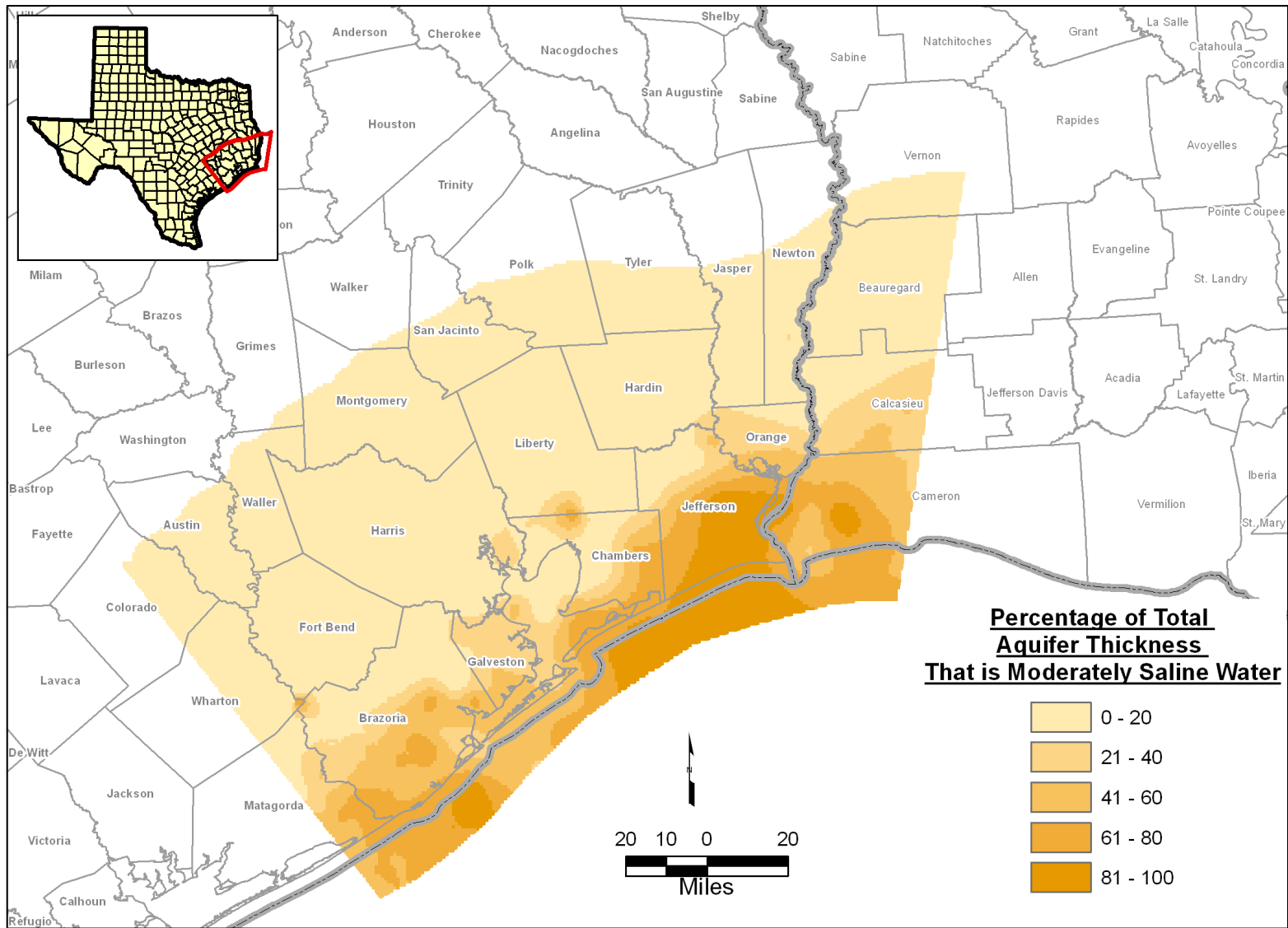


**Figure 9-4** Percentage of the Chicot Aquifer estimated to be moderately saline water with a TDS concentration more than 3,000 ppm, as determined by the analysis of geophysical logs.





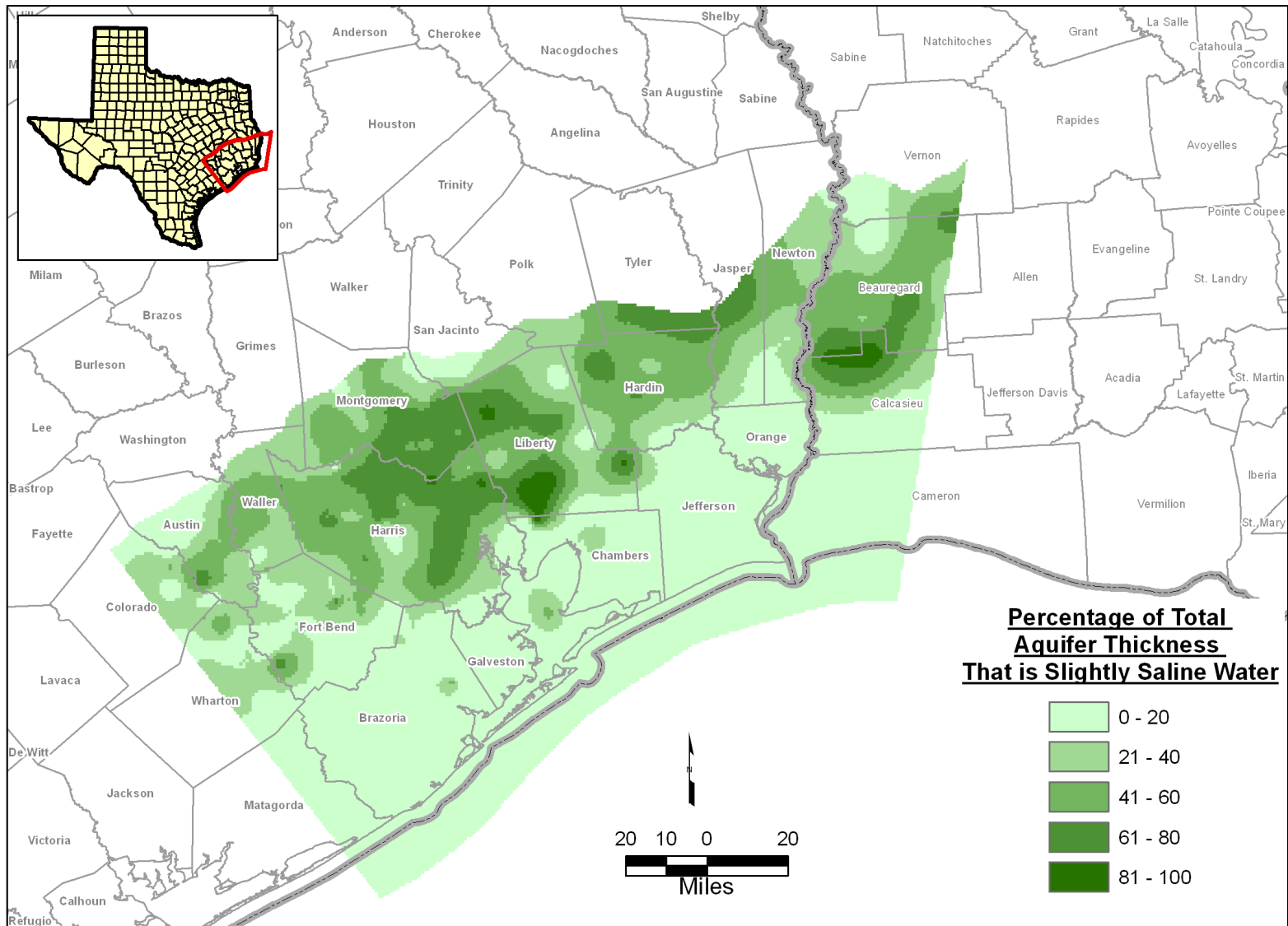


**Figure 9-6** Percentage of the Evangeline Aquifer estimated to be slightly saline water with a TDS concentration between 1,000 ppm and 3,000 ppm, as determined by the analysis of geophysical logs.

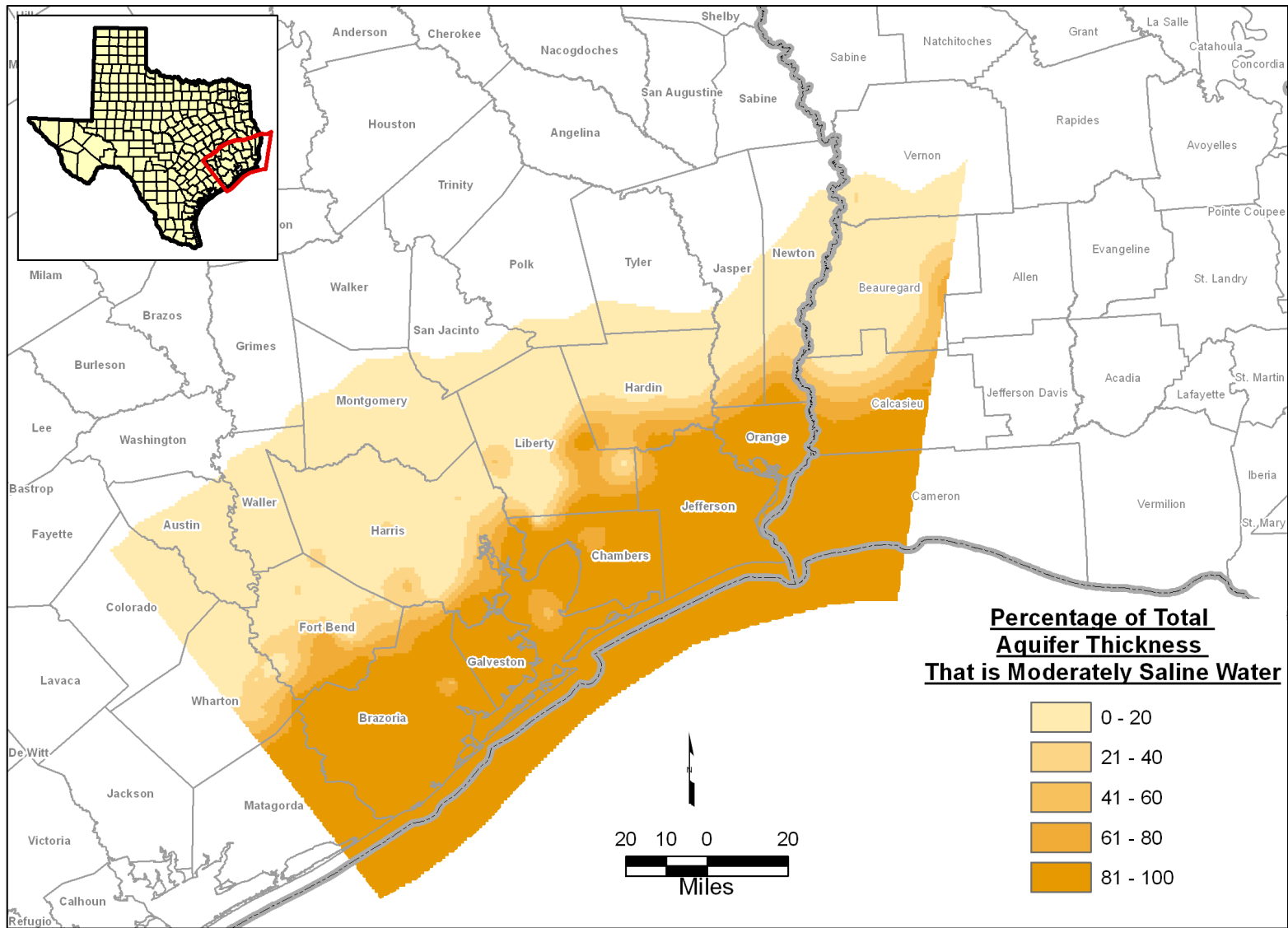


**Figure 9-7** Percentage of the Evangeline Aquifer estimated to be moderately saline water with a TDS concentration more than 3,000 ppm, as determined by the analysis of geophysical logs.

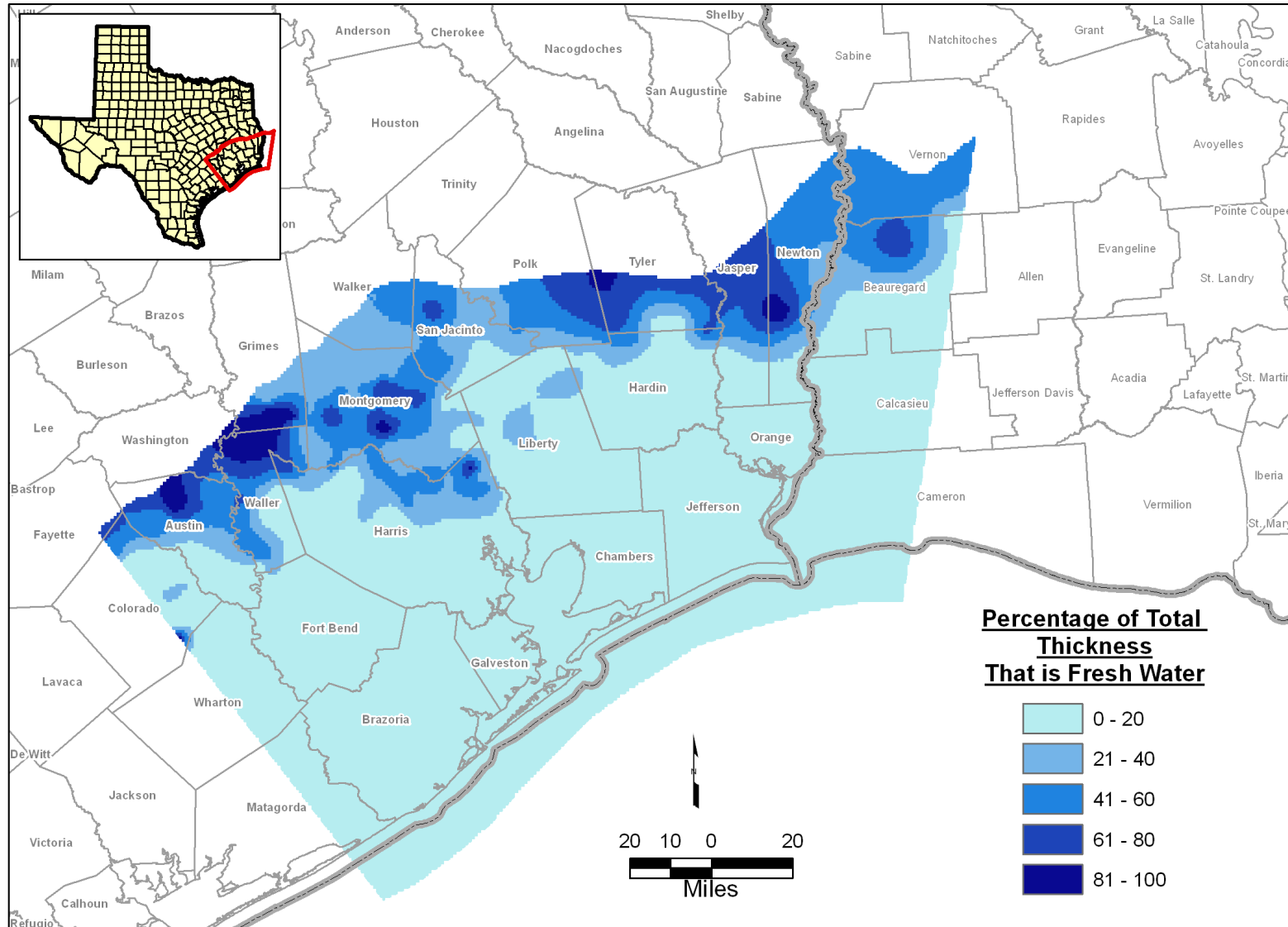


**Figure 9-8** Percentage of the Burkeville confining unit (middle Lagarto Formation) estimated to be fresh water with a TDS concentration less than 1,000 ppm, as determined by the analysis of geophysical logs.

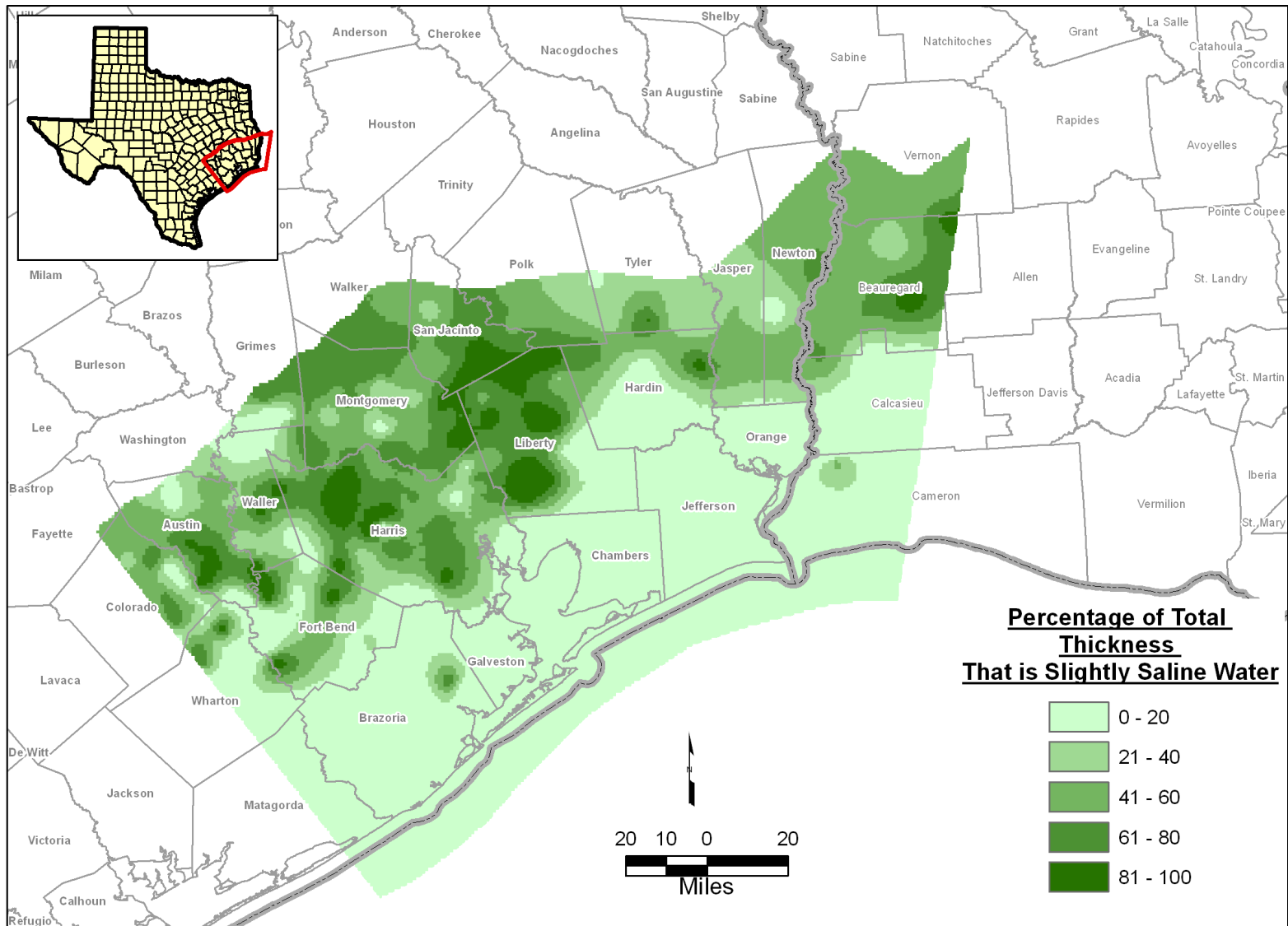


**Figure 9-9** Percentage of the Burkeville confining unit (middle Lagarto Formation) estimated to be slightly saline water with a TDS concentration between 1,000 ppm and 3,000 ppm, as determined by the analysis of geophysical logs.

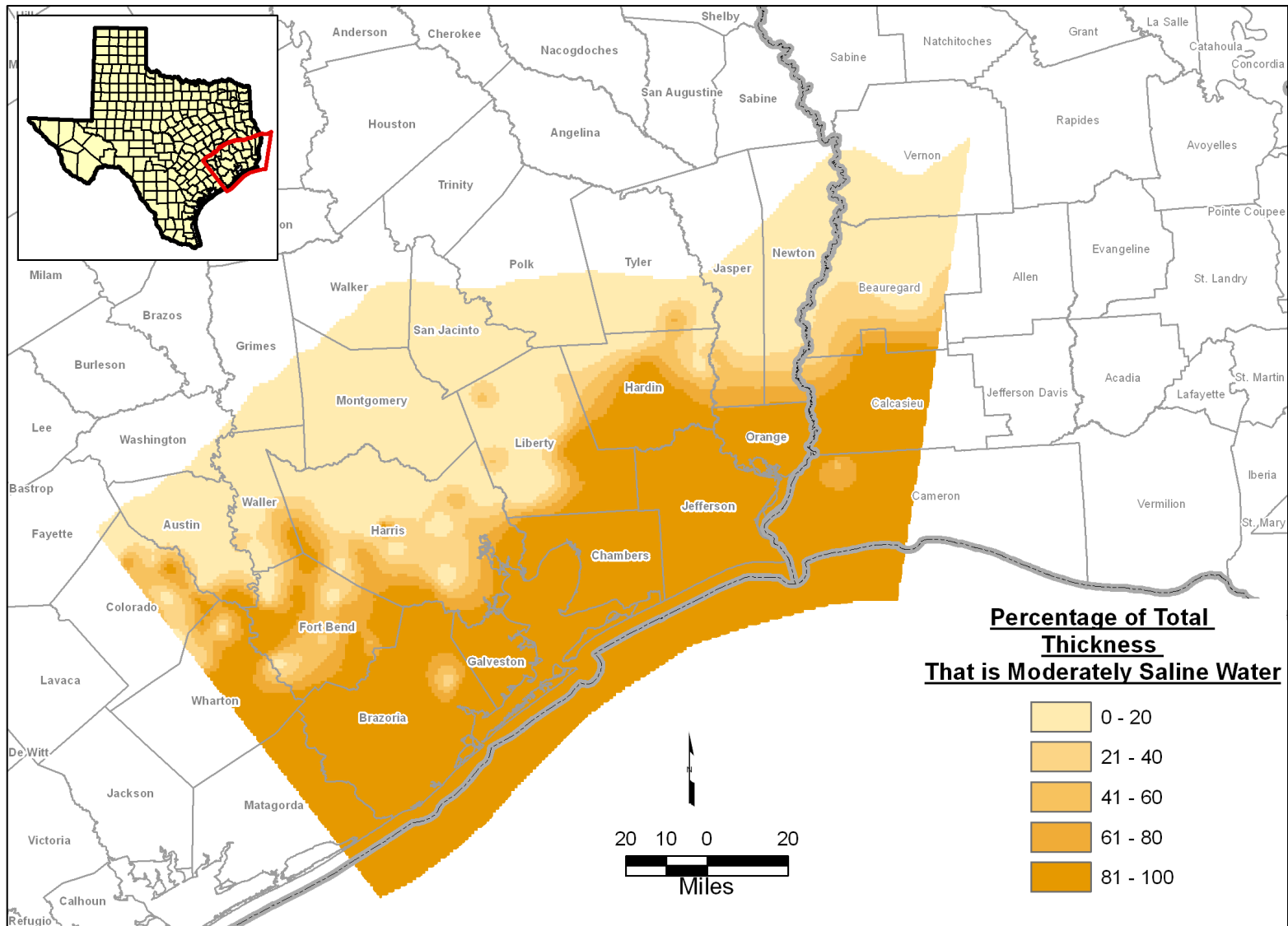


**Figure 9-10** Percentage of the Burkeville confining unit (middle Lagarto Formation) estimated to be moderately saline water with a TDS concentration more than 3,000 ppm, as determined by the analysis of geophysical logs.

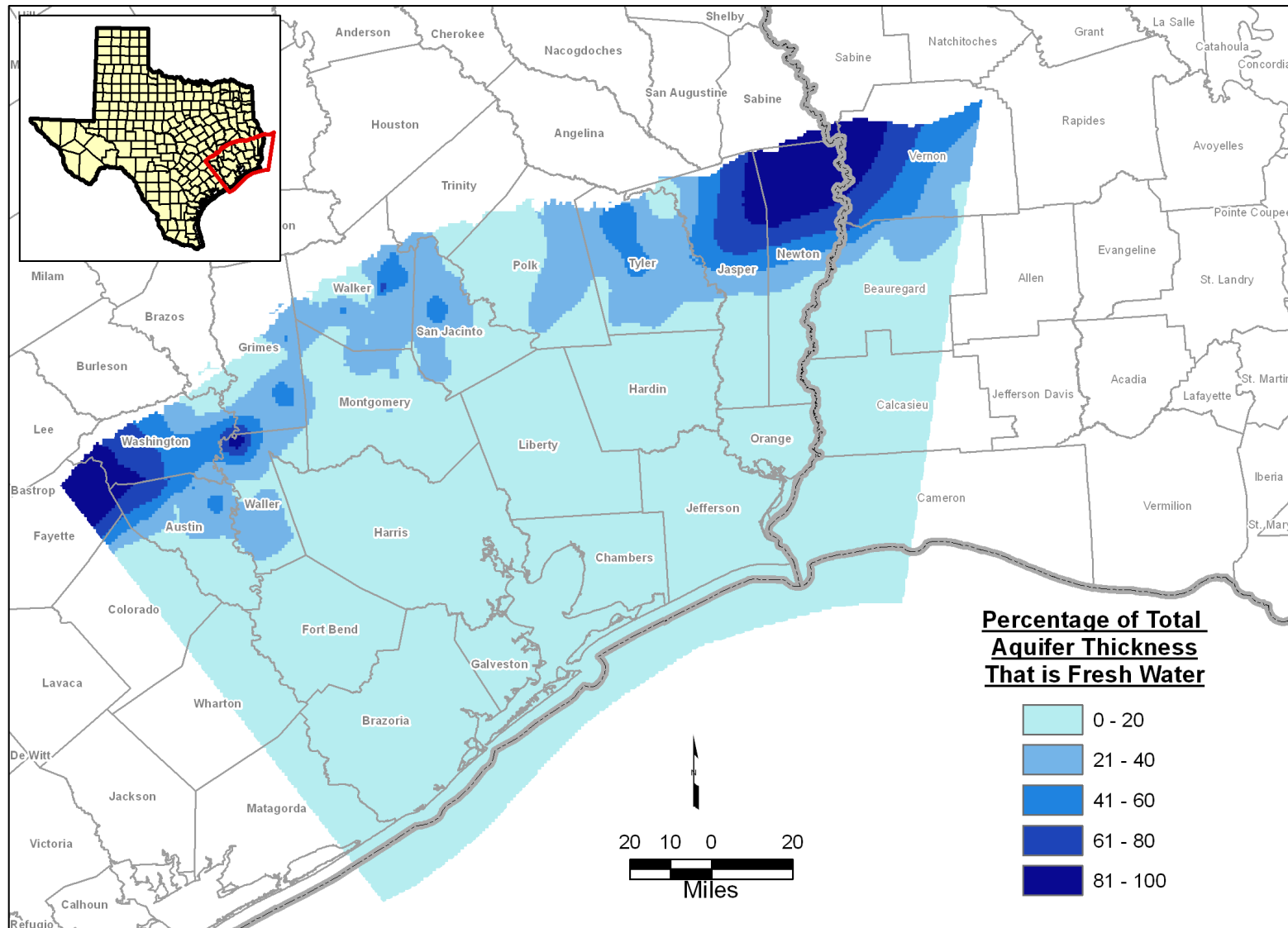


**Figure 9-11** Percentage of the Jasper Aquifer estimated to be fresh water with a TDS concentration less than 1,000 ppm, as determined by the analysis of geophysical logs.

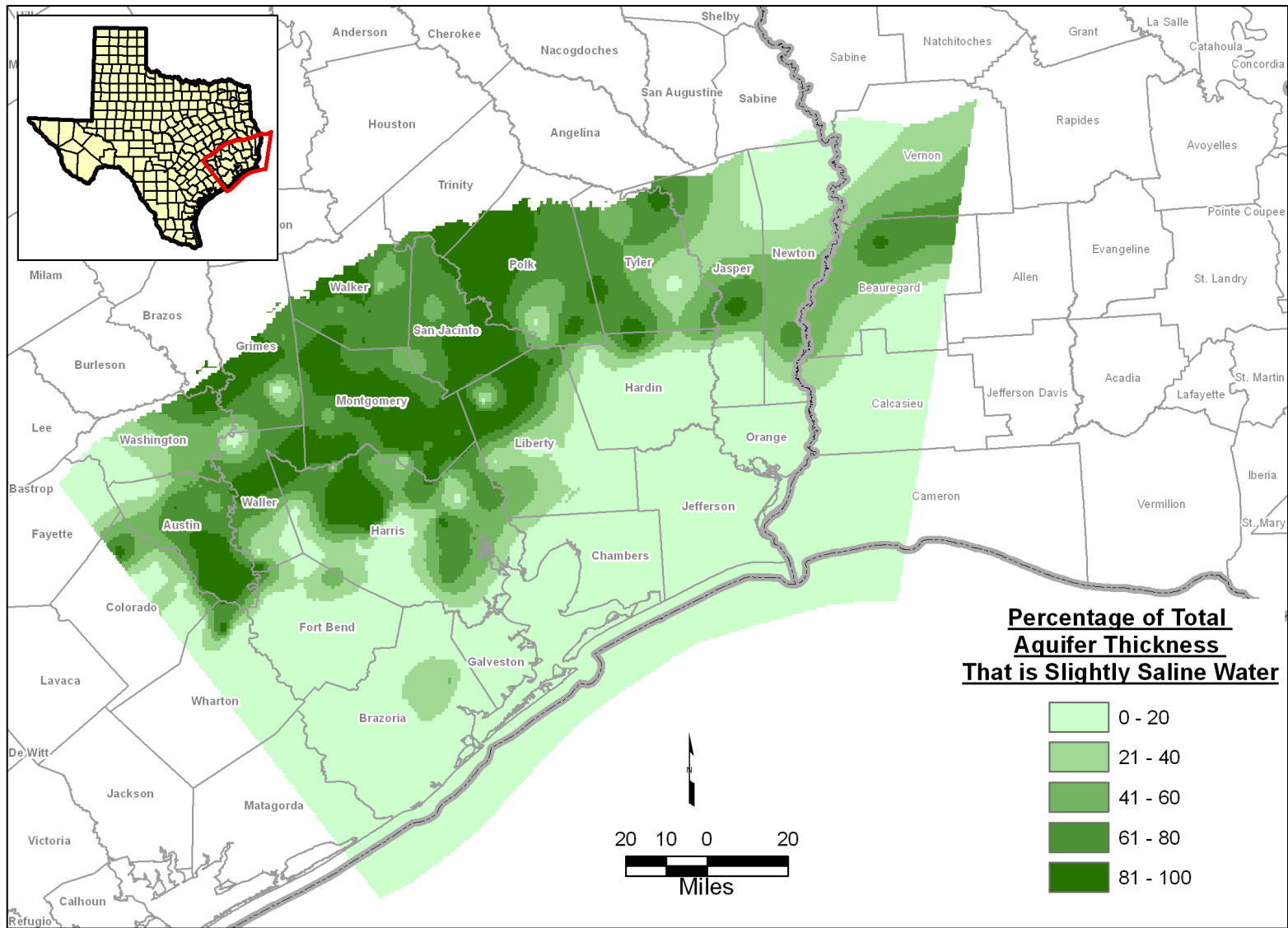


**Figure 9-12** Percentage of the Jasper Aquifer estimated to be slightly saline water with a TDS concentration between 1,000 ppm and 3,000 ppm, as determined by the analysis of geophysical logs.

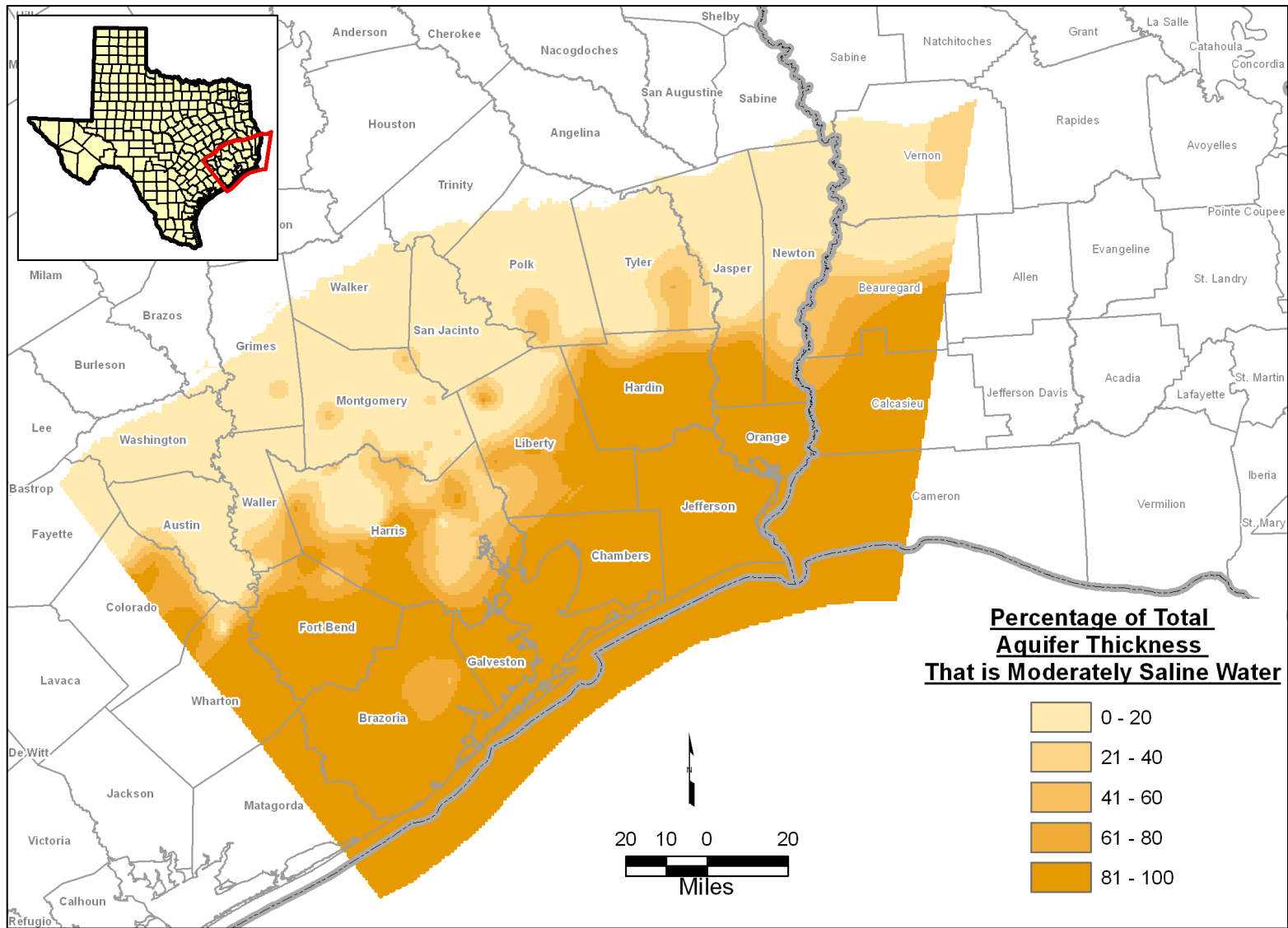


**Figure 9-13** Percentage of the Jasper Aquifer estimated to be moderately saline water with a TDS concentration more than 3,000 ppm, as determined by the analysis of geophysical logs.



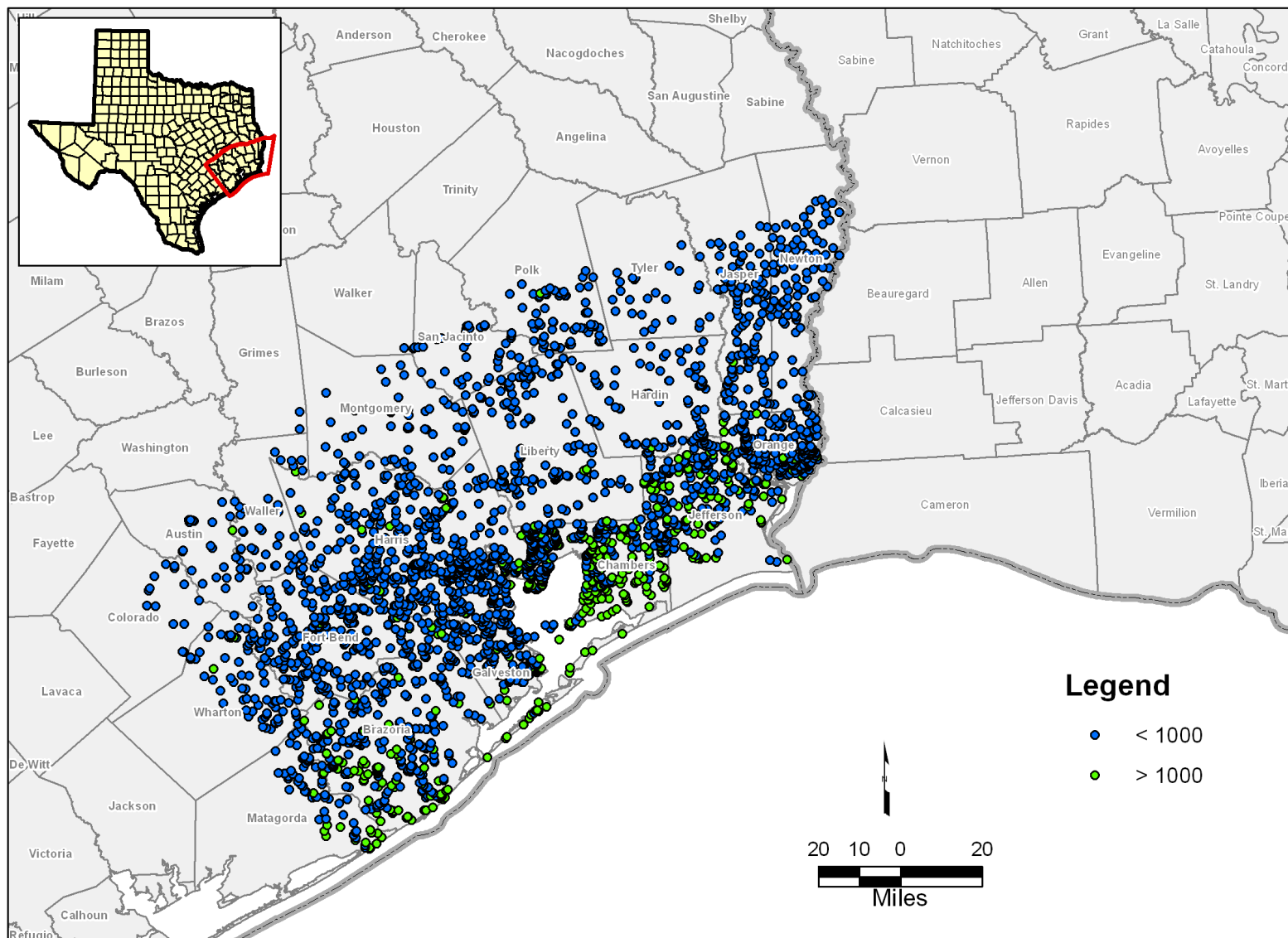


Figure 9-14 Map of water well locations in the Chicot Aquifer with at least one measurement of TDS concentrations.

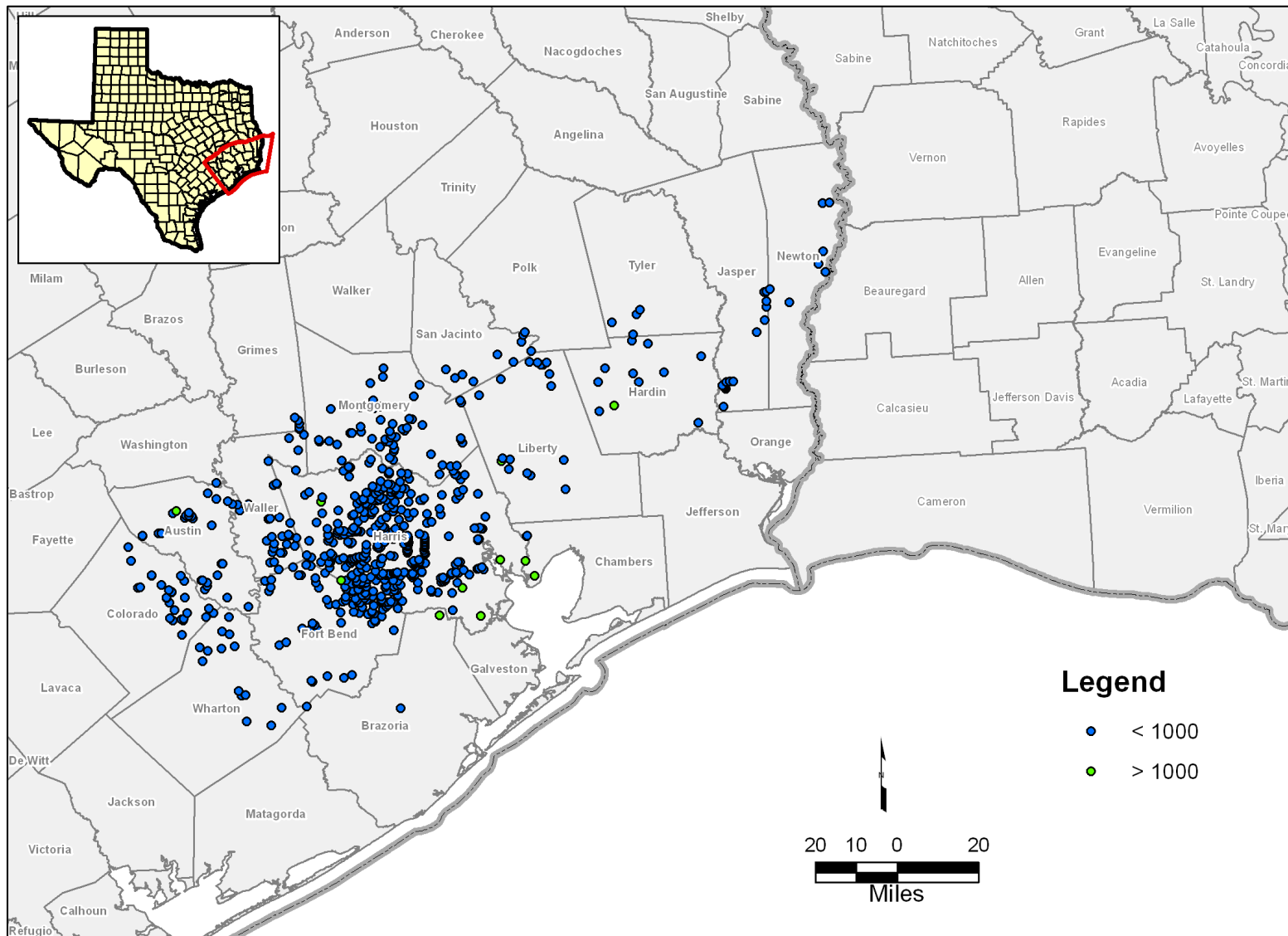


Figure 9-15 Map of water well locations in the Evangeline Aquifer with at least one measurement of TDS concentrations.

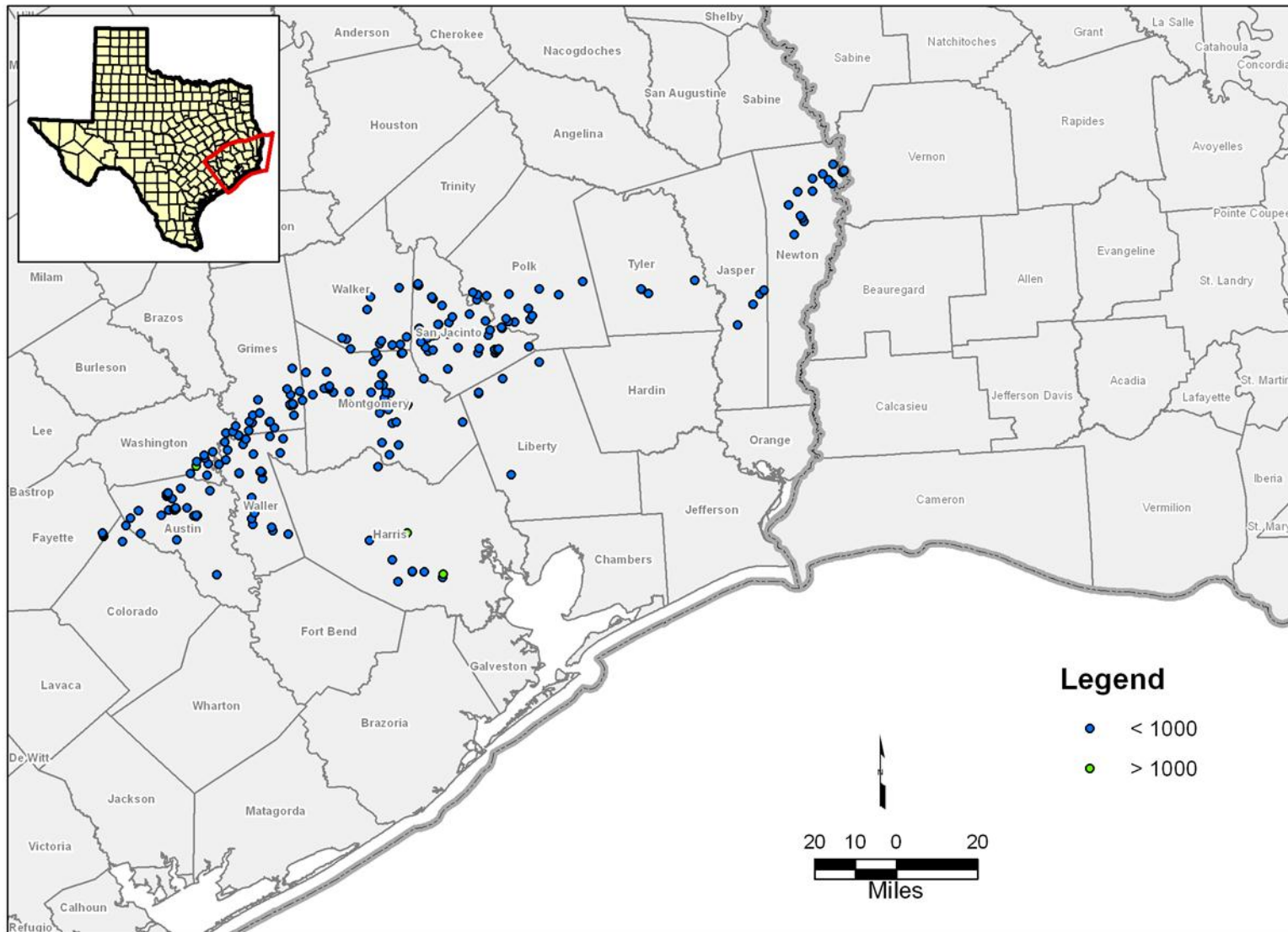


Figure 9-16 Map of water well locations in the Burkeville confining unit with at least one measurement of TDS concentrations.

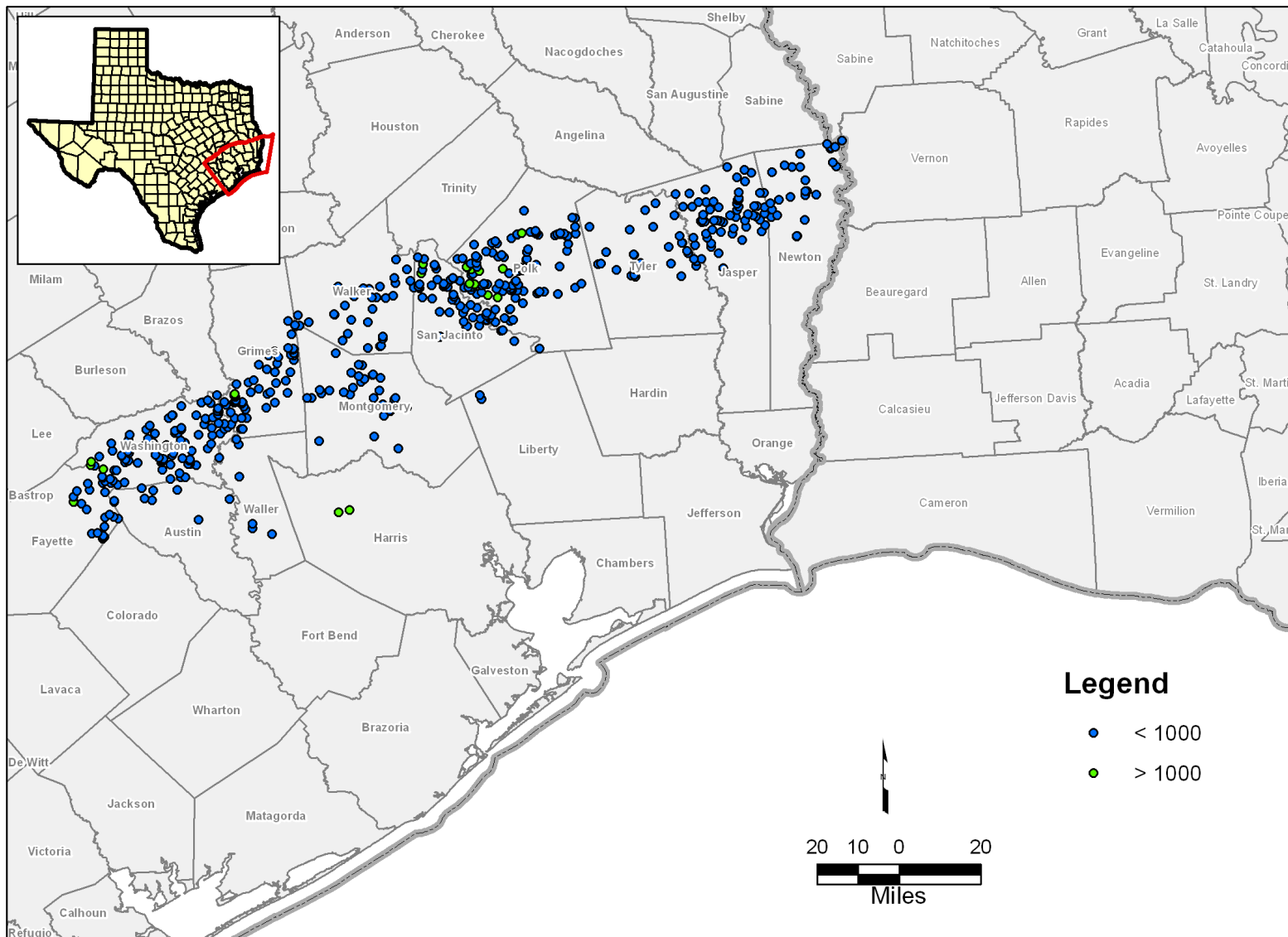


Figure 9-17 Map of water well locations in the Jasper Aquifer with at least one measurement of TDS concentrations

*This page intentionally left blank.*

## 10.0 References

- Alger, R.P., 1966, Interpretation of electric logs in fresh water wells in unconsolidated formations, paper CC, in 7<sup>th</sup> Annual Symposium Transactions: Society of Professional Well Log Analysts, 25 p.
- Anders, R.B., 1957, Ground-water geology of Wilson County, Texas: Texas Water Commission Bulletin 5710, 62 p.
- Anders, R.B., and Baker, Jr., E.T., 1961, Ground-Water Geology of Live Oak County, Texas: Texas Board of Water Engineers Bulletin 6105, 93 p.
- Anderson, J.B., and Milliken, K., 2005, Long-term subsidence along the west Louisiana and east Texas coast (abs.), *in* Coastal subsidence, sea level and the future of the Gulf Coast: The Houston Geological Society, p. 1
- Anderson, J.B., and Fillon, R.H., eds., 2004, Late Quaternary stratigraphic evolution of the northern Gulf of Mexico margin: SEPM Special Publication No. 79, 314 p.
- Applin, E.R., Ellisor, A.E., and Kniker, H.T., 1925, Subsurface stratigraphy of the Coastal Plain of Texas and Louisiana: American Association of Petroleum Geologists Bulletin, v. 9, p. 79–122.
- Aronow, S., and Barnes, V.E., 1968, Geologic atlas of Texas, Houston sheet: The University of Texas at Austin, Bureau of Economic Geology.
- Aronow, S., and Barnes, V.E., 1975, Geologic atlas of Texas, Corpus Christi sheet: The University of Texas at Austin, Bureau of Economic Geology.
- Aronow, S., Brown, T.E., Brewton, J.L., Eargle, D.H., and Barnes, V.E., 1975, Geologic atlas of Texas, Beeville-Bay City sheet: The University of Texas at Austin, Bureau of Economic Geology.
- Ashworth, J.B., and Hopkins, J., 1995, Aquifers of Texas: Texas Water Development Board Report 345, 69 p.

- Autin, W.J., Burns, S.F., Miller, B.J., Saucier, R.T., And Snead, J.I., 1991, Quaternary Geology of the Lower Mississippi Valley, *in* Morrison, R.B., ed., Quaternary Nonglacial Geology; Conterminous U.S.: Boulder, Colorado, Geological Society of America, The Geology of North America, v. K-2, p. 547–581.
- Baker, E.T., Jr., 1964, Geology and Ground-water resources of Hardin County, Texas: Texas Water Commission Bulletin 6406, 174 p.
- Baker, R.C., Dale, O.C., and Baum, G.H., 1965, Ground-Water Condition in Menard County, Texas: Texas Water Commission Bulletin 6519, 92 p.
- Baker, Jr., E.T., 1979, Stratigraphic and hydrogeologic framework of part of the coastal plain of Texas: Texas Department of Water Resources Report 236, 43 p.
- Baker, Jr., E.T., 1986, Hydrology of the Jasper Aquifer in the Southeast Texas Coastal Plain: Texas Water Development Board Report 295, 64 p.
- Banga, T., Capuano, R.M., and van Nieuwenhuise, D.S., 2002, Fluid flow, stratigraphy and structure in the vicinity of the South Liberty salt dome, Texas: Gulf Coast Association of Geological Societies Transactions, v. 52, p. 25–36.
- Barnes, V.E., 1992, Geologic map of Texas: The University of Texas at Austin, Bureau of Economic Geology, State Map No. 3.
- Barton, D.C., 1930, Surface geology of coastal southeast Texas: American Association of Petroleum Geologists Bulletin, v. 14, p. 1301–1320.
- Barton, D.C., Ritz, C.H., and Hickey, M., 1933, Gulf Coast geosyncline: American Association of Petroleum Geologists Bulletin, v. 17, p. 1446–1458.
- Baskin, J.A. and Hulbert, Jr. R.C., 2008, Revised biostratigraphy of the middle Miocene to earliest Pliocene Goliad Formation of South Texas. Gulf Coast Association of Geological Societies Transactions, v. 58, P. 93-101.
- Bates, R.L., and Jackson, J.A., 1983, Dictionary of Geological Terms. Prepared by the American Geological Institute. Doubleday Publishers, New York. 570 pp.

- Beckman, J.D., and Williamson, A.K., 1990, Salt-dome locations in the Gulf Coastal Plain, south-central United States: U.S. Geological Survey Water-Resources Investigations Report 90-4060, 44 p.
- Berggren, W.A., Kent, D.V., Swisher, C.C., and Aubry, M.P., 1995, A revised Cenozoic geochronology and chronostratigraphy: Society of Sedimentary Geology (SEPM) Special Publication 54, p. 129–212.
- Bernard, H.A., and LeBlanc, R.J., 1965, Resume of the Quaternary geology of the northwestern Gulf of Mexico province, *in* H.E. Wright and D.G. Frey, eds., *The Quaternary of the United States*: Princeton University Press, Princetown, New Jersey, p. 137–185.
- Blum, M.D., and Price, D.M., 1998, Quaternary alluvial plain construction in response to glacio-eustatic and climatic controls, Texas Gulf Coastal Plain: Society of Sedimentary Geology (SEPM) Special Publication No. 59, p. 31–48.
- Bodenlos, A.J., 1970, Cap-rock development and salt-stock movement, *in* Kupfer, D.H., editor, *Geology and technology of Gulf Coast salt domes*: Baton Rouge, Louisiana, School of Geosciences, Louisiana State University, p. 73–86.
- Bornhauser, M., 1947, Marine sedimentary cycles of Tertiary in Mississippi Embayment and central Gulf Coast area: *American Association of Petroleum Geologists Bulletin*, v. 31, p. 698–712.
- Bornhauser, M., 1958, Gulf coast tectonics: *American Association of Petroleum Geologists Bulletin*, v. 42, p. 339–370.
- Boyd, D.B., and Dyer, B.F., 1964, Frio barrier bar system of South Texas: *Gulf Coast Association of Geological Societies Transactions*, v. 14, p. 309–322.
- Brewton, J.L., Owen, F., Aronow, S., and Barnes, V.E., 1976a, Geologic atlas of Texas, Laredo sheet: The University of Texas at Austin, Bureau of Economic Geology.
- Brewton, J.L., Owen, F., Aronow, S. and Barnes, V.E. 1976b, Geologic atlas of Texas, McAllen-Brownsville sheet: The University of Texas at Austin, Bureau of Economic Geology.



- Brown, L.F., Jr., and others, 1976, Environmental geologic atlas of the Texas coastal zone—Corpus Christi area: The University of Texas at Austin, Bureau of Economic Geology, 123 p.
- Brown, L.F., Jr., and others, 1977, Environmental geologic atlas of the Texas coastal zone—Kingsville area: The University of Texas at Austin, Bureau of Economic Geology, 131 p.
- Brown, L.F., Jr., and others, 1980, Environmental geologic atlas of the Texas coastal zone—Brownsville-Harlingen area: The University of Texas at Austin, Bureau of Economic Geology, 140 p.
- Bruno, R.S., and Hanor, J.S., 2003, Large-scale fluid migration driven by salt dissolution, Bay Marchand Dome, offshore Louisiana: Gulf Coast Association of Geological Societies Transactions, v. 53, p. 97–107.
- Bryant, W.R., Lugo, J., Cordova, C. and Salvador, A., 1991, Physiography and bathymetry, *in* A. Salvador, ed., The geology of North America: the Gulf of Mexico basin, v. J: Boulder, Colorado, Geological Society of America, p. 13–30.
- Carr, J.E., Meyer, W.R., Sandeen, W.M., and McLane, I.R., 1985, Digital models for simulation of ground-water hydrology of the Chicot and Evangeline aquifers along the Gulf Coast of Texas: Texas Department of Water Resources, Report 289, 101 p.
- Catuneanu, O., and 27 others, 2009, Towards the standardization of sequence stratigraphy: Earth-Science Reviews, v. 92, p. 1–33.
- Chowdhury, A.H. and Mace, R.E., 2003, “A groundwater availability model of the Gulf Coast Aquifer in the Lower Rio Grande Valley, TX – Numerical simulations through 2050: Texas Water Development Board Report,” 171 pp.
- Chowdhury, A., Wade, S., Mace, R.E., and Ridgeway, C., 2004, *Groundwater Availability of the Central Gulf Coast Aquifer System: Numerical Simulations through 1999*. Texas Water Development Board, unpublished report.

- Chowdhury, A.H., and Turco, M.J., 2006, Geology of the Gulf Coast aquifer, Texas, *in* Mace R.E., and others, eds., *Aquifers of the Gulf Coast of Texas: Texas Water Development Board Report 365*, p. 23–50.
- Chowdhury, A., and Mace, R.E., 2007, Groundwater Resource Evaluation and Availability Model of the Gulf Coast Aquifer in the Lower Grande Valley of Texas, *Texas Water Development Board Report 368*, p. 120.
- Collier, H., 1993, Borehole Geophysical Techniques for Determining the Water Quality and Reservoir Parameters of Fresh and Saline Water Aquifers in Texas, *Report 343*, Texas Water Development Board, Austin, TX.
- Collins, E.W., 1986, Salt diapirism-sedimentation relationships at Damon Mound Dome: stop1, *in* Seni, S.J., and Kyle, J.R., editors, *Comparison of cap rocks, mineral resources, and surface features of salt domes in the Houston diapir province: Geological Society of America, Field Trip Guidebook*, p. 103–118.
- Coleman, J.M., 1990, Depositional systems and the tectonic/eustatic of the Oligocene Vicksburg episode of the Northern Gulf Coast, Ph.D. Dissertation, University of Texas. Austin, TX.
- Coplin, L.S., and Galloway, D., 1999, Houston-Galveston, Texas—managing coastal subsidence, *in* Galloway, D., Jones, D.R., and Ingebritsen, S.E., eds., *Land subsidence in the United States: U.S. Geological Survey Circular 1182*, p. 35–48.
- Dale, O.C., 1952, Ground-Water Resources of Starr County, Texas: *Texas Board of Water Engineers Bulletin 5209*, 47 p.
- Deussen, A., 1914, Geology and underground waters of the southeastern part of the Texas Coastal Plain: *U.S. Geological Survey Water-Supply Paper 335*, 365 p.
- Deussen, A., 1924, Geology of the coastal plain of Texas west of Brazos River: *U.S. Geological Survey Professional 126*, 145 p.
- Deutsch, C.V., and Journel, A.G., 1998, *GSLIB Geostatistical Software Library and User's Guide*, Oxford University Press, New York, 340 p.

- Dodge, M.M., and Posey, J.S., 1981, Structural cross sections, Tertiary formations, Texas Gulf Coast: University of Texas at Austin, Bureau of Economic Geology.
- Doering, J.A., 1935, Post-Fleming surface formations of southeast Texas and south Louisiana: American Association of Petroleum Geologists Bulletin, v. 19, 651–688.
- Doering, J.A., 1956, Review of Quaternary surface formations of the Gulf Coast region: American Association of Petroleum Geologists Bulletin, v. 40, 1816–1862.
- Doyle, J.D., 1979, Depositional patterns of Miocene facies, middle Texas Coastal Plain: The University of Texas at Austin, Bureau of Economic Geology Report of Investigations No. 99, 28 p.
- Driscoll, F.G., 1986, Groundwater and Wells, Johnson Filtration Systems, Inc., St. Paul, MN, 1079 p.
- Dubar, J.R., 1983, Miocene depositional systems and hydrocarbon resources: the Texas Coastal Plain: The University of Texas at Austin, Bureau of Economic Geology, report prepared for U.S. Geological Survey under contract no. 14-08-0001-G-707, 99 p.
- Dubar, J.R., Ewing, T.E., Lundelius, Jr., E.L., Otvos, E.G., and Winker, C.D., 1991, Quaternary Geology of the Gulf of Mexico Coastal Plain, *in* Morrison, R.B., ed., Quaternary Non-Glacial Geology of the Conterminous United States: Boulder, Colorado, The Geological Society of America, The Geology of North America, v. K-2, p. 583–610.
- Dutton, A.R., and Richter, B.C., 1990, Regional geohydrology of the Gulf Coast Aquifer in Matagorda and Wharton Counties: Development of a numerical model to estimate the impact of water-management strategies: Contract report prepared for Lower Colorado River Authority, Austin, Texas, under Contract IAC (88-89) 0910, 116 p.
- Engelkemeir, R.M., and Khan, S.D., 2007, Near-surface geophysical studies of Houston faults: The Leading Edge, August 2007, p. 1004–1008.
- Engelkemeir, R.M., and Khan, S.D., 2008, Lidar mapping of faults in Houston, Texas, USA: Geosphere, v. 4, p. 170–182.

- Evans, D.G., Nunn, J.A., and Hanor, J.S., 1991, Mechanisms driving groundwater flow near salt domes: *Geophysical Research Letters*, v. 18, n. 5, p. 927–930.
- Ewing, T.E., 1990, Tectonic map of Texas: University of Texas at Austin, Bureau of Economic Geology, scale 1:750,000, 4 sheets.
- Ewing, T.E., 1991, Structural framework, *in* A. Salvador, ed., *The geology of North America: the Gulf of Mexico basin*, v. J: Boulder, Colorado, Geological Society of America, p. 31–52.
- Fillon, R.H., and Lawless, P.N. 2000, Lower Miocene-early Pliocene deposystems in the Gulf of Mexico: Regional sequence relationships: *Gulf Coast Association of Geological Societies Transactions*, v. 50, p. 411–428.
- Fisher, W.L., Brown, L.F., McGowen, J.H., and Groat, C.G., 1972, Environmental geologic atlas of the Texas coastal zone—Galveston-Houston area: The University of Texas at Austin, Bureau of Economic Geology, 91 p.
- Fisher, W.L., Brown, L.F., McGowen, J.H., and Groat, C.G., 1973, Environmental geologic atlas of the Texas coastal zone—Beaumont-Port Arthur area: The University of Texas at Austin, Bureau of Economic Geology, 93 p.
- Fisher, W.L., and McGowen, J.H., 1967, Depositional systems in the Wilcox Group of Texas and their relationship to occurrence of oil and gas: *Gulf Coast Association of Geological Societies Transactions*, v. 17, p. 105–125.
- Fogg, G.E., Seni, S.J., and Kreitler, C.W., 1983, Three-dimensional ground-water modeling in depositional systems, Wilcox Group, Oakwood salt dome area, East Texas: The University of Texas at Austin, Bureau of Economic Geology, Report of Investigations No. 133, 55 p.
- Fowler, T, 2011, Natural gas facility in Mont Belvieu explodes (updated): Fuelfix (insert website address).

- Frazier, D.E., 1974, Depositional episodes; Their relationship to the Quaternary stratigraphic framework in the northwestern portion of the Gulf Basin: The University of Texas at Austin, Bureau of Economic Geology Geological Circular 74-1, 28 p.
- Gagliano, S.M., 1999, Faulting, subsidence and land loss in coastal Louisiana, *in* Coast 2050: toward a sustainable coastal Louisiana, the appendices, Louisiana Department of Natural Resources, Baton Rouge, Louisiana, p. 1–45.
- Gagliano, S.M., 2005, Effects of earthquakes, fault movements, and subsidence on the south Louisiana landscape: The Louisiana Civil Engineer Journal of the Louisiana Section of the American Society of Civil Engineers, v. 13, p. 5–22.
- Galloway, W.E., Kreitler, C.W., and McGowen, J.H., 1979, Depositional and ground-water flow systems in the exploration for uranium: The University of Texas at Austin, Bureau of Economic Geology, 267 p.
- Galloway, W.E., 1981, Depositional architecture of Cenozoic Gulf Coastal Plain fluvial systems: SEPM Special Publication No. 31, p. 127–155.
- Galloway, W.E., Henry, C.D., and Smith, G.E., 1982, Depositional framework, hydrostratigraphy, and uranium mineralization of the Oakville Sandstone (Miocene), Texas Coastal Plain: The University of Texas at Austin, Bureau of Economic Geology Report of Investigations No. 113, 51 p.
- Galloway, W.E., Jirik, L.A., Morton, R.A., and DuBar, J.R., 1986, Lower Miocene (Fleming) depositional episode of the Texas Coastal Plain and continental shelf: The University of Texas at Austin, Bureau of Economic Geology Report of Investigations No. 150, 50 p.
- Galloway, W.E., 1989a, Genetic stratigraphic sequences in basin analysis I: Architecture and genesis of flooding-surface bounded depositional units: American Association of Petroleum Geologists Bulletin, v. 73, p. 125–142.
- Galloway, W.E., 1989b, Genetic stratigraphic sequences in basin analysis II: application to northeast Gulf of Mexico Cenozoic basin: American Association of Petroleum Geologists Bulletin, v. 73, p. 143–154.

- Galloway, W.E., Bebout, D.G., Fisher, W.L., Cabrera-Castro, R., Lugo-Rivera, J.E., and Scott, T.M., 1991, Cenozoic, in A. Salvador, ed., *The geology of North America: the Gulf of Mexico basin*, v. J: Boulder, Colorado, Geological Society of America, p. 245–324.
- Galloway, W.E., Liu, X., Travis-Neuberger, D., and Xue, L., 1994, Reference high-resolution correlation cross sections, Paleogene section, Texas Coastal Plain: The University of Texas at Austin, Bureau of Economic Geology.
- Galloway, W.E., and Hobday, D.K., 1996, *Terrigenous clastic depositional systems*: 2<sup>nd</sup> ed., New York, Springer-Verlag, 489.
- Galloway, W.E., Ganey-Curry, P.E., Li, X., and Buffler, R.T., 2000, Cenozoic depositional history of the Gulf of Mexico basin: *American Association of Petroleum Geologists Bulletin*, v. 84, p. 1743–1774.
- Galloway, W.E., 2005, Gulf of Mexico Basin depositional record of Cenozoic North American drainage basin evolution: *International Association Sedimentologists Special Publication* 35, p. 409–423.
- George, P.G., Mace, R E., and Petrossian, R., 2011, *Aquifers of Texas*, Report 380, Texas Water Development Board, Austin, TX.
- Grubb, H.F., 1984, Planning report for the gulf coast regional aquifer-system analysis in the Gulf of Mexico Coastal Plain, United States: U.S. Geological Survey Water-Resources Investigations Report 84-4219, 30 p.
- Grubb, H.F 1987, Overview of the Gulf Coast Regional Aquifer-System Analysis, *in* Vecchioli, J., and Johnson, A.I., eds., *Aquifers of the Atlantic and Gulf Coastal Plain*: American Water Resources Association Monograph no. 9, p. 101-118.
- Guevara-Sanchez, E.H., 1974, Pleistocene facies in the subsurface of the southeast Texas Coastal Plain: Ph.D. dissertation, The University of Texas at Austin, 133 p.
- Halbouty, M.T., 1979, *Salt domes—Gulf region, United States and Mexico*, 2nd edition: Houston, Texas, Gulf Publishing, 561 p.

- Hamlin, H.S., 1986, Texas coastal salt domes—Stratigraphic and structural interrelationships, *in* Seni, S.J., and Kyle, J.R., editors, Comparison of cap rocks, mineral resources, and surface features of salt domes in the Houston diapir province: Geological Society of America, Field Trip Guidebook, p. 27–42.
- Hamlin, H.S., Smith, D.A., and Akhter, M.S., 1988, Hydrogeology of Barbers Hill salt dome, Texas coastal plain: The University of Texas at Austin, Bureau of Economic Geology, Report of Investigations no. 176, 41 p.
- Hamlin, H.S., 2006, Salt domes in the Gulf Coast aquifer, *in* Mace, R.E., and others, eds., Aquifers of the Gulf Coast of Texas: Texas Water Development Board Report 365, p. 217–230.
- Hammond, Jr., W.W., 1969, Ground-Water Resources of Matagorda County, Texas: Texas Water Development Board Report 91, 163 p.
- Haq, B.U., Hardenbol, J., and Vail, P.R., 1987, Chronology of fluctuating sea levels since the Triassic: *Science*, v. 235, p. 1156–1167.
- Harris, H.B., 1965, Ground-water resources of LaSalle and McMullen counties, Texas: Texas Water Commission Bulletin 6520, 59 p.
- Hem, J.D., 1982, Conductance, a collective measure of dissolve ions, *in* R.A. Minear and Keigh, L.H. editors, *Water analysis*, v. 1, Inorganic species, pt. 1: Academic Press, p. 137-161.
- Hem, J.D., 1985, Study and interpretation of the chemical characteristics of natural water: U. S. Geological Survey Water Supply Paper 2254, 249 p.
- Hernandez-Mendoza, J.J., T.F. Hentz, L.H., DeAngelo, M.V., Wawrzyniec, T.F., Sakurai, S., Talukdar, S.C., and Holtz, M.H., 2008, Miocene chronostratigraphy, paleogeography, and play framework of the Burgos Basin, southern Gulf of Mexico: *American Association of Petroleum Geologists Bulletin*, v. 92, p. 1501–1535.
- Hoel, H.D., 1982, Goliad Formation of the south Texas Gulf Coastal Plain: regional genetic stratigraphy and uranium mineralization: Master's thesis, The University of Texas at Austin, 173 p.

- Holzer, T.L., 1984, Ground failure induced by ground water withdrawal from unconsolidated sediment, *in* Holzer, T.L., ed., *Man-induced land subsidence: Geological Society of American Review of Engineering Geology*, v. 6, p. 67–105.
- Holzer, T.L., and Gabrysch, R.K., 1987, Effect of water-level recoveries on fault creep, Houston, Texas: *Ground Water* v. 25, p. 392–397.
- Horswell, C., 2009, Daisetta sinkhole still a mystery 8 months after it formed: *Houston Chronicle*, January 5, 2009.
- Hosman, R.L., 1996, Regional stratigraphy and subsurface geology of Cenozoic deposits, Gulf Coastal Plain, South-Central United States—Regional aquifer system analysis—Gulf Coastal Plain: U.S. Geological Survey Professional Paper 1416-G, 35 p.
- Hosman, R.L. and Weiss, J.S., 1991, Geohydrologic units of the Mississippi.
- IHS, 2009, User’s Manual for PETRA. Information Handling Services, Houston, TX.
- Jones, P.H. and Buford, T.B., 1951, Electric logging applied to ground-water exploration: *Geophysics*, v. 16, no. 1, p. 115–139.
- Jones, P.H. 1956,. *Water Resources of Southwest Louisiana*. U. S. Geological Water Supply Paper 1364, 460 p.
- Jones, J.O., and Freed R.L., 1996, *Structural Framework for the Northern Gulf of Mexico: Gulf Coast Association of Geological Societies*, 754 pages.
- Jorgensen, D.G., 1975, *Analog-model studies of the ground-water hydrology in the Houston District, Texas: Austin: Texas Water Development Board Report 190*, 84 p.
- Kasmarek, M.C., Gabrysch, R.K., and Johnson, M.R., 2009, *Estimated land-surface subsidence in Harris county, Texas, 1915-17 to 2001: U.S. Geological Survey Scientific Investigation Map 3097*.
- Kasmarek, M.C., and Robinson, 2004, *Hydrogeology and Simulation of Groundwater Flow and Land-Surface Subsidence in the Northern Part of the Gulf Coast Aquifer System, Texas. Scientific Investigation Report 2004-5102: United States Geological Society*.



- Keys, W.S., and MacCary, L.M., 1971, Application of borehole geophysics to water-resources investigations: U.S. Geological Survey Techniques of Water-Resources Investigations, Book 2, Chapter E1, 126 p.
- Klinge, H., Schelkes, K., Rubel, A., Suckow, A., Schildknecht, F., and Ludwig, R., 2002, The saltwater/freshwater regime in the sedimentary cover of the Gorleben salt dome: *Transport in Porous Media*, v. 47, p. 125–148.
- Knox, P.R., Young, S.C., Galloway, W.E., Baker, Jr., E.T., and Budge, T., 2006, A stratigraphic approach to Chicot and Evangeline aquifer boundaries, central Texas Gulf Coast: *Gulf Coast Association of Geological Societies Transactions*, v. 56, p. 371–393.
- Konikow, L.F., Sanford, W.E., and Campbell, P. J., 1997, Constant-concentration boundary condition—Lessons from the HYDROCOIN variable-density groundwater benchmark problem: *Water Resources Research*, v. 33. no. 10, p. 2253–2261.
- Kreitler, C. W., 1976, Lineations and faults in the Texas coastal zone: The University of Texas at Austin, Bureau of Economic Geology Report of Investigations No. 85, 32 p.
- Kreitler, C.W., 1977, Fault control of subsidence, Houston, Texas: *Ground Water*, v. 15, p. 203-214.
- Kreitler, C.W., Guevera, E., Granata, G., and McKalips, D., 1977, Hydrogeology of Gulf Coast aquifers, Houston-Galveston area, Texas: *Gulf Coast Association of Geological Societies Transactions*, v. 27, p. 72–89.
- Kuecher, G.J., Roberts, H.H., Thompson, M.D., and Matthews, I., 2001, Evidence for active growth faulting in the Terrebonne delta plain, south Louisiana: implications for wetland loss and vertical migration of petroleum: *Environmental Geosciences*, v. 8, p. 77–94.
- Kyle, R.J., and Price, P.E., 1986, Sulfide mineralization in salt dome cap rocks, *in* Seni, S.J., and Kyle, J.R., editors, Comparison of cap rocks, mineral resources, and surface features of salt domes in the Houston diapir province: *Geological Society of America, Field Trip Guidebook*, p. 43–63.

- Lang, J.W., Winslow, A.G., and White, W.N., 1950, Geology and ground-water resources of the Houston district, Texas: Texas Board of Water Engineers, Bulletin 5001, 37 p.
- Lawless, P.N., Fillon, R.H., and Lytton III, R.G., 1997, Gulf of Mexico Cenozoic biostratigraphic, lithostratigraphic, and sequence stratigraphic event chronology: Gulf Coast Association of Geological Societies Transactions, v. 47, p. 271–282.
- LBG-Guyton and NRS Consulting, 2003, Brackish Groundwater Manual for Texas Regional Water Planning Groups, Texas Water Development Board, Austin, Texas.
- Loskot, C.L., Sandeen, W.M., and Follett, C.R., 1982, Ground-Water Resources of Colorado, Lavaca, and Wharton Counties, Texas: Texas Department of Water Resources Report 270, 199 p.
- Lundelius, E.L., 1972, Fossil vertebrates from the late Pleistocene Ingleside fauna, San Patricia County, Texas: The University of Texas at Austin, Bureau of Economic Geology Report of Investigations No. 77, 74 p.
- Marvin, R.F., Shafer, G.H., and Dale, O.C., 1962, Ground-Water Resources of Victoria and Calhoun Counties, Texas: Texas Board of Water Engineers Bulletin 6202, 147 p.
- Mason, C.C., 1963, Ground-Water Resources of Refugio County, Texas: Texas Water Commission Bulletin 6312, 115 p.
- Maury, C.J., 1920, Recent mollusks of the Gulf of Mexico and Pleistocene and Pliocene species from the Gulf states. Part I. Pelecypoda. Bull. Am. Paleontol. 8 (34): 115 pp.
- Maury, C.J.-Continued 1922, Recent Mollusca of the Gulf of Mexico and Pleistocene and Pliocene species from the Gulf States. Part II. Scaphopoda, Gastropoda Amphineura Cephalopoda. Bull. Am. Paleontol. 9, (38): 34-142.
- McCoy, T.W., 1990, Evaluation of Ground-Water Resources in the Lower Rio Grande Valley, Texas: Texas Water Development Board Report 316, 48 p.
- McGowen, J.H., Brown, Jr., L.F., Evans, T.J., Fisher, W.L., and Groat, C.G., 1976a, Environmental geologic atlas of the Texas coastal zone—Bay City-Freeport area: The University of Texas at Austin, Bureau of Economic Geology, 98 p.

- McGowen, J.H., Brown, Jr., L.F., Evans, T.J., Fisher, W.L., and Groat, C.G, 1976b, Environmental geologic atlas of the Texas coastal zone–Port Lavaca area: The University of Texas at Austin, Bureau of Economic Geology, 107 p.
- Miller, J.A., 1986, Hydrogeologic framework of the Floridian aquifer system in Florida and in parts of Georgia, Alabama, and South Carolina: U.S. Geological Survey Professional Paper 1403-B, 91 p.
- Miyazaki, B., 2009, Well integrity: an overlooked source of risk and liability for underground natural gas storage. Lesson learned from incidents in the USA: Geological Society, London, Special Publications, v. 313, p. 163–172.
- Moore, E.J., 1966, A graphical description of new methods of determining equivalent NaCl concentration of chemical analysis, in 7<sup>th</sup> annual symposium transactions: Society of Professional Well Log Analysts, Houston, TX, 34 p.
- Morton, R.A., and McGowen, J.H., 1980, Modern depositional environments of the Texas Coast: The University of Texas at Austin, Bureau of Economic Geology Guidebook 20, 167 p.
- Morton, R.A., Jirik, L.A., and Foote, R.Q., 1985, Structural cross sections, Miocene series, Texas continental shelf: University of Texas at Austin, Bureau of Economic Geology.
- Morton, R.A., Jirik, L.A., and Galloway, W.E., 1988, Middle-Upper Miocene depositional sequences of the Texas Coastal Plain and continental shelf: The University of Texas at Austin, Bureau of Economic Geology Report of Investigations No. 174, 40 p.
- Morton, R.A., and Galloway, W.E., 1991, Depositional, tectonic and eustatic controls on hydrocarbon distribution in divergent margin basins: Cenozoic Gulf of Mexico case history: Marine Geology, v. 102, p 239–263.
- Morton, R.A., Sams, R.H., and Jirik, L.A., 1991, PlioPleistocene depositional sequences of the southeastern Texas continental shelf and slope: geologic framework, sedimentary facies, and hydrocarbon distribution: The University of Texas at Austin, Bureau of Economic Geology Report of Investigations No. 200, 80 p.

- Mullican, W.F., III, 1988, Subsidence and collapse at Texas salt domes: The University of Texas at Austin, Bureau of Economic Geology, Geological Circular 88-2, 35 p
- Murray, G.E., 1961, Geology of the Atlantic and Gulf Coastal province of North America: New York, Harper and Brothers, 692 p.
- Myers, B.N., and O.C. Dale, 1966, Ground-Water Resources of Bee County, Texas: Texas Water Development Board Report 17, 101 p.
- Myers, B.N., and O.C. Dale, 1967, Ground-Water Resources of Brooks County, Texas: Texas Water Development Board Report 61, 87 p.
- Nehring, R., 1991, Chapter 15: oil and gas resources, in A. Salvador, ed., The geology of North America: the Gulf of Mexico basin, v. J: Boulder, Colorado, Geological Society of America, p. 445–494.
- Paine, J.G., 1993, Subsidence of the Texas coast: inferences from historical and late Pleistocene sea levels: Tectonophysics, v. 222, p. 445–458.
- Paleo-data. 2009, [www.paleodata.com](http://www.paleodata.com).
- Peckham, R.C., 1965, Availability and quality of ground water in Leon County, Texas: Texas Water Commission Bulletin 6513, 43 p.
- Plummer, F.B., 1933, Cenozoic systems in Texas, in Sellards, E.H., Adkins, W.S., and Plummer, F.B., eds., The geology of Texas, v. 1, stratigraphy: The University of Texas at Austin, Bureau of Economic Geology Bulletin No. 3232, p. 519–818.
- Preston, R.D., 1983, Occurrence and Quality of Ground Water in the Vicinity of Brownsville, Texas: Texas Department of Water Resources Report 279, 98 p.
- Price, W.A., 1933, Role of diastrophism in topography of Corpus Christi area, south Texas: American Association of Petroleum Geologists Bulletin, v. 17, p. 907–962.
- Price, W.A., 1934, Lissie Formation and Beaumont Clay in south Texas: American Association of Petroleum Geologists Bulletin, v. 18, p. 948–959.

- Price, W.A., 1958, Sedimentology and Quaternary geomorphology of south Texas. Supplementary to Field Trip Manual: Sedimentology of south Texas, Corpus Christi Geol. Soc. Spring Field Trip, 1958: Gulf Coast Assoc. Geol. Soc, Trans., v. 8, p. 41-75. (Abstract in Geoscience Abstracts, v. 1, no. 7, p. 4 (No. 1-1630), 1959.
- Proctor, C.V., Brown, T.E., Waechter, N.B., Aronow, S., and Barnes, V.E., 1974, Geologic atlas of Texas, Seguin sheet: The University of Texas at Austin, Bureau of Economic Geology.
- Rainwater, E.H., 1964, Regional stratigraphy of the Gulf Coast Miocene: Gulf Coast Association of Geological Societies Transactions, v. 14, p. 81–124.
- Reeves, R.D., 1967, Ground-Water Resources of Kendall County, Texas: Texas Water Development Board Report 60, 90 p.
- Rezak, R., 1984, Local carbonate production on a terrigenous shelf: Gulf Coast Association of Geological Societies Transactions, v. 35, p. 477–484.
- Rogers, L.T., 1967, Availability and Quality of Ground Water in Fayette County, Texas: Texas Water Development Board Report 56, 117 p.
- Rose, N.A., 1943, Progress report on the ground-water resources of the Texas City area, Texas: U.S. Geological Survey open-file report, 45 p.
- Ryder, P.D., 1988, “Hydrogeology and predevelopment flow in the Texas Gulf Coast Aquifer Systems,” United States Geological Survey Water-Resources Investigations Report 87-4248, 109 p.
- Ryder, P.D., and Ardis, A.F., 2002, Hydrology of Texas Gulf Coast aquifer systems: U.S. Geological Survey Professional Paper 1416-E, 77 p.
- Salvador, A., 1991, Introduction, *in* A. Salvador, ed., The geology of North America: the Gulf of Mexico basin, v. J: Boulder, Colorado, Geological Society of America, p. 1–12.
- Saribudak, M., and Van Nieuwenhuise, B., 2006, Integrated geophysical studies over an active growth fault in Houston: The Leading Edge, March 2006, p. 332–334.

Shafer, G.H., 1968, Ground-Water Resources of Nueces and San Patricio Counties, Texas.

Schlumberger, 1972, Log Interpretation Volume I, Principals. Schlumberber Wireline and Testing, Sugarland, TX 130 p.

Schumm, S.A., 1977, The fluvial system: New York, John Wiley, 338 p.

Seni, S.J., 1986, Texas coastal salt domes—Introduction and overview, *in* Seni, S.J., and Kyle, J.R., editors, Comparison of cap rocks, mineral resources, and surface features of salt domes in the Houston diapir province: Geological Society of America, Field Trip Guidebook, p. 3–24.

Seni, S.J., Collins, E.W., Hamlin, H.S., Mullican, III, W.F., and Smith, D.A., 1985, Phase III—Examination of Texas salt domes as potential sites for permanent storage of toxic chemical waste: The University of Texas at Austin, Bureau of Economic Geology, report prepared for Texas Water Commission under interagency contract no. IAC (84-85)-2203, 310 p.

Seni, S.J., Hamlin, H.S., and Mullican, III, W.F., 1984a, Technical issues for chemical waste isolation in solution-mined caverns in salt domes: The University of Texas at Austin, Bureau of Economic Geology, report prepared for Texas Department of Water Resources under interagency contract no. IAC (84-85)-1019, 8 p.

Seni, S.J., Kreitler, C.W., Mullican, III, W.F., and Hamlin, H.S., 1984b, Utilization of salt domes for chemical-waste disposal: The University of Texas at Austin, Bureau of Economic Geology, report prepared for Texas Department of Water Resources under interagency contract no. IAC (84-85)-1019, 161 p.

Seni, S.J., Mullican, III, W.F., and Hamlin, H.S., 1984c, Texas salt domes—Aspects affecting disposal of toxic-chemical waste in solution-mined caverns: The University of Texas at Austin, Bureau of Economic Geology, report prepared for Texas Department of Water Resources under interagency contract no. IAC (84-85)-1019, 94 p.

Seni, S.J., Mullican, III, W.F., and Hamlin, H.S., 1984d, Texas salt domes—Natural resources, storage caverns, and extraction technology: The University of Texas at Austin, Bureau of

Economic Geology, report prepared for Texas Department of Water Resources under interagency contract no. IAC (84-85)-1019, 161 p.

Seni, S.J., and Jackson, M.P.A., 1984, Sedimentary record of Cretaceous and Tertiary salt movement, East Texas basin—Times, rates, and volume of salt flow and their implications for nuclear waste isolation and petroleum exploration: The University of Texas at Austin, Bureau of Economic Geology Report of Investigations No. 139, 89 p.

Seni, S.J. and Mullican, III, W.F., 1986, Topography over domes—Implications for dome growth and dissolution, *in* Seni, S.J., and Kyle, J.R., editors, Comparison of cap rocks, mineral resources, and surface features of salt domes in the Houston diapir province: Geological Society of America, Field Trip Guidebook, p. 89–100.

Shah, S.D., and Lanning-Rush, J., 2005, Principal faults in the Houston, Texas, metropolitan area: U.S. Geological Survey Scientific Investigation Map 2874.

Shafer, G.H., 1965, Ground-Water Resources of Gonzales County, Texas: Texas Water Development Board Report 4, 89 p.

Shafer, G.H., 1968, Ground-Water Resources of Nueces and San Patricio Counties, Texas: Texas Water Development Board Report 73, 129 p.

Shafer, G.H., 1970, Ground-Water Resources of Aransas County, Texas: Texas Water Development Board Report 124, 81 p.

Shafer, G.H., and Baker, Jr., E.T., 1973, Ground-Water Resources of Kleberg, Kenedy, and Southern Jim Wells Counties, Texas: Texas Water Development Board Report 173, 153 p.

Shafer, G.H., 1974, Ground-Water Resources of Duval County, Texas: Texas Water Development Board Report 181, 117 p.

Sharp, Jr., J.M., and Hill, D.W., 1995, Land subsidence along the northeastern Texas Gulf coast: effects of deep hydrocarbon production: *Environmental Geology*, v. 25, p. 181–191.

- Sharp, Jr., J.M., Kreitler, C.W., and Lesser, J., 1991, Ground water, *in* A. Salvador, ed., The geology of North America: the Gulf of Mexico basin, v. J: Boulder, Colorado, Geological Society of America, p. 529–543.
- Shelby, C.A., M.K. Pieper, J., Aronow, S., and Barnes, V.E., 1968, Geologic atlas of Texas, Beaumont sheet: The University of Texas at Austin, Bureau of Economic Geology.
- Spradlin, S.D., 1980, Miocene fluvial systems: southeast Texas: The University of Texas at Austin, Master's thesis, 139 p.
- Solis I., 1981, Upper Tertiary and Quaternary depositional systems, Central Coastal Plain, Texas, The University of Texas at Austin, Bureau of Economic Geology Report of Investigations No. 108, 89 p.
- Strom, E.N., Houston, V.E., and Garcia, A., 2003, Selected hydrogeologic datasets for the Jasper Aquifer, Texas. Open File Report 2003-299: United States Geological Survey, Reston, VA.
- Tedford, R.H., and Hunter, M.E., 1984, Miocene marine-nonmarine correlations, Atlantic and Gulf Coastal Plains, North America: *Palaeography, Palaeoclimatology, Palaeoecology*, vol. 47, pp.129-151.
- Thompson, G.L., 1966, Groundwater-resources of Lee County, Texas: Texas Water Development Board Report 20, 131. p.
- Trowbridge, A.C., 1932, Tertiary and Quaternary geology of the Lower Rio Grande region, Texas: U.S. Geological Survey Bulletin 837, 260 p.
- Van Wagoner, J.C., Mitchum, R.M., Campion, K.M., and Rahmanian, V.D., 1990, Siliciclastic sequence stratigraphy in well logs, cores, and outcrops: concepts for high-resolution correlation of time and facies: American Association of Petroleum Geologists Methods in Exploration Series No. 7, 55 p.
- Verbeek, E.R., 1979, Surface faults in the Gulf Coastal Plain between Victoria and Beaumont, Texas: *Tectonophysics*, v. 52, p. 373–375.



- Verbeek, E.R., and Clanton, U.S., 1979, Clodine fault, southwestern Houston metropolitan area, Texas: U.S. Geological Survey Open-file Report 79-947, 25 p.
- Weeks, A.W., 1933, Lissie, Reynosa, and upland terrace deposits of coastal plain of Texas between Brazos River and Rio Grande: American Association of Petroleum Geologists Bulletin, v. 17, p. 453–487.
- Weeks, A.W., 1945, Quaternary deposits of the Texas Coastal Plain between Brazos River and Rio Grande: American Association of Petroleum Geologists Bulletin, v. 29, p. 1693–1720.
- Weiss, J., 1992, Geohydrologic Units of the Coastal Lowland Aquifer System South-Central United States, Professional Paper 1416-C: U.S. Geological Survey, Denver, CO., 42 p.
- Wesselman, J.B., 1967, Ground-water resources of Jasper and Newton Counties, Texas: Texas Water Development Board Report 59, 167 p.
- Wesselman, J.B., 1971, Ground-water resources of Chambers and Jefferson counties, Texas: Texas Water Development Board Report 133, 173 p.
- Wesselman, J.B., 1972, Ground-water resources of Fort Bend County, Texas: Texas Water Development Board Report 155, 176 p.
- Whitman, H.M., 1965, Estimating Water Quality From Electric Logs, Department of Conservation, Louisiana Geological Survey and Louisiana Department of Public Works in cooperation with the United States Geological Survey
- Williamson, J.D.M., 1959, Gulf Coast Cenozoic History: Gulf Coast Association of Geological Societies Transactions, v. 9, p. 15–29.
- Williamson, A.K., and H.F., Gurb, 2001, Groundwater Flow in the Gulf Coast Aquifer Systems South-Central United States Regional Aquifer System Analyses –Gulf Coast Plains: USGS Professional Paper 1416-F
- Winker, C.D., 1979, Late Pleistocene fluvial-deltaic deposition Texas Coastal Plain and shelf: Master's thesis: The University of Texas at Austin, 187 p.

- Winker, C.D., 1982, Cenozoic shelf margins, northwestern Gulf of Mexico: Gulf Coast Association of Geological Societies Transactions, v. 32, p. 427–448.
- Winker, C.D., and M.B. Edwards, 1983, Unstable progradational clastic shelf margins, in Stanley, D.J., and Moore, G.T., eds, The shelfbreak; Critical interface on continental margins: SEPM Special Publication 33, p. 139-157.
- Winker, C.D., and Buffler, R.T., 1988, Paleogeographic evolution of early deep-water Gulf of Mexico and margins, Jurassic to middle Cretaceous (Comanchean): American Association of Petroleum Geologists Bulletin, v. 72, p. 318–346.
- Wood, L.A., Gabrysch, R.K., and Marvin, R., 1963, Reconnaissance investigation of the ground-water resources of the Gulf Coast region, Texas: Texas Water Commission Bulletin 6305, 114 p.
- Young, S.C., and Kelley, V., eds., 2006, A site conceptual model to support the development of a detailed groundwater model for Colorado, Wharton, and Matagorda Counties: unpublished report prepared for the Lower Colorado River Authority, xxx p.
- Young, S.C., Kelley, V., Budge, T., Deeds, N., and Knox, P., 2009, Development of the LCRB Groundwater Flow Model for the Chicot and Evangeline Aquifers in Colorado, Wharton, and Matagorda Counties, prepared for the Lower Colorado River Authority, Austin, TX.
- Young, S.C., Knox, P.R., Baker, E., Budge, T., Hamlin, S., Galloway, B., Kalbous, R., and Deeds, N., 2010, Hydrostratigraphic of the Gulf Coast Aquifer from the Brazos River to the Rio Grande: Texas Water Development Board Report, 203 p.

*This page intentionally left blank.*

## **APPENDIX A**

### **Geophysical Logs Listing, including Location and Use**

*This page intentionally left blank.*

## Appendix A Geophysical Logs Listing, including Location and Use

API number or ID	NAD27 latitude	NAD27 longitude	Dip section/ position	Strike section/ position	Company	Lease	County	State	Lithology and water qual data	Paleo Data
171152004000	31.228681	-92.957056	-1/1		Domestic Oil	Pardee	Vernon	LA	X	
171150002000	31.177184	-93.07196	-1/2		Gamble, B.E.	Pickering Lbr	Vernon	LA		
171150002100	31.172684	-93.118861	-1/2A		McElwee, W.T.	Martin's Devel Fee	Vernon	LA	X	
171150002200	31.029688	-93.002156	-1/3	D-D'/16	Burton, W.T.	Fee	Vernon	LA	X	
171158800300	30.96809	-93.092758	-1/4	D-D'/15	Union Pacific Res	Crosby 21 SWD	Vernon	LA	X	
171152017900	30.926891	-93.119859	-1/5	D-D'/14	UPRC	USA 31	Vernon	LA		
171152013500	30.89056	-93.17287	-1/6	D-D'/13	Union Pacific Res	Quinn 15	Vernon	LA		
170112090100	30.865993	-93.105958	-1/7		Chesapeake Oper	Triple R 20	Beauregard	LA	X	
170112059000	30.742296	-93.17896	-1/8		Smith Petroleum Company	Ensminger	Beauregard	LA		
170110016900	30.597198	-93.154058	-1/9	C-C'/16	Magnolia Pet	Four 'C' McPherson	Beauregard	LA		
170112053200	30.576498	-93.270061	-1/9A	C-C'/14	Goldking Pdn	Jones, S.M.	Beauregard	LA	X	
170110029800	30.513799	-93.234859	-1/10	C-C'/15	Texas Co	Hollingsworth, I. Etal	Beauregard	LA		
170110090600	30.416501	-93.290959	-1/11		Shell Oil	Edgewood Land & Logging	Beauregard	LA		
170192183600	30.378302	-93.258857	-1/12		Neumin Pdn	Mayo Realty	Calcasieu	LA	X	
170190045900	30.354702	-93.40106	-1/12A		Union Prod	Davis	Calcasieu	LA		
170190116300	30.32772	-93.23687	-1/13		Shell Oil	Lake Charles Naval Stores	Calcasieu	LA		
170190145800	30.214206	-93.307555	-1/14		Magnolia Pet	Bordages, I.R.	Calcasieu	LA	X	
170192162100	30.20016	-93.30406	-1/14A		Mobil E&P	Farquhar	Calcasieu	LA		
170190167400	30.143808	-93.309355	-1/15		Hankamer Inv	James, B	Calcasieu	LA		
170192020200	30.118409	-93.320055	-1/15A	B-B'/17	Damson Expl	Louisiana Farm & Livestock	Calcasieu	LA	X	
170190184900	30.09673	-93.40586	-1/16	B-B'/16	Union Sulphur	Ellender, E.	Calcasieu	LA		
170230020800	30.026912	-93.361856	-1/17		Stanolind O&G	Gulf Land	Cameron	LA	X	
170230050900	30.000513	-93.359356	-1/18		Mecom (US Oil of LA)	Ellender, J.	Cameron	LA	X	
170230159900	29.984214	-93.389356	-1/19		Hurt, H.	Vincent, N et al	Cameron	LA	X	
170232228000	29.951415	-93.414956	-1/20		The Expl	Miami Corp	Cameron	LA	X	
170230156200	29.895418	-93.435656	-1/21		Texaco	Miami - Back Ridge	Cameron	LA	X	
170230177200	29.83212	-93.43961	-1/22		Magnolia Pet	Lutcher 'C'	Cameron	LA		
170232122500	29.77681	-93.39369	-1/23		Amoco Pdn	Vincent Heirs	Cameron	LA		
177004121502	29.56011	-93.43163	-1/24	A-A'/12	BHP Billiton Pet	OCS-G-09387	Offshore-Cameron	LA		
177004084000	29.33696	-93.46457	-1/25		Odeco O&G	OCS-G-2828	Offshore-Cameron	LA		
177014015000	29.23642	-93.64023	-1/26		Hall-Houston Oil	OCS-G-7615	Offshore-Cameron	LA		
177014031202	29.173744	-93.46166	-1/27		Forcenergy	OCS-G-16141	Offshore-Cameron	LA		
177014036000	29.073046	-93.436859	-1/28		Mariner En	OCS-G-24733	Offshore-Cameron	LA	X	
177014018600	29.059745	-93.676963	-1/29		Texas Gas Expl	OCS-G-5308	Offshore-Cameron	LA	X	

Final Report – Updating the Hydrogeologic Framework for the Northern Portion of the Gulf Coast Aquifer

API number or ID	NAD27 latitude	NAD27 longitude	Dip section/ position	Strike section/ position	Company	Lease	County	State	Lithology and water qual data	Paleo Data
170850422200	31.286983	-93.472072	0/1		Thompson Expl Drlg	Pickering Lbr	Sabine	LA	X	
171150002700	31.190687	-93.489872	0/2		Riley, F., Jr.	Dixon	Vernon	LA	X	
171152000400	31.107089	-93.499572	0/3		Mallard Drlg	Olin Un	Vernon	LA	X	
171158800000	30.944494	-93.47407	0/4	D-D'/11	Sonat Expl	Sonat Minerals 27 SWD	Vernon	LA	X	
171152012000	30.968593	-93.401768	0/4A	D-D'/12	Sonat Expl	Sonat Minerals	Vernon	LA		
170112061600	30.864497	-93.518272	0/5	D-D'/10	ARCO (Atlantic Richfield)	Singletery (Joshlin)	Beauregard	LA	X	
170112080000	30.78462	-93.49522	0/6		Falcon En of Tx	Riceland Lbr	Beauregard	LA		
170112040700	30.6501	-93.50307	0/7		Kirby Expl	Boise Southern	Beauregard	LA		
170110064200	30.6115	-93.53987	0/8		Magnolia Pet	Lutcher-Moore	Beauregard	LA	X	
170110075500	30.5325	-93.554269	0/9	C-C'/13	Union Sulphur & Oil	Lutcher-Moore	Beauregard	LA		
170112105800	30.4753	-93.560268	0/10		Aminex USA	Olympia Minerals	Beauregard	LA		
170190001800	30.362803	-93.583164	0/11		Lamson-Bennett & Cole	Lutcher-Moore	Calcasieu	LA		
170190025500	30.280005	-93.54016	0/12		Jayred, W.B.	Industrial Lbr	Calcasieu	LA		
170190258300	30.26112	-93.61978	0/12A		Breder, G.W.	Industrial Lbr	Calcasieu	LA		
170190197200	30.178608	-93.619662	0/13		xxx-Moore Oil Inds	Brooks, W.F>	Calcasieu	LA		
170190207200	30.155108	-93.56326	0/13A		Cox & Hamon	Jardell, J.	Calcasieu	LA		
170190206500	30.08671	-93.5564	0/14	B-B'/14	Nabors, W.C.	C.O.G.	DeSo	LA		
170190189600	30.09361	-93.542359	0/14A	B-B'/15	Union Sulphur	Burton-Bank	Calcasieu	LA	X	
170232012700	30.039211	-93.627362	0/15	B-B'/13	Shell Oil	Watkins, J.B.	Cameron	LA	X	
170230011100	30.014612	-93.54886	0/16		Magnolia Pet	Moore, R.A.	Cameron	LA		
170230187700	29.85354	-93.65672	0/17		Texas Co	Miami Corp Fee	Cameron	LA		
170230196800	29.830819	-93.627059	0/18		Magnolia Pet	Cameron Land Co	Cameron	LA	X	
170230204500	29.771222	-93.600058	0/19		Callery, F.A.	Erselding, F. et al	Cameron	LA	X	
177002020800	29.74685	-93.63524	0/20		Amerada Hess	SL 10368	Cameron	LA		
177004106800	29.69852	-93.65901	0/21		IS/Chevron	OCS-G-21531	Offshore-Cameron	LA		
177000005500	29.537832	-93.594961	0/24	A-A'/11	British American Oil	OCS 0847	Offshore-Cameron	LA		
177014031600	29.36355	-93.71683	0/25		Basin Expl	OCS-G-21053	Offshore-Cameron	LA		
177014015000	29.23642	-93.64023	0/26A		Texas Gas Expl	OCS-G-5308	Offshore-Cameron	LA		
177014018600	29.059745	-93.676963	0/27		Hall-Houston Oil	OCS-G-7615	Offshore-Cameron	LA	X	
424033027800	31.292386	-93.878986	1/1		Coffman, T.D.	Temple-Eastex 90	Sabine	TX	X	
424033019600	31.237488	-93.918587	1/2		Coffman, T.D.	Temple-Eastex	Sabine	TX		
424033034300	31.17107	-93.84428	1/3		N/A	N/A	Sabine	TX		
423513052100	31.153391	-93.847284	1/3A		Maersk En	Texaco	Newton	TX	X	
423513052600	31.14586	-93.89397	1/3B		Union Pacific Res	ARCO	Newton	TX		
423510004800	30.95765	-93.82187	1/4		Pan American	Brown, E.W., jr.	Newton	TX	X	
423513072600	30.794102	-93.835981	1/5	D-D'/9	Geosouthern En	Seybold	Newton	TX	X	

Final Report – Updating the Hydrogeologic Framework for the Northern Portion of the Gulf Coast Aquifer

API number or ID	NAD27 latitude	NAD27 longitude	Dip section/ position	Strike section/ position	Company	Lease	County	State	Lithology and water qual data	Paleo Data
423510047800	30.729603	-93.791579	1/6		Kerr-McGee	Sinclair-Atlantic	Newton	TX		
423513003300	30.71436	-93.85365	1/6A		White Shield O&G	Kirby-Arco	Newton	TX		
422410009100	30.674804	-93.879881	1/7		Atlantic Refg - Sinclair	Henderson, D.M.	Jasper	TX		
423510009600	30.556304	-93.834877	1/8		Atlantic Refg - Sinclair	Holmes, M.	Newton	TX	X	
423510022600	30.466204	-93.824375	1/9	C-C'/12	Humble O&R	Kurth, J.H.	Newton	TX		
423513038100	30.403906	-93.854874	1/10		Arco O&G	Arco B.E. Quinn 26	Newton	TX		
423510028900	30.297007	-93.841871	1/11		Humble O&R	Dyer et al	Newton	TX	X	
423613081000	30.181809	-93.85807	1/12		Range Res	Smith, L.C.	Orange	TX	X	
423610047400	30.11941	-93.85017	1/13		Sun Oil	Stark, W.J.L.	Orange	TX		
423610055500	30.077411	-93.869871	1/14	B-B'/11	Sun Oil	Lutcher-Moore Lbr Co	Orange	TX		
423610049000	30.042512	-93.822469	1/15	B-B'/12	Scurlock Oil	Phares	Orange	TX		
423610131800	29.942814	-93.828368	1/16		Humble O&R	Sabine Lake ST 8	Orange	TX		
170230205500	29.864116	-93.835866	1/17		California	SL 3463	Cameron	LA	X	
170230207900	29.784417	-93.906667	1/18		British American Oil Pdcg	La 'G' SL 2875	Cameron	LA		
422453035800	29.720819	-93.878265	1/19		McCormick O&G	Kountze Arco Fee	Jefferson	TX	X	
422450334300	29.679222	-93.847665	1/20		Hugh xxxouren etal	Kountze-Stuart	Jefferson	TX		
427153001100	29.545828	-93.799364	1/21	A-A'/9	Superior Oil	ST 14-L	Offshore-Cameron	TX	X	
427084057200	29.438131	-93.874168	1/22	A-A'/8	Spinnaker Expl	OCS-G-23193	Offshore-Jefferson	TX	X	
427104013100	29.24994	-93.85949	1/24		Prime Nat Res	OCS-G-14883	Offshore-Jefferson	TX		
427104005600	29.029945	-93.864768	1/26		Champlin Pet	OCS-G-8169	Offshore-Jefferson	TX	X	
420050019200	31.21599	-94.3519	2/1		Walker, R.Y.	Angelina Hardwood	Angelina	TX	X	
G0030024A	31.134445	-94.263054	2/2		Key WW Co	Caney Creek Rec Area	Angelina	TX	X	
420053011900	31.108394	-94.260197	2/2A		Cox, Cox & Goldking?	USA	Angelina	TX	X	
422410025300	31.0529	-94.24066	2/3		Atlantic Refg	H&TC RR Sec 249 Fee	Jasper	TX		
424573011900	30.985697	-94.291597	2/4		Sun Oil	Shivers, A.	Tyler	TX	X	
424570004100	30.843301	-94.242794	2/5		Dishman & Lucas	Angelina Lumber	Tyler	TX	X	
424570004300	30.788302	-94.208892	2/6	D-D'/8	Spidle, A.A.	International Paper	Tyler	TX		
424570025600	30.72077	-94.19273	2/7		San Patricio Oil	Cain	Tyler	TX		
424570024500	30.680904	-94.256692	2/8		Texas Co	Gouger GU 20/A	McMullen	TX	X	
424570025400	30.638305	-94.258191	2/9		Atlantic Refg	Rice	Tyler	TX		
424570037700	30.555906	-94.24689	2/10		Amer Repub - Hou- Sohio	Kirby Lbr Co	Tyler	TX	X	
421990011600	30.508307	-94.136586	2/11		Stanolind	Dy-Jackson	Hardin	TX	X	
1-9	30.451007	-94.108184	2/12	C-C'/11	Gulf Oil	Temple Lbr Co	Jasper	TX		
421993181100	30.386908	-94.155584	2/13	C-C'/10	Arco O&G	Bankston Fee	Hardin	TX	X	
421990035600	30.315209	-94.200685	2/14		Atlantic Refg - Sinclair	Nona Mills	Hardin	TX	X	
423610000400	30.21311	-94.068279	2/15		Gulf Oil	Miller-Vidor Land Co	Orange	TX		



Final Report – Updating the Hydrogeologic Framework for the Northern Portion of the Gulf Coast Aquifer

API number or ID	NAD27 latitude	NAD27 longitude	Dip section/ position	Strike section/ position	Company	Lease	County	State	Lithology and water qual data	Paleo Data
422450016900	30.118412	-94.140781	2/16		Sun Oil	Seale, W.	Jefferson	TX	X	
422453257200	30.005214	-94.11788	2/17	B-B'/10	PB Energy Storage Svcs	Drig Disposal Well	Jefferson	TX		
422450165400	29.955215	-94.106579	2/18		Humble O&R	Texas Rice Land Co	Jefferson	TX		
422450163700	29.911816	-94.104478	2/19		Union Sulphur & Oil	Aubey, L. etal Un A	Jefferson	TX	X	
422450211000	29.848917	-94.093877	2/20		Shell Oil	Hebert-Broussard	Jefferson	TX		
422453014300	29.796318	-94.120378	2/21		Amoco Pdn	Broussard & Hebert	Jefferson	TX	X	
422450299600	29.70562	-94.086076	2/22		Shell Oil	McFaddin State	Jefferson	TX	X	
426060001000	29.648121	-94.005471	2/23		Hunt Oil	ST 43-S	Offshore-Jefferson	TX		
427080001000	29.564524	-94.004372	2/24		Magnolia Pet	SL 41142 HI Area	Offshore-Jefferson	TX	X	
427084046800	29.20282	-93.98412	2/29		Vastar Res	OCS-G-14869	Offshore-Jefferson	TX		
2-6	31.275087	-94.691007	3/1		Byers & Kurth	Southern Pine Lbr	Angelina	TX		
420053017100	31.193988	-94.717507	3/2		Redd & Willingham	Copes Hrs	Angelina	TX	X	
423733048400	31.08869	-94.694006	3/3		Cities Service	Champion Intl Corp	Polk	TX	X	
423730000300	31.01856	-94.65104	3/4		Rinehart	Carter, W.T.	Polk	TX	X	
423730000600	30.8959	-94.6469	3/4A		Plummer, A.	Pierce	Polk	TX		
424573010100	30.863897	-94.552803	3/5		Watson Oil	Carter, W.T. & bros	Tyler	TX	X	
2-10	30.812698	-94.615004	3/6		Justiss-Mears Oil	Carter, W.T., & Bro	Tyler	TX		
424570047700	30.700702	-94.565202	3/7	D-D'/7	Gulf Oil	Carter-Camden	Tyler	TX	X	
2-12	30.575205	-94.538999	3/8		Shell Oil	Kirby Lbr Co	Tyler	TX		
424570006300	30.562105	-94.519599	3/9		Sinclair - Atlantic	Chambers, T.W.	Tyler	TX	X	
421993311900	30.41234	-94.50264	3/10	C-C'/7	Kerr-McGee	BlackStone	Hardin	TX		
G1000055B	30.396222	-94.448789	3/11	C-C'/8	Lanford Drig	W Hardin WSC Honey Island	Hardin	TX	X	
421990063400	30.39544	-94.38392	3/11A	C-C'/9	Atlantic - Sinclair	Works, P.A. Fee	Hardin	TX	X	
421990067400	30.300009	-94.420792	3/12		Jones, R.N. - Darcy H.P.	Kirkpatrick etal	Hardin	TX	X	
421990214800	30.170112	-94.39109	3/13		Humble O&R	Piloff	Hardin	TX	X	
422453156200	30.102313	-94.374189	3/14		Arco O&G	Arco Fee	Jefferson	TX	X	
422450012300	30.063014	-94.335288	3/15		Sun Oil	Kolander etal 'A'	Jefferson	TX		
422453195500	30.01734	-94.39853	3/15A	B-B'/8	Coalinga	Carpenter, A.M.	Jefferson	TX		
422450223800	29.939617	-94.350588	3/16	B-B'/9	Chavanne, H.J. Trustee	Gilbert, W.C.	Jefferson	TX		
422450226500	29.892118	-94.295486	3/17		Stanolind	Marrs McLean	Jefferson	TX	X	
422450265800	29.800021	-94.319487	3/18		McCarthy	Plant Sivelair	Jefferson	TX		
422450268900	29.777921	-94.268686	3/19		McCarthy O&G	Gill	Jefferson	TX	X	
422450286600	29.713323	-94.246685	3/20		Austral Oil Expl	WHP McFaddin	Jefferson	TX		
426060005500	29.585427	-94.264085	3/21		Texas Crude Oil	ST 83-8 SL 10209	Offshore-Jefferson	TX	X	
	#N/A	#N/A	3/		Conoco	ST 31-L	Offshore-	TX		
427083031300	29.47505	-94.2122	3/21A	A-A'/5	Kilroy of Texas	ST 30-L	Offshore-Jefferson	TX		

Final Report – Updating the Hydrogeologic Framework for the Northern Portion of the Gulf Coast Aquifer

API number or ID	NAD27 latitude	NAD27 longitude	Dip section/ position	Strike section/ position	Company	Lease	County	State	Lithology and water qual data	Paleo Data
427080005700	29.224838	-94.116777	3/24		Shell - Phillips	Fed Block 161	Offshore-Jefferson	TX		
427084012800	28.981845	-94.067874	3/26		Exxon	OCS-G-4737	Offshore-Jefferson	TX		
424553048500	31.232783	-95.110914	4/1?		Range Pdn	Baker, J.	Trinity	TX	X	
424550002200	31.190784	-95.060613	4/2		N/A	N/A	Trinity	TX		
424550003200	31.065385	-95.064512	4/3		N/A	N/A	Trinity	TX		
423730003000	30.964087	-95.018811	4/4		Werdy, J.Z.	Saner-Ragley Lbr Houston Sch	Polk	TX	X	
423733012000	30.846891	-94.947912	4/5		Macpet etal	Southland Paper Co	Polk	TX	X	
423733097500	30.657999	-94.897411	4/6	D-D'/6	Prime Oprtg	Stephens	Polk	TX	X	
423730035900	30.577903	-94.832708	4/7		Continental	Carter, W.T.	Polk	TX	X	
422910018900	30.428207	-94.768905	4/8		Texam O&G	Garner, A.	Liberty	TX	X	
422910022100	30.326809	-94.765703	4/9	C-C'/6	Atlantic Refg	Nona Mills	Liberty	TX		
422910032500	30.26171	-94.678899	4/10		Texas Co.	Tortoris	Liberty	TX		
422910180200	30.149012	-94.654098	4/11		Mecom, J.W.	White	Liberty	TX	X	
422910167000	30.063514	-94.616996	4/12		Mecom, J.W.	Haas	Liberty	TX		
422910476500	29.920818	-94.575794	4/13	B-B'/6	Harrison, D.J. Jr.	Rich, J.M. etal	Liberty	TX		
420713130200	29.833221	-94.495291	4/14		HNG Fossil Fuels	Devilier, O.C.	Chambers	TX	X	
420710217700	29.744923	-94.46989	4/15		Meredith & Co.	Tyrrell Dubois	Chambers	TX	X	
427080002200	29.499531	-94.383388	4/16		British American Pdn	SL 52155 Blk 27-L	Offshore-Galveston	TX		
427083033200	29.452232	-94.325086	4/16A	A-A'/4	ANR Production	SL 56-L	Offshore-Galveston	TX		
424710019900	31.044084	-95.44612	5/0		Deupree, S.J.	Texas Longleaf Lbr Co	Walker	TX	X	
424710001400	30.925287	-95.439319	5/1		Union Pdeg	Smither	Walker	TX	X	
424710009700	30.842089	-95.355018	5/2		Humble O&R	Gibbs Bros &Co	Walker	TX	X	
4-6	30.864588	-95.352918	5/2A		Tidewater	Newman, A.D. Un	Walker	TX	X	
424070012700	30.715893	-95.279318	5/3		Stanolind	Carey Ld &	San Jacinto	TX	X	
424073003300	30.622197	-95.247717	5/4		Glen Rose	Gary Hrs	San Jacinto	TX	X	
424073007800	30.546301	-95.163716	5/4.5	D-D'/5	Houston Pet	Childerss, D. un	San Jacinto	TX	X	
424070015600	30.457705	-95.175215	5/5		Amerada	Foster Lbr	San Jacinto	TX	X	
424070021400	30.393207	-95.145013	5/6		Amerada - Mid States	Central Coal & Coke	San Jacinto	TX	X	
4-12	30.361108	-95.112212	5/6.5		Mitchell & Assoc	Cherry, H.R.	Liberty	TX	X	
422910391400	29.973819	-94.965604	5/?		General Crude	Davis	Liberty	TX		
422910008600	30.30651	-95.05961	5/7		Karsten (Shell)	Grogan	Liberty	TX	X	
4-13	30.281911	-95.11541	5/7A		Superior	Hightower, T.J.	Liberty	TX	X	
422910501800	30.249512	-95.042408	5/8	C-C'/5	Humble O&R	Quinn, R.E.	Liberty	TX	X	
422913252800	29.923718	-94.455391	5/?	B-B'/7	Rising Star En	Aldrich, R.C. &c	Liberty	TX		
422910388000	30.080816	-95.026806	5/9		W.H. Hunt Tr Est	Simmons	Liberty	TX	X	
422910391400	29.973819	-94.965604	5/10N		Amerada	Brown, R.C.	Liberty	TX		

Final Report – Updating the Hydrogeologic Framework for the Northern Portion of the Gulf Coast Aquifer

API number or ID	NAD27 latitude	NAD27 longitude	Dip section/ position	Strike section/ position	Company	Lease	County	State	Lithology and water qual data	Paleo Data
422910438400	29.943119	-94.893102	5/11		General Crude	Moore's Bluff	Liberty	TX	X	
420710022600	29.862822	-94.900203	5/12		Sunray-MidContinent	Barber	Chambers	TX	X	
4-18	29.867121	-94.868302	5/12N		Halbouty	Wilburn, E.	Chambers	TX	X	
420713145800	29.813022	-94.830601	5/13	B-B'/5	Texas Crude	Weakley, C.L.	Chambers	TX	X	
420710097200	29.756924	-94.8218	5/14		Humble O&R	Cton Lake S GU 1	Chambers	TX	X	
420710269600	29.685825	-94.790099	5/15		Continental	ST 2-3A	Offshore-	TX	X	
420710274000	29.641026	-94.754697	5/16		Humble O&R	State 'Q'	Offshore-	TX	X	
420710246600	29.597328	-94.713596	5/17		Humble O&R	Mayes, M.E.	Chambers	TX	X	
420710243200	29.566429	-94.718696	5/18		Humble O&R	Mayes, M.E.	Chambers	TX	X	
421670095600	29.464232	-94.726495	5/19		Std of Texas		Offshore-	TX	X	
421670095900	29.445733	-94.675894	5/20		Abercrombie	Boyt, E.W.	Galveston	TX		
427063011100	29.274738	-94.657992	5/21				Offshore-Galveston	TX		
427063004200	29.249039	-94.642192	5/21.5	A-A'/2	GMA Offshore	ST 150-L	Offshore-Galveston	TX		
427084042900	28.752051	-94.250678	5/26		Pogo Pdcg	G-15787 HI A-94	Offshore-Galveston	TX	X	
424713002200	30.760393	-95.766626	6/1		Moran	Gibbs Bros	Walker	TX	X	
424710014800	30.6995	-95.7391	6/2		Markle, C.W. etal	Davis, T.H.	Walker	TX	X	
424710018000	30.646896	-95.634623	6/3		Marr, M.H. & Moran	Ward, K.	Walker	TX	X	
424710018900	30.564399	-95.572922	6/4		Moran	Central Coal & Coke	Walker	TX	X	
423390086800	30.447704	-95.51382	6/5		Superior - Speed, C.C.	Sykes, J.B.	Montgomery	TX	X	
423390090100	30.396606	-95.50602	6/6	D-D'/3	Sunray - Atascosa Drlg	M. Sykes	Montgomery	TX	X	
423390008600	30.363808	-95.452718	6/7	D-D'/4	Atascosa Drlg	Foster, T.S. Est.	Montgomery	TX	X	
423390020200	30.287211	-95.451618	6/8		Humble O&R	Grand Lake GU 2	Montgomery	TX	X	
423393082000	30.228114	-95.374715	6/9		Exxon	Conroe Fld Un	Montgomery	TX	X	
423390171800	30.147717	-95.291713	6/10		Humble O&R	Wickizer, W.W.	Montgomery	TX	X	
423393073700	30.13757	-95.3385	6/10A		Murexco Pet	Bahr, C.	Montgomery	TX		
422010760300	30.032119	-95.22571	6/11	C-C'/4	Humble O&R	Foster Lbr Co	Harris	TX	X	
422010272200	29.954921	-95.181809	6/12		Wrightsman, C.B.	Harris Co Land Impvmt	Harris	TX	X	
422013203800	29.89637	-95.16442	6/12.5		Sanchez-O'Brien Oil	King	Harris	TX		
422010280100	29.812925	-95.122709	6/13		Republic Nat Gas	Hornberger, J. etal	Harris	TX		
422013261300	29.743928	-95.15611	6/14		Ballard Expl	Houston Ship Chnl Un	Harris	TX		
422010604400	29.632629	-95.047307	6/15	B-B'/4	Humble O&R	Humble West Fee	Harris	TX	X	
420710309600	29.556929	-94.968804	6/16		Humble O&R	Galveston Bay State R	Offshore-Galveston	TX	X	
421670096600	29.434832	-94.912101	6/17		Apache	Dollar Bay Fig	Galveston	TX	X	
421673009100	29.295837	-94.820197	6/18		Mitchell & Assoc	Galveston Twst Un 4	Galveston	TX	X	
427064038000	29.126042	-94.666792	6/19		Seneca Res	OCS-G-6094	Offshore-Galveston	TX	X	
427064044600	28.885648	-94.564789	6/21		APEX O&G	OCS-G-26477	Offshore-Galveston	TX	X	

Final Report – Updating the Hydrogeologic Framework for the Northern Portion of the Gulf Coast Aquifer

API number or ID	NAD27 latitude	NAD27 longitude	Dip section/ position	Strike section/ position	Company	Lease	County	State	Lithology and water qual data	Paleo Data
427084027900	28.80625	-94.448685	6/22		Union Pacific Res	OCS-G-6189	Offshore-Galveston	TX	X	
421850006100	30.589399	-96.040033	7/1		Cooper	Freund	Grimes	TX	X	
421850003400	30.504402	-95.994732	7/2		Exeter Oil	Bradley, I.P.	Grimes	TX	X	
421850015000	30.372007	-95.91223	7/3		Murdick, C.H.	Stoneham	Grimes	TX	X	
421853032100	30.34795	-95.95787	7/3A		J-O'B Oprtg	Law, T.M.	Grimes	TX		
421853000900	30.26691	-95.856629	7/4		Lone Star Pdcg	Goforth	Grimes	TX	X	
424733006600	30.215512	-95.811328	7/5	D-D'/2	High Chapparel Oil	Sabine Rylty	Waller	TX	X	
423390101400	30.133016	-95.751326	7/6		Stanolind	Nichols, H.C.	Montgomery	TX	X	
423393085200	30.109017	-95.703924	7/7		Ultramar O&G	Bayer, G.	Montgomery	TX	X	
422010004800	30.082518	-95.687924	7/8		Humble O&R	Krug, T.	Harris	TX	X	
422010010400	30.066219	-95.678724	7/9		Humble O&R	Theeck, H.	Harris	TX	X	
422013140000	30.0266	-95.64415	7/9.2		Stone & Webster (Jackson Expl)	Klores GU	Harris	TX		
422013167000	29.92215	-95.577	7/9.7		Outline Oil	Northwest Fwy Investors	Harris	TX		
422013162200	29.895225	-95.508919	7/10	C-C'/3	Mahada En	Foley, B.	Harris	TX	X	
422010345500	29.867925	-95.489319	7/10.5		Production Maintenance	Rowsky unit	Harris	TX	X	
422010790400	29.850626	-95.53302	7/10.5A	C-C'/2	Pan American	Houston Un N-6W-10	Harris	TX	X	
422010351000	29.786928	-95.450218	7/11		Sparta Oil	Suttles, J.H. etal	Harris	TX	X	
422010505800	29.655431	-95.398617	7/12		Gulf	Taylor, E.R.	Harris	TX	X	
422013001600	29.66793	-95.246613	7/12N	B-B'/2	Pan American	DrIDist 25	Harris	TX	X	
422010556800	29.626632	-95.304215	7/13		Smith, R.E.	Smith	Harris	TX	X	
422010611400	29.568033	-95.242513	7/14	B-B'/3	Seaboard	Allison, R.H.	Harris	TX		
421670003500	29.521834	-95.216012	7/14.5		Stanolind	Brown, C.	Galveston	TX	X	
420390084700	29.454135	-95.230312	7/15		Placid Oil	Neubauer Hrs	Brazoria	TX		
421670187600	29.404235	-95.163009	7/16		Humble O&R	Algoa Twst	Galveston	TX	X	
421670145300	29.371335	-95.111407	7/17		Hunt, H.L.	Hervey, H.P. et al	Galveston	TX	X	
421670144800	29.334736	-95.082406	7/18		Hunt, H. Tr.	Jensen, M. etal Un	Galveston	TX	X	
421670133600	29.302337	-95.066805	7/19		Texas Eastern Tsmns	Craig	Galveston	TX	X	
421673003900	29.251638	-95.048003	7/20		Mobil Oil	Halls Bayou Ranch	Galveston	TX	X	
421670191600	29.208139	-94.9421	7/20.5		Humble O&R	William Meyer, W.	Galveston	TX	X	
427060008600	29.069443	-94.9176	7/21	A-A'/1	Shell	ST 220-L S.W.	Offshore-Galveston	TX	X	
427060002700	28.982246	-94.867098	7/22		Humble O&R	Blk 253	Offshore-Galveston	TX	X	
427060012400	28.852149	-94.724694	7/23		Shell	Blk 288 Un 96-14	Offshore-Galveston	TX	X	
427064009700	28.766251	-94.641892	7/24		Sohio	OCS G 5179	Offshore-Galveston	TX		
424773062500	30.3299	-96.3944	8/1		Houston, W.S. O&G	CG & HD	Washington	TX		
424770023900	30.260212	-96.400644	8/2		Texas-Harvey Oil	Dallas, F.W.	Washington	TX		
424770027200	30.183115	-96.25494	8/3		Union Sulphur	Kubecza, J.	Washington	TX		

Final Report – Updating the Hydrogeologic Framework for the Northern Portion of the Gulf Coast Aquifer

API number or ID	NAD27 latitude	NAD27 longitude	Dip section/ position	Strike section/ position	Company	Lease	County	State	Lithology and water qual data	Paleo Data
424770029400	30.097419	-96.253741	8/4		Magnolia Pet	Giddings Est	Washington	TX		
420153013800	30.0461	-96.2014	8/4.5		Prairie - Convest	O'Reed Lange etal	Austin	TX		
424730024300	29.9796	-96.0928	8/6		Humble O&R	Hardy, R. 'B'	Waller	TX		
424730031800	29.905526	-95.931732	8/7		Halbouty, M.T.	Harris, J.W. etal	Waller	TX		
420390422400	29.23448	-95.41405	8/14		Humble O&R	Moore, H.	Brazoria	TX		
427060002200	28.9094	-95.1847	8/17		Humble O&R	ST 278-L	Offshore-Galveston	TX		
420150001700	30.008422	-96.449247	9/1		Dakamont Expl	Weise	Austin	TX		
420153053900	29.91718	-96.40987	9/2		Superior	Woods Pet GU 2	Austin	TX		
420150066300	29.8287	-96.2879	9/3		Texas Co	Kollatschny, P.	Austin	TX		
420150026200	29.7606	-96.2016	9/4		Magnum Pdcg (Shell)	Hillboldt, D.C.	Austin	TX		
420150068300	29.6384	-96.1186	9/5		Southern Nat Gas	Uhyrek, F.	Austin	TX		
421573175200	29.5326	-96.0187	9/7		Thompson (Phillips)	Oldag	Fort Bend	TX		
421570167400	29.3212	-95.8488	9/9		Howell, H.H. & Cook	Armstrong, G.W.	Fort Bend	TX		
420390271500	29.2703	-95.7585	9/10		Progress Pet	Gulf Fdn	Brazoria	TX		
420390389800	29.0782	-95.608	9/13		Pan American	Hobbs, I.	Brazoria	TX		
420393035000	28.9813	-95.5783	9/14		Dow Chemical	Bute, J.	Brazoria	TX		
420393211000	28.97789	-95.46545	9/15		BHP Pet (Monsanto)	Beretta, M.A.	Brazoria	TX		
420390481100	28.89909	-95.39908	9/16		Humble O&R	Freeport Sulphur A/C-1	Brazoria	TX		
427064036000	28.5853	-95.1058	9/17		Seagull En	Galveston 392	Offshore-Galveston	TX		
421493208800	30.0748	-96.8488	10/1		GSI	Scht-Rogers	Fayette	TX		
424813403300	29.2858	-96.1627	10/11		Carrizo O&G	McMillan	Wharton	TX		
424810256200	29.15604	-96.01046	10/13		Flaitz & Mitchell (Humble)	Cockburn, H.C.	Wharton	TX		
422310067000	0	0	10/15		Brazos O&G	Findley Est	Matagorda	TX		
427043007300	28.7159	-95.5428	10/18		Corpus Christi O&G	ST 369-L	Offshore-Matagorda	TX		
427043000500	28.443	-95.501	10/20		Forest	Brazos 470	Offshore-Matagorda	TX		
420893145600	29.66568	-96.74452	11/3		Quamagra Ints	Weimar GU	Colorado	TX		
420893163900	29.6296	-96.6908	11/4		McRae-Fleming Ents	Miller, A.L., etal	Colorado	TX		
420893173400	29.54227	-96.58537	11/5		Property Pdcg	Burkitt Fdn	Colorado	TX		
420893215800	29.4341	-96.5178	11/7		Walter O&G	Lehrer 'A'	Colorado	TX		
420890075900	29.4161	-96.4716	11/8		Hamill, C.B. (Shell)	Schiurring, C.R.	Colorado	TX		
424813369000	29.32463	-96.39645	11/10		Talon Dev	Naiser	Wharton	TX		
424810357500	29.1611	-96.1883	11/13		Caribbean Oil	Kluck, A.	Wharton	TX		
424810236800	0	0	11/13.3		Wheelock & Collins	Carville-Humphrey	Wharton	TX		
6663901	0	0	11/14		H.H. Johnson	ww	0	TX		
423210274100	29.02391	-96.10442	11/14.3		Viking Drlg & Pace	Camp, J.	Matagorda	TX		
423210268900	28.8778	-96.0289	11/16		Continental	Fondren, W.W., Jr.	Matagorda	TX		

Final Report – Updating the Hydrogeologic Framework for the Northern Portion of the Gulf Coast Aquifer

API number or ID	NAD27 latitude	NAD27 longitude	Dip section/ position	Strike section/ position	Company	Lease	County	State	Lithology and water qual data	Paleo Data
423210114700	28.8737	-95.9648	11/17		Michael, J.S.	O. Vaughn etal	Matagorda	TX		
426040001200	28.6146	-95.858	11/19		Shell	ST 519-S	Offshore-Matagorda	TX		
427040000700	28.5545	-95.8149	11/20		Shell	ST 440-L NE(W)	Offshore-Matagorda	TX		
5-6	30.901089	-95.644723			Humble O&R	Gibbs Bros	Walker	TX	X	
4-7	30.699994	-95.44792			Marr - Moran	Gibbs Bros	Walker	TX	X	
424713023200	30.5461	-95.357919			Getty Oil	Kelland, T.W.	Walker	TX	X	
6038102	30.4633	-95.3606			Transtate (Keeble)	Foster Est	Montgomery	TX	X	
4-10	30.433905	-95.371918			Moran	Browder	Montgomery	TX	X	
423390187200	30.316511	-95.297015			Texaco	Griffin, D.D.	Montgomery	TX	X	
423390184100	30.192315	-95.16951			Humble O&R	Patton H.L.	Montgomery	TX	X	
422013095800	30.067317	-95.131408			Hester, B.M.	Hirsch, M.	Harris	TX	X	
422010106500	30.028418	-95.089407			Placid Oil	Smith, Mrs. D.F.	Harris	TX	X	
422010265800	29.96442	-95.080607			Texas Co.	Peterson, T.	Harris	TX	X	
6026801	30.5408	-95.8078			Robinson Oil	Walker, L.M.	Montgomery	TX	X	
423390099800	30.461603	-95.798227			Thompson, W.J.	Olson, G.	Montgomery	TX	X	
6043101	30.3647	-95.725			Garvey, O.C.	Martin	Montgomery	TX	X	
423390188700	30.327809	-95.621022			Socony-Mobil Oil	Sealy-Smith Fdn	Montgomery	TX	X	
6052601	30.175	-95.5197			Boyle, W.S.	First National Bank	Montgomery	TX	X	
422013218700	30.093418	-95.518619			Brown, G.R. Ptnrs	Hildebrandt, P.	Harris	TX	X	
422010325200	29.944623	-95.403416			Humble O&R	Polemanakos, A.O.	Harris	TX	X	
422010293600	29.781327	-95.250013			Stanolind O&G	Oates	Harris	TX	X	
422013136800	29.597031	-95.169711			Cavalla En Expl	Eliington AFB	Harris	TX	X	
420513095000	#N/A	#N/A			Daleco Res	Moore, J.	Burleson	TX	X	
7-2	#N/A	#N/A			Phillips Pet	Renchie	Brazos	TX	X	
424553040100	31.031384	-95.364218			Wagner & Brown	Champion Paper	Trinity	TX	X	
424553002300	#N/A	#N/A			Hunt Oil	Hoyt Moore	Trinity	TX	X	
421853002800	30.475903	-95.882129			Victory Pet	Bevans, W.A.	Grimes	TX	X	
423390099800	30.461603	-95.798227			Thompson, W.J.	Olson, G.	Montgomery	TX	X	
424713001600	30.565199	-95.635223			Lone Star Pdcg	Central Coal & Coke	Walker	TX	X	
424070029000	30.79899	-95.191716			Sparta Oil - Thomas Concrete Pipe	Carey & Haley	San Jacinto	TX	X	
6-7	30.191014	-95.87083			Texas Co.	Rice Institute	Waller	TX	X	
423393047800	30.27661	-95.701924			Southland Rylyt	Dean, L.	Montgomery	TX	X	
423390188700	30.327809	-95.621022			Socony-Mobil Oil	Sealy-Smith Fdn	Montgomery	TX	X	
6036904	30.3914	-95.5097			Sunray - Atascosa	Sykes, M.	Montgomery	TX	X	
6037803	30.4061	-95.4447			Wommack, M.K.	Hunt	Montgomery	TX	X	
423390004500	30.463004	-95.374018			Phillips Pet	Fraser	Montgomery	TX	X	

Final Report – Updating the Hydrogeologic Framework for the Northern Portion of the Gulf Coast Aquifer

API number or ID	NAD27 latitude	NAD27 longitude	Dip section/ position	Strike section/ position	Company	Lease	County	State	Lithology and water qual data	Paleo Data
4-9	30.519402	-95.308618			Barnes, J.C.	Johnson	San Jacinto	TX	X	
423730003700	30.685895	-95.017814			HT&B Oil	Brook, Jett	Polk	TX	X	
422013218700	30.093418	-95.518619			Brown, G.R. Ptnrs	Hildebrandt, P.	Harris	TX	X	
6053810	30.1553	-95.4567			Coffey, C.W. etal	Baldwin Bros	Montgomery	TX	X	
423390160400	30.241214	-95.281713			Atlantic Refg	So.Tx. Dev.	Montgomery	TX	X	
6046604	30.3028	-95.2731			Hankamer, C.	Forman	Montgomery	TX	X	
6047404	30.2931	-95.2142			Gray, J.A.	Foster Lbr Co	Montgomery	TX	X	
6047604	30.3211	-95.1642			Amerada	Foster Lbr Co	Montgomery	TX	X	
424070024100	30.441405	-95.051312			Jordan Drlg	Hoard, S.E.	San Jacinto	TX	X	
422010439500	29.74233	-95.325025			Magnolia Pet	Allen, E.W., Hrs	Harris	TX	X	
422010800701	29.809028	-95.604922			Pan American Pet	Miles, L.L.	Harris	TX	X	
6-12	29.856126	-95.54122			Pan American Pet	Houston Unit N-6W-10	Harris	TX	X	
422010334300	29.917124	-95.450517			Union Pdcg	Allen, N.S.	Harris	TX	X	
422010325200	29.944623	-95.403416			Humble O&R	Polemanakos, A.O.	Harris	TX	X	
422010297200	29.961222	-95.359714			Union Pdcg	Deutzer	Harris	TX	X	
422013095800	30.067317	-95.131408			Hester, B.M.	Hirsch, M.	Harris	TX	X	
422910243100	30.226012	-94.964006			Acorn Oil	Berry, C.C.	Liberty	TX	X	
422910016800	30.270112	-95.10641			Superior	Hightower, T.J.	Liberty	TX	X	
6036904	30.3914	-95.5097			Sunray - Atascosa Drlg	M. Sykes	Montgomery	TX	X	
6043101	30.3647	-95.725			Garvey, O.C.	Martin	Montgomery	TX	X	
6043304	30.3594	-95.6433			Callery	Weisinger	Montgomery	TX	X	
6044101	30.3678	-95.5883			Wood, T.J.	Fultz	Montgomery	TX	X	
6036904	30.3914	-95.5097			Sunray - Atascosa	Sykes, M.	Montgomery	TX	X	
6037803	30.4061	-95.4447			Wommack, M.K.	Todd	Montgomery	TX	X	
6038102	30.4633	-95.3606			Transtate (Keeble)	Foster Est	Montgomery	TX	X	
6052704	30.1397	-95.6156			Christie-Mitchell	Neidxxx	Montgomery	TX	X	
6052601	30.175	-95.5197			Boyle, W.S.	First National Bank	Montgomery	TX	X	
6053105	30.2189	-95.4794			Winmill, B.S.	Yost, F.M. etal	Montgomery	TX	X	
6045904	30.2825	-95.405			Humble O&R	So.Tex.Dev.Co.	Montgomery	TX	X	
6046504	30.2925	-95.3283			Humble O&R	Emory, M.	Montgomery	TX	X	
6046604	30.3028	-95.2731			Hankamer, C.	Forman	Montgomery	TX	X	
6047404	30.2931	-95.2142			Gray, J.A.	Foster Lbr Co	Montgomery	TX	X	
6047604	30.3211	-95.1642			Amerada	Foster Lbr Co	Montgomery	TX	X	
6036304	30.475	-95.5292			Hanslip, C.W.	Crawford	Montgomery	TX	X	
6037803	30.4061	-95.4447			Wommack, M.K.	Hunt	Montgomery	TX	X	
6045302	30.3736	-95.3936			Womack, M.K. etal	Hutchings Sealy NB Tr	Montgomery	TX	X	

Final Report – Updating the Hydrogeologic Framework for the Northern Portion of the Gulf Coast Aquifer

API number or ID	NAD27 latitude	NAD27 longitude	Dip section/ position	Strike section/ position	Company	Lease	County	State	Lithology and water qual data	Paleo Data
6046504	30.2925	-95.3283			Humble O&R	Emory, M.	Montgomery	TX	X	
6054302	30.2353	-95.2783			Atlantic Refg	So.Tx. Dev.	Montgomery	TX	X	
6062301	30.1236	-95.2689			C.R. XXXX	C.G.H.Pm.	Montgomery	TX	X	
6026801	30.5408	-95.8078			Robinson Oil	Walker, L.M.	Montgomery	TX	X	
6035203	30.4725	-95.695			Red Bank	Central Coal & Coke	Montgomery	TX	X	
6036403	30.4508	-95.6192			Strum & Womack	Foster Est	Montgomery	TX	X	
6044101	30.3678	-95.5883			Wood, T.J.	Fultz	Montgomery	TX	X	
6044507	30.3172	-95.5622			Fish G&O	Berkley & Hogg	Montgomery	TX	X	
6053105	30.2189	-95.4794			Winmill, B.S.	Yost, F.M. etal	Montgomery	TX	X	
6053810	30.1553	-95.4567			Coffey, C.W. etal	Baldwin Bros	Montgomery	TX	X	
424713019200	30.5414	-95.60509			K & A, INC.	CENTRAL COAL & COKE CORPORATION	Walker	TX	X	
422013079800	30.00976	-95.24512			IPACT	STERLING REFERN FEE	Harris	TX	X	
424713020200	30.723893	-95.47632			SMALL, R.P. CORP.	TIPCO-GIBBS	Walker	TX	X	
422413030800	30.847301	-94.027888			KELLY-BROCK	RHODES, A. B. ET AL	Jasper	TX	X	
422010360700	29.899024	-95.502919			OSBORN,W.B. OIL & GAS OPERATIONS	GOODYGOONTZ "A"	Harris	TX	X	
423213095400	-32.248237	-110.021939			HOUSTON OIL & MINERALS CORP.	RUNNELLS-PIERCE RANCH	Offshore-	TX	X	
423213096100	28.56616	-96.220829			EXXON CORP.	OYSTER LAKE TEMPORARY GAS UNIT	Offshore-Matagorda	TX	X	
421853024100	30.29843	-95.94173			SIDELINE ENERGY INC.	WILLIAM GARDNER	Grimes	TX	X	
421573115200	29.465537	-95.47002			ARCO OIL & GAS CO.	FUQUA INDUSTRIES	Fort Bend	TX	X	
423733050500	30.513305	-94.795107			ADA OIL EXPLORATION CORP.	RACKI	Polk	TX	X	
424713023600	30.72912	-95.49477			ELF AQUITAINE, INC.	GIBBS BROTHERS	Walker	TX	X	
424073045300	30.280206	-95.201538			HOUSTON PETROLEUM COMPANY	U.S.A.	San Jacinto	TX	X	
424073046800	30.55154	-95.12888			COASTAL OIL & GAS CORPORATION	FOSTER MINERALS	San Jacinto	TX	X	
424733037900	30.257853	-95.854708			HIGH CHAPPARAL OIL COMPANY	COWAN-ZOLLMAN-HIGH CHAPPARAL	Waller	TX	X	
423393055300	30.50246	-95.66979			HNG FOSSIL FUELS COMPANY	CENTRAL COAL AND COKE	Montgomery	TX	X	
422013150600	30.02471	-95.90904			LEONARD, J. A.	MATHIS, T. F. JR. ET AL	Harris	TX	X	
421993181600	30.408108	-94.296089			CONOCO INC.	STERNENBERG-PETTY	Hardin	TX	X	
423393056600	30.396607	-95.404018			TXO PRODUCTION CORP.	SEALY	Montgomery	TX	X	
424713024500	30.67368	-95.46794			MCMORAN EXPLORATION CO.	GIBBS BROTHERS	Walker	TX	X	
421853034000	30.41492	-96.01111			OUTLINE OIL CORP.	REUL	Grimes	TX	X	



Final Report – Updating the Hydrogeologic Framework for the Northern Portion of the Gulf Coast Aquifer

API number or ID	NAD27 latitude	NAD27 longitude	Dip section/ position	Strike section/ position	Company	Lease	County	State	Lithology and water qual data	Paleo Data
424073048000	30.51637	-95.23361			OUTLINE OIL CORP.	ELDRIDGE	San Jacinto	TX	X	
420053017400	31.238486	-94.833309			SANTA FE MINERALS, INC.	SANTA FE MINERALS	Angelina	TX	X	
421853036900	30.54704	-95.87937			ARCO OIL & GAS CO.	ASHORN, CHARLIE	Grimes	TX	X	
424713025100	30.66139	-95.42117			WHEELER OPERATING CORP.	AMERADA-RILEY	Walker	TX	X	
421853038400	30.50802	-95.89867			ENERVEST OPERATING, L.L.C.	APOLONIA	Grimes	TX	X	
422013196200	30.06667	-95.62823			TORTUGA OPERATING COMPANY	LEWIS, SAM	Harris	TX	X	
423213148800	28.527008	-96.269544			CORPUS CHRISTI OIL & GAS CO.	STATE TRACT 210	Offshore-Matagorda	TX	X	
421853039900	30.26982	-95.92846			MAGNOLIA ENERGY CO.	CAREY & COROLLA	Grimes	TX	X	
422013205200	29.901123	-95.285812			MARSHALL, A. B.	MARSHALL, A. B. FEE	Harris	TX	X	
422013206200	29.88459	-95.25546			SONORA PETROLEUM CORP.	FULBRIGHT UNIT	Harris	TX	X	
423393077700	30.24002	-95.33677			WAPITI OPERATING, LLC	CONROE FIELD UNIT	Montgomery	TX	X	
423393079400	30.139081	-95.380093			DENBURY ONSHORE, LLC	CONROE FIELD UNIT	Montgomery	TX	X	
422413048700	30.8978	-94.142191			D.J. OILFIELD SALVAGE INC.	CAMERON HEIRS	Jasper	TX	X	
424573042600	31.026194	-94.454501			PECOS PETROLEUM COMPANY	CLARA S. GRISWOLD UNIT	Tyler	TX	X	
421853041900	30.545216	-96.086441			INTERREGIONAL OPERATING SERVICES	JBW-TMPA	Grimes	TX	X	
421853042300	30.51393	-95.18978			COLUMBIA GAS DEVELOPMENT CORP.	UNION FEE	Grimes	TX	X	
423393084900	30.15391	-95.14753			RODEL OIL & GAS COMPANY	BURKETT	Montgomery	TX	X	
423733077700	31.127688	-94.825409			MCBEE COMPANY, THE	CHAMPION INTERNATIONAL	Polk	TX	X	
422013226500	29.9971	-95.0853			NORDSTRAND ENGINEERING, INC.	THARP, KATHLEEN	Harris	TX	X	
421570100400	29.739831	-95.819129			WESTERN GAS RESOURCES STORAGE	BURNEY - UNION	Fort Bend	TX	X	
422413054500	30.585505	-93.991983			ARCO OIL & GAS CO.	ARCO FTD	Jasper	TX	X	
420393250100	29.504836	-95.385117			ARCO OIL & GAS COMPANY	ALBAN FAMILY TRUST	Brazoria	TX	X	
422013236800	29.94331	-95.85063			LONE WOLF OPERATING COMPANY	WARREN RANCH	Harris	TX	X	
422013237500	29.9675	-95.68549			CARNEGIE FINANCIAL CORP.	KITZMANN, J.A.	Harris	TX	X	
423733084000	30.869396	-94.704507			LAKE RONEL OIL COMPANY	ARMADILLO-CARTER, W. T. & BROS.	Polk	TX	X	
421993275400	30.316009	-94.589698			CHEVRON U. S. A. INC.	STONEHILL	Hardin	TX	X	
421573200700	29.459439	-95.562622			JETTA OPERATING COMPANY, INC.	MYERS, A. E.	Fort Bend	TX	X	

Final Report – Updating the Hydrogeologic Framework for the Northern Portion of the Gulf Coast Aquifer

API number or ID	NAD27 latitude	NAD27 longitude	Dip section/ position	Strike section/ position	Company	Lease	County	State	Lithology and water qual data	Paleo Data
424033043600	31.192991	-94.03259			SONERRA RESOURCES CORPORATION	COUNTY LINE	Sabine	TX	X	
427083010100	29.365236	-94.476089			WHITING OIL AND GAS CORPORATION	STATE TRACT 98-L	Offshore-Galveston	TX	X	
420390171100	29.26324	-95.348114			KILMARNOCK OIL COMPANY, INC.	JAMISON, THOS.	Brazoria	TX	X	
424573012100	30.751802	-94.422998			SOUTHERN BAY OPERATING, L.L.C.	CRUSE, C.L.	Tyler	TX	X	
424570020000	30.560406	-94.357193			MILESTONE OPERATING, INC.	EAST TEXAS OIL CO. FEE - G-	Tyler	TX	X	
424713001400	30.541636	-95.606049			MORAN CORPORATION, THE	CENTRAL COAL & COKE	Walker	TX	X	
422910029400	30.366608	-94.953708			ENERGY RESERVES GROUP, INC.	EAST MCCOY GAS UNIT NO. 1	Liberty	TX	X	
423393007200	30.293009	-95.784627			MCCARTHY, GLENN H.	GREGG, SAUNDERS, ET AL	Montgomery	TX	X	
423390110900	30.223013	-95.545619			AXIS ENERGY CORPORATION	ARCENAU, INA	Montgomery	TX	X	
422010394800	29.910524	-95.662123			EXXON CORP.	BISHOP, L.	Harris	TX	X	
420410006800	30.466404	-96.216037			PHILLIPS PET	D B SCHOEPS	Brazos	TX	X	
421570003000	29.76083	-95.780227			UNION PROD	ROESNER	Fort Bend	TX	X	
422410020500	30.426107	-94.083982			GULF OIL CORP.-KILGORE	TEMPLE LUMBER CO., ET AL	Jasper	TX	X	
422910371100	30.010416	-94.7825			TEXAS	CLIFF TEVIS	Liberty	TX	X	
423733021600	30.820197	-94.749508			DEVON ENERGY PRODUCTION CO, L.P.	PARRISH ET AL	Polk	TX	X	
423510042500	31.070093	-93.670377			PAN AMERICAN PET. CORP.		Newton	TX	X	
424573013000	30.949796	-94.446			HUNT OIL	TAPSCOTT	Tyler	TX	X	
422450054100	30.058614	-94.196283			HUMBLE OIL	TYRELL COMBEST RLTY	Jefferson	TX	X	
422910033300	30.052214	-94.489793			HUMBLE OIL	PICKETT MARY E	Liberty	TX	X	
424073001800	30.433606	-95.240116			FAMCOR OIL, INC.	MAYS HEIRS	San Jacinto	TX	X	
424570005700	30.853	-94.355297			PAN AMERICAN PETROLEUM CORP.		Tyler	TX	X	
424710011600	30.86409	-95.616722					Walker	TX	X	
424713029500	30.537856	-95.547261			ICARUS OPERATING CORPORATION	SAM	Walker	TX	X	
423613079100	30.154511	-93.977475			SAMEDAN OIL CORPORATION	MIL-VID WILLIAMS UNIT	Orange	TX	X	
420390451800	29.075243	-95.18951			AMERADA HESS	SHANNON GEORGIA S	Brazoria	TX	X	
422910453700	29.907119	-94.656996			HUMBLE OIL	ROBERTSON-MCDONAL	Liberty	TX	X	
421670127600	29.479334	-95.16351			FIDELITY OIL & RAYALTY	PUTE RANCH	Galveston	TX	X	
420710108300	29.883119	-94.712797			BRITISH AMERICAN OIL COMPANY	CLIVE SHERMAN	Chambers	TX	X	

Final Report – Updating the Hydrogeologic Framework for the Northern Portion of the Gulf Coast Aquifer

API number or ID	NAD27 latitude	NAD27 longitude	Dip section/ position	Strike section/ position	Company	Lease	County	State	Lithology and water qual data	Paleo Data
422910028400	30.29991	-94.880505			GENERAL CRUDE OIL	DAVIS HILL	Liberty	TX	X	
421573039600	29.613835	-95.703826					Fort Bend	TX	X	
420390142000	29.365639	-95.378416			HUMBLE OIL	BELSLEY M E ETAL	Brazoria	TX	X	
420710251300	29.675126	-94.601894			PLACID OIL	BERTHA N JACKSON	Chambers	TX	X	
423610048000	30.080611	-93.805569			PAN AMERICAN PETROLEUM CORP.	BROWN ETAL H L	Orange	TX	X	
421673025300	29.448534	-95.129509			WESLEY WEST		Galveston	TX	X	
420150014600	30.017122	-96.100237					Austin	TX	X	
422450150100	29.920114	-93.974272			CLEGG & HUNT	C DOORBOS	Jefferson	TX	X	
420710306200	29.655928	-94.953004			HUMBLE OIL	CEDAR POINT-STATE	Offshore-Harris	TX	X	
420710120900	29.801621	-94.634395			PETROLEUM DEV ASSOC	STANDLEY FRED	Chambers	TX	X	
422910210400	30.105214	-94.729099			HUNT OIL	A S J STEVENSON	Liberty	TX	X	
421990061800	30.488807	-94.425094			SHELL OIL	KIRBY LUMBER CO	Hardin	TX	X	
424713030400	30.671547	-95.602145			PRIME OPERATING COMPANY	GIBBS GAS UNIT	Walker	TX	X	
424713030500	30.724125	-95.439104			FORTUNE NATURAL RESOURCES CORP.	READER	Walker	TX	X	
424573063000	#N/A	#N/A			SOUTHERN BAY OPERATING, L.L.C.	BSMC GOODE	Tyler	TX	X	
422450131800	30.010514	-94.067478			HUMBLE OIL & REF. COMPANY		Jefferson	TX	X	
423730001000	30.996089	-94.859209					Polk	TX	X	
427083038100	29.454931	-94.247684			SANTOS USA CORP.	S.T. 54-L	Offshore-Jefferson	TX	X	
422010789200	30.078919	-95.88443			ROYIS WARD		Harris	TX	X	
422410030000	30.460506	-93.959479			NECHES EXPLORATION, INC.		Jasper	TX	X	
423510016700	30.688202	-93.665375			HUMBLE OIL AND REFINING COMPANY		Newton	TX	X	
423733009100	30.687201	-94.721807			HASSIE HUNT TRUST		Polk	TX	X	
422410025000	30.763503	-94.074888			AL BROWN		Jasper	TX	X	
423510021300	30.470904	-93.789474			HUMBLE OIL & REFINING COMPANY		Newton	TX	X	
423610032800	30.059612	-93.935073			SHELL OIL CO.		Orange	TX	X	
423730042300	30.542305	-94.683504			CONTINENTAL OIL COMPANY		Polk	TX	X	
423733015400	30.801591	-95.053014			PRAIRIE & CONVST		Polk	TX	X	
423390173100	30.032319	-95.277012					Montgomery	TX	X	
2-17	29.941817	-94.402789				McCarthy 1 Bauer	Jefferson	TX	X	
2-5	31.325786	-94.640307			J.R. Meeker et al	John Massingill 1	Angelina	TX	X	
2-14	30.234413	-95.077409					0	TX	X	

Final Report – Updating the Hydrogeologic Framework for the Northern Portion of the Gulf Coast Aquifer

API number or ID	NAD27 latitude	NAD27 longitude	Dip section/ position	Strike section/ position	Company	Lease	County	State	Lithology and water qual data	Paleo Data
2-15	30.190113	-94.953906					0	TX	X	
2-17	30.031717	-94.922203					0	TX	X	
4-3	31.146483	-95.565124			Reynolds Mining Corp.	J. T. Knox 1	Houston	TX	X	
4-4	31.022984	-95.47962			MAGNOLIA PETROLEUM C	Thompson Long Leaf LBR Co A-1	Walker	TX	X	
4-8	30.652496	-95.371919			PLACID OIL COMPANY	Gibbs Bros. 2	Walker	TX	X	
5-8	30.525801	-95.654224			PHILLIPS PETROLEUM C	Coke A 1	Montgomery	TX	X	
5-9	30.440305	-95.533021			The Superior Oil & Carlton Speed Jr.	James D. Sikes 1	0	TX	X	
6-10	29.898825	-95.692624			Standard Oil Company of Texas	G. J. Mellinger 1 et al 4	Harris	TX	X	
6-11	29.904224	-95.582221			Pan American Petroleum Corporation	Dorothy D Brown 1	Harris	TX	X	
6-17	29.303938	-95.241911			PHILLIPS PETROLEUM Company	Houston 2	Brazoria	TX	X	
6-3	30.607799	-96.196837			Humble Oil & Refining Company	R. P. Trant 1	Brazos	TX	X	
6-4	30.490303	-96.148736			The Texas Company	Orlando 1	Brazos	TX	X	
6-8	30.025321	-95.698024			Texaco, Inc.	M. N. Mergele 1	Harris	TX	X	
6-9	29.954123	-95.696224			Texaco, Inc.	J. J. Sweeney Estate 1	Harris	TX	X	
8-12	29.396944	-95.943833			Ft. Bend Oil Co.	D. Moore 1	Fort Bend	TX	X	
8-16	29.102946	-95.532322			Mobil Oil Corporation	Retrieve State Farm Tract	Brazoria	TX	X	
8-8	29.82623	-96.155839			Lueth & Robinshaw	O. C. Kurtz 1	Austin	TX	X	
8-9	29.747833	-96.004434			John H. England	Mound Company	Waller	TX	X	
9-12	29.689036	-96.241341			Humble Oil and Refining Company	Charles Kaechele B1	Austin	TX	X	
9-13	29.525142	-96.159439			Getty Oil Company	W. S. Leveridge 1	Wharton	TX	X	
G0030002D	31.287451	-94.661148			Lanford Drilling Company Inc.	Fuller Springs Water Improvement Dist. Well No. 4	Angelina	TX	X	
G0030019D	31.40666	-94.762558			Lanford Drilling Company Inc.	Central 3	Angelina	TX	X	
G0030019E	31.430719	-94.811039			Central CWID		0	TX	X	
G0030020A	31.26339	-94.577766			Layne - Texas Company	Four Way Water Supply Corp Well 1	Angelina	TX	X	
G0030020B	31.269699	-94.578911			Water Resources Inc.	Four Way Water Supply Corp Well 2	Angelina	TX	X	
G0030020D	31.275555	-94.535004			Key Drilling Co.	Lufkin Industries Water Well 1	Angelina	TX	X	
G0030020E	31.287291	-94.630638			Russell Drilling Inc.	Four Way Water Supply Corp Well 5	Angelina	TX	X	
G0030020F	31.345881	-94.57917			Russell Drilling Inc.		6	Angelina	TX	X
G0030028A	0	0					0	TX	X	
G0030080J	31.419445	-94.655281			Layne - Texas Company	Test Hole CW-28	Angelina	TX	X	

Final Report – Updating the Hydrogeologic Framework for the Northern Portion of the Gulf Coast Aquifer

API number or ID	NAD27 latitude	NAD27 longitude	Dip section/ position	Strike section/ position	Company	Lease	County	State	Lithology and water qual data	Paleo Data
G0030080K	31.430555	-94.662224			Layne - Texas Company	Southland Paper Mills CW 33	Angelina	TX	X	
G0030080N	31.434723	-94.734169			Layne - Texas Company	Test Hole CW-32	Angelina	TX	X	
G0840063A	29.494673	-94.942092			Water Resources Inc.	San Leon Test Well 1	Galveston	TX	X	
G0930003D	30.747953	-96.058815			Snook Drilling Company	Carlos Water Supply Corp. 4D	Grimes	TX	X	
G0930003E	30.755636	-96.047546			Snook Drilling Company	Carlos Water Supply Corp. 5E	Gaines	TX	X	
G0930020A	30.423081	-95.937469			Layne Western Katy Division	Grimes Co. MUD 1	Grimes	TX	X	
G0930048C	30.336075	-95.957739			G&W Water Supply Corp.	Weisinger T.H. 5	Grimes	TX	X	
G0930049A	0	0					0	TX	X	
G0930049B	30.350729	-95.926704			Lanford Drilling Company	Plantersville Water Supply Corp. 2	Grimes	TX	X	
G1000016C	30.152149	-94.321877			J&S Water Wells	Hardin Co. WCID 1	Hardin	TX	X	
G1000055A	30.407209	-94.617134			Lanford Drilling Company, Inc.	West Hardin Water Supply Corp, Thicket 1	Hardin	TX	X	
G1010003C	29.74674	-94.981216			Layne Texas Company	Layne Texas Co 10	Harris	TX	X	
G1210003C	30.44549	-93.969902			Holly Water Wells	Well 4	Jasper	TX	X	
G1210016B	30.621144	-93.906039			Pender	Kirbyville 2	Jasper	TX	X	
G1210064A	30.822779	-93.975281			Upper Jasper W/S	Well 3	Jasper	TX	X	
G1460006B	0	0					0	TX	X	
G1610086B	0	0					0	TX	X	
G1700026A	30.379341	-95.495193					0	TX	X	
G1700039A	30.236706	-95.446167			Lazy River Imp Dis	Well 1	Montgomery	TX	X	
G1700197R	30.156017	-95.454163					0	TX	X	
G1700578A	30.335888	-95.621147					0	TX	X	
G1700742A	30.132549	-95.377899			Johnston Water Well	Creek Side Village 1	Montgomery	TX	X	
G1700764A	30.376089	-95.669456					0	TX	X	
G2040005B	30.657419	-95.126625			Layne Western Company Inc.	Cape Royal Utility District Well 2	San Jacinto	TX	X	
G2360040A	30.745556	-95.68222			Lanford Drilling Company, Inc.	Pine Prairie Water Supply Corporation Well 2	Walker	TX	X	
G2360052B	30.698958	-95.617764			J.L. Myers Company	Pine Prairie Water Supply Corporation Highway 30 Well	Walker	TX	X	
LBGGRIM06	30.352777	-96.061944			Layne Texas Company	City of Navasota 1102 5484 Well 6	Grimes	TX	X	
LBGGRIM11	30.362551	-96.083524			Layne Texas Company	Layne Texas Company Well 11	Grimes	TX	X	
LBGGRIM14	30.349119	-96.059411			City of Navasota	Water Well 14	Grimes	TX	X	
LBGGRIM15	30.34149	-96.05269			Layne Texas Company	City of Navasota Well 15	Grimes	TX	X	
LBGMONT01	30.38055	-95.64555			Weisinger Inc	Stanley Lakes MUD Well 4 Test Well	Montgomery	TX	X	
LBGWALK11	30.714166	-95.548055			Layne Texas Company	Layne Texas Company Well 11A	Walker	TX	X	

Final Report – Updating the Hydrogeologic Framework for the Northern Portion of the Gulf Coast Aquifer

API number or ID	NAD27 latitude	NAD27 longitude	Dip section/ position	Strike section/ position	Company	Lease	County	State	Lithology and water qual data	Paleo Data
LBGWALK12	30.706388	-95.54111			Texas Water Wells Inc	City of Huntsville Water Well 12	Walker	TX	X	
LBGWALK13	30.695833	-95.529721			Texas Water Wells Inc	City of Huntsville Water Well 13	Walker	TX	X	
LBGWALK14	30.700833	-95.533888			Texas Water Wells Inc	City of Huntsville Water Well 14	Walker	TX	X	
LBGWALK15	30.690277	-95.53611			Layne Texas Company	City of Huntsville Water Well 15A	Walker	TX	X	
LBGWALK16	30.701944	-95.527499			Layne Texas Company	City of Huntsville Water Well 16A	Walker	TX	X	
LBGWALK17	30.69111	-95.544721			Layne Texas Company	City of Huntsville Water Well 17A	Walker	TX	X	
LBGWALK18	30.686388	-95.549721			Layne Texas Company	City of Huntsville Water Well 18A	Walker	TX	X	
LBGWALK19	30.67861	-95.550277			Layne Texas Company	City of Huntsville Water Well 19A	Walker	TX	X	
177004009300	29.656623	-93.669624	0/22		Chevron Oil	OCS 1437	Offshore-Cameron	LA		X
177004028600	29.597597	-93.654756	0/23	A-A'/10	Chevron USA	OCS-G-3259	Offshore-Cameron	LA		X
427103000800	29.316264	-93.856781	1/23		Texaco	OCS-G-1845	Offshore-Jefferson	TX		X
427104001700	29.184273	-93.849026	1/25		Atlantic Richfield	OCS-G-4741	Offshore-Jefferson	TX		X
427104002200	29.168288	-93.83093	1/25A		Atlantic Richfield	OCS-G-4741	Offshore-Jefferson	TX		X
427084004000	29.487348	-94.015437	2/25	A-A'/7	Mesa Pet	OCS-G-3114	Offshore-Jefferson	TX		X
427084007700	29.386965	-94.009614	2/26		Atlantic Richfield	OCS-G-3745	Offshore-Jefferson	TX		X
427083004500	29.348933	-94.004773	2/27		Texaco	OCS-G-1819	Offshore-Jefferson	TX		X
427084016000	29.236674	-93.985528	2/28		Atlantic Richfield	OCS-G-4731	Offshore-Jefferson	TX		X
427084030000	29.15714	-93.956071	2/30		Sun E&P	OCS-G-6173	Offshore-Jefferson	TX		X
427084013800	29.418664	-94.156993	3/22	A-A'/6	Atlantic Richfield	OCS-G-6145	Offshore-Jefferson	TX		X
427084001400	29.343034	-94.18968	3/23		Cities Service	OCS-G-2352	Offshore-Jefferson	TX		X
427084032300	29.109841	-94.054974	3/25		Oryx	OCS-G-9093	Offshore-Jefferson	TX		X
427084013000	29.306436	-94.343985	4/17		Atlantic Richfield	OCS-C-4574	Offshore-Galveston	TX		X
427084015400	29.237838	-94.234381	4/18		Superior	OCS-G-6161	Offshore-Jefferson	TX		X
427084008500	29.133641	-94.195979	4/19		Getty	OCS-G-3747	Offshore-Jefferson	TX		X
427084012600	28.994248	-94.173195	4/20		Atlantic Richfield	OCS-C-4735	Offshore-Jefferson	TX		X
427064003100	29.206367	-94.594635	5/22	A-A'/3	Gulf	G-2667, Gal 181-L	Offshore-Galveston	TX		X
427084014500	29.129769	-94.467073	5/23		Atlantic Richfield	G-6166, HI 194	Offshore-Galveston	TX		X
427084028900	28.993842	-94.50886	5/24		CNG Producing	G-7292m HI 260	Offshore-Galveston	TX		X
427084062600	28.685053	-94.31038	5/27		BP E&P	G-26519 HI A-119	Offshore-Galveston	TX		X
427064009000	28.975797	-94.642709	6/20		Mark Pdcg	OCS-G-5004	Offshore-Galveston	TX		X
427040007100	28.5478	-95.4866	10/19		Sun	Brazos 433	Offshore-Matagorda	TX		X
427040007000	28.3688	-95.3998	10/21		Phillips	Brazos 505	Offshore-Matagorda	TX		X

Final Report – Updating the Hydrogeologic Framework for the Northern Portion of the Gulf Coast Aquifer

API number or ID	NAD27 latitude	NAD27 longitude	Dip section/ position	Strike section/ position	Company	Lease	County	State	Lithology and water qual data	Paleo Data
177004063900	29.648757	-93.346364			Atlantic Richfield C	OCS-G-5274 Well #1	Offshore-Cameron	LA		X
177004123200	29.682415	-93.43751			Chevron USA Inc	OCS-G 22500 002 ST00	Offshore-Cameron	LA		X
427060003400	28.645863	-94.960261			Mobil Oil	Federal BL 385 OCS 0	Offshore-Brazoria	TX		X
427064037200	28.719124	-95.263082			Wacker Oil Company	OCS-G-6105 No. 10	Offshore-Brazoria	TX		X
427083002300	29.374632	-93.974972			Texaco Inc.	A-2 Federal Block 71	Offshore-Jefferson	TX		X
427083002500	29.374632	-93.974972			Texaco Inc.	A-3 Federal Block 88	Offshore-Jefferson	TX		X
427083002800	29.374632	-93.974972			Texaco Inc,	A-4, OCS-G-1818, Fed	Offshore-Jefferson	TX		X
427044002600	28.3638	-95.3552			Shell Oil Company	State Tract 405-L (N	Offshore-Matagorda	TX		X
177004039200	29.703419	-93.236286			McMoran Offshore Exp	CS G 3317 Well #1	Offshore-Cameron	LA		X
427064006100	28.581634	-95.156722			AMINOIL U.S.A., Inc.	OCS-G-3742 Well #2	Offshore-Brazoria	TX		X
427064012200	28.768615	-95.015093			Arco Oil and Gas Com	OCS-G-7247 No. 1	Offshore-Brazoria	TX		X
427084010400	29.328456	-94.353828			Atlantic Richfield C	OCS-G-4575 Well #1	Offshore-Galveston	TX		X
427084015300	29.418686	-94.156992			Arco Oil and Gas	OCS-G-6145 A-3	Offshore-Jefferson	TX		X
427083002200	29.374632	-93.974972			Texaco Inc.	A-1 FB72, OCS-G-1815	Offshore-Jefferson	TX		X
427084015000	29.319635	-93.972372			Atlantic Richfield C	OCS-C-6156 Well #1	Offshore-Jefferson	TX		X
427084060800	29.16064	-94.138477			Spinnaker Exploratio	OCS-G-9086 Well No.	Offshore-Jefferson	TX		X
170030029000	30.5163	-93.020553			TEXACO OIL	Power Lumber LLC	Allen	LA	X	
170110008700	30.797397	-93.396968			SUTTON JOINT ACCOUNT	Stella Oftin 1	Beauregard	LA	X	
170110009500	30.761197	-93.307065			MOBIL OIL CORPORATIO	Magnolia Four C 1	Beauregard	LA	X	
170110013500	30.609898	-93.101956			MOBIL OIL CORPORATIO	Ragler LBR CC 1	Beauregard	LA	X	
170110039800	30.520999	-93.479867			MOBIL OIL CORPORATIO	Lutcher 1	Beauregard	LA	X	
170112089800	30.875892	-93.014956			UNION PACIFIC RESOUR	Crosby 19 1	Beauregard	LA	X	
170190000400	30.395003	-93.646567			SOUTHWEST GAS PRODUC	Lutcher Moore Lumber Co 3	Beauregard	LA	X	
170190036900	30.393301	-93.458662			SHELL OIL COMPANY		0	LA	X	
170190184300	30.107809	-93.395956			UNION SULPHUR COMPAN	A R West 1	Calcasieu	LA	X	
170190199700	30.117509	-93.700065			SUN OIL COMPANY	H L Brown 1	Calcasieu	LA	X	
170192046300	30.134309	-93.599361			TRIBAL OIL & AUSTER	Matilda Gray Stream No J-14	Calcasieu	LA	X	
170192095600	30.303005	-93.105752			AMOCO PRODUCTION COM	Betty A Hein et al No 1	Calcasieu	LA	X	
170230124200	29.999012	-93.218854			HUMBLE OIL & REFININ	Miami Corp L-1	Cameron	LA	X	
170230140000	29.864818	-93.262253			HUMBLE OIL & REFININ	Lake State Lease 1255 Well 1	Cameron	LA	X	
170230178800	29.786023	-93.441955			AUSTRAL OIL COMPANY	Ray B Peveto	Cameron	LA	X	
170230187300	29.830518	-93.737262			TEXACO OIL	Cameron Meadows Land Company 2	Cameron	LA	X	
170232013100	30.017012	-93.617862			SHELL OIL COMPANY	J B Watkins 134	Cameron	LA	X	
170792031700	31.239682	-92.822051			DOMESTIC OIL COMPANY	1 Pardee	Rapides	LA	X	
171150004600	30.917693	-93.274063			SUNRAY DX OIL COMPAN	Fletcher EST 1	Vernon	LA	X	
171152005500	31.172286	-93.316867			ROSSON & LAYMAN	Frank Leach 2	Vernon	LA	X	

Final Report – Updating the Hydrogeologic Framework for the Northern Portion of the Gulf Coast Aquifer

API number or ID	NAD27 latitude	NAD27 longitude	Dip section/ position	Strike section/ position	Company	Lease	County	State	Lithology and water qual data	Paleo Data
171152011400	31.029888	-92.877652			CHESAPEAKE OPERATING	Lawton 27A 1	Vernon	LA	X	
171152019800	30.883392	-92.945954			PILOT RESOURCES INCO		0	LA	X	
177000003900	29.646827	-93.627359			MAGNOLIA PETROLEUM C	A-1	Offshore-Cameron	LA	X	
177000004600	29.704522	-93.75176			MAGNOLIA PETROLEUM C	LA ST LSE 2922 Blk I7 Well A-1	Offshore-Cameron	LA	X	
177004056700	29.714524	-93.254953			Chevron U.S.A. Inc.	OCS-G-3489 No 1	Offshore-Cameron	LA	X	
420390006400	29.528235	-95.348516			HUMBLE OIL & REFININ	Humble 1 de Lorenz	Brazoria	TX	X	
420410006300	30.484104	-96.145736			TEXAS COMPANY	LOUISE ORLANDO	Brazos	TX	X	
420410010200	30.345609	-96.154637			LEWIS J K	G W Lott 1	0	TX	X	
420710288000	29.53153	-94.835699			HUMBLE OIL & REFININ	State A-72	Offshore-Harris	TX	X	
421570083600	29.562536	-95.601923			HUMBLE OIL & REFININ	1 Stancliff	Fort Bend	TX	X	
421670114200	29.364934	-94.961402			MIDSTATES OIL COMPAN	Westerlage Unit 1	Galveston	TX	X	
421850002400	30.661097	-95.92803			WOODLEY PETROLEUM CO	Hattie F Wilson	Grimes	TX	X	
421990033500	30.393708	-94.219287			SINCLAIR	Henry Binns 9	Hardin	TX	X	
421990075700	30.458707	-94.6107			SHELL OIL COMPANY	Kirby Lmbr. Co 1	Hardin	TX	X	
422010353300	29.960123	-95.515919					0	TX	X	
422010406800	29.756929	-95.574522			MORAN CORPORATION TH	Hayes 1	0	TX	X	
422010622300	29.725927	-94.991906			SPARTA OIL COMPANY T	M. H. Bielstein 1	Harris	TX	X	
422910030200	30.366408	-94.740703			ATLANTIC REFINING CO	Kirby A-1	Liberty	TX	X	
422910216900	30.213211	-94.758001			UNION PRODUCING COMP	Smith B-1	Liberty	TX	X	
422910242600	30.132314	-94.886603			SHELL OIL COMPANY	S Macy 1	Liberty	TX	X	
422910484100	29.901218	-94.495592			HUMBLE OIL & REFININ	Boyt B-1	Liberty	TX	X	
423390099400	30.355207	-95.661323			LESTER EMANUEL	Earl White	Montgomery	TX	X	
423390103900	30.213113	-95.636922			ACCO ROBERTS & MURPH	H Roberts	Montgomery	TX	X	
423390110200	30.140016	-95.621122			MITCHELL CHRISTIE	Neidick 1	Montgomery	TX	X	
423390173700	30.109517	-95.395115			HUMBLE OIL & REFININ	Bender 2	Montgomery	TX	X	
424070002100	30.540903	-94.92731			SUNRAY OIL CORPORATI	H Leary	San Jacinto	TX	X	
424573063001	30.769102	-94.310695			RANGE PRODUCTION COM	BSMC Goode Unit 1	Tyler	TX	X	
424710004200	30.539801	-95.47912			BISHOP H C	G W Beardsley Estate 1	Walker	TX	X	
424730000300	30.117918	-96.165438			WILLIAMS H E	T-1169 David Moore Survey	Waller	TX	X	
424730004900	29.938325	-95.975234			PHEFFER & HOGUE	Pfeffer & Hogue 1	Waller	TX	X	
427060008800	28.986745	-95.108107			SHELL OIL COMPANY	ST TR 248L-SW-1	Offshore-Brazoria	TX	X	
427064019700	28.747752	-94.902801			Walter Oil & Gas Cor	OCS-G 4721 Well 3	Offshore-Brazoria	TX	X	
427064036300	29.014045	-94.751494			SPN Resources, LLC	OCS-G 1772 B-3	Offshore-Galveston	TX	X	
427080010000	29.108942	-94.375784			Skelly Oil Company	OCS-G 1830 Block 205	Offshore-Galveston	TX	X	
427084012700	29.125141	-94.074075			Shell Offshore Inc.	OCS-G 4576 18-2	Offshore-Jefferson	TX	X	
427084038400	28.974645	-94.243679			Statoil Exploration	OCS-G 13799 No 1	Offshore-Galveston	TX	X	



Final Report – Updating the Hydrogeologic Framework for the Northern Portion of the Gulf Coast Aquifer

API number or ID	NAD27 latitude	NAD27 longitude	Dip section/ position	Strike section/ position	Company	Lease	County	State	Lithology and water qual data	Paleo Data
427084043600	29.323036	-94.337985			IP Petroleum Company	OCS-SG 15776 2	Offshore-Galveston	TX	X	
427084052300	29.29279	-94.01169			Merit Energy Company	OCS-G 18938 3	Offshore-Jefferson	TX	X	
427104007600	29.441732	-93.789965			Mobil Producing Texa	OCS-G 5180 2	Offshore-Cameron	TX	X	
3-14	29.736623	-94.656095			Pan Am	C.A. Kleke	Chambers	TX	X	
4-14	30.234413	-95.077409			Mobile	B.E. Quinn	Liberty	TX	X	
4-15	30.190113	-94.953906			Shell Oil Company	KIRBY LUMBER CO	Liberty	TX	X	
4-17	30.031717	-94.922203			Amerada	RC Brown #1	Liberty	TX	X	
G0300080N	31.434883	-94.734409					Angelina	TX	X	
Q-323	0	0			Moore and Womack	Wysinger # 1	Montgomery	TX	X	
6035902	0	0			Strake	Peel TJ #1	Montgomery	TX	X	
Q-41	0	0			Gabriel and Womack	Foster Estate #1	Montgomery	TX	X	
420150023000	30.0098	-96.1293	8/5	D-D'/1	Humble O&R	Sherrod, L.R.	Austin	TX	X	
421570000100	29.7538	-95.8705	8/8		Humble O&R	Albright, F.C.	Fort Bend	TX	X	
421570102600	29.6699	-95.8494	8/9	C-C'/1	Mobil (Magnolia - Seaboard)	McKennon, E.	Fort Bend	TX	X	
421573198300	29.5983	-95.8187	8/10		Petroleum Resource Mgmt	Foster Farms	Fort Bend	TX	X	
421570089400	29.5853	-95.6728	8/11		Cockburn, H.C.	Clayton Fdn	Fort Bend	TX	X	
421570245900	29.4568	-95.6113	8/12	B-B'/1	Humble O&R	Lockwood & Sharp	Fort Bend	TX	X	
420390145200	29.3163	-95.4703	8/13		Group Oil	Grey, J.A.-2nd NB	Brazoria	TX	X	
420390427700	29.1295	-95.3051	8/15		Texaco	General Amer Life	Brazoria	TX	X	
420390429100	29.0239	-95.2919	8/16		Brazos O&G	Fletcher Tr	Brazoria	TX	X	
420153073800	29.6167	-96.0497	9/6		Phillips	Sommers	Austin	TX	X	
421573180500	29.46309	-95.9521	9/8		Greenhill Pet	Patterson, A.E. II	Fort Bend	TX	X	
420390286500	29.1862	-95.7075	9/11		Pan American (Stanolind)	Robertson, W.T.	Brazoria	TX	X	
421493132900	29.9842	-96.6822	10/2		Daleco Res	Halamiccek	Fayette	TX	X	
420893153100	29.8066	-96.5792	10/3		Superior Pdn	Werland, A.	Colorado	TX	X	
420890005700	29.7798	-96.5494	10/4		Quintana Pet	Cullen etal	Colorado	TX	X	
420890009000	29.7736	-96.4365	10/5		Paul, W.U.	Reinhardt, H.	Colorado	TX	X	
420893124600	29.6453	-96.3891	10/6		Ponexco	Dixon, L. etal	Colorado	TX	X	
424810121800	29.4747	-96.2802	10/8		General Crude	Northington	Wharton	TX	X	
424810120500	29.4738	-96.1920	10/9		BBM Drlg	Wintermann, D.	Wharton	TX	X	
424813344200	29.3679	-96.1512	10/10		Greenhill	Sorrel, M.	Wharton	TX	X	
424813294400	29.2353	-96.0156	10/12		Ashland Expl	Fields, R.L.	Wharton	TX	X	
423210083600	28.9496	-95.7766	10/16		British-American Oil	M.B. Guess	Matagorda	TX	X	
423210082400	28.8138	-95.6907	10/17		Gulf	O.E. Phillips	Matagorda	TX	X	

## **APPENDIX B**

### **Listing of Geophysical Logs Stratigraphic Contacts**

*This page is intentionally left blank.*

## Appendix B Listing of Geophysical Logs Stratigraphic Contacts

See Table 5-2 for a definition of the column headers.

UWI/API	Dip Section/ Position		Strike Section/ Position		KB	Stratigraphic Contacts (ft, msl)								
						Beaumont	Lissie	Willis	Upper Goliad	Lower Goliad	Upper Lagarto	Middle Lagarto	Lower Lagarto	Oakville
171152004000	-1	1			202	-	-	-	-	-	-	-	-	-
171150002000	-1	2			350	-	-	-	-	-	-	-	-	-856
171150002100	-1	2A			351	-	-	-	-	-	-	-	-	-788
171150002200	-1	3	D	16	243	-	-	-	-	-	-	-	-1628	-2078
171158800300	-1	4	D	15	266	-	-	-63	-	-490	-906	-1332	-1876	-2346
171152017900	-1	5	D	14	232	-	-	-118	-	-486	-988	-1303	-1878	-2403
171152013500	-1	6	D	13	215	-	-	-252	-	-686	-1062	-1503	-2118	-2603
170112090100	-1	7			209	-	-	-278	-343	-828	-1216	-1508	-2258	-2828
170112059000	-1	8			185	-	-	-	-858	-1438	-1748	-2178	-2848	-3620
170110016900	-1	9	C	16	111	-	-133	-496	-1588	-2173	-2603	-2943	-3724	-4378
170112053200	-1	9A	C	14	128	-	-166	-618	-1498	-2018	-2449	-2758	-3580	-4188
170110029800	-1	10	C	15	96	-	-268	-678	-1928	-2438	-2899	-3218	-4108	-4753
170110090600	-1	11			47	-	-308	-848	-2068	-2650	-3078	-3428	-4308	-5010
170192183600	-1	12			55	-	-498	-976	-2398	-3020	-3505	-3908	-4812	-5525
170190045900	-1	12A			56	-18	-616	-998	-2153	-2768	-3265	-3668	-4601	-5378
170190116300	-1	13			64	-98	-658	-1108	-2618	-3308	-3868	-4396	-5301	-6193
170190145800	-1	14			27	-158	-668	-1238	-1958	-2668	-3223	-3867	-4868	-5824
170192162100	-1	14A			31	-158	-724	-1248	-2205	-2898	-3509	-4094	-5100	-6238
170190167400	-1	15			24	-224	-828	-1350	-2748	-3698	-4323	-4918	-6128	-7378
170192020200	-1	15A	B	17	17	-258	-908	-1418	-3218	-4168	-4809	-5528	-6808	-7963
170190184900	-1	16	B	16	16	-273	-983	-1558	-3286	-4053	-4658	-5463	-6810	-7778
170230020800	-1	17			18	-348	-1093	-1603	-3403	-4660	-5123	-6058	-8038	-8624
170230050900	-1	18			20	-203	-888	-1418	-2438	-3211	-3616	-4266	-	-4493
170230159900	-1	19			22	-206	-820	-1411	-2108	-2528	-2788	-	-	-
170232228000	-1	20			24	-378	-1121	-1528	-3398	-4668	-5249	-6259	-8304	-

Final Report – Updating the Hydrogeologic Framework for the Northern Portion of the Gulf Coast Aquifer

UWI/API	Dip Section/ Position		Strike Section/ Position		KB	Stratigraphic Contacts (ft, msl)								
						Beaumont	Lissie	Willis	Upper Goliad	Lower Goliad	Upper Lagarto	Middle Lagarto	Lower Lagarto	Oakville
170230156200	-1	21			20	-498	-1210	-1828	-3664	-4930	-5510	-6690	-8863	-
170230177200	-1	22			19	-513	-1314	-1713	-3773	-5108	-5788	-6908	-9018	-
170232122500	-1	23			27	-638	-1378	-2003	-4153	-5358	-6085	-7223	-9498	-
177004121502	-1	24	A	12	110	-913	-1873	-2938	-5748	-6988	-7697	-8813	-10968	-
177004084000	-1	25			98	-1028	-1990	-3033	-6053	-7528	-8248	-9838	-	-
177014015000	-1	26			75	-1548	-2726	-4134	-	-	-	-	-	-
177014031202	-1	27			119	-	-	-	-	-	-	-	-	-
177014036000	-1	28			82	-2288	-4413	-7068	-	-	-	-	-	-
177014018600	-1	29			68	-2568	-	-	-	-	-	-	-	-
170850422200	0	1			310	-	-	-	-	-	-	-	-	-
171150002700	0	2			195	-	-	-	-	-	-	-	-	-184
171152000400	0	3			179	-	-	-	-	-	-	-155	-578	-930
171158800000	0	4	D	11	175	-	-	-28	-381	-778	-978	-1253	-1748	-2168
171152012000	0	4A	D	12	220	-	-	-	-	-	-	-	-	-
170112061600	0	5	D	10	126	-	-	-228	-728	-1139	-1330	-1640	-2108	-2523
170112080000	0	6			169	-	-23	-445	-978	-1428	-1688	-1978	-2503	-2910
170112040700	0	7			158	-	-208	-588	-1078	-1603	-1876	-2323	-2873	-3338
170110064200	0	8			152	-	-229	-643	-1108	-1633	-1949	-2408	-2968	-3458
170110075500	0	9	C	13	126	-	-278	-708	-1306	-1904	-2256	-2668	-3408	-3936
170112105800	0	10			86	-	-348	-800	-1512	-1946	-2423	-2798	-3710	-4228
170190001800	0	11			58	-	-	-890	-1791	-2388	-2818	-3248	-4030	-4583
170190025500	0	12			41	-48	-518	-878	-1973	-2628	-3138	-3678	-4658	-5496
170190258300	0	12A			20	-	-568	-933	-1444	-2018	-2573	-3366	-	-
170190197200	0	13			31	-278	-848	-1388	-3249	-3880	-4316	-4899	-5908	-6731
170190207200	0	13A			28	-138	-688	-988	-2518	-3176	-3572	-4203	-4880	-5648
170190206500	0	14	B	14	8	-	-	-	-	-	-	-	-	-
170190189600	0	14A	B	15	20	-	-	-	-2814	-3554	-4018	-4612	-5788	-6748
170232012700	0	15	B	13	20	-248	-758	-1328	-2828	-3758	-4062	-4588	-5420	-

Final Report – Updating the Hydrogeologic Framework for the Northern Portion of the Gulf Coast Aquifer

UWI/API	Dip Section/ Position		Strike Section/ Position		KB	Stratigraphic Contacts (ft, msl)								
						Beaumont	Lissie	Willis	Upper Goliad	Lower Goliad	Upper Lagarto	Middle Lagarto	Lower Lagarto	Oakville
170230011100	0	16			20	-308	-968	-1373	-3603	-4470	-5008	-5600	-6728	-7718
170230187700	0	17			30	-128	-738	-1276	-2206	-2830	-3446	-4278	-5898	-
170230196800	0	18			18	-128	-668	-1228	-1793	-2458	-2978	-3473	-4509	-
170230204500	0	19			18	-348	-1018	-1900	-4350	-5138	-5752	-6590	-8016	-
177002020800	0	20			59	-408	-1048	-1965	-4284	-5109	-5696	-6555	-8153	-12953
177004106800	0	21			57	-428	-1148	-2001	-4408	-5318	-5991	-6983	-8659	-14398
177004009300	0	22			47	-408	-1188	-2148	-4368	-5413	-6124	-7208	-8998	-14628
177004028600	0	23	A	10	72	-	-1288	-2404	-4576	-5738	-6546	-7723	-9788	-
177000005500	0	24	A	11	73	-888	-1673	-2725	-5328	-6563	-7248	-8745	-	-
177014031600	0	25			103	-1393	-2238	-3763	-7798	-10298	-	-	-	-
177014015000	0	26A			68	-1488	-2651	-4228	-	-	-	-	-	-
177014018600	0	27			75	-2038	-3148	-4858	-	-	-	-	-	-
424033027800	1	1			270	-	-	-	-	-	-	-	-	-
424033019600	1	2			279	-	-	-	-	-	-	-	-	-
424033034300	1	3			306	-	-	-	-	-	-	-	-	-
423513052100	1	3A			294	-	-	-	-	-	-	-	-	-
423513052600	1	3B			308	-	-	-	-	-	-	-	-	-
423510004800	1	4			318	-	-	-	-	-	-	-	-212	-543
423513072600	1	5	D	9	247	-	-	-	-	-	-	-	-	-
423510047800	1	6			136	-	-	-	-	-	-	-	-	-
423513003300	1	6A			117	-	-	-	-	-971	-1348	-1623	-2135	-2518
422410009100	1	7			118	-	-68	-558	-	-1153	-1488	-1803	-2374	-2848
423510009600	1	8			108	-	-	-	-	-1408	-1738	-2216	-2828	-3343
423510022600	1	9	C	12	67	-	-418	-748	-1013	-1810	-2163	-2648	-3273	-3813
423513038100	1	10			69	-	-608	-948	-1221	-2011	-2412	-2941	-3628	-4158
423510028900	1	11			54	-58	-638	-1070	-2086	-2928	-3388	-4188	-5328	-5926
423613081000	1	12			45	-58	-688	-1065	-2208	-2923	-3464	-4223	-5308	-5938
423610047400	1	13			29	-163	-718	-1154	-2233	-3058	-3618	-4470	-5623	-6368

Final Report – Updating the Hydrogeologic Framework for the Northern Portion of the Gulf Coast Aquifer

UWI/API	Dip Section/ Position		Strike Section/ Position		KB	Stratigraphic Contacts (ft, msl)								
						Beaumont	Lissie	Willis	Upper Goliad	Lower Goliad	Upper Lagarto	Middle Lagarto	Lower Lagarto	Oakville
423610055500	1	14	B	11	23	-148	-733	-1083	-1675	-2519	-3043	-3718	-4828	-5448
423610049000	1	15	B	12	25	-238	-788	-1138	-1860	-2732	-3200	-3826	-4938	-5398
423610131800	1	16			23	-438	-1068	-1412	-3061	-3938	-4490	-5468	-7008	-7573
170230205500	1	17			18	-458	-1138	-1763	-3399	-4400	-4948	-5908	-7458	-8278
170230207900	1	18			18	-358	-1048	-1568	-3376	-4483	-5086	-5943	-7698	-8335
422453035800	1	19			18	-	-	-	-3548	-4453	-5246	-6258	-8223	-
422450334300	1	20			16	-	-1208	-1953	-3818	-4738	-5528	-6508	-8218	-
427153001100	1	21	A	9	96	-558	-1350	-2473	-4848	-5844	-6578	-7618	-8888	-
427084057200	1	22	A	8	90	-633	-1568	-2438	-5300	-6320	-7103	-8208	-9718	-
427103000800	1	23			85	-	-	-2684	-6418	-8028	-9108	-10263	-	-
427104013100	1	24			96	-1052	-2039	-3060	-7298	-8978	-	-	-	-
427104001700	1	25			106	-1168	-2186	-3394	-8944	-	-14423	-	-	-
427104002200	1	25A			100	-1186	-2238	-3458	-8406	-	-	-	-	-
427104005600	1	26			100	-1318	-2458	-4248	-	-	-	-	-	-
420050019200	2	1			141	-	-	-	-	-	-	-	-	-
G0030024A	2	2			202	-	-	-	-	-	-	-	-	-
420053011900	2	2A			219	-	-	-	-	-	-	-	-	-
422410025300	2	3			203	-	-	-	-	-	-	-	-	-
424573011900	2	4			225	-	-	-	-	-	-	-	-	-
424570004100	2	5			166	-	-	-	-	-	-	-	-	-
424570004300	2	6	D	8	218	-	-	-	-	-	-	-	-496	-800
424570025600	2	7			192	-	-	-	-	-	-	-	-915	-1190
424570024500	2	8			454	-	-	-	-	-	-	-	-	-
424570025400	2	9			177	-	-198	-528	-	-	-	-528	-1056	-1409
424570037700	2	10			97	-	-158	-478	-	-	-713	-988	-1613	-2010
421990011600	2	11			60	-	-206	-660	-	-703	-1044	-1308	-2108	-2626
1-9	2	12	C	11	50	-	-223	-818	-	-1313	-1733	-1973	-2833	-3338
421993181100	2	13	C	10	58	-	-283	-953	-	-1333	-1775	-2168	-2978	-3486

Final Report – Updating the Hydrogeologic Framework for the Northern Portion of the Gulf Coast Aquifer

UWI/API	Dip Section/ Position		Strike Section/ Position		KB	Stratigraphic Contacts (ft, msl)								
						Beaumont	Lissie	Willis	Upper Goliad	Lower Goliad	Upper Lagarto	Middle Lagarto	Lower Lagarto	Oakville
421990035600	2	14			42	-	-290	-998	-	-1518	-1978	-2498	-3328	-3823
423610000400	2	15			43	-9	-488	-1038	-1788	-2528	-3003	-3530	-4366	-4856
422450016900	2	16			48	-128	-620	-1128	-2186	-2938	-3428	-3923	-4813	-5323
422453257200	2	17	B	10	21	-193	-708	-1378	-2618	-3414	-3980	-4398	-5259	-6102
422450165400	2	18			23	-310	-908	-1518	-2736	-3610	-4183	-4618	-5688	-6490
422450163700	2	19			28	-358	-1113	-1646	-2926	-3818	-4428	-4855	-5950	-6888
422450211000	2	20			23	-	-	-	-3178	-4131	-4808	-5113	-6428	-7454
422453014300	2	21			20	-493	-1208	-1968	-3348	-4499	-4918	-5308	-6513	-7323
422450299600	2	22			20	-592	-1198	-1734	-2405	-3256	-3953	-4488	-5890	-6588
426060001000	2	23			33	-653	-1328	-1748	-3056	-3888	-4626	-5358	-6640	-7488
427080001000	2	24			52	-843	-1488	-1938	-3590	-4568	-5598	-6428	-7728	-
427084004000	2	25	A	7	78	-988	-1780	-2174	-4078	-5268	-6216	-7188	-	-
427084007700	2	26			96	-1054	-1596	-2158	-4971	-5963	-7004	-8099	-10231	-
427083004500	2	27			47	-	-	-2420	-5406	-6359	-7448	-8190	-	-
427084016000	2	28			103	-1628	-2143	-3268	-6836	-8710	-9703	-11153	-14063	-
427084046800	2	29			95	-1598	-2188	-3520	-	-	-	-	-	-
427084030000	2	30			100	-	-	-	-7833	-12178	-	-	-	-
2-6	3	1			260	-	-	-	-	-	-	-	-	-
420053017100	3	2			230	-	-	-	-	-	-	-	-	-
423733048400	3	3			182	-	-	-	-	-	-	-	-	-
423730000300	3	4			191	-	-	-	-	-	-	-	-	-
423730000600	3	4A			261	-	-	-	-	-	-	-	-	-
424573010100	3	5			378	-	-	-	-	-	-	-	-148	-128
2-10	3	6			368	-	-	-	-	-	-	-	-	-
424570047700	3	7	D	7	291	-	-	47	-	-	-13	-311	-764	-1138
2-12	3	8			156	-	-	-303	-	-683	-880	-1138	-1594	-1878
424570006300	3	9			146	-	-	-213	-	-595	-800	-1098	-1508	-1780
421993311900	3	10	C	7	145	-	-	-323	-	-	-	-	-2643	-3178



Final Report – Updating the Hydrogeologic Framework for the Northern Portion of the Gulf Coast Aquifer

UWI/API	Dip Section/ Position		Strike Section/ Position		KB	Stratigraphic Contacts (ft, msl)								
						Beaumont	Lissie	Willis	Upper Goliad	Lower Goliad	Upper Lagarto	Middle Lagarto	Lower Lagarto	Oakville
G1000055B	3	11	C	8	100	-	107	-434	-1057	-	-	-	-	-
421990063400	3	11A	C	9	110	-	-	-473	-1063	-1528	-1833	-2228	-2748	-3258
421990067400	3	12			86	-	-	-658	-1373	-1970	-2246	-2718	-3282	-3873
421990214800	3	13			55	-	-218	-878	-1354	-2036	-2374	-2899	-3494	-4275
422453156200	3	14			57	82	-443	-1083	-1618	-2308	-2668	-3228	-3941	-4748
422450012300	3	15			56	57	-498	-1199	-1676	-	-	-	-	-
422453195500	3	15A	B	8	51	-	-733	-1315	-1837	-2782	-3056	-3606	-4611	-5393
422450223800	3	16	B	9	39	-53	-803	-1410	-2189	-3030	-3658	-4478	-5506	-7108
422450226500	3	17			32	-228	-1012	-1588	-2608	-3516	-4388	-5313	-7038	-8718
422450265800	3	18			25	-178	-768	-1128	-2654	-3833	-4603	-5368	-6678	-8038
422450268900	3	19			25	-248	-988	-1614	-2628	-3734	-4380	-5153	-6123	-7353
422450286600	3	20			22	-280	-1203	-1678	-3083	-4219	-4763	-5418	-6258	-8083
426060005500	3	21			54	-378	-1300	-1968	-3198	-4603	-5058	-5718	-6438	-
427083031300	3	21A	A	5	98	-	-	-2228	-4228	-5453	-6430	-7328	-9081	-
427084013800	3	22	A	6	101	-868	-1753	-2468	-4388	-5373	-6158	-	-8853	-
427084001400	3	23			86	-828	-1628	-2488	-5078	-	-7244	-	-10678	-
427080005700	3	24			82	-	-	-	-5846	-	-7813	-	-11851	-
427084032300	3	25			95	-	-	-	-9263	-12058	-	-	-	-
427084012800	3	26			101	-1218	-2278	-3373	-11948	-	-	-	-	-
424553048500	4	1?			352	-	-	-	-	-	-	-	-	-
424550002200	4	2			378	-	-	-	-	-	-	-	-	-
424550003200	4	3			253	-	-	-	-	-	-	-	-	-
423730003000	4	4			277	-	-	-	-	-	-	-	-	-
423733012000	4	5			234	-	-	-	-	-	-	-	-	-218
423733097500	4	6	D	6	313	-	-	-8	-	-	-	-	-946	-1408
423730035900	4	7			223	-	-	-228	-	-	-398	-728	-1228	-1718
422910018900	4	8			105	-	-	-623	-	-	-868	-1318	-1838	-2395
422910022100	4	9	C	6	68	102	-368	-658	-	-	-828	-1398	-1978	-2594

Final Report – Updating the Hydrogeologic Framework for the Northern Portion of the Gulf Coast Aquifer

UWI/API	Dip Section/ Position		Strike Section/ Position		KB	Stratigraphic Contacts (ft, msl)								
						Beaumont	Lissie	Willis	Upper Goliad	Lower Goliad	Upper Lagarto	Middle Lagarto	Lower Lagarto	Oakville
422910032500	4	10			102	-16	-628	-993	-	-1268	-1742	-2358	-3328	-4248
422910180200	4	11			87	-168	-768	-1178	-1488	-2091	-2618	-3251	-4178	-4887
422910167000	4	12			76	-68	-698	-1068	-	-1618	-2130	-2790	-3738	-4420
422910476500	4	13	B	6	56	-188	-843	-1235	-1766	-2385	-3065	-3683	-4705	-5551
420713130200	4	14			49	-	-	-	-2048	-2680	-3399	-4175	-5415	-6383
420710217700	4	15			32	-423	-1063	-1478	-2528	-3318	-4170	-4880	-5988	-7028
427080002200	4	16			40	-548	-1194	-1555	-3658	-4430	-5359	-6073	-7243	-8878
427083033200	4	16A	A	4	89	-	-	-	-3754	-5618	-5442	-6108	-7574	-
427084013000	4	17			106	-758	-1503	-1900	-4028	-4978	-5554	-6048	-7640	-
427084015400	4	18			104	-663	-1795	-2725	-6140	-8678	-9943	-11198	-15258	-
427084008500	4	19			100	-1238	-2668	-4078	-7368	-9825	-11343	-	-	-
427084012600	4	20			101	-1538	-2913	-3968	-8558	-11368	-12403	-	-	-
424710019900	5	0			298	-	-	-	-	-	-	-	-	-
424710001400	5	1			153	-	-	-	-	-	-	-	-	-
424710009700	5	2			218	-	-	-	-	-	-	-	-	-
4-6	5	2A			148	-	-	-	-	-	-	-	-	-
424070012700	5	3			349	-	-	-	-	-	-	-	-	-
424073003300	5	4			315	-	-	-	-	-	-	12	-548	-998
424073007800	5	4.5	D	5	240	-	-	-	-	-	-	-478	-1018	-1438
424070015600	5	5			199	-	-	-163	-	-	-358	-804	-1218	-1718
424070021400	5	6			194	-	-	-208	-	-	-483	-878	-1438	-2003
4-12	5	6.5			154	-	-	-	-	-	-	-	-	-
422910391400	5	?			78	-	-	-	-	-	-	-	-	-
422910008600	5	7			150	-	-8	-348	-	-566	-983	-1363	-1943	-2568
4-13	5	7A			120	-	-	-	-	-	-	-	-1948	-2644
422910501800	5	8	C	5	144	-	-8	-328	-	-668	-1034	-1442	-2058	-2728
422913252800	5	?	B	7	69	-	-	-	-	-	-	-	-	-
422910388000	5	9			90	75	-646	-1298	-	-1889	-2376	-3143	-4038	-4926

Final Report – Updating the Hydrogeologic Framework for the Northern Portion of the Gulf Coast Aquifer

UWI/API	Dip Section/ Position		Strike Section/ Position		KB	Stratigraphic Contacts (ft, msl)								
						Beaumont	Lissie	Willis	Upper Goliad	Lower Goliad	Upper Lagarto	Middle Lagarto	Lower Lagarto	Oakville
422910391400	5	10N			93	-	-	-	-	-1588	-2028	-2573	-3368	-4131
422910438400	5	11			90	-96	-488	-868	-	-	-1463	-2320	-3463	-4412
420710022600	5	12			53	-	-	-	-	-	-	-	-	-
4-18	5	12N			55	-	-	-	-1733	-2348	-2788	-3508	-4448	-5324
420713145800	5	13	B	5	54	-78	-703	-1018	-1738	-	-2998	-3606	-4573	-5498
420710097200	5	14			39	-128	-718	-1203	-1863	-2553	-3223	-3913	-4948	-5666
420710269600	5	15			19	-233	-783	-1298	-2278	-2990	-3835	-4463	-5358	-6233
420710274000	5	16			20	-248	-848	-1348	-2239	-2939	-3803	-4608	-5478	-6391
420710246600	5	17			16	-283	-893	-1348	-2382	-3138	-3990	-4701	-5588	-6653
420710243200	5	18			25	-328	-938	-1373	-2453	-3241	-4258	-4964	-5811	-7058
421670095600	5	19			19	-378	-968	-1613	-2523	-3278	-4393	-5153	-5803	-7268
421670095900	5	20			18	-393	-1048	-1668	-2568	-3360	-4478	-5491	-6368	-6588
427063011100	5	21			80	-	-	-	-	-	-	-	-	-
427063004200	5	22	A	2	75	-578	-1168	-1938	-3788	-4588	-5608	-6983	-7998	-
427064003100	5	22	A	3	90	-	-1198	-1828	-4033	-5415	-6411	-7968	-9558	-
427084014500	5	23			100	-888	-1608	-2388	-5463	-7218	-9328	-	-	-
427084028900	5	24			101	-1578	-2688	-	-	-	-	-	-	-
427084042900	5	26			95	-	-	-	-	-	-	-	-	-
427084062600	5	27			148	-	-	-	-	-	-	-	-	-
424713002200	6	1			407	-	-	-	-	-	-	-	-	-
424710014800	6	2			272	-	-	-	-	-	-	-	-	-
424710018000	6	3			363	-	-	-	-	-	-	-	-	12
424710018900	6	4			308	-	-	-	-	-	-	42	-233	-558
423390086800	6	5			316.2	-	-	-	-	-	-158	-438	-763	-1203
423390090100	6	6	D	3	343	-	-	-	-	-	-375	-904	-1228	-1653
423390008600	6	7	D	4	249	-	-	-	-	-	-740	-1108	-1438	-1858
423390020200	6	8			184	-	-	-78	-	-	-513	-1008	-1428	-1893
423393082000	6	9			172	-	-	-188	-	-	-	-	-1403	-1678

Final Report – Updating the Hydrogeologic Framework for the Northern Portion of the Gulf Coast Aquifer

UWI/API	Dip Section/ Position		Strike Section/ Position		KB	Stratigraphic Contacts (ft, msl)								
						Beaumont	Lissie	Willis	Upper Goliad	Lower Goliad	Upper Lagarto	Middle Lagarto	Lower Lagarto	Oakville
423390171800	6	10			127	-	-43	-353	-	-633	-988	-1714	-2218	-2868
423393073700	6	10A			97	-	-	-	-	-	-	-	-	-2738
422010760300	6	11	C	4	98	-	-348	-773	-845	-1338	-1699	-2183	-2738	-3281
422010272200	6	12			70	22	-438	-913	-1120	-1553	-1928	-2443	-3028	-3648
422013203800	6	13			65	-	-	-	-	-	-	-	-3223	-3833
422010280100	6	13			58	-48	-	-	-	-	-	-	-3863	-4533
422013261300	6	14			42	-113	-678	-1298	-1580	-2070	-2508	-3223	-3958	-4633
422010604400	6	15	B	4	34	-188	-796	-1338	-1633	-2478	-2978	-3808	-4648	-5413
420710309600	6	16			21	-218	-668	-1478	-2278	-3231	-3928	-4783	-5648	-6518
421670096600	6	17			22	-268	-818	-1661	-2470	-3603	-4603	-5308	-6220	-7098
421673009100	6	18			17	-603	-1165	-2130	-4578	-5823	-6968	-8348	-9363	-
427064038000	6	19			82	-548	-1038	-1720	-	-	-6200	-	-8098	-
427064009000	6	20			67	-868	-1598	-2398	-6778	-8878	-	-	-	-
427064044600	6	21			97	-	-	-	-	-	-	-	-	-
427084027900	6	22			81	-1598	-2683	-	-	-	-	-	-	-
427084062600	6	23			147	-	-	-	-	-	-	-	-	-
421850006100	7	1			267	-	-	-	-	-	-	-	-	-
421850003400	7	2			300	-	-	-	-	-	-	-	-	-
421850015000	7	3			350	-	-	-	-	-	-	-98	-233	-648
421853032100	7	3A			361	-	-	-	-	-	-	-	-288	-696
421853000900	7	4			341	-	-	77	-	-	-338	-684	-983	-1348
424733006600	7	5	D	2	292	-	-	-	-	-148	-590	-1015	-1343	-1753
423390101400	7	6			240	-	-	-188	-	-539	-922	-1340	-1698	-2168
423393085200	7	7			210	-	-	-198	-	-513	-913	-1328	-1676	-2190
422010004800	7	8			231	-	-	-208	-	-418	-920	-1298	-1608	-2188
422010010400	7	9			220	-	-	-218	-	-471	-947	-1368	-1678	-2244
422013140000	7	9.2			175	-	-	-	-	-	-	-	-	-
422013167000	7	9.7			137	-	-	-	-	-1178	-1628	-2048	-2533	-3038

Final Report – Updating the Hydrogeologic Framework for the Northern Portion of the Gulf Coast Aquifer

UWI/API	Dip Section/ Position		Strike Section/ Position		KB	Stratigraphic Contacts (ft, msl)								
						Beaumont	Lissie	Willis	Upper Goliad	Lower Goliad	Upper Lagarto	Middle Lagarto	Lower Lagarto	Oakville
422013162200	7	10	C	3	123	-	-128	-693	-	-1086	-1595	-2018	-2523	-3078
422010345500	7	11			104	22	-175	-650	-760	-1386	-1804	-2153	-2678	-3270
422010790400	7	10.5A	C	2	120	97	-138	-651	-	-1243	-1715	-2046	-2658	-3293
422010351000	7	11			88	97	-124	-698	-	-1201	-1698	-2138	-2748	-3580
422010505800	7	12			80	-38	-168	-938	-	-1388	-1958	-2368	-3173	-
422013001600	7	12N	B	2	48	-	-	-1173	-	-1926	-2403	-2968	-3458	-3953
422010556800	7	13			63	-75	-404	-1064	-1283	-1903	-2408	-2888	-3623	-4278
422010611400	7	14	B	3	61	-140	-438	-1070	-1376	-2196	-2688	-3508	-4293	-5133
421670003500	7	15			45	-188	-488	-1126	-1688	-2593	-3048	-3771	-4508	-5275
420390084700	7	15			52	-273	-600	-1268	-1698	-2660	-3248	-4018	-4668	-5540
421670187600	7	16			61	-418	-750	-1438	-2076	-3199	-3898	-4808	-5518	-6618
421670145300	7	17			50	-	-	-	-2230	-3368	-4109	-4993	-5813	-7015
421670144800	7	18			43	-413	-860	-1488	-2293	-3430	-4204	-5053	-5888	-7098
421670133600	7	19			42	-418	-904	-1536	-2371	-3478	-4148	-5018	-5878	-7188
421673003900	7	20			26	-498	-908	-1608	-2478	-3733	-4408	-5298	-6338	-7633
421670191600	7	21			26	-630	-1078	-1668	-2881	-4308	-5038	-5998	-7153	-8733
427060008600	7	21	A	1	52	-528	-985	-1558	-3272	-4943	-5863	-7158	-	-
427060002700	7	22			68	-688	-1120	-1858	-4418	-6606	-7508	-8678	-11006	-
427060012400	7	23			85	-	-	-2678	-6988	-	-	-	-	-
427064009700	7	24			90	-	-2328	-	-	-	-	-	-	-
424773062500	8	1			276	-	-	-	-	-	-	-	-	-
424770023900	8	2			362	-	-	-	-	-	-	-	-	52
424770027200	8	3			195	-	-	-	-	-	-	-	-	-
424770029400	8	4			214	-	-	-	-	-148	-348	-633	-863	-1243
420153013800	8	4.5			267	-	-	62	-53	-298	-500	-801	-1073	-1433
420150023000	8	5	D	1	160	-	-	22	-238	-378	-591	-808	-1118	-1493
424730024300	8	6			152	-	-	-78	-478	-778	-878	-1058	-1398	-1753
424730031800	8	7			211	-	-28	-268	-643	-1003	-1478	-1918	-2428	-3138

Final Report – Updating the Hydrogeologic Framework for the Northern Portion of the Gulf Coast Aquifer

UWI/API	Dip Section/ Position		Strike Section/ Position		KB	Stratigraphic Contacts (ft, msl)								
						Beaumont	Lissie	Willis	Upper Goliad	Lower Goliad	Upper Lagarto	Middle Lagarto	Lower Lagarto	Oakville
421570000100	8	8			158	-	-146	-378	-738	-1043	-1468	-1908	-2383	-2898
421570102600	8	9	C	1	123	-	-286	-583	-818	-1258	-1813	-2248	-2788	-3340
421573198300	8	10			102	124	-305	-593	-838	-1323	-1788	-2328	-3038	-3529
421570089400	8	11			89	22	-388	-665	-1143	-1800	-2368	-2848	-3773	-4277
421570245900	8	12	B	1	75	-88	-573	-843	-1478	-2093	-2618	-3093	-3953	-4683
420390145200	8	13			54	-216	-720	-1018	-2048	-2675	-3328	-3928	-4868	-6008
420390422400	8	14			45	-258	-793	-1118	-2103	-2823	-3488	-4128	-5188	-6978
420390427700	8	15			22	-381	-978	-1288	-2658	-3338	-4205	-4778	-5828	-7748
420390429100	8	16			14	-458	-983	-1318	-2783	-3593	-4543	-5358	-	-
427060002200	8	17			25	-653	-1193	-1548	-3538	-4783	-6018	-7378	-8798	-
420150001700	9	1			335	-	-	-	-	-	-	-	-	-
420153053900	9	2			314	-	-	-	-	-	-	-	-	-
420150066300	9	3			263	-	-	-38	-	-458	-668	-978	-1358	-1798
420150026200	9	4			212	-	-	-108	-23	-628	-893	-1193	-1650	-2120
420150068300	9	5			152	-	-	-298	-538	-1128	-1518	-1843	-2408	-2928
420153073800	9	6			129	-	-68	-428	-678	-1348	-1818	-2100	-2698	-3211
421573175200	9	7			141	-	-198	-428	-798	-1428	-1908	-2208	-2758	-3501
421573180500	9	8			124	-	-188	-550	-878	-1518	-2028	-2388	-3000	-3776
421570167400	9	9			84	-98	-458	-798	-1423	-2148	-2820	-3298	-3948	-4748
420390271500	9	10			61	-188	-403	-738	-1168	-1868	-2328	-3018	-4168	-5053
420390286500	9	11			57	-328	-633	-1183	-1653	-2518	-3158	-	-	-
420390389800	9	13			48	-528	-888	-1358	-1778	-2638	-3463	-4168	-5098	-6588
420393035000	9	14			33	-668	-1128	-1638	-2248	-3088	-3898	-4428	-5558	-7318
420393211000	9	15			43	-	-	-	-2813	-3708	-4500	-4988	-6583	-
420390481100	9	16			23	-598	-1123	-1418	-2933	-3898	-4708	-5848	-8148	-
427064036000	9	17			98	-	-	-3768	-5528	-6748	-	-	-	-
421493208800	10	1			388	-	-	-	-	-	-	-	-	-
421493132900	10	2			417	-	-	-	-	-	-	-	-63	-368

Final Report – Updating the Hydrogeologic Framework for the Northern Portion of the Gulf Coast Aquifer

UWI/API	Dip Section/ Position		Strike Section/ Position		KB	Stratigraphic Contacts (ft, msl)								
						Beaumont	Lissie	Willis	Upper Goliad	Lower Goliad	Upper Lagarto	Middle Lagarto	Lower Lagarto	Oakville
420893153100	10	3			293	-	-	-	-93	-376	-453	-618	-828	-1128
420890005700	10	4			250	-	-	-	-193	-528	-596	-728	-958	-1245
420890009000	10	5			331	-	-	-113	-548	-807	-933	-1118	-1348	-1745
420893124600	10	6			232	-	74	-123	-453	-872	-1140	-1378	-1718	-2264
424810121800	10	8			176	-	-21	-304	-755	-1228	-1638	-1866	-2351	-2980
424810120500	10	9			155	-	-48	-305	-926	-1408	-1645	-1968	-2488	-
424813344200	10	10			136	-	-98	-453	-933	-1488	-1858	-2248	-2673	-3390
424813403300	10	11			125	-	-120	-386	-1308	-1838	-2208	-2585	-3048	-3768
424813294400	10	12			121	-31	-303	-596	-1550	-2348	-2721	-3468	-4270	-5021
424810256200	10	13			92	-90	-353	-638	-1228	-1888	-2338	-3028	-3878	-4683
423210034100	10	14			70	-	-	-	-1524	-2138	-2878	-3518	-4668	-5783
422310067000	10	15			56	-315	-798	-1110	-1643	-2308	-3468	-4213	-5548	-6628
423210083600	10	16			45	-388	-923	-1218	-1678	-2318	-3825	-4498	-5823	-7598
423210082400	10	17			27	-458	-1038	-1158	-2428	-3103	-4431	-5018	-6808	-
427043007300	10	18			71	-628	-1288	-1376	-2853	-3633	-5375	-6736	-	-
427040007100	10	19			74	-768	-1448	-1508	-4213	-5268	-7528	-	-	-
427043000500	10	20			84	-	-	-1653	-4258	-5848	-	-	-	-
427040007000	10	21			77	-	-1958	-1958	-	-	-	-	-	-

## **APPENDIX C**

### **Estimated Total Sand Thickness at Each Geophysical Log Location**



*This page is intentionally left blank.*

**Appendix C Estimated Total Sand Thickness at Each Geophysical Log Location**

Well ID/API Number	Easting (ft)	Northing (ft)	Beaumont	Lissie	Willis	Upper Goliad	Lower Goliad	Upper Lagarto	Middle Lagarto	Lower Lagarto	Oakville
424810138700	6035547	18997873		129	196	175	220	165			
424810140100	6025918	18957772				187	125	151	155	195	335
424810114000	6135892	19014986				294	203	40			
424810067100	6229756	18982945	20	205	0	265	170	205	175	190	105
EBD_5	6200122	18995993			20	270	120	59			
EBD_6	6192590	19043826			0	85	190	0			
EBD_7	6053655	19069378			60	40	30	90	96		
420890035400	5999163	19131456						155	33	77	100
EBD_12	6061928	19050395			3	118	84	130			
420890044800	6003638	19084883					68	150	78		
420890001500	6022609	19186912						91			
420890044000	6000214	19087263					61	155	80		
420890005700	6013839	19166222						181	88		
EBD_17	6090905	19191390					0	185	90		
EBD_18	6057533	19223214							116		
EBD_19	6128111	19238651							235	202	8
420150062400	6073749	19238385							230	142	44
EBD_225	6151561	19120146			280	238	132	185	130	310	25
420150023000	6143877	19254370			105		58	169	198	215	110
EBD_24	6096029	19187933					26	240	75	195	
EBD_25	6047703	19256823								115	275
EBD_26	6050847	19208397						163			
EBD_44	6070047	18874065		74	11	190	60				
423210254700	6240661	18798392	220	130	95	385	289	305	561	230	
423210098800	6191378	18885869	119	155	185	195	60	175			
423210253900	6228962	18792716		123	117	290	397				
EBD_75	6155852	18849776		86	136	200	85				
EBD_76	6192898	18799336		130	85	210	85				
423210107500	6269562	18843776	255	125	0	238	242	55	119	651	
423210130600	6147221	18879363	83	207	0	55	25	145			
EBD_81	6146544	18890828		157	105	160	135	124	40	0	175
423010250700	6178707	18755395	185	195	29	166	239				
423210067000	6265951	18914119	140	100	0	85	220				
EBD_86	6204097	18930261	141	115	0	185	45	75			
EBD_87	6253457	18807755		260	310	555	276				
423210083800	6264301	18884252	230	100	0	160	150	131	479	190	
423210251400	6190532	18757551	131	79	30	240					

Final Report – Updating the Hydrogeologic Framework for the Northern Portion of the Gulf Coast Aquifer

Well ID/API Number	Easting (ft)	Northing (ft)	Beaumont	Lissie	Willis	Upper Goliad	Lower Goliad	Upper Lagarto	Middle Lagarto	Lower Lagarto	Oakville
422850002900	5937646	19070286						133	67	60	60
422850003000	5958331	19062729					31	190			
422850019100	5927649	19056557						87			
422850032600	5975280	19018207				70	45	105	97	85	140
420890009000	6049648	19165097			195		115	250	75	0	325
EBD_104	6056075	19023200		113	115	157	140	115	139	40	
EBD_105	6055086	19062786		81	118	75	109	129	118	69	195
420890034500	6022033	19141083					78	133	85	20	80
420893059400	6089433	19134546					100	190	0	31	30
420893057000	6041813	19103284			120	16	142	137	115		
420890097000	6072598	19106978			198	62	185	75			
420893102900	6076947	19086154			158	117	270	250	55	0	50
420893122100	5975303	19090595					45	120	90	70	
EBD_116	6042997	19067670			118	60	118	137	138		
420893137600	6106355	19114492			133	94	83	149	106		
420893107600	6122197	19118420		113	134	116	217	228			
420890008800	6064495	19176688					120	180			
420890072400	6080152	19064741			244	171	196	100	139		
424810002000	6111819	19083227		140	204	167	255	70	50	40	100
424810121800	6102782	19057901			171	53	228	29	70		
424810094300	6148386	19046336			221	208	295	153	232	125	389
424813344200	6145093	19020425		188	236	347	194	130	86	125	300
424813326000	6120115	19016247		125	195	225	145				
424813376900	6094382	19011199		149	205	165	131	84			
424813336100	6079109	18991918		193	77	350	146	136	98	50	220
424810147800	6068314	18956092		145	153	281	187	75	150		
424813147700	6100928	18951830		137	63	180	185				
EBD_131	6135287	18939030		144	190	541					
424810280200	6167272	18936731		115	190	562	236				
424813252100	6215588	18988959	181	195	264	340					
423210011600	6184689	18917157	142	216	178	569	110	157	48	60	
423210061200	6244259	18948676	257	77	146	565	140	112			
423210196700	6151230	18798446	166	224	209	616	273				
423210204300	6158877	18823819	104	151	145	460	185	234	0	110	
423210211900	6178236	18838273	197	227	143	641	249				
423213115900	6182739	18865643	52	193	66	344	330	20	90	33	259
423210102600	6214550	18883181	140	90	108	417	210	140	135	0	205
423210262100	6233281	18860934	207	208	140	360	205				
423210067100	6251340	18912232	298	308	164	429	301				

Final Report – Updating the Hydrogeologic Framework for the Northern Portion of the Gulf Coast Aquifer

Well ID/API Number	Easting (ft)	Northing (ft)	Beaumont	Lissie	Willis	Upper Goliad	Lower Goliad	Upper Lagarto	Middle Lagarto	Lower Lagarto	Oakville
423213082100	6297027	18874213	317	225	260	563					
423210217100	6101058	18864866	134	214	103	432	457				
423210229500	6110938	18821009	124	179	130	282	155				
423210013200	6192878	18902144	110	131	154	680	125	40			
423210083600	6269996	18872635	270	214	61	595	116				
423210082800	6306492	18840234	185	263	188	550	176	354	600	0	
420890075500	6040184	19035415		139	162	145	144	140	80		
420893059200	6029435	19082663			155	20	160	100	180	69	
420893022900	6068958	19156790			221		132	170	50		
EBD_159	5957261	19082322			23			160			
420893153100	6004105	19175688						178	117	0	50
EBD_161	6025240	18994211			146	170	261	111	65		
420893124600	6066177	19118867			178	63	152	202	145	173	105
420893160400	6002847	18989784				135	209	133			
420890067400	6019512	19012185				96	230	115	90		
420890048400	5974620	19059675					155	202			
420890043600	6004449	19097783					40	235	85	80	
424810067200	6232571	18983071	135	214	248	296	167	245	75	135	160
424810128800	6111701	18980214		159	239	444	243	151			
424813307900	6108106	19010674		185	209	325	278	190	80		
424813010500	6151231	19074697		102	203	161	222	73	25	20	290
EBD_171	6061751	18979796		69	106	235	80	105			
424813294400	6189931	18973689		164	202	566	210	270	115	144	381
424813058100	6025630	18987848			200	200	67	128			
424810098900	6168613	19046742		157	243	293	418	154			
424810354400	6078085	18895342		207	167	408	170				
424810140900	6026778	18940103			191	287	185	145			
424810355000	6046916	18957081			128	211	199	115			
424813162200	6179990	19068456		218	242	107	95	105			
EBD_179	6049076	18934575			105	271	185				
424813336500	6189263	18968935	30	184	159	556	219				
EBD_181	6149334	19036390		104	148	148	240	175	95		
EBD_182	6074555	18908110		110	115	180	140	55	65	42	
424813127300	6136168	18966466	0	73	131	382	260	115			
EBD_184	6119399	19099603		13	188	71	82	120	96		
423210257700	6266273	18777941	105	60	45	395					
423210214800	6188071	18823512	226	250	164	571	261	229	45	212	
423210077400	6312524	18857548	245	130	98	442					
423210257800	6277044	18791497	100	245	179	511	65	484	321		

Final Report – Updating the Hydrogeologic Framework for the Northern Portion of the Gulf Coast Aquifer

Well ID/API Number	Easting (ft)	Northing (ft)	Beaumont	Lissie	Willis	Upper Goliad	Lower Goliad	Upper Lagarto	Middle Lagarto	Lower Lagarto	Oakville
423210112000	6230278	18841983	216	339	263	397	225				
423213017100	6253662	18804959	80	180	330	485					
423210082400	6299307	18824202	310	235	120	410					
423210262600	6147983	18856948		222	127	460	280	176	4	115	
423210214700	6177638	18828994	211	239	130	545	65				
423210171200	6118886	18882327	103	184	128	500	280	93	0	0	
423210030800	6235611	18942219	233	283	252	622	273	85			
423210257600	6263408	18777305	160	106	190	280					
423210111400	6225170	18843419	248	238	224	575	310				
EBD_202	6108467	19010651		0	87	225	203	145	160		
EBD_204	6185295	18755000		101	60	330	345	470	462	588	
EBD_205	6281591	19027769		141							
421570137400	6189383	19046016				381	259	135	115	40	
421570102600	6236891	19133823		226	273	190	225	30	246		
421570000100	6229066	19164117		252	214	274	81	199	135	230	
421570245900	6315402	19059169		498	293	420	325	99	85	30	280
421570094000	6279327	19145816		384	235	171	234	106	85	66	
421570135000	6193749	19152656		112	172	185	110	177	218		
EBD_212	6195036	19096741	67	232	238	275	317	65	137		
421573038600	6282950	19117531		287	324	207	351	141			
421570134900	6193081	19149909				165	100	157	263		
421570099600	6250102	19162276		284	124	177	55	160	0		
421570188700	6272422	19064320		313	185	197	85	80	223		
EBD_217	6303491	19073050		169	215	227	308	210			
420390406900	6292992	18896903	266	206	239	488	217	483	152	650	
420390191000	6341751	18987784		214	324	582	185	170	40	235	
420390448100	6464519	18984140	145	330	40	305	455				
420390427700	6417671	18944064	240	348	120	640	305				
420390387800	6323921	18936857	179	240	247	328					
EBD_225	6279915	18904543	140	210	191	479	250				
420390103200	6451019	19001078	105	280	383	457	270	334	266	484	496
420390090300	6441119	19022759	43	155	190	435	250				
420390387800	6323921	18936857	120	50	90	322	318				
420390096500	6435791	19017796	217	100	288	444	466				
EBD_230	6272385	18990290	190	120	239	406	120	230	185	530	
EBD_231	6461942	18867280		363	140	540					
EBD_232	6309095	18942604	145								
420390001500	6393949	19093435		501	223	359	227	193	42	0	20
420390098400	6434456	19013797		109	265	490	506				

Final Report – Updating the Hydrogeologic Framework for the Northern Portion of the Gulf Coast Aquifer

Well ID/API Number	Easting (ft)	Northing (ft)	Beaumont	Lissie	Willis	Upper Goliad	Lower Goliad	Upper Lagarto	Middle Lagarto	Lower Lagarto	Oakville
420390392700	6286757	18924965		220	227	453	203	252	65	40	
420390446700	6370308	18934177	336	279	200	808	122	140	0	295	875
EBD_237	6393456	18884323	220	325	286	679	425	228	966		
421570089400	6294046	19105171	27	310	322	281	320	162	219	210	249
424810189100	6097247	18925473	110	75	140	480	180	193			
424810188500	6103214	18925496	110	100	101	318	211	90			
424810138700	6035629	18997786			196	175	200	90	130		
EBD_244	6072374	18903525			180	439	179	155			
424810120500	6130797	19058526			256	155	346	136	133		
EBD_246	6112175	19035449			218	250	253	185	135	384	100
EBD_247	6144736	18944436		86	221	428	249	176			
EBD_248	6276521	18854390	233	225	230	447	128				
423210033700	6225629	18917704				206	25	172	160		
423210168300	6157303	18866550	85	65	86	464	120	70			
EBD_251	6195757	18877908	129	176							
EBD_252	6150730	18893582	30	161							
EBD_253	6338665	18885975	216								
420390286500	6288679	18959489	125	155	155	615	130				
EBD_255	6366107	18892648	212	118	101	246	284	65			
420153073800	6174120	19112131		130	223	192	75	20	100		
420393256500	6404696	18919506	190								
EBD_260	6429280	19082415						113	72	140	151
420393189100	6346955	18863970	140								
EBD_263	6368079	19047839	70	175	305						
420390426300	6407996	18984584	135	120	155	320	334				
420393229400	6416088	18935653	289	290	142	733	240	175	45		
420893112000	6014502	19044835					125	160	130		
420893161100	5939001	19130198							60	116	49
EBD_269	5988239	19082798			110		119	165	50		
420893193200	5953273	19082449						134			
420893198100	6068393	19027571			72	273	110	130			
EBD_274	6008063	19158368			66			186			
421573200200	6330100	19057069				260					
421573116500	6288958	19078577		284	237	269	328	107			
EBD_278	6359625	19102949		230	268	52	331	164	10	220	130
421573173200	6200028	19093983		72	0	0	0	0	0	20	170
421573169500	6196609	19116839		205	313	232	158	185	235	0	
421573181500	6238903	18996338		197	240	529	64	166			
421573180500	6207094	19057332		179	227	353	233	212	180		

Final Report – Updating the Hydrogeologic Framework for the Northern Portion of the Gulf Coast Aquifer

Well ID/API Number	Easting (ft)	Northing (ft)	Beaumont	Lissie	Willis	Upper Goliad	Lower Goliad	Upper Lagarto	Middle Lagarto	Lower Lagarto	Oakville
EBD_283	6274356	19024285		130	255	565	170	175			
422853177700	5923737	19084585							130		
422853195700	5907566	19105247							70		
EBD_290	6153423	19323612							75	365	
424733043200	6177972	19317170							140	244	211
EBD_292	6184616	19171764			114	110	46	179	240	192	138
424813307900	6108186	19010587		163	177	312	268	190	117		
424813327400	6100732	19005183		153	219	309	212	45			
424813211700	6227114	18999540	131	175	85	185					
424813352200	6214022	19003346	157	201							
EBD_298	6318618	18968396		228	295	429	160	175			
EBD_299	6308343	18901208	310	180	185	557	299				
EBD_300	6349299	18931569		237	138	448					
421570113700	6192548	19094449	70	226	235	272	271	65	117		
EBD_302	6236256	19132172		294	218	160	232	65	153		
EBD_303	6262293	19039402		123	310	424					
EBD_304	6252548	19095403		324	187	150	197				
EBD_305	6315523	19046382	58	354	218	279	150				
EBD_306	6274778	19010070	143	172	271	325	165				
EBD_307	6215320	19070822	40	218	59	113					
EBD_308	6303389	19074491		207	193	285	295	185			
EBD_309	6190673	18822650	176	245	164	476	190	250	40	197	
423210260000	6293447	18833299	255	284	140	546					
423210083600	6269485	18872399	310	214	88	638	151				
EBD_313	5977545	19059836			133		76				
EBD_314	6076088	19133270		50	80	30	170	55			
EBD_315	6004101	19049339			175	20	204	84	149		
EBD_316	6101940	19105517			159	89	228	125	135	60	85
EBD_317	6111003	19092066			196	139	223	110			
EBD_318	6120761	19266850						90	130	135	
EBD_319	6157586	19244142				3	99	185	200	142	
EBD_320	6162314	19185674				30	0	130	174		
421573198300	6247603	19108125		194	246	120	150	95	75	75	
420390145200	6362263	19009842	233	277	333	366	275	310			
EBD_323	6360775	18976334				357	343	340	120		
420390429100	6423511	18905824	255	255	179	601	335	380			
EBD_325	6175801	19177208			160	45	20	245	234		
421670105400	6475045	19001591	157	291	214	375	360	290			
EBD_329	6338123	18924765	175	295	338	577	165				

Final Report – Updating the Hydrogeologic Framework for the Northern Portion of the Gulf Coast Aquifer

Well ID/API Number	Easting (ft)	Northing (ft)	Beaumont	Lissie	Willis	Upper Goliad	Lower Goliad	Upper Lagarto	Middle Lagarto	Lower Lagarto	Oakville
EBD_330	6321900	18921416	130	260	239	431	180				
EBD_332	6209155	18841392	119	270	181	582	158				
EBD_334	6241789	19006834		155	206	534	167	308			
EBD_346	6151903	19163141					55	145	45		
EBD_347	6229839	19200035						161	168	271	
EBD_354	6196274	19231333			20	85	0	121	214		
EBD_355	6344977	19073228		302	243	235	190	105	0	70	
EBD_357	6360494	18831855	83	122	0	655	275	0	0		
EBD_358	6099044	18896535		254	231	472	167	115	0	35	210
424810138700	6050833	18985898								120	
421493204900	5931159	19170265								70	35
421493262000	5902102	19112993								54	
420390006400	6397739	19088576		290	195	64	101	110	15		
420393250100	6386483	19079573		200	270	332	298	130	45		
427060008800	6482716	18894852		0	70	216	397	117	300		
420710246600	6597932	19122763	195	100	0	310	265	165	200	400	465
420710243200	6596852	19111443	65	225	0	290	290	495	228	522	470
420710274000	6584152	19138044	70	129	141	0	215	390	243	367	110
420710309600	6517714	19104289	85	56	283	75	55	170	106	214	270
420710097200	6560919	19179218		240	352	353	125	135	120	215	
420710022600	6534334	19216606	119	238	202	116	0	0	75		
420710269600	6572169	19153816		194	145	255	175	232	82	81	520
420713130200	6662843	19211970					160	140	335	280	415
420710217700	6672479	19180242	150	160	215	460	205	335	260	545	420
420710108300	6593213	19226774	128	207	0	0	45	132	253		
420713145800	6557180	19199503	45	329	26	455	170	105	195	250	270
421573115200	6360127	19064157		211	266	252	53	225	70		
421570100400	6245520	19159642		301	184	200	165	125	60	90	30
421573200700	6330819	19060746						0	145		
421570003000	6257544	19167754		329	227	176	79	154	75	145	140
421573039600	6283805	19115175		139	330	181	190	124	156	137	
421570083600	6316849	19097772	95	234	221	92	316	107	75	150	
421670095600	6596153	19074141	65	175	0	297	213	250	295	213	392
421670144800	6485285	19021817	153	398	2	113	317	220	190	495	440
421670003500	6439874	19088039	71	342	120	0	35	130	110		
421670127600	6457206	19073297	149	262	273	0	195	231	169		
421670096600	6537738	19060684	347	470	165	50	255	315	130	430	60
421670114200	6523244	19034535	234	306	85	263	583	255	353	426	130
421673009100	6569284	19011469	335	177	139	544	190	160	180	245	620



Final Report – Updating the Hydrogeologic Framework for the Northern Portion of the Gulf Coast Aquifer

Well ID/API Number	Easting (ft)	Northing (ft)	Beaumont	Lissie	Willis	Upper Goliad	Lower Goliad	Upper Lagarto	Middle Lagarto	Lower Lagarto	Oakville
421670145300	6475479	19034725					255	525	190	425	275
421670191600	6531985	18977770	413	192	135	470	360	75	380	355	25
421673003900	6497573	18992070	273	253	170	300	440	355	360	475	160
421670187600	6458560	19045976	105	163	7	178	417	320	110	105	
421673025300	6468490	19062563	231	280	175	55	255	328	131	190	
421670133600	6490770	19010249	31	388	67	113	351	121	265	480	82
427064036300	6595991	18909996		0	230	505	525	0	85		
427064019700	6552209	18810889		300	305						
427060002700	6559667	18896699	214	196	183	530	915	115	115		
427083010100	6677418	19042007	116	70	0	457	208	160	170	509	176
427064038000	6621033	18952023		129	61	225	250	0	315	71	819
427060008600	6542100	18927673		180	135	190	665	70	370		
427060012400	6607345	18851523			310	880	255	0	45		
421853000900	6226459	19351112						110	245	110	45
421850015000	6207538	19388735								65	136
421850003400	6179843	19436005									45
421993181100	6759574	19418957		290	562	25	224	270	280	265	125
421993181600	6715021	19424367		215	315	25	238	140	90	180	191
421990033500	6739426	19420379		296	389	20	185	151	144	344	171
421990214800	6689564	19336220		190	285	75	310	15	280	245	
421990063400	6687658	19418344		189	176	285	238	167	63	117	216
421990067400	6677823	19383023				380	266	165	211	253	
421990075700	6615265	19437827		143	142		30	55	260	105	55
421990011600	6763202	19463454		218	312			35	295	450	285
421990061800	6673005	19451673			181		190	173	142	270	90
421990035600	6746770	19392117		302	444	11	310	205	305	540	340
422013205200	6411847	19225140			278	37	135	56	185	115	15
422013095800	6457974	19287751			320	77	191	114	355	200	255
422013001600	6427881	19140791	95	275	145	35	265	180	135	70	55
422010789200	6220253	19282328				17	18	155	296	149	102
422010293600	6425032	19182019		107	95	28	269	33	155	85	
422010604400	6491587	19130714	170	350	225	85	180	150	380		
422010406800	6322709	19168878		408	196	135	228	188	75	205	260
422010394800	6292789	19223697		160	240	110	195	70	135	95	40
422010790400	6334467	19203515		410	216	128	385	1	125	195	30
422010325200	6374025	19239412		387	446	12	110	135	260	200	248
422013136800	6453367	19116043	113	127	70	120	160	35			
422010800701	6312333	19187461		494	141	125	423	36	231	125	190
422010439500	6291106	19162306			90	180	325	170	155	230	160

Final Report – Updating the Hydrogeologic Framework for the Northern Portion of the Gulf Coast Aquifer

Well ID/API Number	Easting (ft)	Northing (ft)	Beaumont	Lissie	Willis	Upper Goliad	Lower Goliad	Upper Lagarto	Middle Lagarto	Lower Lagarto	Oakville
422010505800	6379919	19134206		258	167	30	170	70	40	150	100
422010760300	6428781	19273641		90	245	35	165	85	285	135	125
422010351000	6361602	19181395		346	160	151	80	260	105	245	285
422010622300	6507604	19165458	145	330	249	271	195	70	165		
422010556800	6410273	19124981	120	455	152	71	336	211	125	250	165
422010004800	6282194	19286000		92	143	0	84	321	110	85	195
422010334300	6359558	19228786		90	200	0	45	50	15	90	250
422010345500	6348028	19210373		320	208	77	278	84	85	209	179
422010272200	6443858	19246140		382	352	85	148	130	175	140	191
427084012700	6809788	18961303					30	0	0		
427084027900	6696328	18839148		400	188						
427084042900	6760611	18822676	529	485	220						
427084043600	6722072	19028876	60	0	0	229	304	132	150	740	140
427084057200	6867127	19078588		260	340	555	409	26	450	400	
427080010000	6714021	18950395	103	10							
422413054500	6807057	19493985		155	80				444	516	105
422410025000	6777588	19557366									261
422410020500	6781312	19434419		295	464	21	20	194	292	429	225
422413030800	6790652	19588656									420
422410030000	6819735	19449051					227	346	422	275	85
422453035800	6860134	19181335					245	140	835	835	
422450150100	6825806	19252168			195	405	270	271	494	755	260
422450054100	6753055	19298814	60	90	55	259	266	345	345		
422450131800	6794610	19283468	110	270	0	245	295	25	166	669	455
422450226500	6724897	19236601	171	259	190	300	330	200	384		
422450016900	6769404	19321496	149	196	180	287	193	260	268		
422450163700	6784852	19246933	80	527	143	235	250	265	190	520	160
422450299600	6794675	19172227	175	445	180	675	365	573	177	541	
422453014300	6782065	19204644	125	267	248	630	490	261	174	637	443
422453156200	6696143	19311817		275	255	185	184	146	280		
422450268900	6735517	19195489	95	292	273	95	430	210	350	305	280
427104005600	6878346	18930326		75	120						
427080001000	6823316	19122295	120	254	298	563	325	305	409	601	275
427083038100	6748272	19078332					323	220	170	10	300
426060005500	6740605	19125533		45	291	404	315	165	200	190	
427084052300	6826349	19023338	85	0	0	130	205	35	0		
422910484100	6661516	19236709	105	145	205	75	65	65	375	455	
422910438400	6535229	19245935		320	285	270	120	150	230	134	316
422910371100	6569002	19272058		335	277	253	205	99	141	315	

Final Report – Updating the Hydrogeologic Framework for the Northern Portion of the Gulf Coast Aquifer

Well ID/API Number	Easting (ft)	Northing (ft)	Beaumont	Lissie	Willis	Upper Goliad	Lower Goliad	Upper Lagarto	Middle Lagarto	Lower Lagarto	Oakville
422910243100	6508147	19347883				0	30	159	126	70	135
422910210400	6584210	19307361	40	240	41	151	158	205	170	80	
422910242600	6534097	19314894		263	274	17	107	126	106	203	184
422910216900	6573235	19346238		399	209	22	152	108	185	380	
422910033300	6660610	19291750		170	205	185	115	150	135		
422910029400	6509054	19399214			120			180	130	155	170
422910018900	6566099	19424338						8	196	159	157
422910028400	6533195	19375991						101	150	190	250
422910453700	6610423	19236356	120	205	30	150	260	65	165		
422910180200	6607083	19324437		385	236	119	95	110	310		
422910388000	6490748	19294133		330	377	25	18	110	110	120	190
422910008600	6476732	19375831			208	17	55	113	182	135	277
422910030200	6576030	19402262		150	255			37	330	273	246
423390187200	6401877	19376216			72	13	184	111	325	201	99
423390184100	6443968	19332729		343	162	35	0	255	235	145	110
423390173700	6374148	19299552		90	160	15	50	115	270	75	0
423390099800	6242155	19422707							181	118	25
423390110200	6302438	19307763					145	219	191	30	175
423390110900	6325024	19338933				4	202	225	227	64	208
423390008600	6352177	19391390						269	134	53	149
423390171800	6406161	19314832		45	30	10	0	140	165	40	100
423390004500	6375417	19428536			20			20	115	215	120
423393047800	6275032	19356503					40	195	130	25	35
423393082000	6378775	19343000								0	40
423390188700	6299763	19376145					40	185	155	70	36
423510016700	6907323	19537070			174	0	309	186	235	100	45
423510042500	6897800	19675953									295
423510021300	6872898	19455792		175	65	90	188	269	278	360	
423510009600	6856912	19486070						254	222	228	0
423510004800	6852830	19632356								282	305
423510028900	6859974	19391595		338	136	349	381	292			
423613079100	6820149	19337396		487	100	315	125	250			
423610048000	6875801	19313501	85	284	11	267	443	195	555	691	179
423613081000	6857207	19349397							366		
423610032800	6835399	19303597	88	400	180	439	398	356	362		
423730003700	6483661	19514550									80
423730042300	6590935	19467153			200				335	160	115
423730035900	6543506	19477894			188				35	281	151
423733012000	6502889	19574164									113

Final Report – Updating the Hydrogeologic Framework for the Northern Portion of the Gulf Coast Aquifer

Well ID/API Number	Easting (ft)	Northing (ft)	Beaumont	Lissie	Willis	Upper Goliad	Lower Goliad	Upper Lagarto	Middle Lagarto	Lower Lagarto	Oakville
423733097500	6521861	19506113									72
423733050500	6556408	19454929			216			13	247	169	228
423733009100	6576397	19519328							90	196	169
424070002100	6514444	19463049							289	131	65
424070024100	6477146	19425059			82		65	60	87	53	165
424073001800	6417944	19419616			140			0	366	247	107
424070015600	6437956	19429274			153				253	114	255
424073003300	6412605	19488184			0				59	196	147
424570037700	6727681	19478960		150	135				65	405	156
424570006300	6642012	19476871			297		179	116	262	138	125
424570047700	6625226	19526619							258	221	165
424570024500	6722243	19524297			139					415	0
424573012100	6668835	19547439								339	105
424710018000	6290898	19492178									42
424710018900	6311449	19462903								175	120
424713020200	6339392	19522213								78	25
170112090100	7078464	19612229			202	7	203	130	40	265	225
170110064200	6948259	19511436		170	15	145	180	105	170	250	125
170110013500	7085528	19519145			30	343	153	61	148	350	285
170110039800	6969007	19479613		349	243	260	155	230	180	353	
170110008700	6989005	19581718			406	140	170	276	239	190	250
170110009500	7017922	19570238				140	125	160	195	0	179
170112089800	7106674	19617615			152	51	68	44	115	220	97
170112061600	6949631	19603888				269	316	56	71	55	70
170112053200	7033590	19503747		235	255	180	0	215	90	315	235
170190189600	6958485	19322976				350	144	211	352	628	545
170190145800	7029815	19371241	195	350	212	3	290	51	150	534	470
170190184300	7004309	19330866	55	465	100	535	295	215	480	811	544
170190000400	6919344	19430724		318	301	356	65	200	270	535	
170190036900	6978408	19433548		402	183	150	20	128	182	330	114
170192020200	7027987	19336158	221	577	67	568	331	239	322	764	560
170192183600	7041500	19431862						190	94	266	244
170192046300	6939665	19336737	175	345	80	497	203				
170190199700	6908291	19328803		349	71	45	492	199	294	416	578
170230187300	6902485	19223735	141	242	228	495	365	140	535	950	350
170230140000	7051816	19245034	170	399	317	434	310	122	748	380	
170230124200	7062529	19294675	70	480	135	362	113	60	455	1105	185
170232012700	6932839	19301632	171	462	87	180	30	40	132	528	648
170230159900	7009076	19286035	134	285	40	635	265	25			

Final Report – Updating the Hydrogeologic Framework for the Northern Portion of the Gulf Coast Aquifer

Well ID/API Number	Easting (ft)	Northing (ft)	Beaumont	Lissie	Willis	Upper Goliad	Lower Goliad	Upper Lagarto	Middle Lagarto	Lower Lagarto	Oakville
170230050900	7018183	19292531	160	494	106	305	320	211	59		
170232228000	7001711	19273624	265	455	41	519	393	347	538	1164	148
170230156200	6996388	19252868	518	244	28	227	215	235	475	935	135
177000003900	6941066	19158910	77	425	585	845	650	142	528	540	
170230178800	6996760	19212964	250	394	258	528	565	400	705	560	270
170230205500	6870643	19234206	187	397	150	452	393	379	612	737	267
170230204500	6947091	19204651	274	340	280	685	120	240	515	856	420
170230196800	6937304	19225835	40	390	284	1001	417	203	15	0	
170232013100	6936300	19293730	82	290	319	454	480	325	405		
170230020800	7016818	19302085		420	268	472	135	144	403	1313	
177000004600	6900494	19177646	185	282	343	364	181	246	245	701	
177014036000	7013761	18953823		1180	517	133	15				
177014018600	6937571	18944531		432	502						
427104007600	6893773	19081388		224	546						
171150004600	7024783	19627802			153			102	235	340	205
171150002200	7107131	19673816									225
171158800300	7080268	19649629			190		239	151	265	130	170
171150002700	6951518	19723106									163
171158800000	6961729	19633810			90	101	341	180	156	361	133
171152000400	6950285	19692507							170	270	155
8-8	6137820	19187234						270	200	109	128
420150014600	6152959	19257358				19	58	138	136	72	23
9-12	6112469	19136351			132	51	115	129	35	57	68
420390142000	6390726	19029005	115	90	60	231	174	155	160		
420390171100	6401922	18992147		100	75	140	460	180	202		
420390451800	6455349	18925907	180	0	95	325	390	110	561	44	
8-16	6345678	18931404	250	50	120	290	80	170	188	422	
6-17	6435069	19008393		120	227	128	335	70	45	470	
420410010200	6131626	19376386									15
420710120900	6619426	19198310	84	81	40	409	181	140	310	340	180
420710251300	6631951	19152781	44	271	30	250	130	345	210	315	450
420710288000	6560351	19096993		150	63	460	125	347	120	385	245
420710306200	6521080	19140544		135	25	65	120	195	330	242	
8-12	6210615	19033351				300	90	30	30	205	
2-17	6690084	19252954			0	115	295	160	280	419	276
5-8	6286484	19447835								95	60
5-9	6325797	19418216						34	161	75	191
424573010100	6626183	19586222								155	3
424570020000	6692993	19478815			255				174	281	67

Final Report – Updating the Hydrogeologic Framework for the Northern Portion of the Gulf Coast Aquifer

Well ID/API Number	Easting (ft)	Northing (ft)	Beaumont	Lissie	Willis	Upper Goliad	Lower Goliad	Upper Lagarto	Middle Lagarto	Lower Lagarto	Oakville
424710004200	6341255	19455136								210	100
4-7	6348648	19513874								114	15
4-8	6373190	19497566								110	20
424730000300	6131102	19293345								278	100
424730004900	6193467	19230080			216	99	7	114	121	335	125
8-9	6186746	19160387		76	179	150	7	248	120	130	90
9-13	6140487	19077574			225	78	252	75	25	20	160
G0840063A	6527220	19082022	130								
G0930048C	6193703	19375123							95	136	136
G0930049B	6203271	19380818							95	75	
G0930020A	6198917	19407043									115
G1000055B	6667258	19417599		154	81	0					
G1000055A	6614156	19418983		250	126		71	59			
G1000016C	6711702	19330796	40	158							
G1010003C	6510644	19173186	125								
G1210016B	6833291	19508429		260	155						
G1210064A	6807589	19580624								501	
G1210003C	6816760	19443408		410							
G1700026A	6338588	19396499			60			185	186		
G1700578A	6299607	19379085			75		0	22			
G1700039A	6356143	19345195			85	0	80				
G1700742A	6379226	19308164		108	115						
G1700764A	6283835	19393126							315		
G1700197R	6354832	19315712			247	17	90				
G2040005B	6450017	19502661			25				13	126	
G2360052B	6295433	19511347									24
6036904	6333848	19400705						257	180	25	85
6043304	6292300	19387372						227	317	9	0
6037803	6354065	19406893							200	180	70
6043101	6266528	19388300							0	0	15
6038102	6379628	19428820									0
6044101	6309478	19391117								45	75
6047604	6443591	19379689			44	76	220	80	110	40	0
6047404	6428302	19368810				90	125	204	21	0	0
6046604	6409614	19371545					130	176	161	83	72
6046504	6392402	19367057		160	0	0	85	194	276	0	40
6045904	6368414	19362404		64	26		61	94	25	60	170
6052601	6333896	19321781				15	121	225	101	83	161
6052704	6304184	19307717					175	215	160	35	75

Final Report – Updating the Hydrogeologic Framework for the Northern Portion of the Gulf Coast Aquifer

Well ID/API Number	Easting (ft)	Northing (ft)	Beaumont	Lissie	Willis	Upper Goliad	Lower Goliad	Upper Lagarto	Middle Lagarto	Lower Lagarto	Oakville
6053105	6345942	19338282						125	291	56	85
6062301	6413727	19306359			112	13	270	178	132	24	26
6054302	6409027	19346899			46	40	87	147	171	25	120
6045302	6370621	19395724							191	77	155
6036304	6326487	19430899								115	95
6044507	6318425	19373019							106	115	60
6053810	6354043	19315418				21	142	260	157	136	133
6036403	6298562	19420955									135
6035203	6274436	19427923							170	110	35
6026801	6238054	19451436									116
421853002800	6215597	19426924									75
422013218700	6335440	19292091		222	223	0	60	105	205	25	30
422013162200	6341428	19220060		258	277	9	188	133	155	220	175
422010360700	6343269	19221520		175	125	15	85	85	0	145	45
422010353300	6338258	19243596		285	260	0	160	60	195	50	190
422010297200	6387575	19246031		185	246	32	107	85	150	40	45
422010265800	6475665	19251004		207	278	111	19	155	52	153	110
422010106500	6471852	19274177		343	246	54	0	105	120	50	70
422910501800	6483075	19355323			205	10	46	94	90	100	70
422910016800	6462593	19361925		154	116	0	55	85	140	95	35
4-13	6459571	19366096								17	200
4-14	6472300	19349334			170	0	75	96	148	151	85
4-15	6511924	19334960									40
423390090100	6334928	19402648						254	232	80	80
423390086800	6331721	19421155						52	144	149	65
423393007200	6248768	19361473			110			75	205	50	70
423390173100	6412588	19273018		305	219	66	135	40	250	15	185
423390160400	6407861	19349006			25	20	66	133	89	17	100
423390101400	6261488	19303614			177	8	205	234	169	157	10
423390103900	6296407	19334182					48	287	206	129	85
423390099400	6286691	19385622								162	50
423390020200	6353670	19363513					0	165	210	175	100
424070021400	6448475	19406206			65			150	50	75	110
4-9	6395093	19449937									80
424713023200	6379205	19459006							80	85	105
LBG MONT01	6291289	19395046							200	35	65
LBG WALK11	6317058	19517758								60	0
LBG WALK12	6319349	19515013								50	81
LBG WALK13	6323073	19511313								25	25

Final Report – Updating the Hydrogeologic Framework for the Northern Portion of the Gulf Coast Aquifer

Well ID/API Number	Easting (ft)	Northing (ft)	Beaumont	Lissie	Willis	Upper Goliad	Lower Goliad	Upper Lagarto	Middle Lagarto	Lower Lagarto	Oakville
LBGWALK14	6321694	19513082									15
LBGWALK15	6321152	19509209									0
LBGWALK16	6323680	19513567								25	15
LBGWALK17	6318441	19509404									0
LBGWALK18	6316943	19507621								30	45
LBGWALK19	6316883	19504781								60	0
LBGGRIM06	6160698	19380023								55	30
LBGGRIM11	6153783	19383342								0	80
LBGGRIM15	6163756	19376016								45	
424073007800	6440158	19461691								173	100
424713001600	6291884	19462417								66	86
424733006600	6241432	19332932						224	131	65	55
6-12	6331793	19205413		350	190	67	373	0	175	85	0
6-11	6318130	19222403		260	252	103	300	105	153	187	230
6-10	6283316	19219061			207	160	233	75	188	62	125
424713019200	6301685	19454125									250
424713025100	6357613	19500162								125	45
421853039900	6203803	19351332								186	91
424073048000	6418690	19449840								198	182
421853024100	6199243	19361597							175	100	134
424713024500	6342767	19504034								150	17
424713023600	6333534	19523880								104	41
424713029500	6319892	19453560								110	59
424713001400	6301381	19454199								51	37
422013079800	6423005	19265237		139							
422013236800	6232768	19233349				105	0	65	150	50	40
424733037900	6227188	19347836							240	127	198
424073045300	6432490	19364288			48	56	6	130	90	40	63
422013206200	6421696	19219532			328	98	126	83	255	175	
423393077700	6390542	19347836								25	175
422013237500	6284595	19244152			156	18	191	190	148	92	115
423393079400	6378435	19310513								60	90
422013150600	6213218	19262301					45	117	109	186	0
424073046800	6451008	19464078								209	50
422013196200	6301253	19280969		124	151	2	144	206	50	40	0
423393084900	6451506	19319051					40	169	181	40	197
421853042300	6432490	19449547			85				70	25	130
422013226500	6473654	19262834	80	425	315	67	73	95	294	131	190
424070012700	6401238	19521879								105	0



Final Report – Updating the Hydrogeologic Framework for the Northern Portion of the Gulf Coast Aquifer

Well ID/API Number	Easting (ft)	Northing (ft)	Beaumont	Lissie	Willis	Upper Goliad	Lower Goliad	Upper Lagarto	Middle Lagarto	Lower Lagarto	Oakville
423393085200	6276772	19295452			140	5	138	187	73	44	158
422010010400	6285328	19280179			160	0	105	205	130	125	50
4-17	6524557	19277760						108	225	239	353
4-18	6544344	19218637				155	60	130	140	115	307

## **APPENDIX D**

### **TWDB Comments on Draft Hydrostratigraphic Report and Responses**

*This page intentionally left blank.*

## **D. TWDB Comments on Draft Report and Responses to Comments**

This section lists the comments provided by the TWDB on the draft report and INTERA responses to the comments. The comments were received on May 4, 2012 from the contract manager Cindy Ridgeway.

### **D.1 Report Comment**

- Comment 1.** Page viii, Figure 6-10: please change “Upper” Lagarto to “Lower” Lagarto for consistency with data used to develop the referenced figure.
- Response 1.** The suggested changed has been made.
- Comment 2.** Page xi, bottom paragraph: please insert "geophysical logs" after "650" or please clarify what was examined. If the intent is to reference geophysical logs, please note that number changes to 660 elsewhere in the report; for example, page 4-6 and page xi, paragraph 4, sentence 1. Please adjust values so they are consistent throughout the report and/or match the data provided in the geodatabase.
- Response 2.** Report has been changed so that 666 geophysical logs” instead of “approximately 650” or “660”. The 666 value is consistent throughout the rest of the modified report and is the number of logs listed in Appendix A.
- Comment 3.** Page 1-3, paragraph 2: Please clarify second sentence. It is unclear if the wrong dip sections were referenced and therefore if the intent was to describe preference for Mr. Knox’s picks were used for dip section 9 and preference was given for Dr. Ewing’s picks for dip section 8.
- Response 3.** To clarify the second sentence, the sentence was replaced with the two following sentences: “For dip section 9, Mr. Knox’s picks were given preference over Dr. Ewing’s picks. For dip section 8, Mr. Ewing’s picks were given preference over Mr. Knox’s picks.”
- Comment 4.** Page 1-3, Section 1.2, paragraph 1: please explain why only 500 geophysical logs were used for the lithologic analyses instead of the 650-660 used for the stratigraphic correlations and on page 1-4, last paragraph, please explain why only 632 logs were used for developing the sand maps.
- Response 4.** The report has been modified state that result from approximately 800 log analyses were used as part of this study (these locations shown in Figure 4-4). Of the 800 log analysis, 666 new analyses were generated as part of this study. This study used lithologic picks from approximately 600 logs to generate the sand maps. Not all of the logs were used to generate the sand maps because some of the “stratigraphic” logs and “paleomarker logs” were not analyzed for lithology. In general, the “stratigraphic logs” are located along our dip and strike lines, the “lithologic” logs were more spatially scattered, and the paleomarker logs are near the coast.
- Comment 5.** Page 2-2, line 1; page 3-21; and Figures 3-8 and 3-9: cited Weiss (1992) however this reference was not provided in the reference section. Please either adjust the citation or update the reference section accordingly.
- Response 5.** We have added Weiss (1992) to the reference section.

- Comment 6.** Page 2-5, paragraph 2, line 5; page 2-23, Figure 2-6; page 3-14, paragraph 2, line 3; and page 3-22, Figure 3-10 (in figure caption): please specify "a" or "b", or both, after the citation of "McGowen and others (1976)" for consistency with the reference section.
- Response 6.** We have modified the citation to McGowen and others (1976) to McGowen and others (1976a,b).
- Comment 7.** Page 2-7, last line: please update "Figure 1" with the appropriate figure in the report—possibly with Figure 2-8.
- Response 7.** Figure 1 has been renumbered to Figure 2-8.
- Comment 8.** Pages 2-10 to 2-11, Table 2-2: please update header from “Map Number (See Figure 3-8)” to “Map Number (See Figure 2-8)” and please add comma to the numbers greater than 999 in the table.
- Response 8.** The suggested change has been made.
- Comment 9.** Page 2-18, line 8: please update reference to “(3-21)” to “(Figure 2-21)”.
- Response 9.** The suggested change has been made.
- Comment 10.** Page 2-19, line 6: cited Tedford and Hunter (1984) and Baskin and Hulbert (2008); however, these references were not provided in the reference section. Please either adjust the citations or update the reference section accordingly.
- Response 10.** The two missing references have been added to the bibliography.
- Comment 11.** Page 2-24, Figure 2-7: please label counties on map to assist with identifying where in the Houston area subsidence and active surface faults exist.
- Response 11.** The counties in Figure 2-7 have been labeled.
- Comment 12.** Page 2-25, Figure 2-8: please adjust reference “Line of cross section (Figure 3)” to “Line of cross section (Figure 2-10)”.
- Response 12.** The suggested change has been made.
- Comment 13.** Page 3-1, line 2: please update reference to Table 3-1 to Table 2-1.
- Response 13.** The suggested change has been made.
- Comment 14.** Page 3-2, paragraph 2, line 5: cited Jones and others (1956); however, this reference was not provided in the reference section. Please either adjust the citation or update the reference section accordingly.
- Response 14.** The missing reference has been added to the bibliography. The correct reference is Jones (1956) and not Jones and others (1956).
- Comment 15.** Page 3-3, paragraph 1, line 4: cited Grubb (1984, 1987), Ryder (1988), Weiss (1992), Hosman (1996), Williamson and Grubb (2001); however, these references were not provided in the reference section. Please either adjust the citations or update the reference section accordingly.
- Response 15.** The bibliography was updated to include these citations.
- Comment 16.** Page 3-3, paragraph 2, line 8 and 12: cited Jorgensen (1975); however, this reference was not provided in the reference section. Please either adjust the citation or update the reference section accordingly.
- Response 16.** The bibliography was updated to include this citation.

- Comment 17.** Page 3-3, paragraph 2, line 15: cited Chowdhury and Mace (2003); however, this reference was not provided in the reference section. Please either adjust the citation or update the reference section accordingly.
- Response 17.** The bibliography was updated to include this citation.
- Comment 18.** Page 3-6, line 3: please update reference to Table 4-2 to Table 3-2.
- Response 18.** The suggested change has been made.
- Comment 19.** Page 3-8, paragraph 1, line 3: cited Baskin and Hulbert (2008); however, this reference was not provided in the reference section. Please either adjust the citation or update the reference section accordingly.
- Response 19.** The bibliography was updated to include this citation.
- Comment 20.** Pages 3-8 to 3-11, Section 3.3: please re-visit all references to tables in this section. Tables 3-3 and 3-4 are provided and not referenced.
- Response 20.** We identify seven correct references to tables and figures on pages 3-8 through 3-11 and have corrected references.
- Comment 21.** Page 3-12, Section 3.4, line 14: please update reference to Figure 2-7—possibly with Figure 2-23.
- Response 21.** The reference to Figure 2-7 has been changed to reference 2-23.
- Comment 22.** Page 3-13, paragraph 1, line 8: cited Morton and others (1991); however, this reference was not provided in the reference section. Please either adjust the citation or update the reference section accordingly.
- Response 22.** The reference has been included in the revised bibliography.
- Comment 23.** Page 3-14, line 1: cited Maury (1920, 1922); however, this reference was not provided in the reference section. Please either adjust the citation or update the reference section accordingly.
- Response 23.** The references have been included in the revised bibliography.
- Comment 24.** Page 3-14, line 1: cited Plummer (1933); however, this reference was not provided in the reference section. Please either adjust the citation or update the reference section accordingly.
- Response 24.** The reference has been included in the revised bibliography.
- Comment 25.** Page 3-14, paragraph 1, line 6: cited Price (1958); however, this reference was not provided in the reference section. Please either adjust the citation or update the reference section accordingly.
- Response 25.** The reference has been included in the revised bibliography.
- Comment 26.** Page 3-14, paragraph 1, line 11: references Figure 2-10, please clarify the connection to this figure, please remove the reference, or please update with an appropriate figure.
- Response 26.** The reference to Figure 2-10 has been removed.
- Comment 27.** Page 3-14, paragraph 1, line 14: cited Morton et al. (1991); however, this reference was not provided in the reference section. Please either adjust the citation or update the reference section accordingly.
- Response 27.** We have added the reference to the bibliography.

- Comment 28.** Page 3-14, paragraph 2, line 5 and Page 3-15, last line: cited Autin and others (1991); however, this reference was not provided in the reference section. Please either adjust the citation or update the reference section accordingly.
- Response 28.** We have added the reference to the bibliography.
- Comment 29.** Page 4-6, Section 4.2.2, paragraph 1, sentence 1: please replace " Figure 5-4" with "Figure 4-4".
- Response 29.** The suggest modification was made.
- Comment 30.** Pages 4-7 and 4-8, section 4-3: cites the following references: Estepp (2004), Morton and Jirik (1989), Jones and Freed (1996), Coleman (1990), Shafer (1960), Preston (1963), Harris (1965), Thompson (1966), Peckham (1965), Anders (1957), Myers and Dale (1961), Baker and Dale (1961), and Paleo-Data, Inc. (2009); however, these references were not provided in the reference section. Please either adjust the citations or update the reference section accordingly.
- Response 30.** We have removed two of the references from the report and added the remaining references to the bibliography.
- Comment 31.** Page 4-8, Section 4.4, last sentence: please include address of website for the Bureau of Ocean Energy Management, Regulation, and Enforcement.
- Response 31.** The URL for the Bureau of Ocean Energy Management, Regulation, and Enforcement was added to the report.
- Comment 32.** Page 4-11, Figure 4-4, caption: please reword to "...of the northern portion of the Gulf Coast Aquifer System" and remove "...from the Brazos to the Rio Grande".
- Response 32.** The suggested rewording of the caption was made.
- Comment 33.** Page 5-1, Section 5.1, 4th sentence: please update reference to Figure 2-5 to a figure in the report that shows an example of a depositional environment that includes a fluvial system connected to a delta with flanking bay-lagoon systems.
- Response 33.** The reference to Figure 2-5 has been corrected to Figure 2-21
- Comment 34.** Section 5.2: Exhibit B, page 5 of the Scope of Work indicated PETRA software would be used for stratigraphic correlations. Please update the report, as applicable, on how the software was used and to what extent.
- Response 34.** A paragraph has been added to Section 5.2 to explain the use of PETRA for stratigraphic correlations.
- Comment 35.** Page 6-2: Section 6.2, paragraph 1: please insert River after Brazos.
- Response 35.** The suggested change has been made.
- Comment 36.** Page 6-4, paragraph 1, line 4: please replace "Anahua" with "Anahuac".
- Response 36.** The suggested change has been made.
- Comment 37.** Page 6-4, Section 6.2: some paleomarkers are identified on Figure 6-1; however, these do not track well with the paleomarkers listed in the text. Please update text and/or figure so there is agreement between figure and text.
- Response 37.** The text and Figure 6-1 has been modified so that they are in agreement.
- Comment 38.** Page 6-5, paragraph 1, line 4: please insert "Formation" after "Oakville".
- Response 38.** The suggested change has been made.

- Comment 39.** Figure 6-9: please clarify the basis for interpreting the irregular contacts (finely undulating, especially with depth) between the well control.
- Response 39.** The surfaces shown in Figures 6-3 through Figure 6-9 are based on sampling the same rasters for each geologic unit. Figure 6-9 shows surfaces cut along strike whereas the other cross-sections are cut along dip. The surfaces are generally smooth along the dips because sampling occurs in a direction aligned with the direction of decreasing elevations in the geologic surface. The surfaces are more irregular along strike because the sampling occurs in a direction that is at a skewed angle to the decreasing trend. This non alignment causes the “stair-step” change or irregular surfaces observed in Figure 6-9. The irregular surfaces observed in Figure 6-9 will diminished with decreases in the raster resolution, which is 4000 feet. The report has been modified to indicate that the irregular contacts are not a result of well control but a function of the sampling process.
- Comment 40.** Page 6-18: please adjust figure 6-10 and/or the geodatabase. Data from the geodatabase suggests Figure 6-10 should be labeled as the Lower Lagarto not the Upper Lagarto.
- Response 40.** The caption for Figure 6-10 has been changed to refer to Lower Lagarto and not Upper Lagarto.
- Comment 41.** Table 7-1: please spell out LCRA-SAWS Water Project in the caption.
- Response 41.** The suggested change has been made.
- Comment 42.** Pages 7-4 and 7-5, Table 7-2: please explain either in footnotes or expand in the text (or both) the flow characteristics. Understanding that the scale is relative; however, the Kh/Kv ratios do not appear to make sense in the table. In addition, please explain the rationale behind assigning the Kh and Kv values to the particular units.
- Response 42.** The report has been modified provide additional explanation for the values assigned to Kh, Kv, and Kv/Kh. The table provides Kv/Kh values that vary between 1 and 0.1. This means that Kv will range between Kh and  $0.01 * Kh$  for the different facies. There are different values for Kv/Kh for the sands and clays because of the different sorting, packing, and layering that occurs between sand and clays beds. Relative rankings of Kh and Kv values were provided to provide a general framework estimating the relative differences in K provided by the facies maps.
- Comment 43.** Table 7-2 (and figures in Section 8): please clarify if Bayfill (BF) is the same as Bayfill/Lagoon and update text for consistency, as applicable.
- Response 43.** Bayfill and Bayfill/Lagoon are the same. Table 7-2 has been modified.
- Comment 44.** Page 7-8, Figure 7-3: please correct spelling of fluvial for fluvial facies (F).
- Response 44.** The suggested change has been made.
- Comment 45.** Page 8-2, paragraph 1, line 2: cited Young and others (2009); however, this reference was not provided in the reference section. Please either adjust the citation or update the reference section accordingly.
- Response 45.** The missing reference has been added.
- Comment 46.** Page 8-2, Section 8.1.1, line 6: please update figure for Willis unit from 8-5 to 8-6.
- Response 46.** The suggested change has been made.
- Comment 47.** Section 8 figures of sand percentages and total sand thicknesses do not agree in the overlap area with Young and others (2010). Please clarify how to proceed and which study to use.



- Response 47.** Section 8.1 has been amended to acknowledge that the sand map may not agree with those in Young and others (2010) in the overlapping area. This occurs for three reasons. One reason is that the contouring in the overlapping area is influenced by new information gather slightly outside of the overlapping area that was not available for contouring by Young and others (2010). A second reason is that addition sand information in the overlapping area is included in this study. A third reason is that there are some adjustments to the top and bottom boundaries of the geology units north of dip-section 10, which affects the intervals over which sand thicknesses and sand percentages are tallied. Because sand thickness contours & percentages in this report are based on more information than the corresponding figures in Young and others (2010), the information provide by this report supersedes information presented by Young and others (2010).
- Comment 48.** Page 8-19, Figure 8-13b: overlap with Young and others (2010) does not agree in overlap (northern Wharton County) with Figure 9-13b of the southern hydrostratigraphy study. Please adjust or clarify.
- Response 48.** We agree with the findings in comment 48. Please see response to comment 47.
- Comment 49.** Page 8-23: Figure 8-17: Figure 8-17 does not match s\_t\_jp\_cp in geodatabase, please adjust figure accordingly. A review of the geodatabase suggests Figure 8-17 (a) is the contour of Chicot Aquifer base elevation and Figure 8-17 (b) is the Willis geological unit thickness, neither of which relate to the caption which indicates the map(s) should reflect the Jasper Aquifer showing total sand thickness.
- Response 49.** Figure 8-17 has been modified to show the a single figure that is the sand thickness of the Jasper aquifer. The draft report did not show information associated with the Jasper aquifer.
- Comment 50.** Section 9 (figures): Exhibit B, page 6, Task 4 of the Scope of Work states that water quality maps will include the 3-group classification of water quality (fresh, slightly saline, moderately saline). Please update the section to include these maps as well as the ones with the percent of freshwater in each of the four-aquifer units already provided or clarify in more detail why percent may be more feasible due to the geometry of saltwater divide in the subsurface.
- Response 50.** The additional water quality maps have been provided for slightly saline and moderately saline for the Chicot Aquifer, Evangeline Aquifer, Jasper Aquifer, and the Burkeville confining unit.
- Comment 51.** Page 9-1, paragraph 2, lines 4 and 8: cites LBG-Guyton and NRS Consulting (2003); however, this reference was not provided in the reference section. Please either adjust the citation or update the reference section accordingly.
- Response 51.** The missing reference has been added to the bibliography.
- Comment 52.** Figure 9-6: figure illustrates wells for all aquifers and indicates which are fresh versus saline; however, the reader cannot tell the distribution of wells and water quality in the different aquifer units. Please resubmit figures showing the distribution of water quality-wells per each aquifer unit.
- Response 52.** Figure 9-6 has been parsed out into four separate figures.
- Comment 53.** Pages B-7 and B-8: please clarify the meaning of the two rows of data highlighted in yellow.

**Response 53.** There is no significance of the yellow lines. These lines were accidentally carried over from the Excel spreadsheet and have been removed from the report.

## **D.2 Geodatabase Comments**

**Comment 1.** Northern dip and strike sections are missing from geodatabase. Please update geodatabase with data for these cross-sections including the appropriate metadata.

**Response 1.** We have updated the geodatabase to include the cross-sections from the Southern Gulf Coast Study (Young and others, 2010)

**Comment 2.** Geological Unit Top Elevation rasters are missing from geodatabase. Please update geodatabase with data for these rasters including the appropriate metadata.

**Response 2.** We have updated the geodatabase to include the top elevation rasters for the geologic units.

**Comment 3.** Please verify rasters and cross-sections do not extend above land surface and adjust as needed. Analyses with DEM data indicates several instances where this may occur but may be an artifact of scale.

**Response 3.** We have verified that the rasters do not extend about land surfaces.

**Comment 4.** Please provide metadata in a manner similar to the metadata provided with the project for the update for the framework the southern and central portion of the Gulf Coast Aquifer System (contract 0804830795).

**Response 4.** We have changes the metadata so that it is consistent with the southern Gulf Coast Geologic Study (Young and others, 2010)

**Comment 5.** Please re-visit and update the top of Jasper Aquifer and/or the base of the Burkeville confining unit (Figure 1 below) as these surfaces overlap.

**Response 5.** We have modified the top of the Jasper Aquifer so that it does not overlap with the bottom of the Burkeville confining unit.

## **D.3 Suggestions for Report**

**Comment 1.** Please address consistencies in the capitalizations, for example, Lower Lagarto versus lower Lagarto or Burkeville confining unit versus Burkeville Confining Unit throughout the report.

**Response 1.** The report has been modified to make the capitalization consistent among the geologic units.

**Comment 2.** Please address inconsistencies in referencing up-dip, mid-dip, down-dip and updip, middip, downdip, throughout the report.

**Response 2.** Report has been modified to use updip, middip, and downdip.

**Comment 3.** Please capitalize "aquifer" when used directly after "Gulf Coast" ..

**Response 3.** The suggested change has been made.

**Comment 4.** Page xii, paragraph 2, line 1: please replace "develop" with "developed".

**Response 4.** The suggested change has been made.

**Comment 5.** Page xii, paragraph 4, last sentence: please include a space in "the Chicot", change "Aquifer" to "aquifers", and end the sentence with a period.

- Response 5.** The suggested change has been made.
- Comment 6.** Page 1-1, paragraph 2, sentence 2: please change “use” to “used” and change “South” to “south”.
- Response 6.** The suggested changes have been made.
- Comment 7.** Page 1-3, paragraph 2, line 6: please delete space between "(" and "Young".
- Response 7.** The suggested change has been made.
- Comment 8.** Page 1-3, paragraph 3: please use past tense for references to “work” for example, “...two geologists worked toward...” and “Mr. Knox worked northward...”.
- Response 8.** The suggested changes have been made.
- Comment 9.** Page 2-2, paragraph 2, sentence 2: please remove River after Rio Grande.
- Response 9.** The suggested change has been made.
- Comment 10.** Page 2-9, paragraph 2, line 9: please insert comma after "1970".
- Response 10.** The suggested change has been made.
- Comment 11.** Page 3-1, paragraph 1, line 14 and elsewhere in the report: suggest replacing all references to Ashworth and Hopkins (1995) with the most recent version of the report—TWDB Report 380 (George and others, 2011).
- Response 11.** The suggested change has been made.
- Comment 12.** Page 3-5, Table 3-1: please add commas to thousand placeholder for values listed in “Width” column for consistency throughout the report.
- Response 12.** The suggested change has been made.
- Comment 13.** Page 3-20: please number this page.
- Response 13.** The suggested change has been made.
- Comment 14.** Page 3-20, Figure 3-7: please replace "other" with "others" in figure caption.
- Response 14.** The suggested change has been made.
- Comment 15.** Page 4-1, Section 4.1, paragraph 3, sentence 2: please remove "I" or clarify what this designates.
- Response 15.** The suggested change has been made.
- Comment 16.** Page 4-1, Section 4.1, paragraph 3, sentence 3: please remove "a" before “...100 ft...”
- Response 16.** The suggested change has been made.
- Comment 17.** Table 4-2: please adjust the font for 660 for consistency with font used in the caption.
- Response 17.** The suggested change has been made. The number 660 has been changed to 666 (to be consistent with Appendix A)
- Comment 18.** Page 5-5, Section 5.2, paragraph 3: please use lower case “p” for Previous.
- Response 18.** The suggested change has been made.
- Comment 19.** Page 6-1: Section 6.1, paragraph 4, second sentence: please add a period to the end of the sentence and please consider editing the sentence for clarification.
- Response 19.** The suggested change has been made.

- Comment 20.** Page 6-2: Section 6.2, paragraph 2: please consider combining sentences 2 and 3.
- Response 20.** The two sentences were not combined.
- Comment 21.** Page 6-2, paragraph 3, line 6: please change "8000" to "8,000".
- Response 21.** The suggested change has been made.
- Comment 22.** Page 6-3: last paragraph, first sentence; please change dip sections 6 to dip section 6.
- Response 22.** The suggested change has been made.
- Comment 23.** Page 6-3: third paragraph: please insert “are” between surfaces and several and possibly remove “from the salt dome”. For example, “Near the salt domes the stratigraphic surfaces **are** several hundreds of feet higher than the corresponding surfaces several miles away ~~from the salt dome.~~”
- Response 23.** The suggested change has been made.
- Comment 24.** Page 6-4: please change Mr. Knox picks to Mr. Knox’s picks (third line).
- Response 24.** The suggested change has been made.
- Comment 25.** Page 6-4 first paragraph: please change Dr. Ewing to Dr. Ewing’s (2 times).
- Response 25.** The suggested change has been made.
- Comment 26.** Page 6-5, paragraph 1, line 7: suggest inserting "decreasing" before "age" for clarification.
- Response 26.** The suggested change has been made.
- Comment 27.** 6-6, paragraph 1, line 3: please replace "northern" with "north".
- Response 27.** The suggested change has been made.
- Comment 28.** Page 6-7, paragraph 2, line 6: please replace "exits" with "exist".
- Response 28.** The suggested change has been made.
- Comment 29.** Page 6-7, paragraph 2, line 7: please replace "Chamber" with "Chambers".
- Response 29.** The suggested change has been made.
- Comment 30.** Page 7-2, Section 7.2, last paragraph: the sentence reads as if Galloway's work (2000) was performed after the work done by Young (2006). Please remove “previously” and replace with “have also been used”.
- Response 30.** The suggested change has been made.
- Comment 31.** Page 7-3 bullet 3: please edit “clays, silts, and, rarely, sands”
- Response 31.** No changes made to text.
- Comment 32.** Page 8-1: Section 8.1, second paragraph, last sentence: please change “provide” to “provides”.
- Response 32.** The suggested change has been made.
- Comment 33.** Page 8-3: Section 8.1.2: please change Fort-Bend to Fort Bend.
- Response 33.** The suggested change has been made.
- Comment 34.** Page 9-2, Section 9.1.2, paragraph 3: please update the spelling of Fahrenheit.
- Response 34.** The suggested change has been made.

**Comment 35.** Page 9-3, paragraph 2, line 8: please update string of specific conductivities to, “...of 14,000; 4,000; 1,400; 650; and 325 ...”

**Response 35.** No change was made to the text.

**Comment 36.** Page 9-3: Table 9-2: please change 1400 to 1,400 for consistence with rest of table.

**Response 36.** The suggested change has been made.

**Comment 37.** Pages 9-6 and 9-7: please change all 1000 ppm to 1,000 ppm for consistence in numbering.

**Response 37.** The suggested change has been made.

**Comment 38.** Page 9-6: Section 9.3.2 sentence 2: please remove “the” after the comma. For example, “Except for Chambers and Jefferson Counties, the every county has more wells with TDS concentrations below 1,000 ppm than above 1,000 ppm.”

**Response 38.** The suggested change has been made.

**Comment 39.** Page 9-7, next-to-last line: please replace "brined" with "brine".

**Response 39.** The suggested change has been made.

**Comment 40.** The following publications appear in the list of references but they are not cited in the body of the report. Please either remove the references or update the text with the appropriate citation(s) : Page 10-1: Arroyo (2004);Page 10-2: Baker (1961); Baker, Dale, and Baum (1965); and Beckman and Williamson (1990);Page 10-5: Core Laboratories (1972) -- both entries; Page 10-9: Halbouty (1979);Page 10-12: Lundelius (1972);Page 10-13: Myers and Dale (1966);Page 10-14: Rawson et al. (1967);Page 10-16: Shafer (1970);Page 10-17: Texas Water Commission (1989);Page 10-19: Young et al. (2006a).

**Response 40.** The following publications were omitted from the bibliography: Arroyo (2004); Baker (1961); Core Laboratories (1972) -- both entries; Rawson et al. (1967);Texas Water Commission (1989);Page 10-19: Young et al. (2006a). Citations were added to the report for the publications not omitted.

#### **D.4 Suggestions for Geodatabase**

**Comment 1.** Analyses of the alignment of the base of the Jasper to the TWDB footprint for the Gulf Coast Aquifer show a slight deviation in Brazos County (Figure 2 below). Please clarify or clip this from the dataset.

**Response 1.** The dataset has been clipped.